The Mineralogy of Fluoride Mobilisation to Groundwater from the Peninsular Granite, Andhra Pradesh, India

Bethan Mary Hallett

Department of Earth Sciences

UCL

A thesis submitted for the degree of:

Doctor in Engineering (EngD)

Environmental Engineering Science

2011

I, Bethan Mary Hallett confirm that the work presented in this thesis is my own. Where information has been derived from other sources, I confirm that this has been indicated in the thesis

Signed ……

Date ……

Abstract

This thesis investigates the mineralogical sources of fluoride (F) in groundwater in two gneissic granite bedrock aquifers in Andhra Pradesh, India, with the aim of developing a conceptual framework for describing the mechanisms of F release from mineralogical sources to groundwater. This included an enquiry into the spatial variation and relative importance of the mineralogical F sources, the effect of weathering and regolith development on F distribution, and the processes of water-rock interaction concerning F. The two catchments (Maheshwaram and Wailpally) are underlain by Pre-Cambrian gneissic granite, with groundwater F concentrations often exceeding the WHO guideline limit for F in drinking water (1.5 mg/l). Samples of fresh and weathered rock were collected and analysed using optical petrology, point counting, X-ray diffraction, electron microprobe and whole rock chemical analysis, the results of which were used to develop mass balances of F occurrence through the weathering profile. The availability of fluorine for release to groundwater was investigated through batch leaching experiments.

Results indicate the principal F-bearing rocks to be porphyritic granites in both catchments, with apatite, biotite, fluorite, amphiboles and titanite as the principal F-bearing minerals overall. The relative availability of F for release to groundwater (as indicated by batch leaching experiments) does not directly relate to sample total F content. Weathered samples, with typically low total F content and few F-bearing minerals may provide a source of F to groundwater through the leaching of relatively mobile and water soluble F. High F leached from calcrete samples and mafic vein samples in Wailpally may be important sources of F to groundwater where present. Generalisations of F distribution and release to groundwater at both a catchment scale and local scale are represented by a series of conceptual models, and a semi-quantitative analysis of F-loss through long term weathering presented.

Acknowledgements

I would firstly like to offer my deepest gratitude to my supervisors William Burgess and Eva Valsami-Jones for their instruction, guidance, encouragement, and support.

I would also like to thank EPSRC and the Natural History Museum in London for funding this project.

I am also grateful to the National Geophysical Research Institute (NGRI) in Hyderabad, India, the Indo-French Centre for Groundwater Research and French Geological Survey (The Bureau de Recherché Geologiques et Minieres - BRGM), for allowing me to visit the NGRI headquarters and for support with field work, project development, transport and accommodation while in India. In particular I would like to thank Shakeel Ahmed and Jerome Perrin, as well as Surendra Atal for his assistance with field work and P. Sreedevi and S. Atal for allowing me to use their groundwater fluoride data sets.

At UCL I would like to show my gratitude to Tony Osborne for his help, patience and guidance with leaching experiments and never ending whole rock fluorine analysis, Andy Beard for his training and support with EM analysis and James Davy and Hank Sombroek for instruction and fun in thin section preparation. I would also like to thank Maz Iqbal, Ian Wood, Qiong Li and Hingure Dharmagunawardhane.

At the Natural History Museum I would like to thank Catherine Unsworth, Stanislav Strekopytov, Agnieszka Dybowska and Colin Walker for their help and support with analytical methods and chemical analysis.

Finally, I would like to thank my ever supportive and optimistic husband, Oliver Hallett, who has willingly read and corrected every page of work, as well as my parents, Rachel and Stephen James, and all of my friends and colleagues at UCL for helping me through the past 4 years!

Contents

List of Figures

List of Tables

List of Abbreviations

CIA – Chemical Index of Alteration

EM – Electron Microprobe

EM-EBSD – Electron Microprobe with Electron Backscatter Detection

EM-EDX – Electron Microprobe with Energy Dispersive X-Ray detection

F – Fluorine

F^- – Fluoride

IC– Ion Chromatography

ICP-AES – Inductively Coupled Plasma - Atomic Emission Spectroscopy

ICP-MS – Inductively Coupled Plasma - Mass Spectroscopy

ISE – Ion Selective Electrode

IUGS – International Union of Geological Sciences

NHM – Natural History Museum (London)

RSD – Relative Standard Deviation (%)

SD – Standard Deviation

SI – Saturation Index

UNICEF – United Nations Children's Fund (formerly United Nations International Children's Emergency Fund)

WRF – Whole Rock Fluorine

WRC – Whole Rock Chemistry

WHO – World Health Organisation

XRD – X-Ray Diffraction

XRF – X-Ray Fluorescence

Chapter 1. Introduction

1.1 Background

Fluorine (F) is an essential element for human health, linked to dental and skeletal strength. A lack of fluoride leads to dental caries, however excessive fluoride is also harmful. The main intake of fluoride is through drinking water, with a concentration of between 0.5-1.5 mg/l recommended (Fawell et al., 2006). Consumption of water with a higher concentration of fluoride over prolonged periods is detrimental to health, with concentrations >1.5 mg/l F leading to dental fluorosis and >4 mg/l F leading to skeletal fluorosis or even crippling fluorosis (Fawell et al., 2006). Fluorosis is particularly a problem across large regions of east Africa, India and China, where naturally high-fluoride groundwater is used as drinking water with little or no treatment prior to use. Globally, fluorosis is endemic in more than 25 countries (figure 1-1), with an estimated tens of millions of people affected worldwide (UNICEF, 2008). In India alone it is estimated that approximately 65 million people suffer from some degree of fluorosis (Andezhath and Ghosh, 1999). It is widely accepted that naturally occurring fluoride in groundwater used for drinking water is the cause of this widespread problem.

The World Health Organisation guideline maximum for fluoride in drinking water is 1.5 mg/l, however a variety of guidelines and standards are used in different countries (table 1-1) (WHO, 1993). These depend on the local diet and water consumption. In hot climates water consumption is usually higher and therefore the guideline maximum fluoride concentration is lower (e.g. 1.0 mg/l in India) (Apambire et al., 1997).

Figure 1-1- Countries with endemic fluorosis (adapted from UNICEF, 2008).

Table 1-1 - Local limits of F in water (Edmunds and Smedley, 2005)

Country or Institution	Limit or Guideline		Date	Maximum concentration (mg/l)
Australia	Guideline	Health based guideline	1996	1.5
Canada	Guideline		2003	1.5
India	Guideline		1998	1.0
Japan	Guideline	Health based	1993	0.8
European Commission	Directive		1998	1.5
US EPA	Regulation	Primary standard	2002	4.0
	Guideline	Secondary standard	2002	2.0
WHO	Guideline		2004	1.5

Fluorine is the most electronegative of all the elements, making it very reactive and resulting in the formation of strong ionic bonds (Lindahl and Mahmood, 1995). It therefore only very rarely occurs as elemental fluorine in the natural environment, but is common as a trace constituent in many minerals, a principal constituent of fluoride minerals (e.g. fluorite, CaF_2, and fluor-apatite $Ca_5(PO_4)_3F$), and in solution as F^- (fluoride) ions and ionic complexes (Saxena and Ahmed, 2001). The average crustal content is 625 ppm F (Edmunds and Smedley, 2005) and F content ranges by lithology from <200ppm in ultra-mafic rocks (e.g. peridotite) to >2000ppm in some granites (table 1-2) (Jeffery & Hutchinson, 1986). Fluoride in groundwater ranges in concentration from zero to over 20mg/l. Table 1-3 (page 29) lists a collection of research reports on fluoride in natural waters.

Table 1-2 - Average F content of selected rock types (Levinson, 1974). [+]Extra details for Granite from Jeffery and Hutchinson (1986).

Rock Type	Average F (ppm)
Ultra-mafic Igneous	100
Basalt	400
Granite	735 (up to 2000)[+]
Shale	740
Sandstone	270
Limestone	330
soils	200

Occurrence of high fluoride in groundwater is most common in semi-arid climates and crystalline igneous rock environments (e.g. many parts of India and east Africa) (Gizaw, 1996; Handa, 1975), and on a regional scale is associated with F-bearing lithologies, alkaline soils, high evapotranspiration and Na-HCO_3 type groundwaters with high pH (allowing for statistical regional predictions such as those by Amini et al. (2008)). Significant differences are however evident between catchments with common lithologies and spatial variation is common at a small scale within individual catchments. Despite a large number of documented studies (table 1-3, page 29), few explanations of this spatial variability of F^- have been proposed (e.g. Handa (1975) and Jacks et al. (2005) for India, Kim and Jeong (2005) for south east Korea and Fuhong and Shuqin (1988) for China), none of which provide the basis for process-based prediction of F flux from bedrock to groundwater. Current interest in fluoride in groundwater in India is evident by a recent PhD by Atal (2008) and recent publications (Jha et al., 2010; Mamatha and Rao, 2010; Reddy A. et al., 2010; Reddy D. et al., 2010; Avishek et al., 2010; Chaudhary et al., 2010)

This thesis develops a conceptual framework for describing the mechanisms of F flux to groundwater in two catchments of granitic gneiss in Andhra Pradesh, India, by establishing a quantitative mass balance for the mineralogical sources of F in bedrock and its mobilisation and redistribution as a consequence of regolith development.

1.2 Environmental Sources of Fluoride

1.2.1 Mineral Sources

The principle source of fluoride in groundwater in unpolluted environments is mineralogical, with many common minerals containing small amounts of F. F^- is located within minerals bonded with cations such as Ca, Na or Al as a major constituent (e.g. in fluorite, CaF_2, cryolite Na_3AlF_6 or villiaumite NaF), and substituting for OH^- ions in minerals such as micas or amphiboles.

The accumulation of F in melts and as an elemental volatile in volcanic regions such as the East African Rift Valley and Iceland can lead to the formation of igneous and volcanic rocks with a very high F content. The excessive F content of some groundwater, lakes and rivers of East Africa has been related to leaching of these igneous source rocks, combined with the effects of volcanic HF emissions and contributions from atmospheric dust (Fuge, 1988). Fluoride concentrations as high as 295 mg/l F have been recorded in lakes along the Ethiopian Rift Valley (Gizaw, 1996). Regional concentration of fluoride in volcanic environments is correlated with reports of fluorosis in Sudan, Tanzania, Uganda, Kenya, and Ethiopia (Fawell et al., 2006; Wondwossen et al., 2004)

Crystalline basement environments often contain groundwater with a high fluoride concentration over more extensive regions, as many igneous and metamorphic rocks contain large amounts of fluoride bearing minerals. This is the case over large parts of India (Rao and Devadas, 2003;Sujatha, 2003), Pakistan (Shah and Danishwar, 2003), Korea (Kim and Jeong, 2005), Norway (Banks et al., 1995), Mexico (Valenzuela-Vasquez et al., 2006) and China (Yong and Hua, 1991), as well as Pre-Cambrian basement regions of Africa (Apambire et al., 1997).

1.2.2 Atmospheric Fluoride and Pollution Sources

Atmospheric fluoride content is increased by industrial emissions (e.g. in the production of phosphate fertilisers and coal ash produced by burning coals), as well as by volcanic activity (in the form of hydrogen fluoride gas, HF, and F in ash deposits) (Fuge, 1988). High atmospheric F can lead to a higher F content of rain; however, the total contribution of rainwater to groundwater F is generally estimated

to be small. Polluted rainwater in Norway, for example, contains an average of 0.02 ppm F, and is only a minor source of F to lakes in the area (Skjelkvåle, 2007). Industrial pollution and coal combustion may, however, pollute local soils and river water (e.g. south east Pakistan, Farooqi et al., 2007). In non-industrialised areas atmospheric F is low (0.05-1.90μg/m^3) and is not considered a significant source of fluorine for humans (Fawell et al., 2006).

Inhalation of high fluoride smoke produced from burning coals with high F content is an alternative route for F ingestion that can lead to fluorosis. This is particularly a problem in China, where coals are burnt along with F-bearing clays (~1027 ppm F) in the home with poor ventilation (Lian-Fang and Jian-Zhong, 1995;Dai et al., 2004).

Industrial waste discharge and fluoride-containing fertilisers may be a source of F to groundwater where chemicals are discharged into streams and rivers, and fertiliser chemicals are leached from the soil down into the aquifer (Motalane and Strydom, 2004;Sujatha, 2003). Industrial waste discharged to lakes and rivers from textile factories and rock polishing industries have been found in certain cases to contribute to local groundwater fluoride (Jacks et al., 2005; Tirumalesh et al., 2007).

1.3 Fluoride in Groundwater in India

Fluorosis is endemic in India, with an estimated 60-65 million people drinking water with a F concentration higher than the WHO maximum guideline value of 1.5 mg/l (Andezhath and Ghosh, 1999). The most severely affected states include Rajasthan, Gujarat and Andhra Pradesh where concentrations of groundwater fluoride are high and where untreated groundwater is widely used for drinking water (figure 1-2) (Handa, 1975).

High fluoride groundwater (up to 20 mg/l in Andhra Pradesh – Rao, 1993) is associated with the Archean Granite and Gneiss basement complexes (e.g. in Andhra Pradesh, Gujarat and Karnataka) (see table 1-3 and figure 1-2). However, there is significant spatial variation in groundwater fluoride content between and within catchments of apparently similar geology. Proposed explanations for these variation

are either poorly supported by quantitative analysis e.g. difference in groundwater residence time (Rao and Devadas, 2003), variations in the fluoride content of the aquifer bedrock (Kumar et al., 1991; Mondal et al., 2009), or have only local application e.g. evaporative enrichment of fluoride near the surface soils and subsequent washing into shallow aquifers (Gupta et al., 2005; Sreedevi et al., 2006), and precipitation of calcrete acting as a sink for F (Jacks and Sharma, 1995).

Temporal variation is an important aspect of uncertainty. There is a widespread belief that F concentrations have increased over the past 20-30 years in many areas of India (e.g. Gupta et al., 2005), and there is a common acceptance that F concentration in groundwater is seasonal, increasing after the summer monsoon (e.g. Sreedevi et al., 2006). Neither of these generalisations is well supported by documented field observations. Hydrogeologically, there have been distinct changes over large regions of the basement complexes in India over the past 30 years: the scale of groundwater abstraction has increased dramatically, leading to a decline in groundwater levels. In the 1970s the water table was at a shallow level in the weathered regolith (e.g. in Rushton, 1986), yet now the regolith is largely dewatered over large areas and groundwater levels fluctuate between the deeper regolith and the fractured bedrock. However, evidence for seasonal variation in fluoride and observations of increased groundwater fluoride at and since these earlier times are unavailable. Increased groundwater abstraction in Andhra Pradesh due to an increase in irrigated farm land has been proposed to accelerate weathering of the bedrock and saprolite and, along with the application of fluoride-containing fertilisers, has been suggested as an explanation for increased groundwater fluoride (Rao, 2008).

In Andhra Pradesh, a state distinctly affected by fluorosis, the distribution of groundwater fluoride and the prevalence of fluorosis has been documented at a regional scale e.g. Rao (2006), Sarma and Rao (1997) and Siddiqui (1955). The area is underlain by Precambrian gneissic granite with groundwater present in fractures and fissures within the bedrock and in the weathered regolith. Both spatial and temporal variations have been observed, with large differences in groundwater F between catchments of similar geology. Although the bedrock of high fluoride catchments in Andhra Pradesh is often stated as the principal source of fluoride to groundwater, the mineralogical sources and controls of fluoride mobilisation have not

been established quantitatively. Uncertainties remain concerning the details of geological F occurrence and the patterns and mineralogical associations of its distribution within the weathering profile and within catchments, the behaviour of fluoride on weathering and regolith development, and the mobilisation processes that control groundwater F occurrence and variability.

Figure 1-2 - a) Fluorosis affected states in India (souce: WHO, 1993) b) Map of mean fluoride concentration of groundwater (source: Pauwels and Ahmed, 2007)

Despite these uncertainties, a range of fluoride management responses have been implemented or suggested in Andhra Pradesh, some with contradictory assumptions of F sources and mobilisation to groundwater. The identification of low fluoride wells for drinking (Brinda et al., 2010) makes assumptions of temporal or seasonal variations. The implementation of drip irrigation (rather than flooding) to reduce weathering and leaching (Rao and Devadas, 2003) is based on the assumption that increased groundwater F is due to increased weathering rates. Increasing vegetation cover to reduce evapotranspiration and to prevent the formation of F rich salts (Rao and Devadas, 2003;Brinda et al., 2010) assumes these to be a major source of F to groundwater. The reduction in fertiliser use or use of fertilisers with low F (Rao and Devadas, 2003; Sreedevi et al., 2006) assumes the increase in use of F rich fertilisers to be the cause of high F groundwater. Artificial recharge schemes to 'dilute' high F groundwater including installation of check dams and other surface water management structures (Bhagavan and Raghu, 2005; Rao, 2008; Rao, 2003) assume

long term weathering of the aquifer bedrock as the primary source of F in groundwater .

Choice of appropriate fluoride management techniques should be based on knowledge of the sources of fluoride, their distribution within the catchment and within the weathering profile and the mechanisms of mobilisation of F to groundwater. An adequate knowledge base for these issues does not exist and a more thorough understanding of the sources and controls of fluoride in groundwater is needed to support the development of appropriate management techniques.

1.4 Research Aim and Approach

The aim of this research is to develop a conceptual framework for describing the mechanisms of F release from mineralogical sources to groundwater in hard rock regions.

This research is based on parallel studies of two catchments in Andhra Pradesh with apparently similar geology but differing groundwater fluoride concentrations (the Maheshwaram Catchment in the Ranga Reddy district and the Wailpally Catchment in the Nalgonda district). The following research questions have been addressed:

- What is the relative importance of the numerous mineralogical sources of fluoride in bedrock/regolith aquifers?
- How does the relative mineralogical distribution of F change as a consequence of regolith development?
- What is the magnitude of F variation spatially within the bedrock, as determined by geological/mineralogical variation?
- What are the processes of water-rock interaction concerning fluoride?
- How are fluoride distribution and mobilisation to groundwater linked to the hydrological conditions?

These issues have been addressed by development of a mass balance of fluoride occurrence through the weathering profile in each area, including investigation of the distribution and weathering of fluoride bearing minerals, using optical petrology, point counting, X-ray diffraction, electron microprobe analysis and whole rock chemical analysis. The availability of fluorine release to groundwater has been investigated through batch leaching experiments.

1.5 Thesis Structure

The structure of this thesis is as follows:

Chapter 1 – Introduction

Chapter 2 – A review of fluorine bearing minerals in igneous rocks, including details of occurrence, chemistry and weathering, and a summary of the controls of fluoride in groundwater.

Chapter 3 – A review of the geology and hydrogeology of Andhra Pradesh, focusing on the occurrence of groundwater fluoride, and on the two research catchments, Maheshwaram and Wailpally.

Chapter 4 – Methods and results of mineralogical investigations of Maheshwaram and Wailpally. This includes details of sample collection, petrology, X-ray diffraction, electron microscopy and whole rock chemical analysis.

Chapter 5 – The results of the mineralogical investigations are combined to form a mass balance of mineralogical fluoride occurrence through the weathering profile in each sample location. The mass balances are established to determine the relative mineralogical contributions to the total F content of the rock and to quantify F removal and redistribution upon bedrock weathering and regolith development. Further investigation of the weathering profile is carried out through analysis of one profile in each catchment, including sample description, chemistry and whole rock fluorine with depth.

Chapter 6 – An experimental study of water-rock interaction through batch leaching, with the objective to investigate the relative mobility of F to solution from bedrock lithologies and regolith equivalents, and the mobilisation of F from weathered samples at different depths in the regolith profile.

Chapter 7 – Summary and discussion of results, including the development of conceptual models of F release to groundwater, incorporating results from chapters 4, 5 and 6, and groundwater F relationships in Maheshwaram and Wailpally. Suggestions for further research are also presented.

Table 1-3– Research on Fluoride in Natural Waters

Continent	Country/Area	Reference	Subject
Africa	East Africa	Gizaw (1996)	F in waters (groundwater, streams and lakes) up to 295mg/l (in lakes) linked to acid volcanic, high temp rifting, high subsurface CO_2 pressure, low Ca and low salinity
		Kilham and Hecky (1973)	F in lakes and rivers (max 1,627 mg/l). From F rich volcanic rocks
	Eritrea	Srikantha et al. (2002)	F in groundwater (up to 3.73mg/l). Linked to pegmatite intrusion
	Ethiopia - Rift Valley	Rango et al. (2010)	F and As in lakes, groundwater and hot spring (up to 121mg/l in lakes). Linked to weathering of volcanic glass
	Ghana	Apambire et al. (1997)	F in groundwater (up to 4.6 mg/l). Linked to local geology - granites and syenites
	Tanzania	Nkotagu (2009)	F in ground and river water (up to 14mg/l - river water). Linked to sub-surface evaporation processes.
North America	Canada - Alberta	Hitchon (1995)	F in groundwater (up to 22mg/l)
	Canada - Quebec	Boyle and Chagnon (1995)	F in groundwater (up to 28mg/l) sedimentary aquifers
	USA - Nebraska	Gosselin et al. (1999)	F in drinking water (up to 2.60mg/l)
	USA - Wisconsin	Ozvath (2006)	F in groundwater (up to 7.60mg/l) Linked to geology (mainly syenites and granites)
	USA - West	Nordstrom and Jenne (1977)	F in geothermal waters and fluorite saturation
	Mexico - Hermosillo City	Valenzuela-Vasquez et al. (2006)	F in drinking water (up to 7.59mg/l) Local rock type – Granite
	Mexico - San Luis Potosi	Carrillo-Rivera et al. (2002)	F in groundwater linked to groundwater temperatures and depth. Management suggestions.
South America	Argentina - Buenos Aires	Kruse and Ainchil (2003)	F in groundwater (up to 5mg/l). Local geology – Clay, silt, loess
		Paoloni et al. (2003)	F in groundwater (up to 18.2mg/l)
	Argentina - Cordoba	Nicolli et al. (1989)	As and F in groundwater (up to 6.2mg/l F).
	Argentina - La Pampa	Smedley et al. (2002)	As and F in Loess aquifer (up to 28mg/l F)
	Argentina - Tucuman	Warren et al. (2005)	F in groundwater (up to 8.3mg/l)
Asia	Bangladesh - Ganges	Datta et al. (1999)	F in rivers
	China	Fuhong and Shuqin (1988)	Distribution of high F groundwater in China, linked to granites, volcanic, climate (and precipitation of salts) and hot springs

Continent	Country/Area	Reference	Subject
Asia	China	Lian-Fang and Jian-Zhong (1995)	Controls on fluorosis
		Dai et al. (2004)	F in coal and clay
	China - Central	Guo et al. (2010)	F in groundwater (up to 3.67mg/l) linked to hard rock aquifers
		Currell et al. (2011)	F and As in groundwater (up to 6.6mg/l) linked to loess and palaeosols
	China - North	Guo et al. (2007)	F in groundwater (max 6.2mg/l) Geological source
		Yong and Hua (1991)	F in groundwater (up to 10.3mg/l)
	China - North West	Genxu and Guodong (2001)	F distribution in water
	India	Handa (1975)	F in groundwater across India
		Jacks et al. (2005)	Controls on F in groundwater in India – linked to evapotranspiration and precipitation of calcite.
	India - South	Jacks and Sharma (1995)	F linked to carbonate deposition, F content increasing down slope.
	India – Andhra Pradesh	Kumar et al. (1991)	F in groundwater (up to 6.9mg/l). Linked to local geology of pink and grey granites.
		Rao (1993)	F in groundwater (up to 20mg/l). Linked to local geology (granites)
		Sarma and Rao (1997)	F in groundwater in Visakhapatnam city (up to 8mg/l). linked to charnokites and khondolites
		Saxena and Ahmed (2001)	F in groundwater (up to 5.5mg/l). Linked to local geology of granite and gneisses. Alkaline conditions, moderate specific conductivity and residence time important for F concentrations.
		Rao (2003)	F in groundwater (up to 8.35mg/l) Local rock type- Granite/Gneiss
		Rao and Devadas (2003)	F in groundwater (up to 5.8 mg/l) linked to local geology – Gneiss. Seasonal F variation.
		Sujatha (2003)	F in groundwater (up to 4.8mg/l)
		Bhagavan and Raghu (2005)	Installation of check dams to reduce groundwater F (1.7-3.1ppm F before dam construction).
		Rao (2006)	F in groundwater (up to 2.3mg/l). Seasonal F variation. Links with local geology (gneissic granites), irrigation, alkaline env and long residence time.
		Sreedevi et al. (2006)	F in groundwater (up to 3.8mg/l) Local rock type- Biotite Granite. Seasonal variation

Continent	Country/Area	Reference	Subject
Asia		Rao (Rao, 2008)	F in Varaha river basin (up to 2.1mg/l). Enhanced by intensive irrigation, fertilisers, alkaline environment.
		Mondal et al. (2009)	F in groundwater (up to 19mg/l). Linked to local geology (granite and gneiss
		Brinda et al. (2010)	F in groundwater (up to 8.8mg/l) Local Geology - Granitic gneiss.
		Reddy, A. et al. (2010)	F in groundwater (up to 5.83 mg/l). No appreciable change in time or space
		Reddy, D. et al.(2010)	F in groundwater (up to 7.6mg/l). Linked to local whole-rock F content (granite/gneiss), and adsorption to/precipitation with calcrete
	India - Gujarat	Gupta et al. (2005)	F in groundwater (up to 8mg/l)
		Dhiman and Keshari (2006)	F in groundwater (up to 5.6mg/l). Local rock type-Granite/Gneiss
	India - Jharkhand	Avishek et al. (2010)	F in groundwater. Over 1.5mg/l in ~400 wells. Linked to fluorosis
	India - Karnataka	Tirumalesh et al. (2007)	F in groundwater (up to 6.50mg/l) local rock type-granite/gneiss/schist
		Mamatha and Rao (2010)	F in groundwater (up to 5.35mg/l) linked to local geology (granite/gneiss), and calcite precipitation
	India - Orissa	Kundu et al. (2001)	F in groundwater Related to F rich hot spring water
	India - Rajasthan	Madhavan and Subramanian (2002)	Absence of F in soils. High F in clays. Geology aeolian sands.
		Muralidharan et al. (2002)	F in shallow groundwater (up to 14mg/l). local geology aeolian sands
		Chaudhary et al. (2010)	F in groundwater (up to 8.5mg/l) linked to fluorosis
		Gautam and Bhardwaj (2010)	F in groundwater (up to 14.62mg/l)
	India - Uttar Pradesh	Misra et al (2006)	F in groundwater. Local rock type-Alkali sedimentary
		Jha et al. (Jha et al., 2010)	F in groundwater (up to 13.9mg/l) linked to clay content and $CaCO_3$ deposits
	India - West Bengal	Gupta et al. (2006)	F in groundwater
	Iran	Mesdaghinia et al. (2010)	F in groundwater (up to 5mg/l). Advise alternative water sources or defluoridation in high F areas
	Iran - Isfahan	Keshavarzi et al. (2010)	F in groundwater (up to 9.2mg/l) linked to metamorphic and granitic rocks and hydrochemistry

Continent	Country/Area	Reference	Subject
	Iran - Khuzestan	Nouri et al. (2006)	F in groundwater (up to 2.17 mg/l)
	Japan - South West	Aizawa and Akaiwa (1995)	F in groundwater linked to F in limestone (up to 680 ppm)
	Japan - South	Abdelgawad et al. (2009)	Sources of F in groundwater -fluorite and micas (in granite).
	South Korea	Kim and Jeong (2005)	F in groundwater (some >5 mg/l). linked to local geology (granite)
	Sri Lanka	Young et al. (2010)	F in groundwater (up to 4.34 mg/l F) linked to local geology (gneiss), groundwater residence time and intensive agriculture
	Pakistan - Nagar Parkar	Naseem et al. (2010)	F in groundwater (up to 7.85 ppm F) linked to granite rock (ave 1939 mg/kg F) weathering.
	Pakistan - Naranji	Shah and Danishwar (2003)	F in groundwater (1.08-1.38 mg/l) (granite aquifer) and in streams
	Pakistan - Punjab	Farooqi et al. (2007)	F in groundwater (up to 21.1 mg/l) (pollution sources)
Europe	England	Fuge and Andrews (1988)	F in the UK environment (areas of high/low F, sources)
	England – Wessex	Gaus et al. (2002)	F in water. Modelling concentrations.
	Estonia	Haamer (2006)	F in drinking water (up to 7.20 mg/l)
	Estonia - West	Karro and Rosentau (2005)	F in drinking water (up to 3.79 mg/l) Local rock type - Sedimentary
	Italy - Central	Vivona et al. (2007)	F in groundwater. Local rock type – volcanic/sedimentary
	Norway	Skjelkvåle (2007)	F in lakes, linked to local geology
	Norway - Central	Banks et al. (1995)	F in groundwater (up to 4.5 mg/l)
	Serbia	Mandinic et al. (2010)	F in groundwater (up to 14 mg/l). Linked to fluorosis.
	Spain - Central	Perez and Sanz (1999)	Low F in drinking water (less than 0.2 mg/l. Linked to dental carries
	Turkey - South West	Davraz et al. (2008)	F in springs and lakes (up to 5.6 mg/l). Linked to volcanic rocks

Chapter 2. Review of Fluorine Mineralogy and Associated Weathering

2.1 Fluorine Mineralogy in Hard Rock Aquifers

The Earth's crust consists of approximately 0.009% fluorine (F), ranking F as the 13th most abundant terrestrial element (Lindahl and Mahmood, 1995). Fluorine bearing minerals are found in sedimentary, igneous and metamorphic rocks (Table 2-1) with an average of 300 ppm F found in the earth's crust (Tebbutt, 1983). F^- is located within minerals either bonded to cations such as Ca^{2+} or Na^+ in minerals such as fluorite (CaF_2), villiaumite (NaF) or cryolite (Na_3AlF_6), or as a substitute for OH^- ions in minerals such as micas or apatite (e.g. $Ca_5(PO_4)_3(OH,F,Cl)$) as both ions have similar physicochemical properties. In many minerals F is released preferentially on weathering. Table 2-2 lists F-bearing minerals found in igneous, sedimentary and metamorphic rocks and those found in mineral veins.

Table 2-1 - Average Fluorine content in Igneous rocks (Jeffery & Hutchinson, 1986)

Igneous Rock Type	Fluorine content (ppm)
Ultrabasic (e.g. Picrite)	1-20
Basic (e.g. basalt, Gabbro)	300-500
Granitic (e.g. Andesite)	200-2000
Alkalic (e.g. Phonolite)	500-2000

Table 2-2 - Some of the common fluoride bearing minerals and their occurrence

Fluoride-Bearing Mineral	Occurrence	Reference
Fluorite CaF_2	Igneous: In many igneous rocks, esp. granite and syenite Sedimentary: As a detrital mineral or as cementing in sandstones Other: In veins and cavities and in hydrothermal veins	Deer et al. (1992)
Apatite $Ca_5(PO)_4(OH,F,Cl)$	Igneous: In many igneous rocks, especially granitic pegmatites Metamorphic: Common Sedimentary: As a primary deposit, or detrital (especially in carbonates) Other: In hydrothermal veins	Deer et al. (1992)
Titanite $CaTi[SiO_4](O,OH,F)$	Igneous: In calc-alkaline, alkali, nepheline syenites Metamorphic: In gneisses, schists and metamorphosed impure calc-silicate rocks and scarns Sedimentary: Detrital or authigenic	Deer et al. (1992)

Fluoride-Bearing Mineral	Occurrence	Reference
Amphiboles $Ca_2(Mg,Fe)_4Al[Si_7AlO_{22}](OH)_2$	Igneous: In intermediate calc-alkali rocks and plutonic rocks Metamorphic: In regionally metamorphosed rocks. greenschist to lower granulite facies	Deer et al. (1992)
Micas $K_2(Mg,Fe)_4(Fe,Al)_2[Si_6Al_2O_{20}](OH)_2(F,Cl)_2$ (biotite formula)	Igneous: Muscovite and biotite found in granites and granite pegmatites. Biotite very common in igneous rocks Metamorphic: Muscovite, paragonite and biotite found in phyllites, schists and gneisses Sedimentary: Muscovite and paragonite found in detrital and authigenic sediments. Glauconite found in greensands.	Deer et al. (1992)
Tourmaline $NaMg_3Al_6(BO)_3[Si_6O_{18}](OH,F)_4$ (dravite formula)	Igneous: In granitic pegmatites and some Granites Metamorphic: Especially in metamorphosed impure limestones Sedimentary: As a common detrital mineral or as an authigenic mineral in some limestones Other: In pneumatolytic veins	Rutley (1988)
Topaz $Al_2[SiO_4](OH,F)_2$	Igneous: In granites, granite pegmatites, rhyolites Metamorphic: High grade metamorphism Other: In veins and cavities and in pneumatolytic veins	Rutley (1988) Anthony et al. (1997)
Villiaumite NaF	Igneous: In nepheline syenites, nepheline syenite pegmatites Sedimentary: In lake bed deposits	Stormer and Carmichael (1970) Anthony et al. (1997)
Sellaite MgF_2	Igneous: In alkalic granites and volcanic ejecta Metamorphic: In marble and metamorphic magnesite deposits	Anthony et al. (1997)
Cryolite Na_3AlF_6	Igneous: In granites	Stormer and Carmichael (1970)
Epidote $Ca_2Al_3Si_3O_{12}(OH)$	Igneous: Acid Igneous Metamorphic: In regional and contact metamorphism Other: May be formed from hydrothermal alteration	Deer et al. (1992)
Chlorite $(Mg,Fe,Al)_6(Si,Al)_4O_{10}(OH)_8$	Igneous: Common. Chloritisation of biotite common in granites Metamorphic: Common. Especially in low to moderate grade metamorphic rocks Sedimentary: Common in argillaceous sediments Other: May be formed from hydrothermal alteration	Deer et al. (1992)
Clay Minerals	Usually formed as a product of weathering	Deer et al. (1992)

2.1.1 Fluorite CaF_2

Fluorite (CaF_2) forms cubic crystals with each calcium ion surrounded by 8 fluorine ions, which are each coordinated with 4 calcium ions, forming a regular tetrahedron (Deer et al., 1992; Leeuw and Cooper, 2003) (Figure 2-1). Small impurities of Mg, Si or Al may occur, and part of the Ca may be replaced by Sr, Y or Ce (Forming yttrofluorite, $(CaY)F_{2-3}$, for example), although most fluorite is at least 99% CaF_2. Some fluorites may contain free fluorine which on grinding may give an odour of ozone and HF (known as antozonites), or may contain hydrocarbons (e.g. Blue John,

which may contain up to 0.27% carbon) (Deer et al., 1992). Fluorite is often purple in thin section with moderate relief (Rutley, 1988).

Figure 2-1 – Fluorite Structure.(Ca=black, F=pale grey) (Leeuw and Cooper, 2003).

Chemistry and Weathering

The solubility and dissolution rate of fluorite is thought to be slow, and therefore of less importance as a source of F to groundwater (Nordstrom and Jenne, 1977;Chae et al., 2006). The solubility of fluorite is, however, important as a control of $[F^-]$ in solution (Handa, 1975). Fluorite dissolution is dependent on pH, temperature, concentration of dissolved ionic species, and the composition of the water (Saxena and Ahmed, 2001;Nordstrom and Jenne, 1977). Fluorite solubility can be represented by the equations below (Appelo and Postma, 1996):

$$CaF_{2\,(s)} \leftrightarrow Ca^{2+}_{(aq)} + 2F^-_{(aq)}$$

$$K_{Fluorite} = [Ca^{2+}]\,[F^-]^2 = 10^{-10.5} \quad \text{at } 25°C$$

High concentrations of Ca^{2+} in solution are therefore associated with low concentrations of F^- and vice versa (Appelo and Postma, 1996;Saxena and Ahmed, 2001;Handa, 1975;Sujatha, 2003). F mobilisation is prevented at equilibrium if the concentration of Ca^{2+} is above the limit for fluorite solubility, as observed by Kim and Jeong (2005), Rao (1993) and Sreedevi et al., (2006).

The dissociation of fluorite is affected by concentrations of dissolved calcium, bicarbonate, sulphate and sodium in the water. Increasing the concentration of Ca^{2+} in solution by the dissolution of gypsum ($CaSO_4.2H_2O$), for example, will decrease/limit $[F^-]$ in solution, as shown in the equation below:

$$CaSO_4 \leftrightarrow Ca^{2+} + SO_4^{2-}$$

$$K_{(gypsum)} = [Ca^{2+}]\,[SO_4^{2-}] = 10^{-4.60} \text{ at } 25°C$$

The concentration of bicarbonate ions affects calcite dissolution, which in turn affects fluorite dissolution (Rao et al., 1993;Saxena and Ahmed, 2003). This is shown in the following equations:

$$CaCO_{3\,(s)} + H^+ \leftrightarrow Ca^{2+} + HCO_3^-$$

$$K_{(calcite)} = ([Ca^{2+}]\,[HCO_3^-]) / [\,H^+] = 0.97 \times 10^2$$

$$CaCO_{3\,(s)} + H^+ + 2F^- \leftrightarrow CaF_{2(s)} + HCO_3^-$$

$$K_{(cal.\text{-}fluor.)} = [HCO_3^-] / ([F^-]^2\,[H^+])$$

As $K_{(cal.\text{-}fluor.)}$ is constant, there is a positive correlation between bicarbonate (HCO_3^-) and fluoride concentrations, with high bicarbonate concentrations correlating to high fluoride concentrations (Handa, 1975;Sreedevi et al., 2006). Waters rich in sodium bicarbonate ($NaHCO_3$) will therefore act to increase dissolution in the equations below (Saxena and Ahmed, 2001):

$$CaF_2 + Na_2CO_3 \leftrightarrow CaCO_3 + 2F + 2Na$$

$$CaF_2 + 2NaHCO_3 \leftrightarrow CaCO_3 + 2Na + 2F + H_2O + CO_2$$

Alkaline conditions (pH 7.6-8.6) with moderate specific conductivity (750-1,750 µS/cm) have been found to be most favourable to fluorite dissolution (Saxena and Ahmed, 2001;Fuhong and Shuqin, 1988) as they reduce Ca^{2+} activity, allowing higher $[F^-]$ to be sustained (Warren et al., 2005). These conditions are often found in waters in alkaline volcanic rocks (e.g. Edmunds and Smedley, 2005).

Occurrence and distribution

Fluorite is usually formed in igneous rocks, especially granites and syenites as a late-crystallising hydrothermal mineral (e.g. Ozvath, 2006), but can also be found in sedimentary rocks either as a detrital mineral, or as a cementing material (e.g. in sandstones). Fluorite may also occur as veins (Deer et al., 1992).

Fluorite is the main commercial source of fluorine and is used for the production of hydrofluoric acid and hydrogen fluoride (used to manufacture aluminium fluoride and chlorofluorocarbons). North America holds approximately 26% of the world's high quality fluorite deposits (mostly in Mexico) (Lindahl and Mahmood, 1995).

Fluorite is often cited as the principal mineral influencing the concentration of fluoride in groundwater, e.g. Apambire et al., (1997) in Ghana, Karro and Rosentau (2005) in Estonia and Valenzuela-Vasquez et al. (2006) in Mexico. However, as fluorite has a lower solubility than other fluorine bearing minerals such as apatites and micas, it may not always be the main contributor to F in groundwater (Apambire et al., 1997).

2.1.2 Apatite - $Ca_5(PO_4)_3(OH,F,Cl)$

Apatite minerals have the general chemical formula $Ca_5(PO_4)_3(OH,F,Cl)$. Large variations in F, Cl and OH content are possible. Fluorapatite ($Ca_5(PO_4)_3F$) is the most common form of apatite, although pure end-member fluorapatite minerals are uncommon in nature (Deer et al., 1992). Fluorapatite structures may incorporate CO_3, forming carbonate fluorapatite $Ca_5(PO_4CO_3)_3(F,OH)$ (also known as francolite), the F content of which varies depending on CO_3 content. Francolite is often found in sedimentary rocks (Aizawa and Akaiwa, 1995). Small variations in the F, Cl and OH content can lead to large differences in chemical behaviour (Kreidler and Hummel, 1970). For example, fluorapatite is more soluble than other apatites (Edmunds and Smedley, 2005).

Natural apatite structures usually differ from synthetic structures, possibly due to differences in anion ordering caused by impurities and vacancies (Hughes et al., 1989).

Chemistry and Weathering

There are two general equations (below) for describing fluorapatite and hydroxyapatite dissolution, (forming acidic calcium phosphates in the first equation) (Dorozhkin, 1997):

$$Ca_{10}(PO_4)_6(F,OH)_2 + 14H^+ = 10Ca^{2+} + 6H_2PO_4^- + 2HF,H_2O$$

$Ca_{10}(PO_4)_6(F,OH)_2 \leftrightarrow 10Ca^{2+} + 6PO_4^{3-} + 2F^-, OH^-$

As apatite is a major constituent in human bones and teeth and a major source of inorganic phosphorous in nature, much research has been conducted into its formation and reactions (e.g. Varughese and Moreno, 1981; Hughes et al., 1989; Ishikawa et al., 1994).

Dissolution of fluorapatite is a surface controlled process, and incongruent in its early stages, becoming congruent as the dissolution reaction progresses to steady state (Hagen, 1975; Giudry and MacKenzie, 2003; Parkinson, 1999). Fluorapatite reactions with phosphoric acid indicate that fluorine is lost from the surface first, possibly due to replacement with hydroxyl ions or water (equation below) (Dorozhkin, 1997;Tseng et al., 2005).

$Ca_5(PO_4)_3F + H^+ + H_2O = Ca_5(PO_4)_3(H_2O)^+ + HF$

This reaction forms positively charged apatite crystals, and is followed by the dissolution of calcium ions and then phosphate (Dorozhkin, 1997;Tseng et al., 2005). As calcium ions are released prior to phosphate in the initial stages of whole mineral dissolution, ratios of CaO/P_2O_5 are used as indicators of weathering of apatites, with this ratio increasing as weathering progresses (Giudry and MacKenzie, 2003). Toledo et al. (2004) noted that in point analysis Electron Microprobe Energy Dispersive X-ray analysis apatite Si and P content (replaced by C) and Sr and Na content (replaced by Ca) decrease upon weathering, and that F, CO_3^{2-} and Ca content increases (as substituting cations are lost).

The dissolution of fluorapatite depends on the chemical composition of the mineral, as well as the surrounding environment. Igneous fluorapatite releases compounds faster than sedimentary carbonate fluorapatite at a given pH, even though it has a lower solubility (Giudry and MacKenzie, 2003). Like fluorite, fluorapatite dissolution may also be repressed by the presence of dissolved Ca^{2+} at high pH (Tseng et al., 2005). Fluorapatite dissolution is dependent on pH (with little variation above pH 6), and shows retrograde solubility (decreasing solubility with increasing temperature) (Giudry and MacKenzie, 2003).

A study on the precipitation of fluorapatite scale in water supplies in the UK is given in Appendix 1. This study, conducted on generic hard and soft waters, tested the

dosing of fluoride (as NaF) and phosphate (as H_3PO_4) with the aim of investigating the reaction kinetics and factors governing fluorapatite scale formation. Results showed the importance of high temperatures on apatite precipitation (increasing temperatures reducing the solubility of fluorapatite), with high dosing of phosphate decreasing the onset time of precipitation.

Occurrence and distribution

Apatites are common rock forming minerals, occurring as an accessory mineral in almost all igneous (up to 5% volume), sedimentary (as primary deposits or detrital minerals) and metamorphic rocks. Apatites are common in granitic pegmatites, hydrothermal veins and in carbonates (Deer et al., 1992).

Fluorapatite dissolution is considered to be a major source of fluoride in groundwater in areas of the USA (in Wisconsin, Ozvath, 2006), India (Handa, 1975) Tanzania (Parkinson, 1999) and Japan (Aizawa and Akaiwa, 1995).

2.1.3 Cryolite – Na_3AlF_6

Cryolite is monoclinic, with crystals rarely forming in nature. Although cryolite is considered one of the principal fluoride minerals in igneous rocks, it has a restricted occurrence (Stormer and Carmichael, 1970). There is only considered to be one major source of cryolite, in Ivigtut, west Greenland, where cryolite occurs within granites (up to 20% cryolite) and also as a siderite-cryolite body (up to 80% cryolite) along with siderite, quartz and sulphide (Antipin et al., 2006). As this source is now depleted, the use of natural cryolite has been replaced with synthetic cryolite (Rutley, 1988). Cryolite is used in industry for the manufacture of aluminium and porcellanous glass.

Other occurrences of cryolite are recorded in the Pyrenees (Spain), the Ilmen mountains (Russia), and Colorado, USA (Meshri, 1995).

Cryolite usually forms in silica rich and calcium poor salic (silica and/or aluminium rich) rocks (e.g. granites). Large amounts of calcium present would lead to the preferential formation of fluorite (CaF_2), and it is often only in anorthite poor siliceous rocks that cryolite forms instead of fluorite (Stormer and Carmichael, 1970).

Cryolite is less soluble and less common than many other fluoride bearing minerals (Meshri, 1995). Therefore its importance as a potential source of F to groundwater is limited. Cryolite has, however, been suggested as a source of fluoride in drinking waters in Eritrea by Srikantha et al. (2002).

2.1.4 Villiaumite - NaF

Villiaumite occurs in nepheline syenites, nepheline syenite pegmatites and in lake bed deposits (Anthony et al., 1997). Villiaumite is found in association with nepheline, analcite, alkai feldspars and alkali amphiboles, but not with quartz (unlike cryolite) (Stormer and Carmichael, 1970). Examples of occurrence include those in Greenland, Namibia, Québec (Canada) and New Mexico (USA) (Anthony et al., 1997).

Villiaumite is often used as an additive to drinking water supplies in order to increase water F concentration for health reasons (to reduce dental caries) (Mueller, 1995).

2.1.5 Titanite (Sphene) - $CaTi[SiO_4](O,OH,F)$

Titanite is a common accessory mineral, with the general formula $CaTi[SiO_4](O,OH,F)$. Calcium in the structure may be partly replaced by Na, and Ti may be partly replaced by Al or Fe^{3+}. The oxygen atoms within the structure occur in three different positions, one of which is not bound to any of the SiO_4 groups and can be replaced by (OH,F) (Deer et al., 1992). Partial substitution of Ti by Al and Fe is charge compensated by fluoride hydroxide anions substituting for oxygen; therefore titanite with a higher proportion of Ti substituted for Al and Fe should have a higher F content (Malcherek et al., 1999). In thin section titanite is commonly brown, with diamond shaped crystals and simple twinning (Deer et al., 1992).

The stability of titanite is affected by calcite and dolomite dissolution and precipitation (equation below) (Bancroft et al., 1987).

$$CaTiSiO_5 + CaO_2 = CaCO_3 + TiO_2 + SiO_2$$

Titanite weathers to anatase (TiO_2) and smectite (clay), which often form on the surface of the mineral. Calcium is usually completely lost upon weathering, whereas little Ti is lost as it is held within the weathering products (Tilley and Eggleton, 2005). High Ca solutions suppress titanite weathering and may initiate re-growth of the outer surface of the titanite (Bancroft et al., 1987).

Titanite may form upon weathering of biotite due to the release of Ti from the biotite structure. Titanite is most commonly formed in rocks that are rich in calcium with a high Ca/Al ratio, and is more likely to be found in association with hornblendes rather than anhydrous rocks. Titanite may also be formed in the breakdown of hornblende (Frost et al., 2000).

Occurrence and distribution

Titanite is a common accessory mineral in calc-alkaline and alkali igneous rocks, and is abundant in nepheline syenites. Titanite is also found in metamorphic rocks (such as gneisses and schists), in metamorphosed impure calc-silicate rocks and skarns and as a detrital mineral in sedimentary rocks (Deer et al., 1992).

2.1.6 Tourmaline - $XY_3Z_6B_3Si_6(O,OH)_{30}(OH,F)$

There are several different types of tourmaline, the most common being Dravite, Schorl and Elbaite. All three of these varieties contain fluorine in small amounts (Rutley, 1988).

Dravite – $NaMg_3Al_6(BO)_3[Si_6O_{18}](OH,F)_4$

Schorl – $Na(Fe^{2+}Mn)_3Al_6(BO_3)_3[Si_6O_{18}](OH,F)_4$

Elbaite – $Na(Li,Al)_3Al_6(BO_3)_3[Si_6O_{18}](OH,F)_4$

Occurrence and distribution

Tourmaline is found in some granites, granitic pegmatites, pneumatolytic veins (usually forming Dravite in basic igneous rocks), in some metamorphic rocks (especially in metamorphosed impure limestones) and in metasomatic rocks. Tourmaline is also commonly a detrital mineral in sedimentary rocks, and an authigenic mineral in some limestones (Rutley, 1988).

2.1.7 Topaz - $Al_2[SiO_4](OH,F)_2$

Topaz is an orthorhombic mineral, often with well formed crystals. The composition of topaz is usually constant, with limited replacement of F^- by (OH^-) (Deer et al., 1992)..

Occurrence and distribution

Topaz is found in igneous rocks (usually granites, granite pegmatites and rhyolites) and in veins and cavities (Deer et al., 1992). Topaz can also be formed from high grade metamorphism of aluminium and quartz rich rocks (Anthony et al., 1997)

2.1.8 Sellaite – MgF_2

Sellaite is tetragonal, forming prismatic crystals and has the same mineral structure as that of the Rutile group. Each Mg ion is surrounded by 6 F ions at the corners of an octahedron, and each F ion in turn surrounded by 3 Mg ions (Deer et al., 1992). Sellaite is white or transparent in colour, brittle and with a vitreous lustre (Anthony et al., 1997).

Occurrence and distribution

Sellaite is uncommon, but can be found in evaporites, bituminous dolomite-anhydrite rock, volcanic ejecta and fumarolic deposits, marble, alkalic granites and metamorphic magnesite deposits (Anthony et al., 1997).

2.1.9 Amphiboles - $Ca_2(Mg,Fe)_4\ Al[Si_7AlO_{22}](OH)_2$

The Amphibole group consists of minerals with a $(SiAl)O_4$ tetrahedra linked in chains and bonded together by cations (e.g. Mg or Fe). The above formula is for a magnesio-hornblende or ferro-hornblende. OH^- ions within the amphiboles structure can be substituted by F^- ions (Deer et al., 1992).

Amphiboles are divided into three main groups: the calcium-poor amphiboles (e.g. anthophyllite, cummingtonite), the calcium-rich amphiboles (e.g. tremolite, edenite, hornblende) and the alkali amphiboles (e.g. Glaucophane) (Rutley, 1988).

Chemistry and Weathering

Amphiboles are often readily weathered due to planes of weakness in their structure formed by the silica chains. Where cations that bond these chains together are readily soluble, this will result in a rapid breakdown of the structure (Loughnan, 1969). For example, hornblende may weather to chlorite or vermiculite. On weathering, fluorine is usually released from the structure preferentially (Edmunds and Smedley, 2005).

Occurrence and distribution

Amphiboles are commonly found in regionally metamorphic rocks (less common in contact metamorphism) and in intermediate calc-alkaline igneous and plutonic rocks (Deer et al., 1992). Amphiboles are considered a possible source of fluorine to groundwater in several locations (e.g. in Sri Lanka, Young et al., 2010; in Malawi, Msonda et al., 2007).

2.1.10 Micas - Biotite

Micas are phyllosilicate minerals consisting of sheets of SiO_4 tetrahedra between layers of cations (Fe, Mg, Al) and $(OH)^-$. Sheets are held together by weakly bonded cations (K^+ or Na^+). Some common micas include (Rutley, 1988):

Biotite – $K_2(Mg,Fe)_4(Fe,Al)_2[Si_6Al_2O_{20}](OH)_2(F,Cl)_2$

Lepidolite – $K_2(Li,Al)_{5\text{-}6}[Si_{6\text{-}7}Al_{2\text{-}1}O_{20}](OH,F)_4$

Muscovite – $K_2Al_4[Si_6Al_2O_{20}](OH,F)_4$

Phlogopite – $KMg_3AlSi_3O_{10}F(OH)$

Micas may contain fluorine where F^- ions are substituted for $(OH)^-$ ions (Edmunds and Smedley, 2005). Work by Munoz and Ludington (1974) found that phlogopite is more effective at taking up F than iron rich biotites. In many areas biotite mica is an important F-bearing mineral.

Chemistry and Weathering of Biotite

The structure of biotite is shown in figure 2-2. Cation substitutions can occur within the mineral structure with common substitutions including replacement of K for Na or Ca, replacement of Mg or Fe for Al, Mn, Cr, Ti or Li and replacement of Si or Al for Ti or Fe^{3+} (Deer et al., 1992).

Figure 2-2 - Generalised structure of biotite, consisting of alternating layers of linked (SiAl)O4 tetrahedra containing Mg or Fe, and interlayers of octahedrally coordinated cations (K). F^- ions substitute for OH^- ions, seen here coordinated to Mg and Fe. (Source: AIST website, 2009).

Trioctahedral micas (e.g. biotite and phlogopite) are more readily altered than dioctahedral micas (e.g. muscovite) due to the position of the potassium ions within the structure. Muscovite is surprisingly resilient to weathering (Loughnan, 1969). However the greater the ratio of F/OH in trioctahedral micas the more stable they become (as the F^- ion which has no protonic charge, places the K in the mica further away from the hydroxyl group, making it more firmly fixed between the silicate sheets) (Wilson, 1975).

Biotite also usually weathers more rapidly than other silicate minerals in granitic rocks such as apatite, K-feldspars, zircon, epidote (Nesbitt and Young, 1984), and therefore may be an important source of F to groundwater. Often in calc-alkaline granites the majority of whole rock F^- is located in biotites. Biotite in alkali granites are also found to have higher F^- concentrations than in other granite types (Bailey, 1977).

Chemical weathering and alteration of biotite may lead to the formation of chlorite, titanite, ilmenite, epidote or clay minerals. The weathering of biotite commences along the cleavage of the mineral, and results in the loss of the K ions between the layers of linked $(SiAl)O_4$ tetrahedra. A complex array of secondary minerals can be formed between the lamellae (Siddiqui, 1955). The layers of tetrahedra may however be more difficult to break down.

The removal of interlayer K^+ ions from a biotite mineral and the replacement by hydrated exchangeable cations can form 2:1 'swelling' minerals which keep some of the original biotite structure. Where this occurs on some, but not all layers, interstratified minerals are formed (e.g. a biotite-smectite). Where this has occurred at the edges of the mineral, but not the core of the mineral, 'intergrades' (e.g. integrate biotite vermiculite) are formed (Bisdom et al., 1982). Table 2-3 shows weathering of biotite. Mg and K may be retained by the secondary products of biotite weathering (Nesbitt and Young, 1984).

Figure 2-3 - Biotite mica (a), layer weathering (a) and edge weathering (c) (Bisdom et al., 1982)

The products of biotite weathering depend on the environment and the composition and structure of the biotite. The alteration of biotite to form chlorite may occur through layer by layer replacement (forming pseudomorphs of biotite), or by dissolution, transportation and replacement. Alteration from biotite to chlorite involves the removal of interlayer cations (usually K) (Jiang and Peacor, 1994). The chloritisation of biotite in granites is particularly common (Deer et al., 1992). Hydrothermal alteration of biotite to epidote may also occur (Deer et al., 1992).

Biotite often contains inclusions of minerals such as zircon, titanite and apatite (Bisdom et al., 1982).

Occurrence and distribution

Micas are common minerals, found in igneous, metamorphic and sedimentary rocks. In many areas biotite dissolution is thought to contribute to groundwater fluoride, e.g. in the Bongo granitoids of Ghana (Apambire et al., 1997) and in metamorphic rocks and granites in Iran (Keshavarzi et al., 2010). Micas are commonly found in soils, where (with clay minerals) they are thought to be the main source of fluorine. This may contribute to F in groundwater as F in micas is leached out by percolating water. Micaceous clay may have an F content of up to 7,400 ppm (Robinson and Edgington, 1946).

2.1.11 Epidote – $Ca_2Al_3Si_3O_{12}(OH)$ - $Ca_2Fe^{3+}Al_2Si_3O_{12}(OH)$

There are several varieties of epidote, including zoisite (clinozoisite), epidote, piemontite and allanite. The composition of the clinozoite-epidote series is given above. The general formula for epidotes is $(Ca,Sr,Pb,Mn,Th,REE)_2$ $(Al,Fe^{3+},Fe^{2+},Mn,Cr)_3$ Si_3 $(O,OH,F)_{13}$ (Deer et al., 1992). Epidotes generally have a low F content (below detection limits); however fluorian allanites may also form with a higher F content. These have been described in Andhra Pradesh (Rao et al., 1979) and Canada (Pan and Fleet, 1990).

Epidote is usually colourless to green in thin section, and green, grey or yellow in hand specimen. Allanite is brownish yellow or brown (and occasionally colourless) in thin section and light brown to black in hand specimen. Allanites may have a large range of compositions (Deer et al., 1992).

Epidote minerals are found in a variety of lithologies, produced by regional or contact metamorphism and during crystallisation of acid igneous rocks. Epidote may also be formed from hydrothermal alteration of plagioclase. Allanite is usually found in granites, granodiorites, monzonites and syenites (Deer et al., 1992).

2.1.12 Chlorite $(Mg,Fe,Al)_6(Si,Al)_4O_{10}(OH)_8$

The chlorites are a group of minerals with a similar structure to biotite, but without interlayer K ions (figure 2-4). Chlorites are split into the following groups:

- Clinochlore (Mg-rich chlorites) including:
  - Ripidolite
  - Diabantite
  - Pychnochlorite (Fe rich clinochlore)
- Chamosite (Fe-rich chlorites) including:
  - Brunsvigite
  - Pseudothuringite (an Al-rich chamosite)
- Pennanite (Mn-rich chlorite)

Figure 2-4 - General chlorite structure (Source: Anthoni, 2000, Seafriends Website)

The F^- content of chlorites is usually low (at or below detection limits). Chlorite can be primary or secondary as a weathering product (e.g. hydrothermal alteration of amphiboles, pyroxenes and biotite (Deer et al., 1992)). The composition of chlorite formed from alteration will reflect the composition of the original mineral, with alteration often psudomorphous. Primary chlorite can be transformed under weathering into vermiculite/ smectites (as a consequence of preferential leaching of certain cations), or into secondary altered chlorites (Brandt et al., 2003).

2.1.13 Clay Minerals

Clay minerals are hydrous silicates consisting of Si_4O_{10} tetrahedral sheets, with similar structures to micas. There are a large variety of clay minerals including (Deer et al., 1992):

- The Kaolinite group
- The Illite group
- The Smectite group
- Vermiculite
- The Palygorskite group

Chemistry and Weathering

Clay minerals are usually formed by the weathering of other minerals, for example, the weathering of a K-feldspar in the presence of water will give illite, and with further weathering, kaolinite. Clay minerals can also be produced by hydrothermal alteration. Clay minerals are common in most weathering environments, and have a very small grain size (<0.002mm) and therefore cannot be fully identified by an optical microscope (Rutley, 1988).

Most clay minerals have a high sorption capacity, and can be used as geochemical barriers. In the case of fluorine, F^- ions can be sorbed into the clay, replacing the OH^- ions in the mineral structure. Fluoride sorption and desorption in clay minerals is dependent on pH, with sorption of F ions significant at low pH (below 5.5), and desorption more likely at higher pH values (Savenko, 2001;Kau et al., 1997). Rates of sorption-desorption are dependent on clay mineral type, with higher sorption-desorption rates for montmorillonite, then for kaolinite (Savenko, 2001;Agarwal et al., 2002).

Clay minerals that commonly have high F^- content include illite, palygorskite, sepiolite, kaolinite and montmorillonite (Jacks et al., 2005;Savenko, 2001;Agarwal et al., 2002). In soils, most F^- present is within clay minerals. Clays may therefore be an important source of F^- to groundwater (Robinson and Edgington, 1946). Positive correlations between clay content and soil total F content have been reported,

however total soluble fluoride has also been found to decrease with increasing clay content, due to adsorption of F into the clay minerals (Jha et al., 2010).

Areas where clay is thought to contribute significant F^- to groundwater include areas of India (palygorskite and sepiolite, Jacks et al., 2005;Madhavan and Subramanian, 2002), Estonia (bentonite beds, Karro and Rosentau, 2005) and China (Smectite with ~1027ppm F used with coal as fuel, Dai et al., 2004).

2.1.14 Calcite

Calcium carbonate minerals can be used as a method of fluoride reduction in groundwater (either by precipitation or by adsorption of F^-) and calcite is often quoted as a potential sink for groundwater fluoride in natural systems (Jacks and Sharma, 1995; Reddy D. et al., 2010).

The removal of fluoride from water by calcite occurs both as fluorite (CaF_2) is precipitated with calcite, and also through adsorption of F^- onto the surface of the calcite structure. The adsorption of F^- is dependent on the surface area of calcite and the pH (with lower pH increasing the number of sites to which F^- may be adsorbed) (Turner et al., 2005). Jacks and Sharma (1995) found that the F content of carbonates (co-precipitated as fluorite) in a calcite-dolomite precipitation series was higher in dolomite ($CaMg(CO_3)_2$) precipitation rather than calcite as fluorite is precipitated after calcite and dolomite.

Calcite may also act as a source of fluoride to groundwater, as when calcite with adsorbed fluoride comes into contact with water, fluoride may be de-sorbed (Jha et al., 2010). Measurements of total water soluble F from calcite in batch leaching experiments include 7.6mg/kg (by Reddy D. et al, 2010) and 12.5mg/kg (by Jha et al., 2010).

2.1.15 Sorption of F onto Al and Fe minerals

The sorption of F^- in soils is related to clay content (as mentioned above) and also to the presence of Al and Fe oxides (both amorphous and crystalline phases). Sorption of F^- onto Al and Fe oxides is dependent on pH (higher sorption at low pH) and surface area, and occurs through displacement of OH^- ions and water molecules bound to mineral surfaces (ligand exchange) (Harrington et al., 2003). F may also be adsorbed onto positively charged sites through electrostatic force (Zhu et al., 2007). Adsorption through ligand exchange can be shown as follows, leading to an increase in pH (Zhu et al., 2006):

$$\equiv AlOH + H^+ + F^+ \leftrightarrow \equiv AlF + H_2O$$

Or

$$\equiv AlOH + F^- \leftrightarrow \equiv AlF + OH^-$$

Sorption of F^- onto Al minerals is more common than F^- sorption onto Fe minerals due to the higher affinity of Al atoms for F (Harrington et al., 2003), and is also increased by the presence of phosphate (P) due to surface (Al,Fe)-F-P precipitation (Zhu et al., 2007). The addition of phosphate (present in most fertilisers) also allows F to be desorbed from Al and Fe oxides in soils more easily, as the preferential adsorption of P both on the mineral surface (as (Al-Fe)-F-P precipitates) and in the inner binding sites leave F adsorption to be mainly on the surface binding sites, from which F is more easily de-sorbed (Zhu et al., 2007). This may affect the availability of F in soils where fertilisers are used.

Adsorption of F^- in clays is thought to be greater in clays with a high Al content, as sorption mostly occurs at the Al sheets (Kau et al., 1998). Sorption of F^- onto Al minerals is also thought to promote Al dissolution (especially in amorphous phases), as F^- replacing OH^- or H_2O bound to Al weakens the other Al-OH bonds. Al-F complexes (such as AlF^{2+}, AlF_2^+,, AlF_4^- and AlF_3) form in solution with high F and Al content (Harrington et al., 2003).

2.2 The Weathering of Hard Rocks

2.2.1 Saprolite formation

The weathering of bedrock and the breakdown of F-bearing minerals is important as a mechanism for the release of F to groundwater.

Weathering of hard rocks in Andhra Pradesh leads to saprolite formation. A saprolite is a thoroughly decomposed rock in which the texture and structure of the original rock is preserved (Stolt et al., 1992). Saprolite structure may be lost in the upper portion of the saprolite (termed massive saprolite) as the transition to soil occurs. The first stage of saprolite formation consists of the transformation of easily altered minerals into secondary forms, resulting in a weathered rock. This is preceded by oxidation of iron, lowering of pH and the leaching of bases and de-silication. Weathering changes occur most rapidly with depth, in the lower portion of the saprolite and weathered rock (Stolt et al., 1992).

Factors that are important in the weathering process include (Chorley, 1969):

- The bedrock composition, texture and structure
- The topography (as this affects the micro-climate, vegetation and drainage)
- Biological action (such as that from humic and bacterial acids and plant roots)
- Time
- Climate, including:
    - Rainfall (the presence, availability and pH of water)
    - Temperature

The chemical weathering of a rock to form saprolite is an iso-volumetric process, resulting in a porous medium. The mass lost during saprolite formation (often between 20-60%) and the thickness of the resulting saprolite depends on the rock type, its mineralogy, the soil type and the weathering and erosion conditions.

Saprolite thickness is usually greater in summit positions and less in back-slopes and foot-slopes where erosion is greater (Stolt et al., 1992). Research of saprolite formation in Maryland, USA by Costa and Cleaves (1984) found that rocks of greater metamorphism show greater overburdens of saprolite, and back-slops contain little or no saprolite. It was also found that ephemeral and first order streams of the area flowed over saprolite, whereas 2nd order and greater streams flowed over bedrock due to their higher erosion rates. Long term weathering rates can be calculated by differences between elemental or mineral composition in the fresh bedrock and the weathered regolith (White et al., 2002).

The grain size of a rock and the degree of interlocking between minerals affects its permeability and therefore its susceptibility to weathering. Rocks with a smaller grain size generally have a lower permeability and greater strength, and are therefore less susceptible to weathering. Rocks with a porphyritic texture are also less susceptible due to smaller mineral grains in the spaces between the larger mineral grains (Tugrul and Zarif, 1999, Bell, 2000).

In laboratory leaching experiments using crushed samples, the grain size to which samples are crushed affects the rate and concentrations of elements leached. Crushing a sample to a smaller grain size gives a greater overall surface area than using a larger grain size, therefore giving a greater area available for reaction with water, usually resulting in a faster rate of weathering and higher leached element concentration. This has been demonstrated in leaching experiments by Hodson, 2002 and Chae et al., 2006, as illustrated in figure 2-5 (showing batch leaching of F in experiments by Chae et al. 2006).

Figure 2-5 - The affect of grain size on leached F concentrations in granite batch leaching experiments by Chae et al. (2006). Batch leaching experiments preformed in this study (Chapter 6) have a water-rock ratio of 5:1 and grain size of 500-2000μm.

2.2.2 Chemical and Mineralogical Changes

Chemical weathering of minerals results in a portion of the mineral being dissolved into the weathering water, while the insoluble residue is hydrated (Loughnan, 1969). The weathering of rocks leads to a decrease particle size and the formation of new minerals that are more stable under the new conditions (Chorley, 1969). When looking at the weathering of hard rocks it is important to consider the degree of leaching to which the rock has been subjected.

The primary elements that are lost during saprolite formation include Ca, Na and Mg, nearly all of which are lost during the initial stages of weathering (Table 2-3) (Stolt et al., 1992). Al is considered to be essentially insoluble, and therefore remains in the solid phase (Nesbitt and Young, 1984). The solubility of atoms and ions will affect their mobility and the stability of the mineral that they are in. Water pH affects solubility, with solubility usually increasing with decreasing pH. The pH of natural waters is affected by salt deposition, surface wash and drainage from surrounding hills, rainwater pH, and the mineralogy of the rock.

Table 2-3 - Mobility of common cations, from least mobile at the top of the table (lowest loss rate from the environment), to most mobile at the bottom of the table (highest loss rate). (Source: Loughnan, 1969).

Cation	Mobility
Al^{3+}	Immobile in the pH range 4.5-9.5 (normal range for natural waters)
Fe^{3+}	Immobile under oxidising conditions
Ti^{4+}	May show limited mobility if from $Ti(OH)_4$. Immobile if in the form TiO_2
Fe^{++}	Rate of loss depends on redox potential and degree of leaching
K^{+}	Readily lost, but rate may be retarded through fixation (e.g. in the illite structure)
Ca^{++},Na^{+}, Mg^{++}	Readily lost under leaching conditions

Plagioclase is thought to be the most important contributor of cations to weathering solutions in granitic terrain due to its rapid alteration compared to K-feldspars. As albite is weathered to kaolinite, Na^+, HCO_3^- and SiO_2 should increase in solution (see equation below) (Nesbitt and Young, 1984):

$$2H_2CO_3 + 2NaAlSi_3O_8 = Al_2Si_2O_5(OH)_4 + 2Na^+ + 2HCO_3^- + 4SiO_2$$

(aq.) (carbonic acid) (albite) (kaolinite) (dissolved salts)

Weathering solutions should therefore evolve from low concentrations of Na, K, Ca, Mg, HCO_3 and SiO_2 (primitive weathering solutions) to high concentrations of these elements (evolved weathering solutions). Weathering solutions will progressively change as they migrate down the profile. As high concentrations of carbonic acid are leached from the organic zone of the weathering profile, the most extensively weathered minerals should be located within and just below this zone. The weathering profile can thus be divided into three zones (figure 2-6) (Nesbitt and Young, 1984).

Figure 2-6 – Weathering profile zones and evolution of weathering solutions (Nesbitt and Young, 1984).

The Chemical Index of Alteration (CIA) can be used to evaluate the degree of weathering of a sample, the value of CIA increasing as weathering proceeds (equation below) (Rashid, 2008).

$$CIA = [AL_2O_3/(Al_2O_3+CaO^*+Na_2O+K_2O)] \times 100$$

*CaO is the concentration of CaO in silicates only.

Mineral stability depends on mineral structure and element mobility (as discussed earlier - table 2-3). The stability of some common minerals is shown in table 2-4 (Loughnan, 1969). Minerals such as zircon and quartz are fairly resistant to breakdown, with apatite and epidote also among the more stable minerals. Mineral stability is often affected by the pH of the weathering solutions with apatite stability, for example, greatly reduced at low pH values. In granitic bedrock areas the following order of increasing stability is given (Pettijohn, 1941):

Titanite < Hornblende < Epidote < Apatite < Garnet < Zircon.

However at low pH, this order changes (Lang, 2000):

Apatite < Titanite < Hornblende < Garnet < Epidote < Zircon

One of the most common minerals in granites is feldspars. Ca and Na plagioclase feldspars are more easily broken down than K-feldspars (table 2-4). The weathering of feldspars may produce several different minerals including micas, chlorite, gibbsite and kaolinite. Transitions of feldspars to micas can also occur in saprolites (Wilson, 1975).

Table 2-4 The stability of some common minerals, from most stable (botto) to least stable (top) (Loughnan, 1969)

Mineral	Notes
Olivine and Ca^{++} Plagioclase	Ca^{++} Plagioclase - Tectosilicate
	Olivine – Neosilicate. Silica tetrahedra linked by Mg and Fe in octahedral coordination
Augite	Pyroxene chain silicate.
Hornblende	Amphibole – Double chain Si_4O_{11} structure. Double chains bonded together. Readily cleave along the lengths of the chains
Biotite and Na Plagioclase	Biotite -Trioctahedral Mica (phylosilicate) weathers rapidly – commencing along cleavages, removing K ions
K^+ Feldspar	Tectosilicate.
Muscovite	Dioctahedral Mica (Phylosilicate) resilient to break down
Quartz	Tectosilicate. Spiral arrangement of tetrahedra. Very resistant to weathering

The relative stability of fluorine bearing minerals upon weathering, and their solubilities are given in table 2-5. This is based on a combination of several studies on mineral susceptibility to weathering, including Goldich (1938), Petijohn (1941), Loughnan (1969), Bateman and Catt (1985), Gaciri and Davies (1993), Morton and Hallsworth (1999) and Jerzykowska et al. (2007). The order of relative stability of these minerals may vary depending on the environmental conditions (e.g. pH), but the relative order given in table 2-5 is a guide, within which variations may be expected.

Table 2-5 The relative stability of fluorine bearing minerals, from most susceptible to weathering (top) to least susceptible to weathering (bottom). Based on research by Goldich (1938), Petijohn (1941), Loughnan (1969), Bateman and Catt (1985), Gaciri and Davies (1993), Dreever and Clow (1995), Morton and Hallsworth (1999) and Jerzykowska et al. (2007). Solubility product constant values from Gaciri and Davies (1993) and Appelo and Postma (1996) (fluorite).** Values of the Solubility product constant, where available, are included. These values are subject to change depending on environmental conditions, such as temperature.

	Minerals	Solubility Product Constant (K_{sp})**	Comments
Increasing Susceptibility To Weathering	Calcite	$1x10^{-8}$ (at 25°C)	
	Villiaumite		
	Biotite+		+Some research gives hornblende as more susceptible to weathering than biotite (Goldich 1938, Loughnan 1969)
	Hornblende+		
	Sellaite>	$6.4x10^{-9}$ (at 27°C)	>Susceptibility of fluorite and sellaite to weathering may vary. Sellaite is thought to usually be more soluble than fluorite, which in turn is more soluble than apatite (Gaciri and Davies, 1993).
	Epidote		
	Fluorite>	$10^{-10.5}$ (at 25°C)	*Susceptibility to weathering of apatite varies, from it position here, to a stability more similar to biotite. Lang (2000) has shown apatite susceptibility to weathering to change markedly with solution pH (becoming less stable at low pH).
	Apatite*	$2.3x10^{-45}$ (18°C, pH 7)	
	Titanite^		^Position of titanite varies – in some cases regarded as more susceptible to weathering than hornblende (Petijohn, 1941)
	Topaz		
	Tourmaline		
	Clay minerals**		**Clay minerals are generally considered stable

2.3 Controls on fluoride concentrations in groundwater

The concentration of F^- in groundwater is primarily controlled by the weathering of the aquifer bedrock through the release of F from F-bearing minerals, as well as the chemistry of the weathering solution, and in particular, fluorite saturation. Several indirect controls may also affect groundwater fluoride concentrations, some of which are discussed below.

2.3.1 Direct Controls

Aquifer Bedrock Weathering

The primary source of F to groundwaters is the weathering of F-bearing minerals present in the aquifer bedrock. The most common F-bearing minerals (e.g. apatite, biotite) and those containing high F content (e.g. fluorite, cryolite) have been discussed previously in this chapter. Minerals that are commonly cited as the source of F^- in groundwater used for drinking water are biotite (e.g. Apambire et al., 1997;Young et al., 2010), fluorite (e.g. Karro and Rosentau, 2005; Valenzuela-Vasquez et al., 2006) and apatite (e.g. Ozvath, 2006; Aizawa and Akaiwa, 1995), whereas the more restricted presence of cryolite, villiaumite and sellaite (as well as tourmaline and topaz) make these minerals less common as the source of high F^- groundwater used for drinking.

Fluorite Saturation

The concentration of F^- in solution is controlled by fluorite (CaF_2) saturation, as where fluorite saturation is reached this will precipitate out of solution, reducing the F^- concentration of the water. This has been illustrated by Handa (1975) in India and the inverse relationship between F and Ca in many natural waters by various authors (Appelo and Postma, 1996;Saxena and Ahmed, 2001;Sujatha, 2003). High F^- groundwaters are therefore likely to be those with low Ca concentrations, allowing F^- concentration to increase without fluorite saturation being reached. Alkaline conditions promote the precipitation of calcium carbonate, reducing Ca concentration

and allowing higher F^- concentrations. Details of fluorite saturation are given above in section 2.1.1.

2.3.2 Indirect Controls

Spatial and temporal variations (both seasonal and longer term) in groundwater F^- concentration between areas of similar geology and hydrogeology indicate the presence of indirect controls of F^- concentration in addition to those of fluorite saturation and F-bearing mineral weathering. A number of controls have been proposed to explain these variations in different areas of India, as described briefly below.

Residence Time

Longer residence times allow longer reaction times between groundwater and the aquifer bedrock, and therefore may result in higher concentrations of F^- being released to groundwater. In hot, dry climates, groundwater F^- concentrations can be enhanced by high potential evapotranspiration causing low freshwater exchange and therefore longer residence times in the aquifer (Rao and Devadas, 2003;Padfield and Grey, 1971;Young et al., 2010). In areas where dolerite dykes are present these are thought to increase the residence time of groundwater by forming barriers to groundwater movement (Rao, 2003). The pumping of deeper groundwater (with a longer residence time) is also suggested as a cause of high F^- groundwater, although several studies have found there to be no link between residence time and groundwater concentrations (e.g. Gupta et al., 2005).

Precipitation of F-rich salts

The precipitation of F-rich salts in the upper layers, which are then washed down into the aquifer with the monsoon rains, is thought to increase groundwater F^- concentrations and in some cases cause seasonal variations (with F^- concentration increasing after the monsoon) (Rao, 2003; Sreedevi et al., 2006; Rao, 2006; Brinda et al., 2010).

Application of F-rich Fertilisers and Extensive Irrigation

The application of fertilisers with high F-content may cause F to be leached down by monsoon rains into the aquifer (e.g. Rao, 2003). Intensive irrigation is also thought to increase weathering and therefore enhance dissolution and weathering of F-bearing minerals increasing the F^- concentration of the water, thus high groundwater exploitation (for irrigation) is cited as a cause of high F^- groundwater (e.g. Bhagavan and Raghu, 2005).

Precipitation of Calcite and Dolomite

Jacks and Sharma (1995) and Jacks et al. (2005) found that the precipitation of carbonates in relation to hill slope processes can affect groundwater F^- concentrations, with the F content of carbonates (in the form of fluorite) increasing down-slope. Dolomites that precipitate down-slope from calcite were found to have a higher F content. Calcrete may therefore act as both a sink and a source of groundwater F^-, with high F^- groundwaters occurring in valley bottoms as F is allowed to accumulate as the groundwater travels down-slope and calcite and dolomite are precipitated (Jacks et al., 1993). Removal of F^- from groundwater by co-precipitation with calcrete is also suggested by Reddy D. et al. (2010).

Chapter 3. A Review of the Indian Geological Context

3.1 General Geology and Hydrogeology

The geology of Andhra Pradesh is dominated by Peninsular gneiss (Archean to Proterozoic), with hard rocks covering 66% of the area (figure 3-1). Other lithologies include limestones and shales of the Cuddupah and Kurnool formations (16%), Deccan trap basalts (3%), Gondwana soft rocks (7.5%) and river and coastal alluvium (7.5%) (Rao et al., 2001).

Figure 3-1 - Simplified geological map of Andhra Pradesh (Rao et al. 2001).

Local and regional variations in geology are present in different districts of Andhra Pradesh. This study investigates the Pre-Cambrian granite gneiss around the Hyderabad area.

The granite-gneissic rocks consist of grey granites and pink granites with dolerite dykes and quartz veins (Sujatha, 2003). The granite is fissured (with a higher density of fissures near the surface), and weathering has produced a saprolite layer with

preserved fissured. Figure 3-2 shows a generalised cross section through the weathering profile produced by Dewandel et al. (2006) consisting of:

- A thin layer of red soil (10-40 cm)
- A thin sandy saprolite (1-3 m in Maheshwaram)
- A thick layer of laminated saprolite, with a few granite core stones. This is clay rich with a high effective porosity (0.5-10 %) and a low hydraulic conductivity (average 4×10^{-6} m/s) (10-15m thick in Maheshwaram)
- Fissured fresh granite with weathered granite and a few clay minerals partly filling the fissures. The hydraulic conductivity of this layer is estimated at between 5×10^{-6} and 9×10^{-5} m/s (average 1.6×10^{-5} m/s). In Maheshwaram this is the layer that is tapped by most of the wells drilled in the hard rock areas (15-20 m thick in Maheshwaram)
- Un-fissured granite (bedrock), the hydraulic properties of which are highly variable.

Figure 3-2 –Idealised weathering profile in the Maheshwaram catchment (from Dewandel et al., 2006).

Dewandel et al. (2006) suggests that the profile is the product of a multi-phase weathering process whereby the entire saprolite layer was eroded away during the Jurassic and the current profile created by alternate periods of weathering and erosion, involving the re-weathering of the previously truncated profile. This profile is different to a classical weathering profile as the thickness of the laminated saprolite is large compared to the sandy saprolite and the fissured layer. The saprolite contains

preserved fissures which are important for hydraulic conductivity of the saprolite (Dewandel et al., 2006).

Both the saprolite layer and the fractured bedrock can act as aquifers, transmitting or storing water. Aquifers are usually fairly shallow and unconfined, with recharge through rainfall infiltration. Some deeper confined aquifers (up to 120m) also exist that are hydraulically connected to shallow aquifers through fractures and joints etc with low storage and variable transmisivity (depending on geological structures and faults) (Rao et al., 2001).

Hard rock aquifer porosity is secondary, resulting from fractures, joints and weathering within the rock. The hydraulic properties are therefore dependant on fissure density, distribution and connectivity as well as fissure permeability, with the availability of water at a specific point depending on fracture density and connectivity at that location. The depth over which fissures are conductive is known as the 'conductive fissure zone'. At Maheshwaram this is between 9 and 35m deep and roughly follows the topography. Within this, the most conductive layer (the 'Transmission Zone') is found in the first few meters of the fissured layer, where the density of the fissures is greatest and where most groundwater flow occurs (see figure 3-3). Weathering causes the fissures in the saprolite to be filled with clay materials (increasing fill towards the surface), which reduces their porosity (Dewandel et al., 2006).

High conductivity is due to high density and connectivity of fissures, and not necessarily due to the presence of a single more conductive fissure. This, along with spatial heterogeneity in the weathering profile and hydrological conditions, causes spatial variations in groundwater (Dewandel et al., 2006).

Large scale groundwater development in India started in the 1970s and has since increased with the development of new drilling techniques and pumping equipment. In Andhra Pradesh, the total land area irrigated by groundwater more than doubled between 1975 and 1994, from 3.1% to 7.0% of the total land area, with an increase in the number of groundwater abstraction structures from around 800,000 to 1,600,000. This increase in groundwater abstraction has lead to a decrease in the water table and well yield, and is linked to a reported decline in water quality, including the belief

that in some areas groundwater F has increased (Rao et al., 2001). In many areas the water table has declined from within the weathered saprolite into the fractured bedrock, leaving the saprolite largely dewatered (Kumar and Ahmed, 2003).

Figure 3-3 - Generalised geological and hydrogeological conceptual model of the Maheshwaram granite aquifer. dfiss: density of conductive fissures, Kfiss: hydraulic conductivity of fissures and Kglobal: equivalent hydraulic conductivity of the layer.

3.2 Groundwater Fluoride in Andhra Pradesh

Fluorosis is common in Andhra Pradesh especially in the districts of Nalgonda, Visakhapatnam, Mahabubnagar, Anantapur, Kurnool, Chittoor, Ranga Reddy, and Prakasam (figure 3-4). High F concentrations are linked to the presence of F-bearing minerals in the bedrock, as well as groundwater chemistry, groundwater residence times, long term intensive irrigation, F-bearing fertilisers and the monsoon climate. Large spatial variations are common and are thought to be due to the varying distribution and accessibility of F-bearing minerals (such as fluorite, apatite, hornblende) and water chemistry, although few petrographic studies have been made (e.g. Bhagavan and Raghu, 2005; Rao, 2006). High groundwater F concentrations are linked with low Ca and Mg concentrations and high Na (Sarma and Rao, 1997;Rao et al., 1993), as well as high alkalinity (Kumar et al., 1991;Rao, 2008).

Figure 3-4 – Districts of Andhra Pradesh. Districts with high occurrence of fluorosis shaded in grey (adapted from Rao et al., 2001).

The contribution of F from atmospheric rainfall and deposition is thought to be low in Andhra Pradesh. F deposition in the state of Chhattisghar (to the north of Andhra Pradesh) in 1995 was measured as 474 kg/km^2/year with a mean of 0.1431 ppm fluoride in precipitation. This was due to output from an aluminium plant and numerous cement plants (Chandrawanshi and Patel, 1999). Rainwater chemistry from Uttar Pradesh (rural, semi-arid) is given in table 3-1 along with F precipitation data from Atal (2008) in Maheshwaram and Reddy et al. (2009) in Wailpally. Rainwater is neutral to acid, with a low F content in Maheshwaram (0.05-0.08 ppm) (Atal, 2008), although this is higher in Uttar Pradesh (0.30 ppm F). The contribution of F from rainwater to groundwater is therefore thought to be negligible in the Maheshwaram and Wailpally catchments.

A summary of research on groundwater F in some of the more severely affected districts of Andhra Pradesh is given below.

Table 3-1- Rainwater Chemistry for rural semi-arid sites in India. Values in ppm.

pH	Ca	Mg	K	Na	NO_3	SO_4	Cl	F	NH_4	Location	References
6.1 - 7.4	2.68	0.94	0.09	0.45	2.69	0.74	1.09	0.30	0.78	Uttar Pradesh	Satsangi et al. (1998)
								0.05 - 0.08		Andhra Pradesh Maheshwaram	Atal (2008)
6.25							2.15			Andhra Pradesh Wailpally	Reddy et al. (2009)

Anantapur District (South West Andhra Pradesh)

Groundwater in Anantapur district has between 0.6-5.8 mg/l F (91% of wells measured in 1997 above 1.5 mg/l (Rao and Devadas, 2003)), with higher concentrations of F^- post-monsoon than pre-monsoon. The source of groundwater F^- is attributed to F-bearing minerals in the gneissic bedrock (including apatite, fluorite, biotite, muscovite and hornblende), with areas of high groundwater F^- linked to areas of high whole rock fluorine content (Rao and Devadas, 2003). Check dams installed to reduce groundwater F^- have resulted in a decrease in F^- concentrations in just over half of the locations where dams were installed (Bhagavan and Raghu, 2005).

Guntur District (East central Andhra Pradesh)

Groundwater F^- concentrations up to 2.3 mg/l have been measured in Guntur district (Rao, 2003;Rao, 2006). The aquifer geology is proposed as the source of F^-, although no investigation of the F content or F mineralogy of the bedrock has been made. Leaching of F ions into the groundwater is linked to the cycle of wet and dry conditions and therefore is thought to give seasonal variations (Rao, 2003;Rao, 2006).

Nalgonda (Central Andhra Pradesh)

The Nalgonda district is well known for its high groundwater F^-, with F^- concentrations up to 20mg/l (Rao et al., 1993). The area has also given its name to a method of defluoridation called the 'Nalgonda technique'. The geology of the area consist of biotite rich grey granites, granite gneiss and porphyritic gneiss as well as dolerite dykes. Many of the granite gneisses contain fluorite as well as biotite and hornblende. Whole rock fluorine values range from 325-3200 ppm F (Rao et al., 1993). Further details on groundwater F in Nalgonda is given in section 3.4.

Ranga Reddy district (west central Andhra Pradesh)

Kumar et al. (1991) measured up to 6.9 mg/l F in the north of Ranga Reddy district, underlain by pink and grey granites and intruded by dolerite dykes, with 99% of samples having concentrations over 1.5mg/l. High F^- is attributed to local geology, although no investigation of F in the bedrock geology was undertaken. Sreedevi et al. (2006) found seasonal variations in groundwater F^- content.

Visakhapatnam (North East Andhra Pradesh)

Fluorosis was first recognized in Visakhapatnam the 1940s. Groundwater F^- concentrations of up to 8mg/l have been measured around Visakhapatnam city

(Sarma and Rao, 1997). Water samples from the Varaha river basin also have elevated F^- levels (up to 2.1 mg/l) (Rao, 2008). In both cases high water F^- concentrations are thought to be due to the local geology (including charnokites and khondolites) although no detailed F mineralogical study of the area has been conducted. Other factors thought to enhance local groundwater F^- concentrations include the application of fertilisers which may contain F and intensive long term irrigation increasing weathering (Rao, 2008).

Two catchments have been chosen for further investigation, the Maheshwaram catchment in the Ranga Reddy district and the Wailpally Catchment in the Nalgonda district. Both catchments have apparently similar geology, but with very different groundwater F^- concentrations. In Maheshwaram groundwater F^- concentrations are between 0.4-4mg/l, with many areas under 1.5mg/l, whereas in Wailpally groundwater F^- reaches 7.6 mg/l, with the majority of groundwater over 1.5 mg/l F (Sreedevi et al., 2006; Reddy D. et al., 2010).

3.3 The Maheshwaram Catchment, Ranga Reddy District

The Maheshwaram catchment is located 30km south of Hyderabad, and covers approximately 60km^2 at an elevation of 600-670m above mean sea level (figure 3-5) (Sreedevi et al., 2006). The climate is semi-arid, sub-tropical, with temperatures ranging from 22-44 °C, and an annual average rainfall of 812.0mm, most of which falls in the monsoon season (figure 3-6). Due to the high temperatures, potential evapotranspiration rates reach 1800mm/yr and surface streams are often dry except during the monsoon (Marechal et al., 2006b).

The area predominantly consists of pink and grey granites with a few dolerite dykes and quartz veins and is divided into three areas, the biotite granite (which makes up most of the area), the leucogranite and the intermediate granite area (made up of biotite granite with pegmatites and leucogranite dykes) (figure 3-5). The generalised weathering profile from the soil through to the bedrock is described above in section 3.2.

Porosity is secondary, resulting from fractures, joints and weathering. Kumar and Ahmed, (2003) found at least 4 sets of major joints running across the catchment, with the most prominent striking N-S on average, and with a vertical or very steep dip (70-70° to the west). These major joints, along with smaller joints and fractures are thought to enhance water percolation and groundwater transmission. High yielding wells were found to coincide with lineaments which traverse the area.

Figure 3-5 – Location and Geology of Maheshwaram (adapted from Sreedevi et al., 2006).

Figure 3-6 - Average maximum (red) and minimum (blue) monthly temperatures and average monthly precipitation (green bars) for Hyderabad, India (BBC world weather service).

Rainfall is the main source of groundwater recharge, which is estimated at 5% of the rainfall (Chand et al., 2005). Both the weathered saprolite and the fractured bedrock can transmit surface water and may act as aquifers in the region. However, due to declining water levels, groundwater flow is generally restricted to the fractured rock, leaving the weathered zone dry (Kumar and Ahmed, 2003;Sujatha, 2003). Several tanks are used to store monsoon waters (these are dry during the dry season) (Dewandel et al., 2006)

The water table fluctuates with the seasons as well as with pumping cycles. Figure 3-7 shows a typical well hydrograph over one year, showing the decrease in water table depth in the wet season, and the increase in the dry season, as well as the effect of pumping cycles (Marechal et al., 2006b).

Figure 3-7 - Well hydrograph showing seasonal water table fluctuations (from Marechal et al. 2006b).

Approximately 25% of the cropped area of Ranga Reddy is irrigated, with tube wells as the source of the irrigation water (Andhra Pradesh Online, 2008). Crops are irrigated throughout the year including during the monsoon when rates are lower. Many farmers receive free electricity due to regulation policies and can drill at low costs. In 2006, there were 929 borewells tapping the fractured granite in the Maheshwaram watershed, 707 of which were in use, each pumping for ~6-7 hours each day (Marechal et al., 2006a). Groundwater irrigation is mainly used for rice paddy fields (87% of total abstracted groundwater) and vegetable fields (tomatoes,

okra, etc). The large proportion of water used for rice paddy fields will result in large irrigation flow returns to the aquifer (Marechal et al., 2006b).

Large scale groundwater development has thought to have reduced water levels and water quality, with more recent improvements in drilling techniques and pumping equipment increasing abstraction, including abstraction over dry periods (such as 1992-1993) (Rao et al., 2001;Marechal et al., 2006a). Increases in groundwater abstraction are also thought to have changed the regional groundwater flow, causing areas of stagnation in the north west (where there is a concentration of pumping wells for irrigation) and reduced outflow to the north, which previously would generally follow topography, with groundwater outflow into rivers (Figure 3-8).

Figure 3-8 - Piezometric map of the Maheshwaram watershed. Dots indicating pumping wells are proportional to pumping rate. Zone 1 – low lying area where cultivated fields are concentrated, showing the largest water table depletion and groundwater stagnation. Zone 2 and zone 3 also show marked declines in groundwater level (Source Marechal et al., 2006a).

Overall, most groundwater is high in Ca and Mg, and low in Cl and SO_4 with a pH of around 6.5-8.5 (usually low during post-monsoon season) (Sreedevi et al., 2006). Figure 3-9 shows a rough map of variation in groundwater chemistry over the catchment.

Groundwater fluoride concentrations from 0.40 to 4.27 mg/l F have been measured in the Maheshwaram catchment (figure 3-10) (Sreedevi et al., 2006). Other research has measured F concentrations from 0.44 to 1.88 mg/l (Purushotham et al., 2010) and from 0.39 to 4.67 mg/l (Atal, 2008). High groundwater F concentrations are

associated with high pH and oversaturation with respect to calcite (Sreedevi et al., 2006).

The principal source of F in groundwater is thought to be mineralogical. Research into the mineralogy of the fractured bedrock and the saprolite would provide important information as to the source and mobilisation of F in groundwaters.

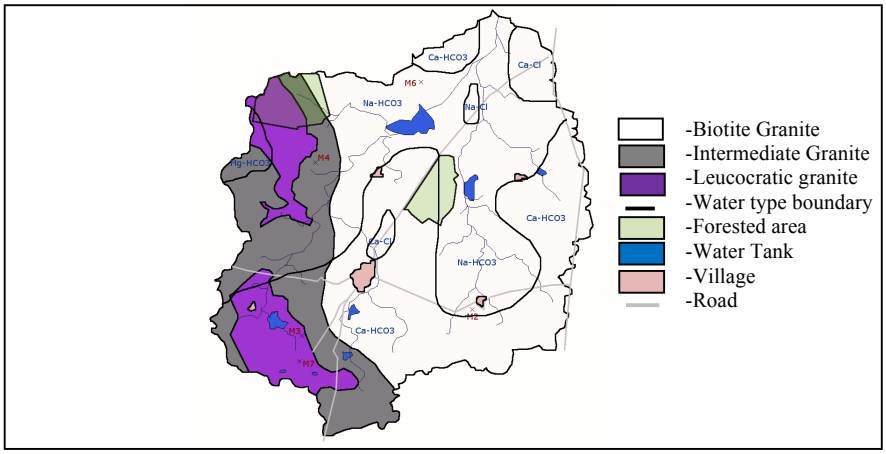

Figure 3-9 – Water chemistry types in the Maheshwaram catchment according to Atal (2008).

Figure 3-10 – Groundwater F values for a) March 2006 (pre-monsoon) and b) January 2006 (post-monsoon) from Sreedevi, (2006). Blue dots indicate groundwater F values 0 - 1.5 mg/l, dark red dots 1.6 - 4.0 mg/l and bright red dots 4.1 – 8.0 mg/l.

It has been suggested that groundwater F concentrations vary with season, increasing after the monsoon (by Sreedevi et al., 2006), although such variations are only seen in

a small proportion of the sites investigated, with many wells showing no variation. Proposed causes of both spatial and seasonal variations include the precipitation of F rich salts in the top layers of the soils and the application of fertilisers with a high F content, which are then leached during the monsoon. Measurements of F in fertilisers show a maximum yield of 0.34 mg/l upon leaching (Sreedevi et al., 2006).

3.3.1 Field Observations - Maheshwaram

The Maheshwaram catchment is flat with occasional rock outcrops forming small hills (figure 3-11). Several large diameter dug wells are located throughout the catchment, most of which are dry, although some still contain water (figure 3-12). Large tanks (figure 3-13) used to store water after the monsoon are located in the south west and north east of the catchment. There are several small villages; the main village being Maheshwaram village (figure 3-13).

Figure 3-11 - Some typical views of Maheshwaram showing the flat landscape. Photos taken in the dry season (June).

Figure 3-12 - Large dug-well containing water. Sides are re-enforced, and steps allow access. Photo taken pre-monsoon (July), water level rises to the water mark during the wet season.

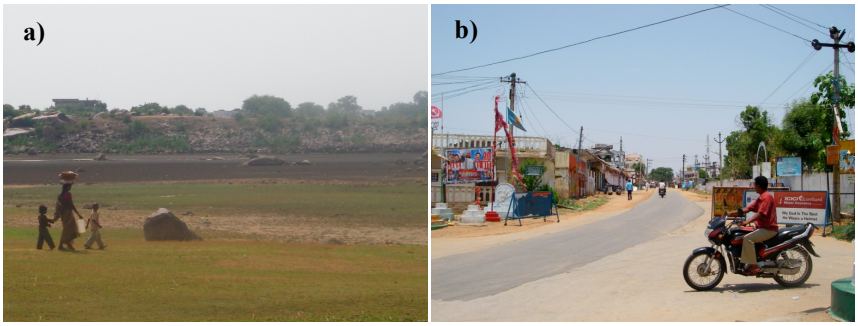

Figure 3-13 - a) Dry tank (dark brown area in background) b) Maheshwaram town centre.

The principal rock types observed are pink and grey gneissic granite. In several locations epidote and pegmatite veins are seen, as well as a gneissic texture. Dolerite dykes are seen cutting across the catchment, as is a quartz vein (figure 3-14 and figure 3-15). The main land use is farming, with much of the area irrigated to form paddy fields (figure 3-16).


Figure 3-14 - Site of Quartz vein, East Maheshwaram.

Figure 3-15 – a) epidote veins in granite with coin for scale b) outcrop in Maheshwaram.

Figure 3-16 – Farming in Maheshwaram, including paddy fields irrigated by groundwater.

3.4 The Wailpally Catchment – Nalgonda District

The Wailpally catchment (~130km^2) is located approximately 70km south east from Hyderabad, in the Nalgonda District, an area known for high fluoride groundwaters. Fluorosis in Nalgonda has been reported since the 1950s (Siddiqui, 1955), and more recently by Khandare et al. (2007), with poor nutrition and low Ca intake enhancing the effects. The area has given its name to a defluoridation technique, the Nalgonda technique, still used in some areas today. The Sai Oral Health foundation has been working in this area since 1989 with domestic de-fluoridators and rainwater harvesting (Narayana et al., 2003).

The climate is semi-arid to arid, with temperatures ranging from 11-42˚C and an average annual rainfall of 632mm/year, most of which falls in the monsoon season (June to September). Rainfall can vary widely, from drought years of ~400mm/year, to high rainfall years of ~1000mm/year. The average potential evapotranspiration is high (Dhakate et al., 2008; Reddy D. et al., 2010).

The west of the catchment is made up of denudation hills and mixed jungle cover, which flattens out in the east to form a plain. The elevation is generally 400m above mean sea level (amsl) in the west, decreasing to 280m amsl in the east (Dhakate et al., 2008).

The catchment's main stream is the Wailpally Vagu, which runs from west to east through the centre of the catchment, terminating at the irrigation tank at Yelmakanna

(Reddy D. et al., 2010). Groundwater is the main source of drinking water and irrigation. Many surface water reservoirs (tanks) are also present (figure 3-17). The area has a large number of paddy fields, which require large amounts of irrigation, as well as areas of cattle grazing and brick making (Reddy D. et al., 2010).

The catchment is underlain by a granite gneiss complex, similar to that seen in the Maheshwaram catchment (figure 3-17). This is divided into pink granite (common), grey granite (confined to local areas), porphyritic granite/gneiss and migmatitic granites. The younger intrusions are of pink granite (Dhakate et al., 2008; Reddy D. et al., 2010). Common minerals include orthoclase feldspar, plagioclase feldspar, quartz, muscovite, biotite and hornblendes. The porphyritic and pink granite is thought to contain more F-bearing minerals than the other rock types present, including fluorite (Reddy D. et al., 2010). Veins of quartz and epidote are also common, as well as deposits of calcrete both at the surface and also at depth in dug-wells. Dolerite dykes trend east-west and northeast-southwest, cutting across the granites and influencing groundwater movement (Dhakate et al., 2008).

Figure 3-17 - Map of the Wailpally catchment (adapted from Dhakate et al., 2008).

Table 3-2 shows whole rock F measurements of rocks in Nalgonda (Natarajan and Mohan Rao, 1974). On average, the porphyritic granites contain the highest F content (average 3300 ppm F) and the grey and pink granites the lowest (average 250 ppm F). Whole rock F measured by Reddy D. et al. (2010) in Wailpally give values of

between 242-990 ppm (measured by XRF). Calcrete is also found to contain between 440-1160 ppm F (Reddy D. et al, 2010).

The weathering profile is 30-40m thick in the west, reducing to less than 10m thick in the east (figure 3-18). This is due to a high density of fractures and fissures in the west allowing greater weathering, as well as accumulation of deposits due to the hilly terrain (Reddy D. et al., 2010). The weathering profile is similar to that described in section 3.2. The major soil types are red soil (derived from weathering of pink granite), loamy soil and sandy soil and a few patches of black soil (from weathering of grey granite) (Dhakate et al., 2008). Soils in the east are generally alkaline, formed due to high evaporation rates and a historic shallow water table (Reddy D. et al., 2010).

Table 3-2 - Fluoride concentrations of rocks in Nalgonda (Natarajan and Mohan Rao 1974).

Rock Type	**F content of the whole rock (ppm)**		
	Min	**max**	**Ave**
Grey Granite gneiss	250	900	600
Grey granite	250	2,500	400
Grey and pink granites	250	400	250
Pink granites	250	1,500	600
Porphyritic granites	600	5,300	3,300
Quartz Veins	250	1,500	500
Epidote veins	400		
Quartzo-feldspathic and pegmatoid rocks	2,500	1,200	600
Aplites	300		
Biotite schist and biotite rick inclusions in grey granite gneiss	250		
Dolerites	250		

Figure 3-18 - Weathering thickness across Wailpally catchment (Dhakate et al. 2008).

Groundwater in Wailpally catchment is semi-confined to unconfined and located in the fractured and fissured granite bedrock and weathered saprolite above. The majority of recharge occurs in the western area in the hills, primarily through vertical fractures, and the general trend of groundwater flow is from the west to the east, with an average gradient of between 7.5 and 9 m/km (Reddy et al., 2009). Significant lateral groundwater movement is thought to occur from west to east with groundwater movement also affected by the presence of dykes (Dhakate et al., 2008; Reddy D. et al., 2010).

The hydraulic characteristics of the aquifer are controlled by the presence of fractures and fissures, and are influenced by the characteristics and thickness of the weathered zone. Pink granites are thought to have greater groundwater potential and storage as the minerals present impart a higher porosity and permeability, whereas mafic minerals of grey granites do not (Dhakate et al., 2008). Groundwater potential varies with fracture and fissure density and weathering profile thickness. Water scarcity and water quality are problems in the catchment. Dhakate et al. (2006) produced a groundwater potential map based on the thickness of the weathered zone and the density of lineaments (figure 3-19).

The groundwater has an average pH of 7.7 (range 6.6-8.9) and temperature of 30 ˚C. Reddy D. et al. (2010) divided the catchment into 4 zones, from west to east, with varying chemical and physical parameters (e.g. decrease in Ca from west to east from 27 to 8 mg/l). Groundwater is saturated with respect to calcite and dolomite in most cases, and under-saturated with respect to fluorite (Reddy D. et al 2010).

Figure 3-19- Wailpally groundwater potential map (Dhakate et al. 2008).

Reddy D. et al. (2010) measured groundwater [F^-] between 0.97 and 5.83 mg/l in Wailpally catchment, with groundwaters saturated with respect to calcite and under-saturated with respect to fluorite (figure 3-20) . A similar study by Reddy, A. et al. (2010) measured groundwater F values of between 0.5 and 7.6 mg/l with an average of 2.88mg/l in the hilly region, 3.26 mg/l in the plains and 4.60 mg/l in the discharge area. The highest groundwater F concentration in this study was measured near Wailpally village.

Figure 3-20- Map of Wailpally with groundwater F values, pre-monsoon 2004-2005 adapted from Reddy D. et al. (2010). Blue dots indicate groundwater F values 0 - 1.5 mg/l, dark red dots 1.6 - 4.0 mg/l and bright red dots 4.1 – 8.0 mg/l. Wailpally map also shows geology and water-table contours (modified from Dhakate et al., 2008; Reddy D. et al., 2010).

The source of F in groundwater is due to minerals with high F content present in many of the rocks in the area (e.g. fluorite (Natarajan and Mohan Rao, 1974)), with variations thought to be due to dilution by surface water tanks and recharged water (Reddy D. et al., 2010). Reddy D. et al. (2010) found no correlation between F and HCO_3, Na, Ca or within the groundwater 'zones', except for areas with low F, where correlation was found between Mg and HCO_3. There was also little/no correlation between F concentrations and topography, gradient or weathered thickness zone.

3.4.1 Field Observations - Wailpally

Low hills are present in the west, flattening out to a plain in the east (figure 3-21). The main town is Wailpally town, with several smaller villages and numerous farms located in the catchment. In Antampet (a large town south of the Wailpally catchment), structures installed by the Sai Oral Health Foundation exist (figure 3-22), indicating that fluorosis is a problem in this area.

There are many dug-wells, most of which are dry and have been replaced by pumped tube-wells (figure 3-23). Much of the area is farmed either for cattle grazing or as paddy fields, requiring large amounts of groundwater (figure 3-24). Locals are advised to drink water pumped from a reservoir near Hyderabad rather than the local groundwater due to high F concentrations (pers. comm. local resident).

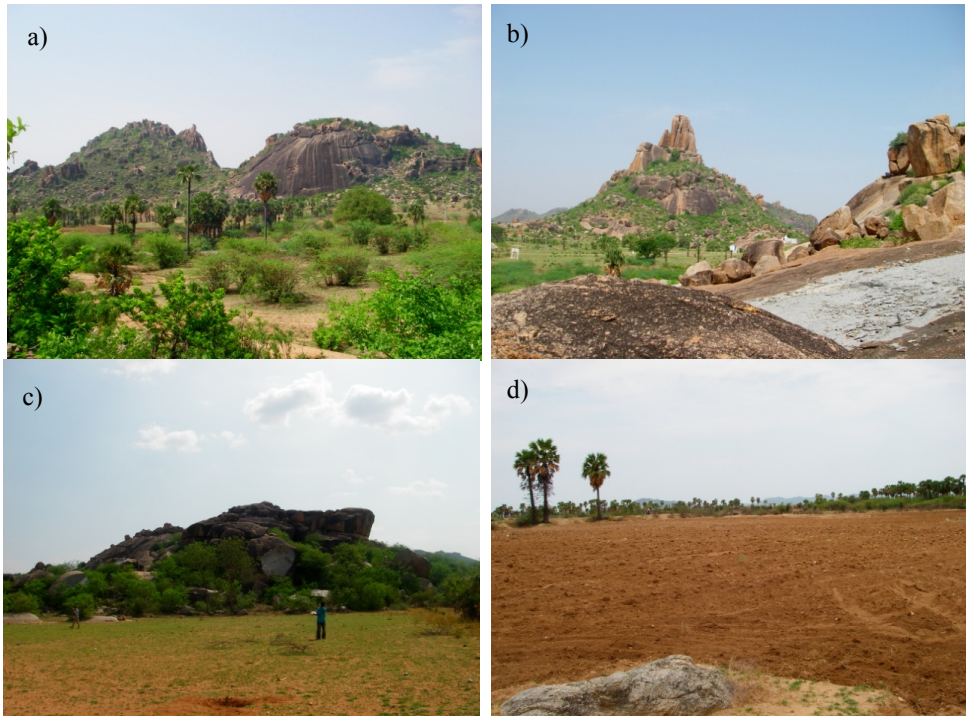

Figure 3-21- a) and b) Hills in the south west of the Wailpally catchment c) Small hills in the central west d) plain in the east of Wailpally with common red soils.

Figure 3-22- Sai Oral Health Foundation Rainwater harvesting structures in Antampet.

Figure 3-23- a) Recent excavation of a large diameter dug-well b) A local farmer and recent tube-well.

Figure 3-24- a) Paddy field with man with possible skeletal fluorosis in west Wailpally b) Paddy field in north of Wailpally.

The geology of the area is spatially variable. The main rock types of the area are granite gneiss, grey granite, and porphyritic granite, with some pegmatites and dolerite dykes. In many locations epidote and pegmatite veins are seen (figure 3-25). Flow banding was noted in two locations as well as large variations in granite colour (and composition) within a single outcrop (figure 3-26).

In many locations calcrete was seen, both as crusts and nodules on the surface and also as layers at depth in the profile (figure 3-27).

Figure 3-25- a) Epidote veins in porphyritic granite b) Thin pegmatite vein in porphyritic granite c) Thick pegmatites vein in finer grained equigranular granite.

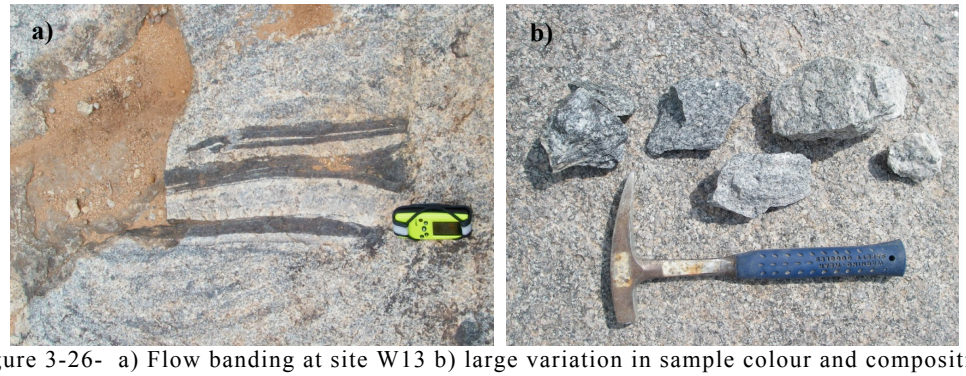

Figure 3-26- a) Flow banding at site W13 b) large variation in sample colour and composition collected from one outcrop. Samples range from very dark (left) to very light (right).

Figure 3-27- a) & b) Calcrete layers within the weathering profile c) Calcrete crust on the surface.

Chapter 4. Mineralogy of Fluoride Occurrence in two Catchments

4.1 Introduction

Paired samples of fresh bedrock and regolith collected from sites across the Maheshwaram and Wailpally catchments (chapter 3) were investigated using a variety of analytical techniques. The results are described in this chapter and have been interpreted as a mass balance of fluorine in the bedrock and regolith and through the weathering profile in chapter 5.

The primary objective of this chapter is to determine the mineralogical sources and distribution of F in the bedrock and regolith of the Maheshwaram and Wailpally catchments. Each F-bearing mineral is a potential source of F^- to groundwater as a consequence of weathering. The two catchments have a similar gneissic granite bedrock geology yet contrasting levels of groundwater F^-. Ultimately, the F^- content of groundwater reflects the weathering flux of F from its primary and secondary mineralogical sources. The mineralogical investigation aims to seek an explanation for the contrasting groundwater F-flux.

4.2 Sample collection

Samples collected and their locations are described in table 4-1 and table 4-2, and are illustrated in figure 4-1 and figure 4-2.

Rock samples were collected from the Maheshwaram and Wailpally catchments during 2008-2009. Locations for collection were chosen so as to ensure a representative spread of samples – both spatially and compositionally. At each location, fresh and weathered samples were taken of between 500-1500g. Samples were collected from dug wells and/or rock outcrops, stored in plastic bags and labelled for transportation back to UCL.

In total, fourteen paired samples of fresh and weathered rock from the Maheshwaram catchment were collected by Dr. W. Burgess (Earth Sciences, UCL) in March 2008 and twenty nine paired samples of fresh and weathered rock from the Wailpally catchment were collected in June 2009.

The Maheshwaram catchment has previously been mapped as exhibiting three gneissic granite lithologies (figure 4-1). The biotite granite covers the majority of the catchment (approximately 70%) and is here represented by samples at site M2. The leucocratic granite covers two small areas in the west of the catchment (approximately 10%), and is represented by samples at M3 and M7. The 'Intermediate' granite consists of biotite granite with pegmatite and leucogranite dykes and makes up the remaining area of the catchment. Sample site M4 is in this area. Sample M6 (epidote chlorite granodiorite) was also taken from the biotite granite area, however the M6 lithology is thought to have limited occurrence in the catchment.

The Wailpally catchment consists predominantly of pink and grey granites (represented by samples at sites W11, W14 and W16), with porphyritic granites in the western hill region (represented by samples W1 and W2). Samples of pegmatite (W17a), calcrete (W-C) and mafic vein material (W13) were also collected.

At one location in each catchment a number of samples were taken through a regolith depth profile (June 2009) where an accessible dug-well allowed safe access. These are discussed in chapter 5, section 5.2.

Table 4-1 - Samples collected from Maheshwaram in March 2008. a: fresh bedrock, b, c and following: regolith. Where thin sections are made, sample mass given is that left after thin section production. TS=thin section made, EM=electron microprobe, WRF=whole rock fluorine, WRC=whole rock chemistry, XRD=X-ray diffraction, BL=batch leaching.

Sample	Location (decimal degrees)	Description	Comments	Mass	Sample Analysis	Illustrative Figure
M2a	Lat: 17.12707 Long: 78.45295	Biotite Granite (porphyritic). From adjacent to dug well	Fresh	390g	TS, EM, WRF, WRC, XRD, BL	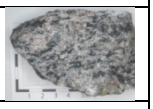
M2b		Weathered biotite granite. From dug well, ~10m depth	Weathered throughout	740g	TS, EM, WRF, WRC, XRD, BL	
M2c		Red sandy saprolite. From dug well, 2m depth.	Weathered throughout	~500g	none	
M2d		Weathered biotite granite. From Dug well ~3m depth	Weathered saprolite with red mineral deposits	540g	TS, EM	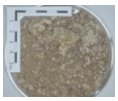
M2 Profile		Samples taken every 0.5m with depth in dug well. Total depth of profile =10.5m.	Various degrees of weathering	~500g each	WRF, WRC, BL	
M3a	Lat: 17.12073 Long: 78.42362	Pink Granite (fine grained). From adjacent to dug-well with artificial recharge	Fresh	800g	TS, EM, WRF, WRC, XRD, BL	
M3b		Weathered saprolite. From within a dug well ~2m depth	Weathered throughout	110g	TS, EM, WRF, WRC, XRD, BL	
M3c		Weathered/sandy saprolite. From dug well ~1m depth	Weathered extensively throughout	600g	none	
M4a	Lat: 17.15671 Long: 78.41321	Grey amphibole granite (med). From adjacent to a dug well	Fresh	1000g	TS, EM, WRC, WRF	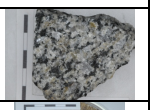
M4b		Weathered saprolite. From within dug well	Weathered	500g	TS, EM, WRF, WRC, XRD	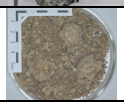
M6a	Lat: 17.16886 Long: 78.47483	Porphyritic pink/green granite (outcrop sample)	Fresh	390g	TS, EM	
M7a	Lat:17.1196 Long:78.4237	Grey granite (fine grained). Leucocratic (outcrop sample)	Localised weathering. Fresh inner	400g	TS, EM, WRF, WRC, XRD, BL	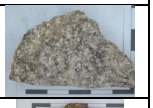
M7b		Weathered saprolite. (no associated depth)	Weathered throughout	600g	TS, EM, WRF, WRC, XRD, BL	
M7c		Weathering crust. (from outcrop)	Weathering crust	150g	TS, EM	

Table 4-2- Summary of Wailpally samples collected. a: fresh bedrock, b, c and following: regolith. Where thin sections are made, sample mass given is that left after thin section production. Sample Analysis includes: TS=thin section made, EM=electron microprobe, WRF=whole rock fluorine, WRC=whole rock chemistry, XRD=X-ray diffraction, BL=batch leaching.

Sample	Location (decimal degrees)	Description	Comments	Mass	Sample Analysis	Illustrative Figure
W1a	Lat: 16.98264 Long: 78.88651	Porphyritic granite (outcrop sample)	Fresh to slightly weathered	500g	TS, EM, BL, WRC, WRF	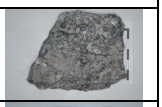
W1b		Porphyritic granite (outcrop sample)	Weathered throughout	450g	TS, EM, BL, WRC, WRF	
W2a	Lat: 16.98264 Long: 78.88651	Porphyritic granite. Collected from outcrop	Fresh	570g	TS, EM	
W2b		Porphyritic granite (outcrop sample)	Localised weathering.	600g	TS, EM	
W2c		Porphyritic granite (outcrop sample)	Weathered throughout	520g	TS, EM	
W11a	Lat: 17.09859 Long: 78.99648	Pink Granite. Collected from dug well. (phaneritic hornblende granodiorite)	Fresh with some light weathering	800g	TS, EM, BL, WRC, WRF	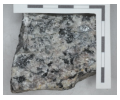
W11 Profile		Samples taken every 1m with depth in dug well. Total depth of profile =6m	Range of weathering	~500g each	BL, WRC, WRF	
W14a	Lat: 17.06751 Long: 78.90794	Pink-Grey granite. (outcrop sample)	Fresh with light weathering	600g	TS, EM	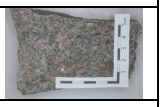
W14b		Weathered sample (outcrop sample)	Weathered throughout.	600g	TS, EM	
W16a	Lat: 17.05814 Long: 78.88583	Grey granite. From outcrop near sample 15. (phaneritic biotite granite)	Fresh	600g	TS, EM, BL, WRC, WRF	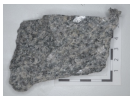
W16b	Lat: 17.05297 Long: 78.88582	Grey granite. From adjacent to dug well	Weathered throughout		TS, EM, BL, WRC, WRF	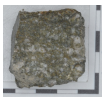
W17a	Lat: 17.13254 Long: 78.89143	Pink Granite pegmatite. From adjacent to Dug well	Fresh	700g	TS, EM, BL, WRC, WRF	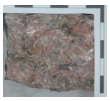
W17b		From adjacent to dug well	Weathered	400g	TS, EM, BL, WRC, WRF	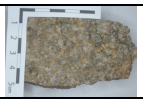
W13	Lat: 17.10071 Long: 78.98107	Mafic vein material within granite (outcrop sample)	Fresh	162g	TS, EM, BL, WRC, WRF	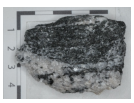
W-C	Lat: 17.10071 Long: 78.98107	Calcrete. From ground surface	Fresh	250g	TS, EM, BL, WRC, WRF	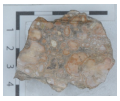

Figure 4-1 – Geology of Maheshwaram and sample locations. Sample locations include fresh (a) and weathered (b,c,d etc) samples. Geology adapted from Sreedevi et al. (2006)

Figure 4-2 – Sample locations and geology of Wailpally. Sample locations 1 and 2 are south of Antampet (not on map). Sample locations include fresh (a) and weathered (b,c,d etc) samples unless otherwise stated. Geology from Dhakate et al., (2008)

4.3 Analytical Methodology

The following methods were applied:

- Optical petrology and point counting
- X-Ray Diffraction (XRD)
- Electron Microscopy (EM):
    - With Electron Backscatter Detection (EBSD)
    - With Energy Dispersive X-ray (EDX) detection for elemental point-analysis and mapping at individual crystal scale
- Whole-rock chemical analysis:
    - Using the Ingram (1970) method for F
    - Using lithium metaborate fusion method for major ions

These methods were used to determine rock sample F content and the principal F-bearing minerals present, as well to investigate differences between fresh rock samples and their weathered equivalents. Samples were first prepared into thin sections and their petrology described and quantified through point counting. Potential F-bearing minerals were identified for further analysis through EM, involving element point analysis, and thus individual mineral fluorine content.

XRD analysis gives an overview of the sample mineralogy, as well as identifying the changes between fresh rock samples and their weathered equivalents. The bulk whole rock chemistry of each sample can also be used for comparison between fresh and weathered rock samples.

Full details of the methods are provided in appendix 2.

4.3.1 Optical Microscopy and Point Counting

Each sample was prepared into one or two covered thin sections. An optical microscope in plane polarised and cross polarised light was used to identify the

minerals present and to characterise the sample mineralogy. Potential F-bearing minerals were identified.

A point counting device was used to estimate percentage occurrence of F-bearing minerals and to assist classification according to the International Union of Geological Sciences (IUGS) igneous rock classification (figure 4-3)

Figure 4-3- IUGS double triangle showing root names for igneous rocks. A=alkali feldspar, P=plagioclase feldspar, Q=quartz, F=feldspathoids. If one or more mafic mineral is present as more than 5%, this mineral is added as a forename of the rock, in order of increasing percentage. Important minerals present in less than 5% are added as 'x-bearing'.

4.3.2 X-Ray Diffraction (XRD)

X-Ray Diffraction (XRD) is used to identify the principal minerals present in a sample, allowing comparison of fresh and weathered samples. The UCL PANalytical X'pert PRO MPD high resolution powder diffractometer was used. Incoming monochromatic X-rays are directed at a sample powdered to <65µm, with random crystal orientation. The X-rays are diffracted by the mineral structures and detected using electronic counters. X-rays will only be diffracted by a mineral if Braggs' law

is satisfied. As the sample is powdered and in random orientation, there should be some crystals from each mineral in the correct orientation to satisfy Braggs' law (Putnis, 1992). The intensity of X-rays detected at each angle of 2Θ is plotted in a diffraction pattern, with intensity relating to abundance and 2Θ related to d-spacing which is characteristic of specific minerals. Each mineral will produce a series of peaks in the diffraction pattern. The peaks are analysed by software that uses the ICDD database for mineral phase identification. A semi-quantitative mineral abundance of the main minerals identified is calculated from the diffraction pattern.

Detection is more difficult if a large number of minerals are present, as some mineral diffraction patterns may be masked by more abundant minerals. In this case the resultant diffraction pattern gives only an approximate abundance of the main minerals present and provides a method of comparison of fresh and weathered samples.

Clay minerals can be identified by separation and alignment prior to XRD analysis.

4.3.3 Electron Microscopy (EM)

Each sample was prepared into one uncovered thin section for use with EM.

In EM, an incident electron beam is directed at the surface of the sample. The interaction between the electron beam and the sample causes the backscattering of electrons from the surface, the detection of which is known as electron backscatter detection (EM-EBSD). The interaction of the primary electron beam and the sample also causes the emission of X-rays which are detected by an energy dispersive system (known as EM-EDX).

The image of the sample produced by EM-EBSD can be used to identify minerals according to the image brightness, determined by the atomic number of the elements present, and features, such as cleavage, that are evident. The energy spectrum of backscattered electrons from specific points on the sample also gives an approximate chemical analysis and so also allows for mineral identification. Unfortunately, EM-

EBSD spectral overlap causes interference between F and Fe (A. Beard, pers. comm.).

The chemical composition of the surface of the sample can also be analysed by individual element using the X-rays emitted using EM-EDX. This is more time consuming but allows the measurement of any element (including F) without overlap or interference. Point analysis using EM-EDX produces a point composition to assist mineral identification and to give the mass percentage F content. Element mapping over an area may also be done (Reed, 1996).

Minerals were identified using EM-EBSD then further analysed in EM-EDX for point analysis and element mapping.

EM-EDX point analysis was used to quantify the average and range of F content of minerals in the rock samples (detection limit for fluoride of 0.05 mass %). The precision of the instrument for fluorine analysis is ±0.12 (this is the standard deviation of F measurement from a standard apatite measured 74 times).

4.3.4 Whole Rock Chemical Analysis – Fluoride

The Whole Rock Fluorine (WRF) content was measured using the Ingram (1970) method and an F Ion Selective Electrode (ISE). The method was modified for use with the samples and equipment available. The method involves 0.2g of powdered sample, 1g sodium carbonate and 0.2g zinc oxide, heated to 950 ˚C for 1.5 hours in a platinum crucible. The crucible with sample is allowed to cool, placed in a beaker filled with water and then placed in a steam bath to digest for 12 hours. This is then filtered, washed down with 0.1 $NaCO_3$ solution, acidified with 2ml 50% HCl and made up to 200ml with deionised water. A 10ml portion of this solution is combined with the same volume of TISAB buffer and measured using the ISE, calibrated to a set of fluorine standards ranging from 0.25 to 10 mg/l F. The ISE was calibrated after every 12 samples measured, and in some cases more frequently than this to check for measurement drift. Where possible repeat samples were prepared. All ISE measurements were repeated. Further details are given in appendix 2.

The results are used to compare total F content between rock samples, between fresh rocks and their weathered equivalents and to combine with other mineralogical investigations (optical, point counting and EM) in determining the distribution and mass balance of F.

4.3.5 Whole Rock Chemical Analysis – Major Ions

The bulk chemistry of the majority of samples was analysed. The sample is powdered and mixed with a lithium metaborate ($LiBO_2$) flux, which is then heated and fused together. This is then dissolved in nitric acid (HNO_3), diluted, and the elements determined using ICP-AES. The required sample: flux ratio should be 1:3 and the final dilution factor should be 1:2500 (see appendix 2 for method details). Analysis of Whole Rock Chemistry (WRC) was carried out at the Natural History Museum, London. This method is effective in dissolving major elements in silicate rocks, although some minerals such as zircon and some metal oxides may not be digested fully (Cremer and Schlocker, 1976). This method is also not suitable for fluorine determination due to the high dilution factors involved in preparation (resulting in fluorine concentrations that are too low for detection) and the poor sensitivity for determination of fluorine by ICP techniques (C. Unsworth, pers. comm.).

4.4 Sample Petrology - Results

Results of optical microscopy and mineral point counting are summarised in table 4-3. The majority of the samples collected are granites. Two non-granite samples were also collected from the Wailpally catchment – one calcrete and one of mafic vein material from a granite outcrop. The granite samples all contained quartz, alkali-feldspar (usually microcline and sometimes orthoclase) and plagioclase feldspar (often with albite twinning, and variable alteration to sericite). Microperthite (the intergrowth of Na rich feldspars in alkali feldspars) is also commonly seen. Compositions range from quartz syenite (a higher proportion of the feldspars are alkali-feldspars) to granodiorite (a higher proportion are plagioclase feldspars). Observations from hand specimen, optical microscope and EM analysis, including textures, relationships between minerals, and identification of potentially F-bearing minerals, are given below.

4.4.1 Point counting

Point counting results of both Maheshwaram and Wailpally rocks, as well as their classification according to the IUGS igneous rock classification scheme are shown in table 4-3. Maheshwaram porphyritic samples are classed as granodiorites (higher proportion of plagioclase feldspar), whereas the medium to fine grained samples are monzogranites (higher proportion of alkali-feldspar). In Wailpally, the medium to fine grained samples are granodiorites, and the porphyritic samples are either monzogranites or granodiorites.

Table 4-3 – Point counting results from Maheshwaram and Wailpally shown in percentages. *Where a mineral is seen but not counted, a value of half of the lower resolution is given. F/W = Fresh or Weathered. Classification according to IUGS scheme, with Po=Porphyritic, Peg=Pegmatite. C=Chlorite, B=Biotite, Fe=Iron oxide, A=Amphibole, Ca=Calcite, E=Epidote. GD=Granodiorite, SG=Syenogranite, MG=Monzogranite, QS=Quartz Syenite. Sample WP 13 is mafic vein material.

	M2a	M2b	M2d	M3a	M3b	M4a	M4b	M7a	M7b	M7c	M6a	W1a	W1b	W2a	W2b	W2c	W16 a	W16 b	W14 a	W14 b	W11 a	W17 a	W17 x	W 13	W-C
F/W:	F	W	W	F	W	F	W	F	W	W	F	F	W	F	W	W	F	W	F	W	F	F	W	F	W
Classification:	C/B GD			MG		A MG		MG			Po E/C GD	Po C MG		Po E GD			B GD		GD		A GD	Peg QS	E QS	-	-
Quartz	21.4	17.9	39.7	28.1	36.3	18.9	9.3	40.4	30.3	37.9	51.0	14.4	31.4	36.1	49.3	31.2	29.8	21.4	35.5	29.7	14.7	7.7	5.0	13.2	1.5
Microper-thite	0.2			4.3	1.6	3.7		21.6	0.6		4.1	14.5	0.7	6.5		2.1	19.6	0.1	15.2	1.0	1.0	2.9			
Plagiocla-se	31.5	19.3	28.7	31.4	27.7	31.6	21.3	15.7	27.7	8.4	22.7	29.4	40.0	25.2	21.0	36.5	31.1	43.7	32.0	29.6	44.2	12.7	53.3	5.3	2.8
K-Feldspar	13.6	47.7	14.8	30.2	25.8	32.2	11.9	17.3	31.4	32.4	4.1	32.6	23.5	11.8	16.8	19.1	10.7	27.8	12.9	34.3	18.4	71.8	20.7	18.8	1.6
Apatite	1.2	0.3	0.1	0.2		0.3		0.05*	0.4		0.1	0.9	0.2	0.5	0.5	0.5	0.6	0.2		0.1	0.2		0.3	0.9	0.1
Biotite	24.0	7.4	4.3	1.5	3.1	3.4	0.8	1.3	3.4	0.4	2.4		2.3	1.2	2.5	5.6	4.9	2.1	1.6	2.4		0.03*	2.8	23.6	0.05*
Chlorite	4.7	1.6		1.7		0.8		0.1	0.3	0.5	8.4	5.3		9.0	3.8	1.8	1.6	0.7	1.0	0.8	1.1	0.1	1.7		0.05*
Iron Oxide	0.6	4.2	11.8	1.9	2.9		11.7	3.3	4.7	20.2	1.6	0.5	0.5	0.2	2.0	1.6	0.6	3.9	0.6	1.1	0.2	0.3	0.3		0.1
Titanite	0.2	0.4	0.05*	0.02*		0.2		0.05*			0.4	1.9	0.4	2.6	2.0	0.3		0.05*	0.6	0.2	0.2		0.7		0.05*
Epidote	2.0	0.7	0.6	0.2	0.1	0.9	0.4	0.3	1.1	0.3	5.0	0.4	0.9	5.5	1.8	1.2	0.7	0.1	0.6	0.6	0.7	4.6	14.4	1.0	
Epidote var2				0.2		0.7							0.1	1.4			0.5	0.1			0.5				
Amphibo-le						7.4															18.7			37.2	
Fluorite				0.2								0.1							0.05*						
Zircon		0.1			0.1											0.1				0.2			0.8		
Calcite		0.5			2.4		44.6																		91.8
Titanium Phosphate															0.3										
TOTAL	100	100	100	100	100	100	100	100	100	100	100	100	100	100	100	100	100	100	100	100	100	100	100	100	100

4.4.2 Maheshwaram samples

Figure 4-1 is reproduced as figure 4-4 below for ease of reference of sample locations.

Figure 4-4 – Geology of Maheshwaram and sample locations. Sample locations include fresh (a) and weathered (b,c,d etc) samples. Geology adapted from (Sreedevi et al., 2006)

M2 Samples – Porphyritic Biotite Granodiorite

M2 samples were collected from within and adjacent to a dug-well. Figure 4-5 and figure 4-6 show the samples and their locations. Photomicrographs are illustrated in figure 4-7 to figure 4-9.

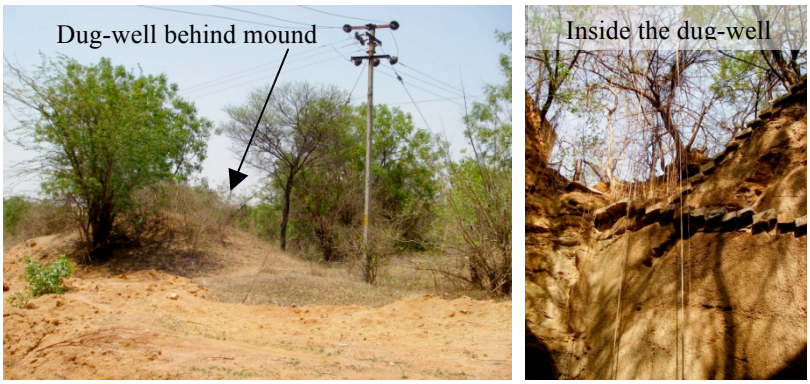

Figure 4-5 – Dug-well from which samples M2b and M2c were taken

Figure 4-6 – Samples collected from location M2.

Sample M2a is a porphyritic fresh rock sample collected from adjacent to the dug well. The sample has microphenocrysts of feldspar (0.5-1.5 cm) and a smaller mass of quartz, biotite, chlorite, epidote, zircon, titanite and apatite (figure 4-7). The sample has a gneissic texture (figure 4-6) and shows foliation in thin section (figure 4-8). Many of the plagioclase feldspars show sericite alteration. Titanite is present as small crystals, a secondary mineral associated with biotite. According to the IUGS Igneous rock classification scheme and point counting this sample is a biotite granodiorite (see table 4-3).

Sample M2b is a loose and friable weathered rock sample from the dug well at ~10m depth. It is medium to coarse grained and weathered throughout. Feldspars commonly show sieve textures and alteration to sericite, principally at the edges of the grains as well as myrmekite textures. Quartz is present as smaller grains and small biotite crystals are fragmented with iron oxide deposits along cleavages. Apatite, epidote and titanite (identified under EM) are also present in small amounts.

Sample M2d is a strongly weathered sample, loose and friable, from the dug-well with a red colour. Feldspar crystals are large (up to 1cm); quartz crystals are smaller. Biotite is fractured and weathered with irregular shapes. Small amounts of titanite, epidote and apatite are found in association with biotite, as well as iron oxides, titanium oxides, and other heavy metal deposits (identified under EM, source of red colour in hand specimen) (figure 4-9).

Potential F-bearing minerals in these samples include:

- M2a – biotite, chlorite, apatite, titanite, epidote
- M2b – biotite, epidote, apatite, titanite
- M2d – biotite, chlorite, titanite, apatite, epidote

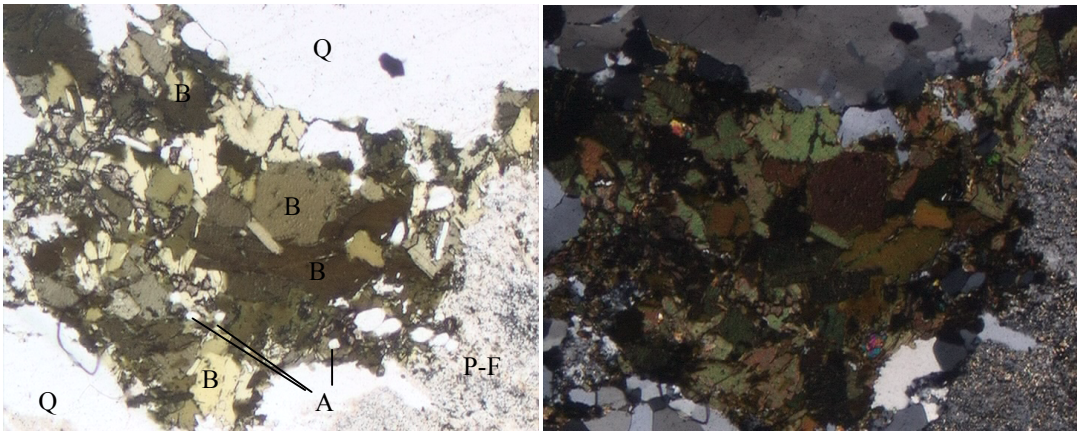

Figure 4-7 - Sample M2a photomicrographs. Plane polarised light (PPL) on left hand side and cross polarised light (XPL) on right hand side. Magnifications x10. Mineralogy: A=apatite, B=biotite mica, MP-F=Microperthitic feldspar, P-F=plagioclase feldspar, Q=Quartz

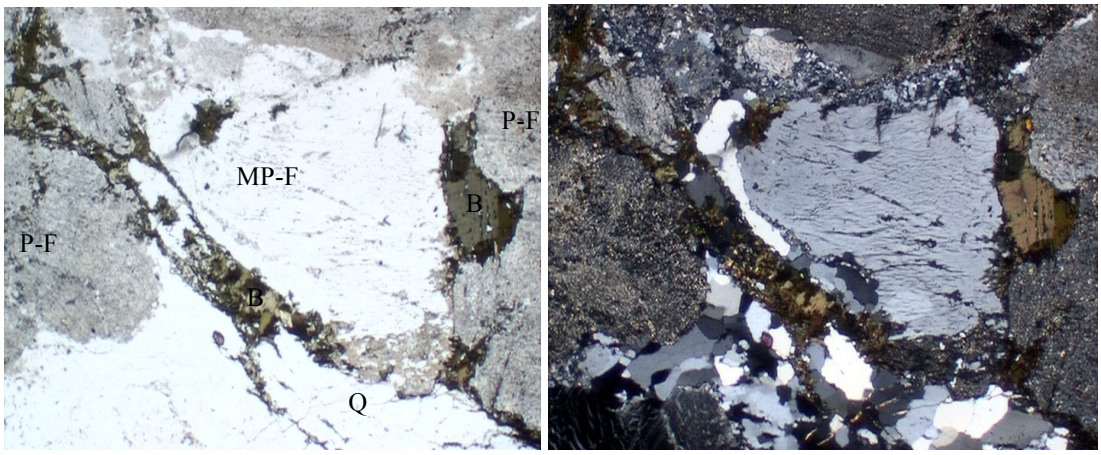

Figure 4-8 - Sample M2a photomicrographs. Plane polarised light (PPL) on left hand side and cross polarised light (XPL) on right hand side. Magnificationsx4. Mineralogy: A=apatite, B=biotite mica, MP-F=Microperthitic feldspar, P-F=plagioclase feldspar, Q=Quartz

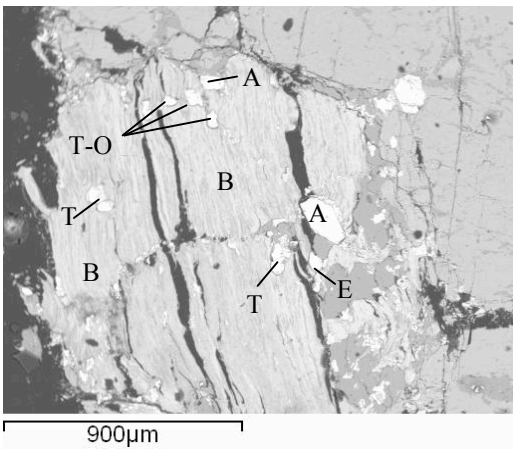

Figure 4-9 Sample M2d – EM-EBSD image. Biotite with apatite, titanite, titanium oxide and epidote. Variation in brightness in the biotite grain showing signs of varying composition. A=apatite, B=biotite, E=epidote, T=titanite, T-O=titanium oxide

M3 Samples – Pink Monzogranite

Samples M3a and M3b were collected from within and adjacent to a dug-well. The location and samples are shown in figure 4-10, and photomicrographs are illustrated in figure 4-11.

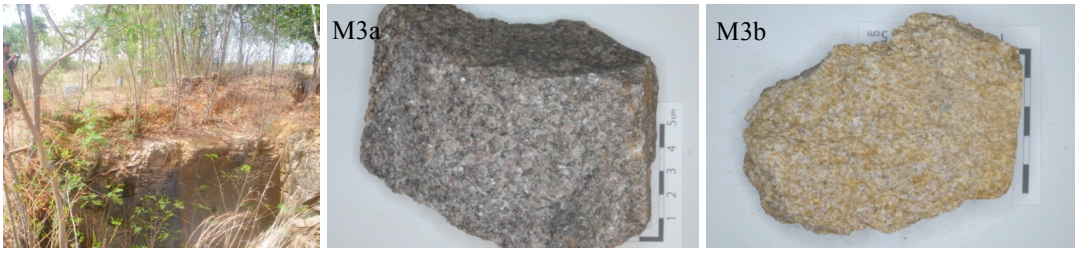

Figure 4-10 - Dug-well from which sample M3b was collected and samples collected

Sample M3a is a fresh rock sample, pink and grey in colour, with a fine-medium grain size (figure 4-10). Feldspars show some alteration as well as myrmekite texture with quartz. Biotite, chlorite, apatite, epidote and fluorite are present (figure 4-11), as well as titanite, formed as an alteration product of biotite. EM identified two varieties of epidote (variety 1 and 2), as well as iron and silver oxides. Variations in biotite composition can be seen across grains indicating weathering and loss of potassium (K). According to the IUGS Igneous rock classification scheme and point counting results this sample is a monzogranite (see table 4-3).

Sample M3b is a weathered sample from the dug-well (at approximately 2m depth). Many of the plagioclase feldspars show alteration (including sericite). Biotite and chlorite crystal remnants are thin and broken along cleavages, often associated with iron oxide deposits (figure 4-11). EM analysis identifies calcite and titanium oxides to be present also but no fluorite.

Potential F-bearing minerals in M3 samples include:

- M3a – biotite, chlorite, apatite, titanite, epidote, epidote var 2, fluorite
- M3b – biotite, chlorite, calcite

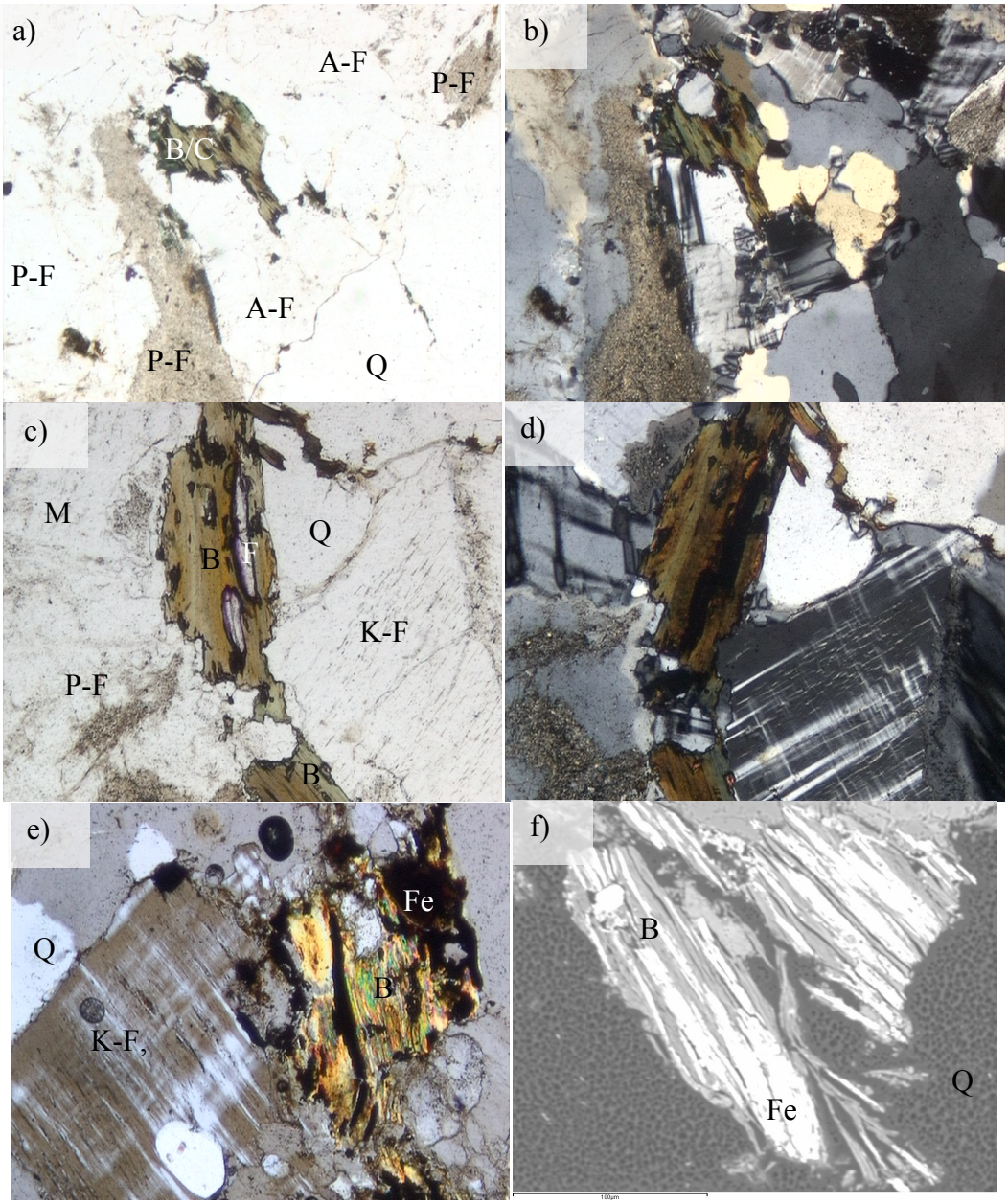

Figure 4-11 - photomicrographs a) M3a, PPL, magnification x4 b) M3a, XPL, magnification x4 c) M3a, PPL, Magnification x10 d) M3a, XPL, magnification x10 e)M3b, XPL, magnification x10 f) M3b, EM-EBSD image, scale bar 100um. B=Biotite, C=Chlorite, F = Fluorite, Fe=iron oxide, K-F=k-Feldspar, M=Microcline, P-F=Plagioclase Feldspar, Q=Quartz.

M4 Samples – Amphibole Monzogranite

Samples M4a and M4b were collected from within and adjacent to a dug-well. Figure 4-12 and figure 4-13 show the samples and collection location. Photomicrographs are illustrated in figure 4-14.

Sample M4a is a fresh rock sample, with medium-coarse grain size (figure 4-12). Feldspars are present as large crystals (0.4-0.8 cm), with smaller quartz, biotite,

amphibole, titanite, apatite, epidote, chlorite and zircon. Many of the amphibole crystals show good examples of twinning (figure 4-14 a&b). Titanite is large (a primary mineral) and shows signs of weathering (figure 4-14 c). EM analysis identifies epidote var 2 to be present (shown in figure 4-14 d). Amphiboles are identified as magnesio-hornblende through EM-EDX point analysis and an amphibole classification spreadsheet (Preston and Smith, 2002). According to the IUGS Igneous rock classification scheme and point counting results this sample is an amphibole monzogranite (see table 4-3).

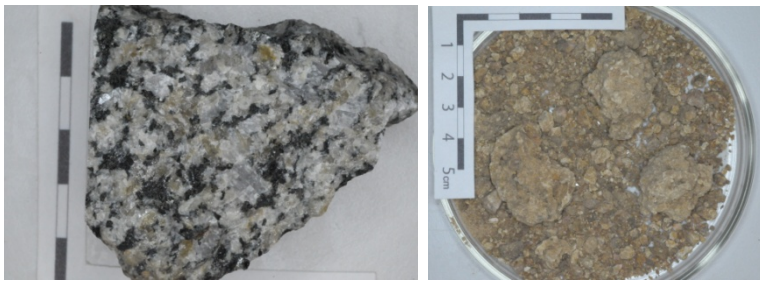

Figure 4-12 - Samples from location M4

Figure 4-13 - Dug-well from which the M4 samples were collected

Sample M4b is a weathered sample with an orange-red colour, and medium-coarse grain size. This sample is highly weathered and is loose and friable. Feldspars are large but mostly fractured and weathered. Most plagioclase feldspars have large areas of alteration, often with Fe oxides present along fractures. An abundance of calcite is present. Small amounts of biotite and epidote are identified in EM analysis (figure 4-14, e&f).

Potentially F-bearing minerals in M4 samples include:

- M4a – biotite, magnesio-hornblende, apatite, titanite, epidote.
- M4b – biotite, epidote

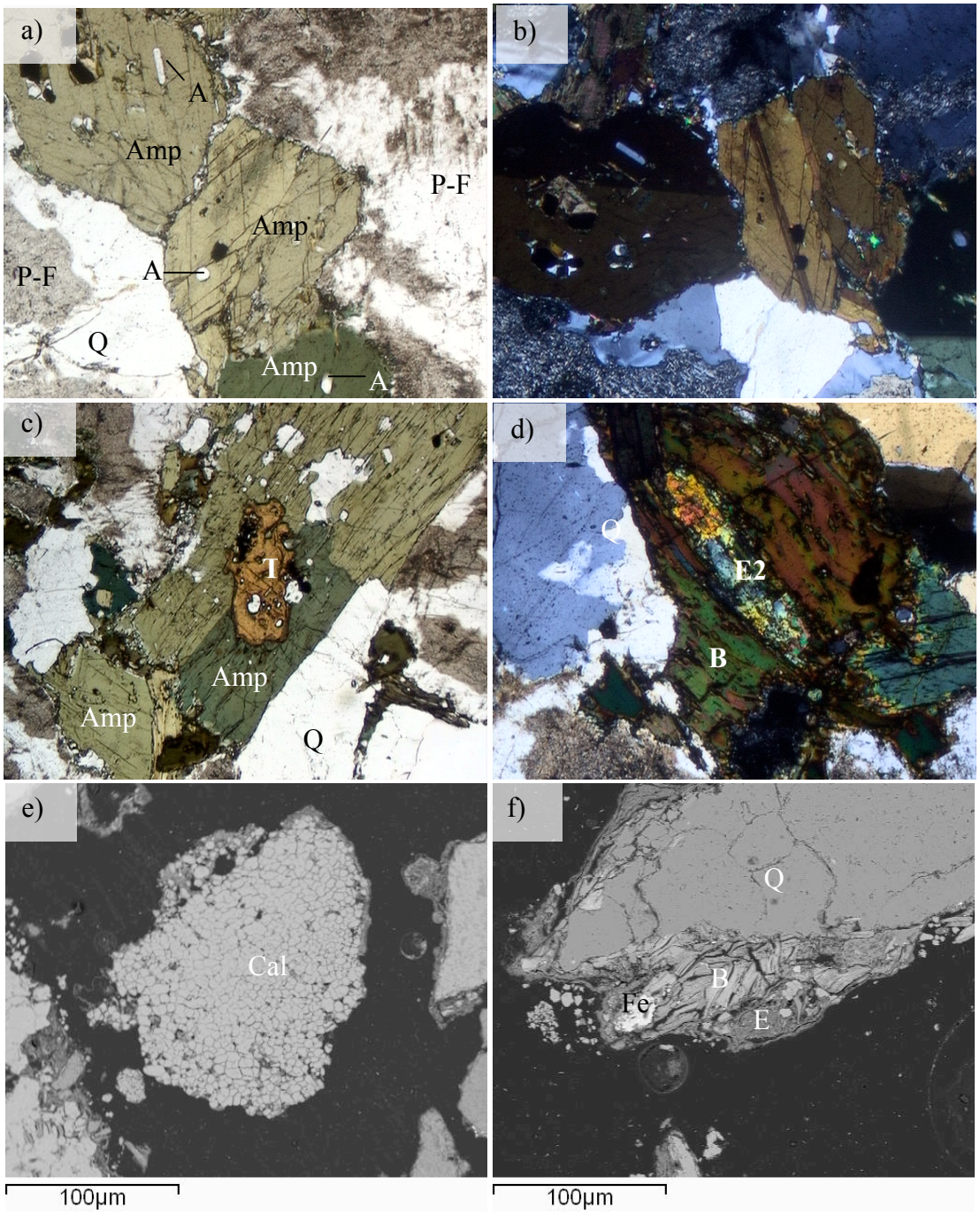

Figure 4-14 – Photomicrographs a) M4a PPL, mag x4 b) M4a XPL, mag x4 c) M4a PPL, mag x10 d) M4a XPL, magx10 e) Electron Microprobe -Electron Back Scatter Detection image of M4b f) Electron Microprobe -Electron Back Scatter Detection image of M4b. A = apatite, Amp=amphibole, B=biotite mica, Cal=calcite, E=epidote, E2=epidote var 2 , Fe=iron oxide, P-F=plagioclase feldspar, Q=quartz, T=titanite

M6 Samples – Porphyritic Epidote-Chlorite Granodiorite

Sample M6a is a porphyritic fresh sample from an outcrop, pink and green in colour (figure 4-15). Feldspars and some quartz crystals are large (up to 3cm), with smaller epidote and chlorite. Chlorite and epidote are found in large amounts, epidote as

either tabular crystals or as long acicular radial crystals, often within plagioclase feldspar (figure 4-16 - a&b) and chlorite as acicular crystals, closely packed together between larger quartz and feldspar (figure 4-16 - c). Titanite, apatite and ilmenite were identified under EM in small amounts. According to the IUGS Igneous rock classification scheme this sample is an epidote-chlorite granodiorite (see table 4-3).

Potentially F-bearing minerals in M6 include:

- M6a – chlorite, epidote, titanite

Figure 4-15 – Sample M6a and the outcrop from where sample M6a was taken.

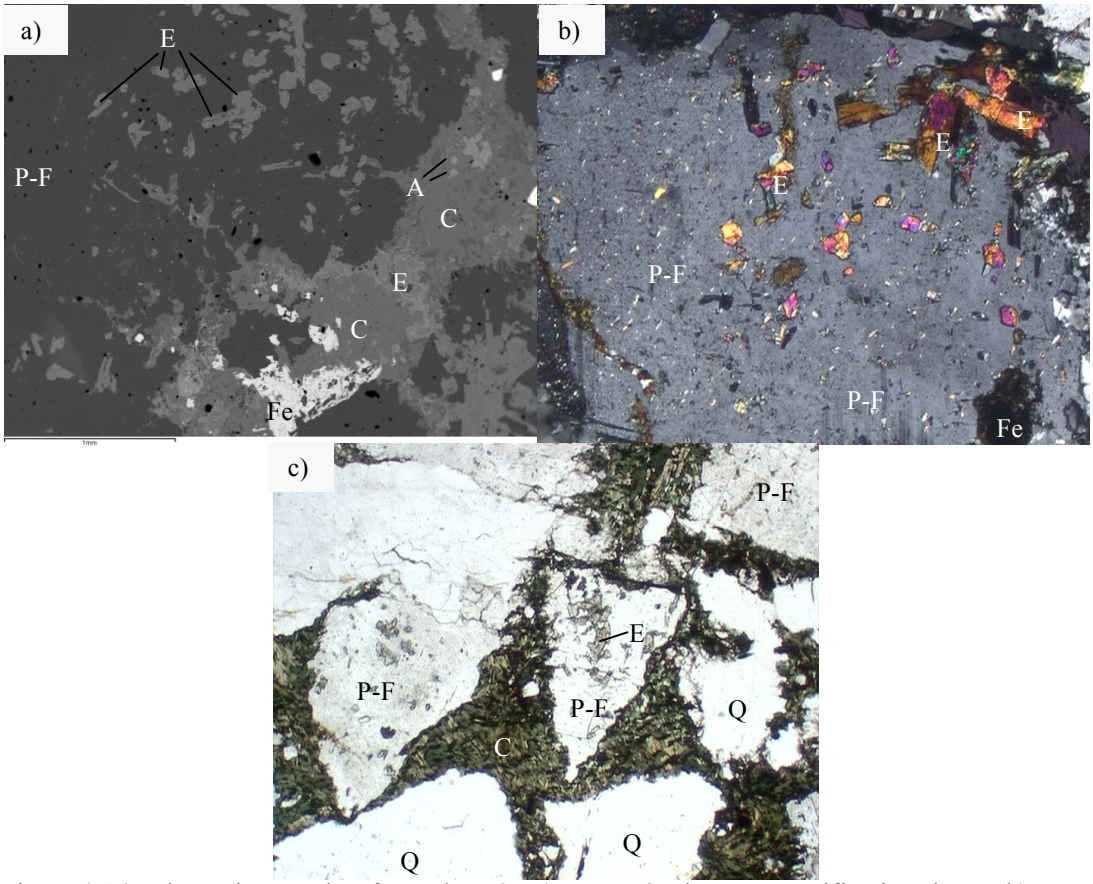

Figure 4-16 - photomicrographs of sample M6a, a) EM-EBSD image, magnification shown. b) XPL image, magnification x10 c) PPL image, magnification x4.
A=apatite, C=chlorite, E=epidote, Fe=iron oxide, P-F=plagioclase feldspar, Q=quartz

M7 Samples – Grey Monzogranite

Sample photos and locations are shown in figure 4-17 and figure 4-18. Sample M7a is a fine grained grey (and pink) fresh rock sample (with some localised weathering) collected from outcrop. Feldspars and quartz make up most of the sample, with subordinate biotite (with iron oxide), chlorite, epidote and apatite (figure 4-19 – a&b). Titanite and ilmenite were identified under EM analysis. According to the IUGS Igneous rock classification scheme and point counting results this sample is a monzogranite (see table 4-3).

Sample M7b is a weathered sample, fine to medium grained. Biotite and chlorite are small and fractured along cleavages. Epidote is found in association with biotite, as are iron oxides. The sample is highly fractured and weathered (figure 4-19 – c&d).

M7c is a weathering crust from the M7 area. The sample shows a large amount of weathering and alteration. The main minerals present include quartz, feldspars, iron oxides, chlorite, epidote, and biotite.

Potentially F-bearing minerals in M7 samples include:

- M7a – biotite, chlorite, epidote, apatite, titanite
- M7b – biotite, chlorite, epidote, apatite
- M7c – biotite, chlorite, epidote

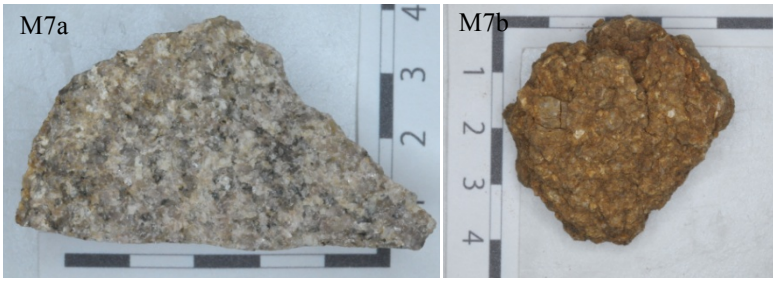

Figure 4-17 – Samples collected from site M7

Figure 4-18 – Outcrop where samples M7a and M7b were collected.

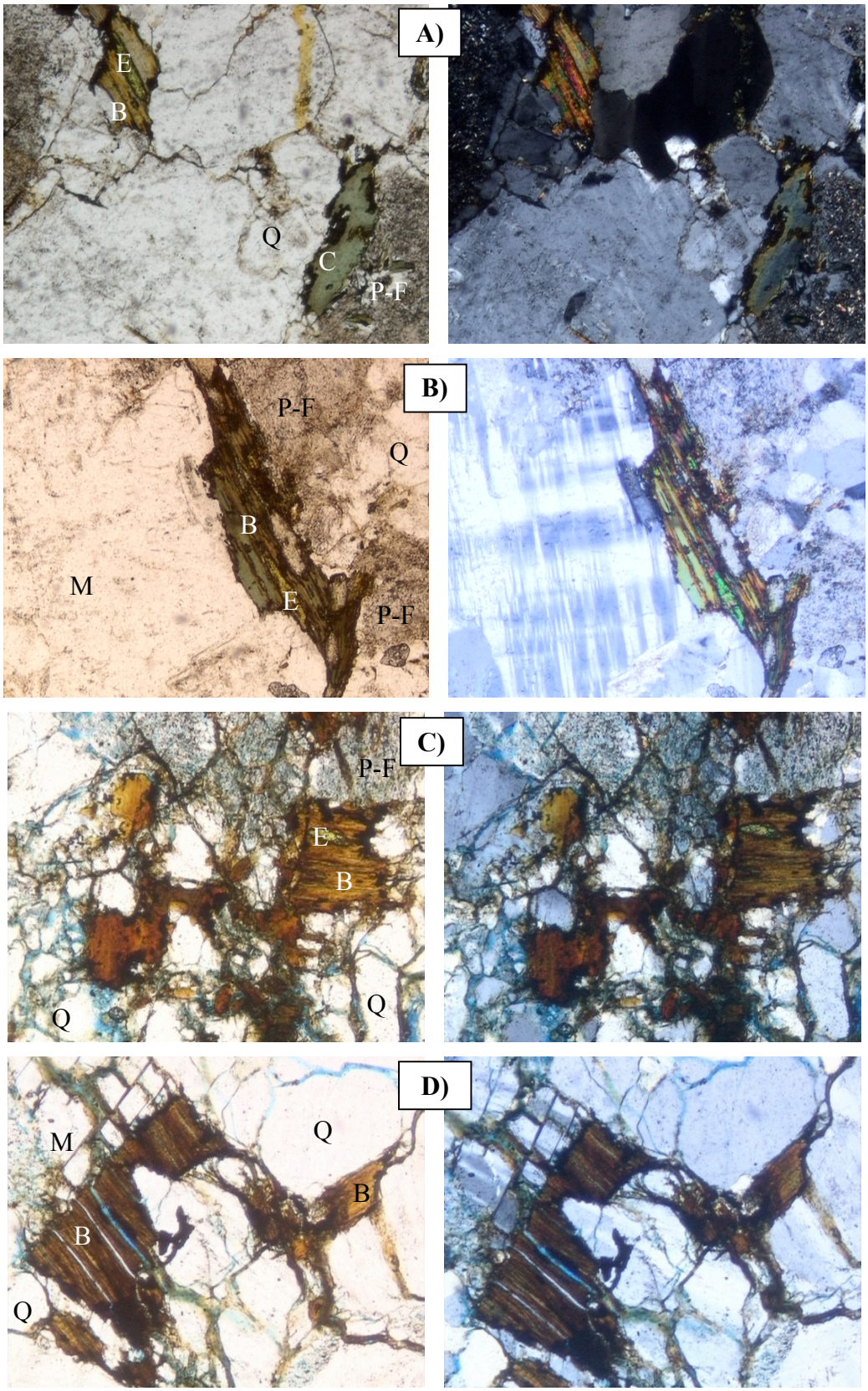

Figure 4-19 - Photomicrographs of sample M7a and M7b. Images through plane polarised light on the left, through crossed polars on the right. A) M7a, magnification x4. B) M7a, magnification x10. C) M7b, magnification x10. D) M7b, magnification x10. Minerals present: B=biotite, Cal=calcite, E=epidote, M=microcline, P-F=plagioclase feldspar, Q=quartz

4.4.3 Wailpally samples

Figure 4-2 is reproduced as figure 4-20 for ease of reference to sample locations.

Figure 4-20 – Sample locations and geology of Wailpally. Sample locations 1 and 2 are south of Antampet (not on map). Sample locations include fresh (a) and weathered (b,c,d etc) samples unless otherwise stated. Geology from Dhakate et al., (2008)

W1 Samples – Porphyritic Chlorite Monzogranite

Samples W1a and W1b were collected from a large outcrop south of Wailpally catchment, and north of Savanagudah. Epidote veins and flow banding were seen in the area. Figure 4-21 and figure 4-22 show the samples and outcrop. These samples (along with W2a, b and c) are representative of the western hill region of the catchment.

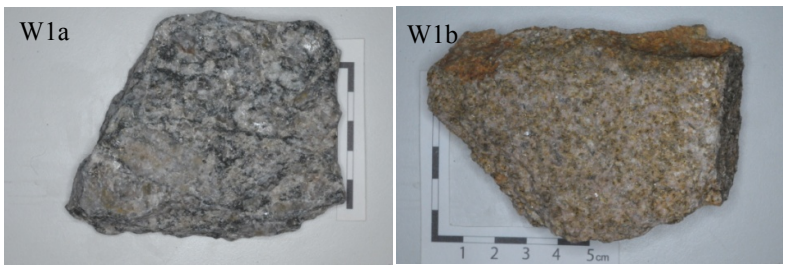

Figure 4-21 - Samples collected from site W1

Fresh rock sample W1a is porphyritic with large feldspars and quartz (0.5-2cm), and smaller mafic minerals. Many feldspars show sericite alteration as well as micrographic textures. Titanite is present as distinct crystals, some of which are heavily altered. Purple fluorite is present in association with chlorite and epidote. EM analysis shows titanite also to be present as veins or rims around chlorite (figure 4-23). Several large and fresh apatite crystals were identified, as well as zircon, iron oxides and ilmenite. This sample has a gneissic texture. According to the IUGS Igneous rock classification scheme and point counting results this sample is a chlorite monzogranite (see table 4-3).

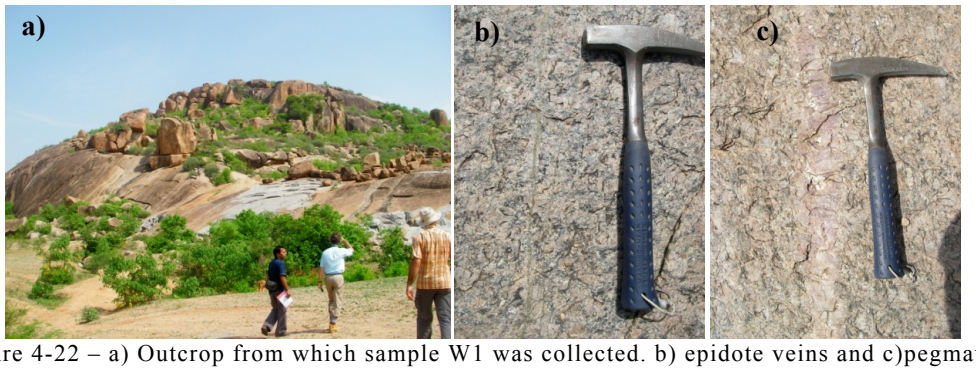

Figure 4-22 – a) Outcrop from which sample W1 was collected. b) epidote veins and c)pegmatite vein

Sample W1b is a weathered sample with fine to medium grain size. Many feldspars show sericite alteration, and are fractured and broken. Biotite is fractured and small, often with iron oxide present at edges, and apatite and epidote present in very small amounts. EM analysis shows titanite as rims or along cleavages of biotite (figure 4-23). No fluorite was found in this sample.

Potentially F-bearing minerals present in W1 samples include:

- W1a – fluorite, apatite, chlorite, titanite, epidote
- W1b – biotite, epidote, apatite, titanite

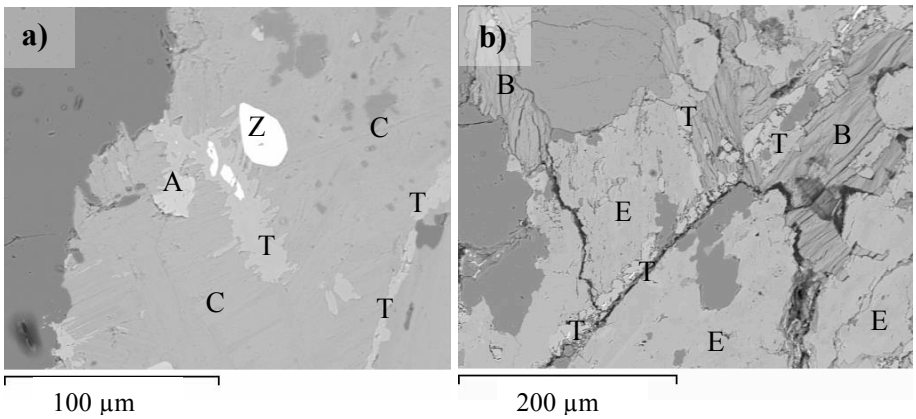

Figure 4-23 – EM-EBSD images a) W1a, chlorite with titanite, apatite and zircon b) W1b, epidote and biotite with titanite precipitated in a vein (bottom left to top right). A = apatite, B=biotite, C=chlorite, E=epidote, T=titanite, Z=zircon

W2 Samples – Porphyritic Epidote Granodiorite

Samples W2a, b and c were collected from the same outcrop as sample W1 (figure 4-22). Sample W2a is similar to W1a but with a larger grain size. Photomicrographs are shown in figure 4-24 and figure 4-25.

Sample W2a is a porphyritic granitic rock with large quartz and feldspars (up to 3 cm), and smaller chlorite, as well as apatite, titanite and epidote. Small amounts of biotite were identified under EM, as well as various forms of titanite and titanium oxides (figure 4-24 and figure 4-25). According to the IUGS Igneous rock classification scheme and point counting results this sample is an epidote granodiorite (see table 4-3).

Sample W2b is a porphyritic, weathered sample. Weathering is local, along fractures and exposed surfaces. Quartz and feldspars have large crystal sizes (up to 1.5 cm), whereas biotite, chlorite, apatite, iron oxides and epidote are present as smaller crystals. EM analysis confirms titanite and epidote as rims or veins within biotite and chlorite. Titanium oxides, ilmenite and a titanium phosphate present as tabular, zoned crystals in association with titanite are also present (figure 4-25 and figure 4-26).

Sample W2c is a highly weathered sample from this location. Many plagioclase feldspars show alteration and sericite. Under EM, biotite and chlorite appear as a mass of small crystals together, and do not appear fresh. Biotite shows alteration to chlorite, with chlorite retaining the biotite structure. Titanite, ilmenite, epidote, apatite and titanium silicates and iron oxides are also present (figure 4-27).

Potential F-bearing samples at W2 include:

- W2a – chlorite, apatite, epidote, titanite, biotite (rare)
- W2b – biotite, chlorite, apatite, epidote, titanite, titanium-phosphate
- W2c – biotite, chlorite, apatite, epidote, titanite

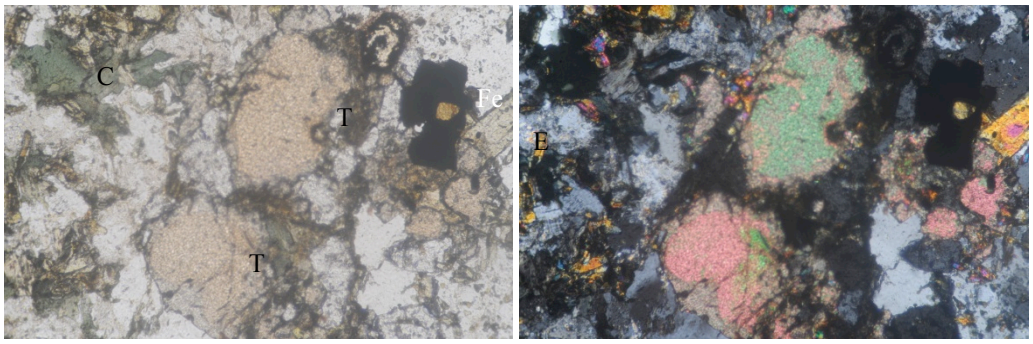

Figure 4-24 – Sample W2a – large titanite crystals. Left=PPL, right=XPL. Magnification x 10. C=chlorite, E=epidote, Fe=iron oxide, T=titanite.

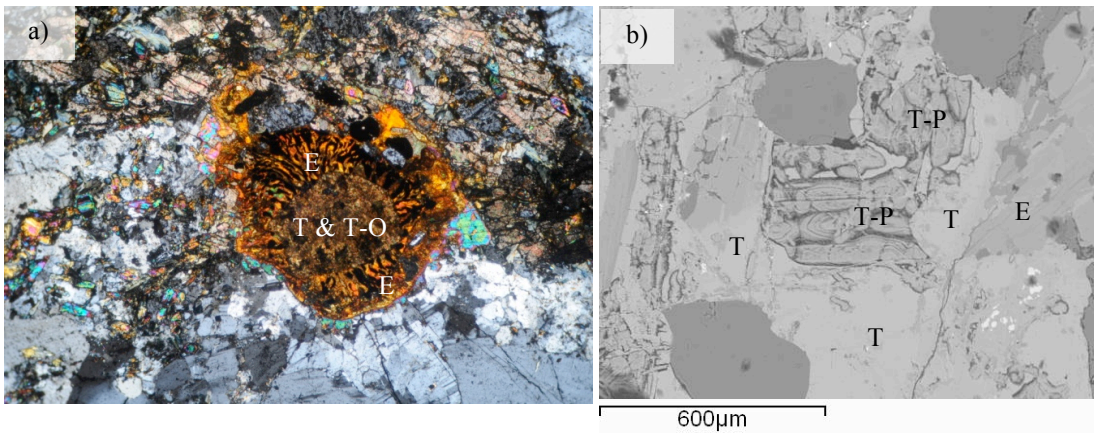

Figure 4-25 – a) W2a – photomicrograph in XPL of titanite and titanium oxide, surrounded by radiating epidote. Magnification x 4.b) W2b – EM-EBSD image of titanium phosphate as tabular zoned crystals, surrounded by titanite and epidote.
E=epidote, T=titanite, T-O=titanium oxide T-P=titanium phosphate

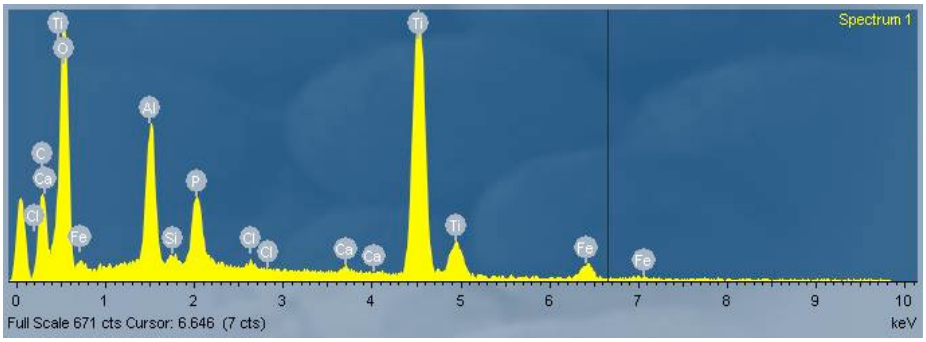

Figure 4-26 - W2b – EM-EBSD graph showing composition of the titanium aluminium phosphate (analysis taken from T-P in figure 4-25).

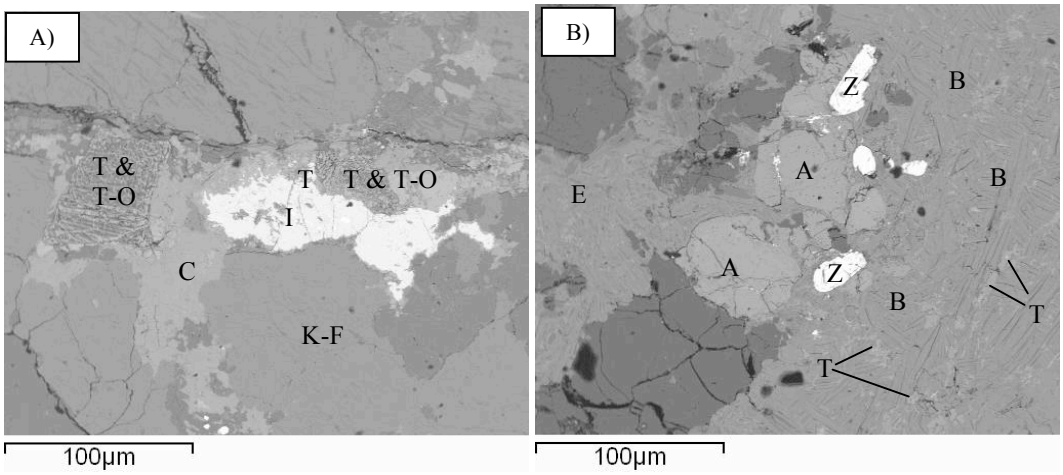

Figure 4-27 – Sample W2c EM-EBSD images. A) titanite, titanium oxides and Ilmenite B) shows biotite as a mass of crystals, largely pitted and unclear cleavage. The large apatite crystals in the centre are relatively fresh under microprobe observation. Zircon present shows zoning. (This area was also mapped). A=apatite, B=biotite, C=chlorite, E=epidote, K-F=k-feldspar, T=titanite, T-O=titanium oxide, I=ilmenite, Z=zircon

W11 Samples – Amphibole Granodiorite

Sample W11a is a medium-coarse grained fresh sample from a dug-well (figure 4-28). As well as quartz and feldspars, this sample contains amphiboles, chlorite, apatite and epidote (figure 4-29). Amphiboles are identified as ferro-edenite through EM-EDX point analysis and an amphibole classification spreadsheet (Preston and Smith, 2002). Epidote is present as veins across the sample, as radial acicular crystals and as tabular, prismatic crystals, usually associated with amphiboles. Many large and well preserved apatite crystals were observed under EM, as well as epidote var 2 and titanite as rims or veins in chlorite (figure 4-29). According to the IUGS Igneous rock classification scheme and point counting results this sample is an amphibole granodiorite (see table 4-3).

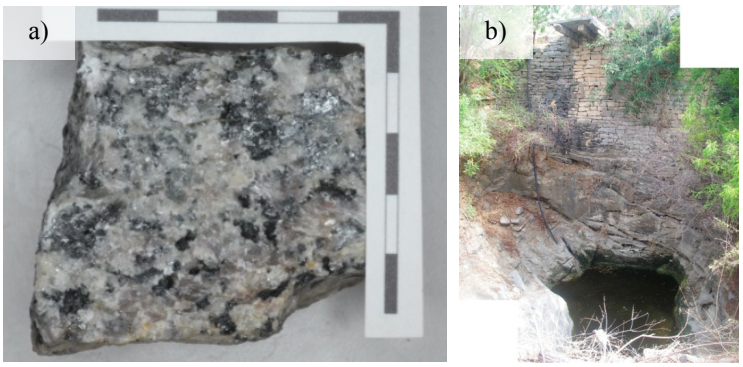

Figure 4-28 – a) Sample W11a b)dug-well from which W11a collected

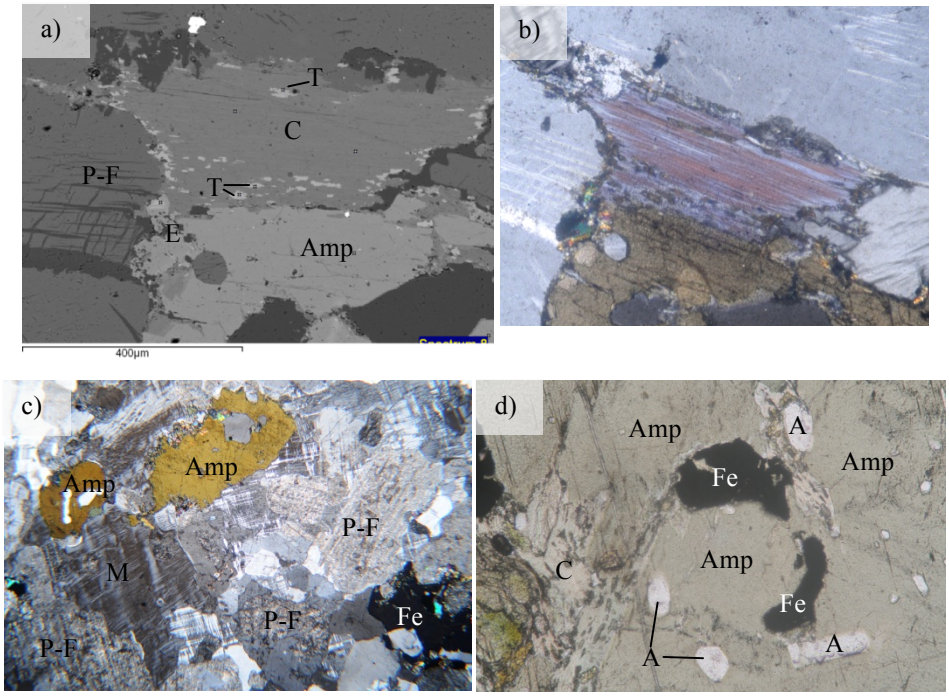

Figure 4-29 – W11a. a) EM-EBSD image - Amphibole and chlorite b) Same location as photo a, XPL, magnification x10. c) XPL image of amphibole and feldspars. d) CPL image of apatite and iron oxide in amphiboles, magnification x10. A = apatite, Amp=amphibole, E=epidote, Fe=iron oxide, P-F = plagioclase feldspar, M=microcline, T = titanite

Weathered samples from the dug well were collected with depth through the profile (see chapter 5, section 5.2). The sample collected at 7m depth is used for comparison with the fresh rock in whole rock chemistry and whole rock fluorine results, labelled W11b, although no thin section was made of this sample.

Potentially F-bearing minerals in this sample include:

- W11a – ferro-edenite, apatite, epidote, chlorite, titanite

W14 Samples – Granodiorite

Sample W14a is a fine grained, pink and grey coloured fresh sample collected from an outcrop where pegmatite and epidote veins were also observed (figure 4-30 and figure 4-31). In thin section, crystals are similar in size, with quartz and plagioclase feldspar slightly larger than chlorite, biotite, epidote, iron oxides and apatite (rare). EM analysis confirmed the presence of fluorite (which could not be identified under optical microscope due to its small size) and titanite, present as an alteration mineral.

According to the IUGS Igneous rock classification scheme and point counting results this sample is a granodiorite (see table 4-3).

Sample W14b is a weathered rock from the same outcrop as W14a. Feldspars show signs of weathering with fractures and sericite formation. Fresh and weathered biotite with iron oxides is present. Apatite is rare, and titanite is present as rims and veins across biotite (identified in EM-EBSD). Two varieties of epidote (var. 1 and var. 2) were identified under EM analysis.

Potentially F-bearing minerals in W14 samples include:

- W14a – fluorite (rare), biotite, chlorite, apatite (rare), epidote, titanite
- W14b – apatite, epidote, biotite, titanite, chlorite, epidote var 2

Figure 4-30 – a) location from which sample W14a was collected b) and c) pegmatite veins within the finer grained granite.

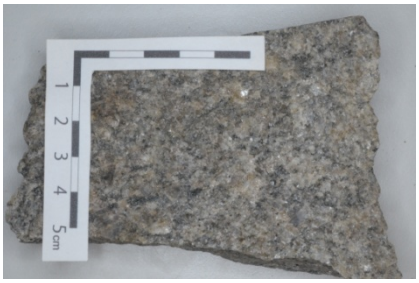

Figure 4-31 – Sample W14a

W16 Samples – Biotite Granodiorite

Sample W16b was collected from recent excavations of a dug-well. Calcrete was seen on the sides of the well (figure 4-32). W16a was collected from a nearby outcrop (figure 4-32). Mafic vein material and large variations in sample colour and composition were noted at this location.

Figure 4-32 – a) outcrop from which sample W16a was collected b) dug-well from which sample W16b was collected

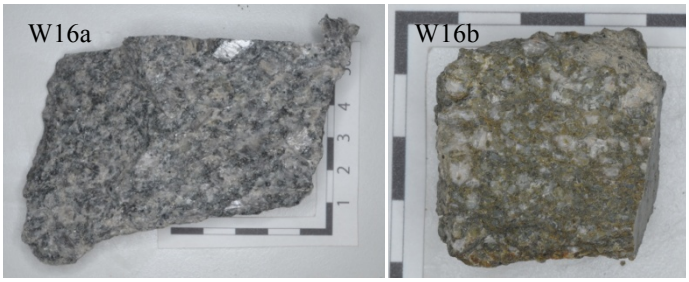

Figure 4-33 – Samples from location W16

Sample W16a is a medium grained fresh sample. Dominant minerals include quartz, plagioclase feldspar and potassium feldspar with biotite, apatite, epidote and chlorite present in small amounts (figure 4-34 - a&b). A small mineral that could be fluorite was observed in thin section, although this was not confirmed or measured under EM. Titanite is present as rims or veins in biotite (identified with EM). According to the IUGS Igneous rock classification scheme and point counting results this sample is a biotite granodiorite (see table 4-3).

W16b is from a dug-well near sample W16a; the sample is weathered throughout. Feldspars are fractured, irregular in shape and show sieve texture and sericite alteration. Highly weathered biotite (small, fragmented crystals) and fresher looking apatites were identified using EM. Titanium oxides and titanite were also identified under EM, in some cases as thin acicular crystals (figure 4-34 - c).

Potentially F-bearing minerals in W16 samples include:

- W16a – biotite, apatite, epidote, chlorite, titanite
- W16b – apatite, biotite, titanite

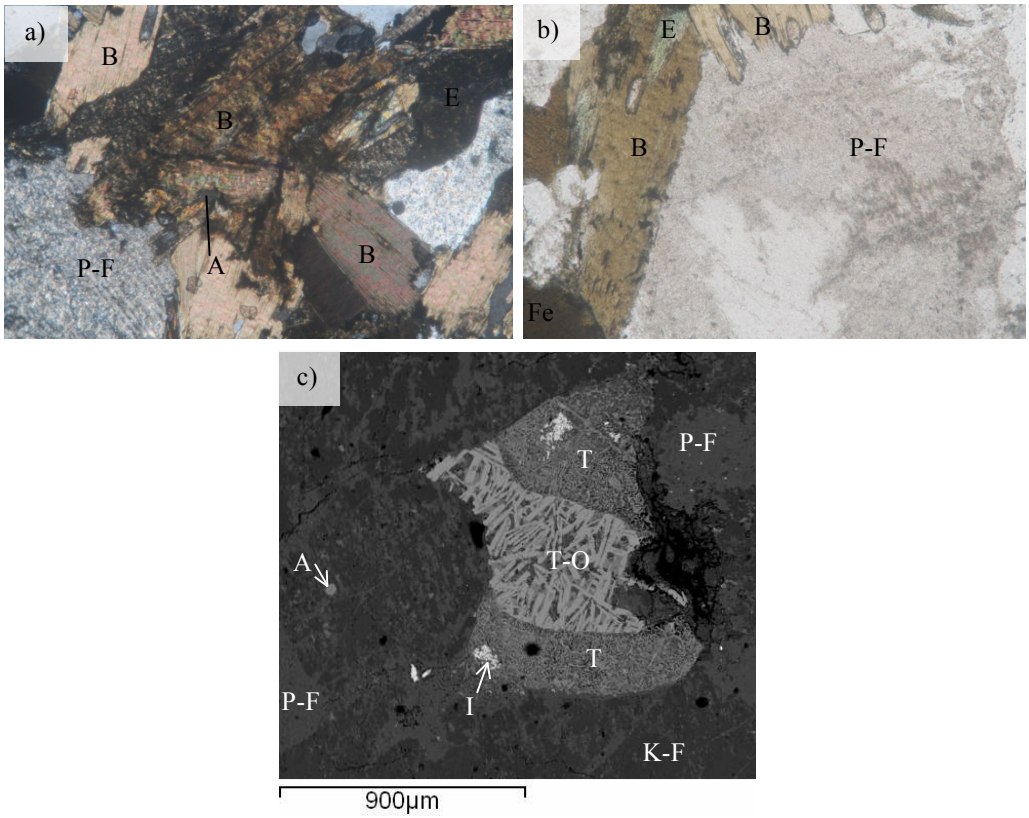

Figure 4-34 – a) Photomicrograph in XPL of W16a, magnification x10 b) Photomicrograph in PPL of W16a, magnification x4. c) EM-EBSD image of W16b. A = apatite, B=biotite, E=epidote, Fe=iron oxide, K-F=K-feldspar, P-F=plagioclase feldspar, T = titanite, I=ilmenite, T-O=titanium oxide

W17 Samples – Pegmatitic Epidote Quartz Syenite

– Weathered epidote Quartz Monzodiorite

Sample W17a is a fresh pegmatite sample from a dug-well (figure 4-35). The dominant minerals present are alkali feldspars (orthoclase and microcline) which make up most of the sample as large phenocrysts (up to 3.5cm, figure 4-36). Plagioclase feldspar (with albite twinning and sericite) and quartz are present as a fine grained groundmass and in much lower quantities. Epidote is also present as small tabular grains in clusters or as veins running through the section. A small amount of iron oxide, titanite and zircon was identified in EM analysis, as well as two small, highly weathered biotite crystals. According to the IUGS Igneous rock classification scheme and point counting results this sample is an epidote quartz syenite (see table 4-3).

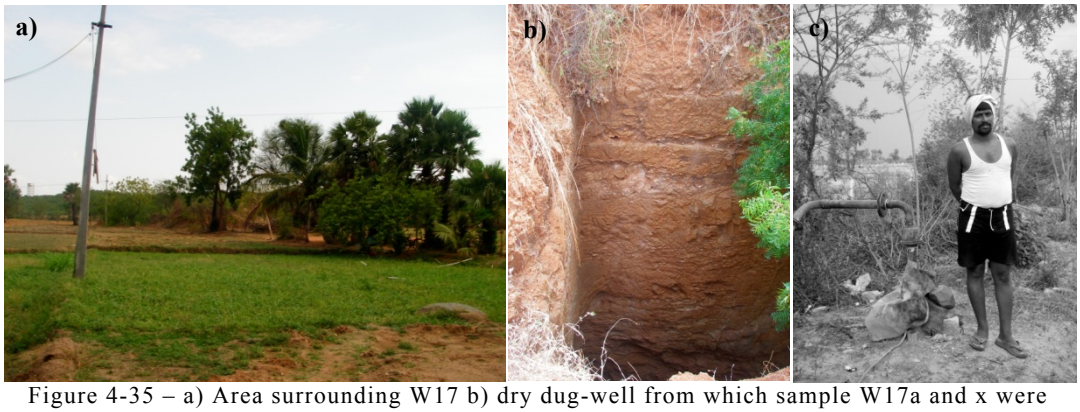

Figure 4-35 – a) Area surrounding W17 b) dry dug-well from which sample W17a and x were collected c) farmer with more recently installed tube-well

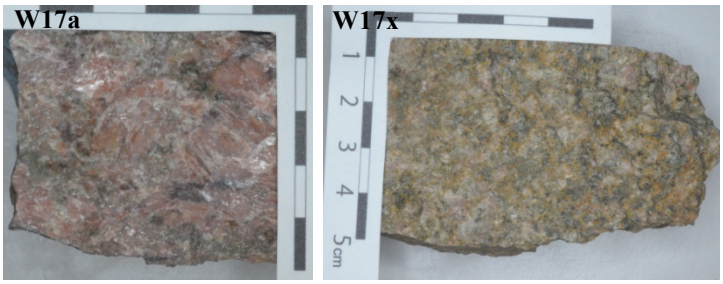

Figure 4-36 – Samples from location W17

The weathered sample from this location has a medium grain size (up to 0.5cm) (figure 4-36) with K-feldspars (orthoclase and microcline) and plagioclase feldspars (with albite twinning) as the principal minerals, present as larger phenocrysts. Quartz, epidote, chlorite, apatite and biotite are present as smaller grains. The larger feldspars contain many fractures, some of which are filled with epidote (figure 4-37). Micrographic and microperthite textures are also seen in the feldspars. The petrography of this sample is very different to the fresh sample collected from this location (W17a), and it is not thought that this sample is the weathered equivalent of W17a. Therefore this sample has been labelled W17x to note its separation from the fresh sample W17a. According to the IUGS Igneous rock classification scheme and point counting results sample W17x is an epidote quartz monzodiorite (see table 4-3).

Potential F-bearing minerals from site W17 include:

- W17a – epidote, biotite (very rare), titanite (very rare)
- W17x – epidote, chlorite, biotite, titanite (rare), apatite (rare)

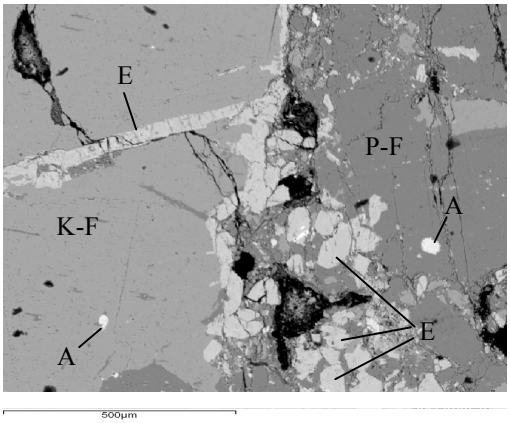

Figure 4-37 – EM-EBSD Image of W17x showing K-feldspar with a vein of epidote and epidote as prismatic crystals along the boundary between K and Na feldspars. A=apatite, E=epidote, K-F=K-feldspar, P-F=plagioclase feldspar.

W13 Sample – Mafic Vein Material

Sample W13 is a fresh sample of mafic vein material, fine-medium grained (figure 4-38), collected from a granite outcrop with flow banding and mafic veins (figure 4-39). The dominant minerals in this sample are biotite and amphiboles which show a schistose texture (figure 4-40 - a). Amphiboles are identified as mostly magnesio-hornblende and some actinolite through EM-EDX point analysis and an amphibole classification spreadsheet (Preston and Smith, 2002). Biotite grains are prismatic, aligned and of roughly equal size, amphiboles are irregular in shape, often showing good cleavage and twinning (figure 4-40 - b). Apatite is present within biotite. Smaller quantities of alkai-feldspars, quartz and plagioclase feldspars are located between layers of biotite and amphibole. Epidote was identified though EM. Point counting results give this mineral to be roughly 37% amphibole, 23% biotite, 18% alkali-feldspar and 13% quartz (see table 4-3 for full point counting results).

Similar mafic vein material has been seen in locations W1, W14 and W16.

Potentially F-bearing minerals in this sample include:

- W13 – biotite, magnesio-hornblende, actinolite, apatite, epidote

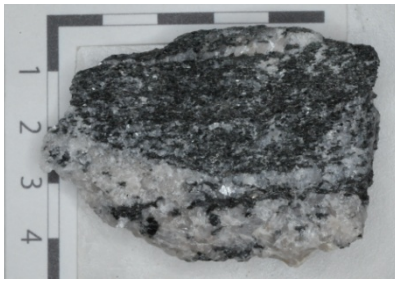

Figure 4-38 –Sample W13

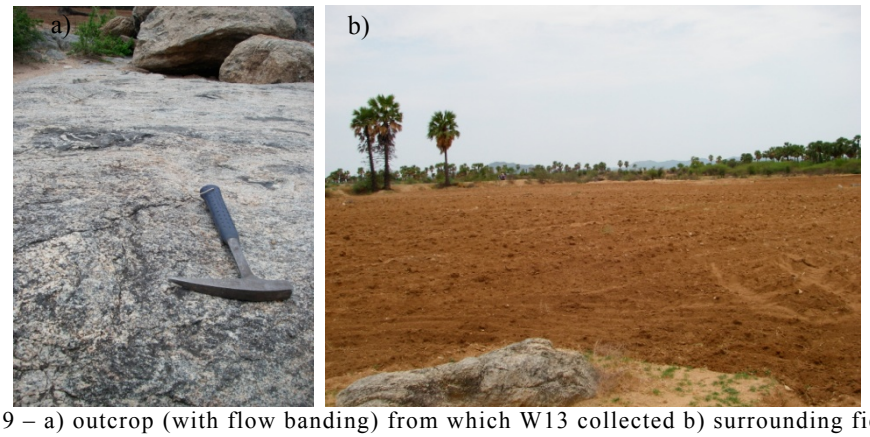

Figure 4-39 – a) outcrop (with flow banding) from which W13 collected b) surrounding fields (from which sample W-C collected).

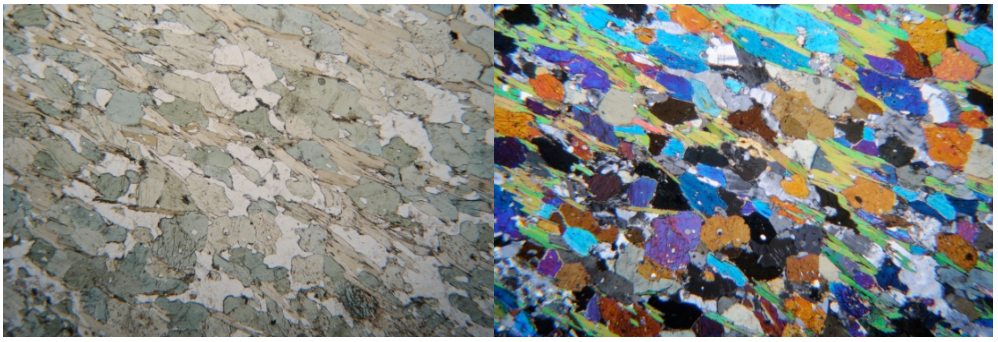

a)

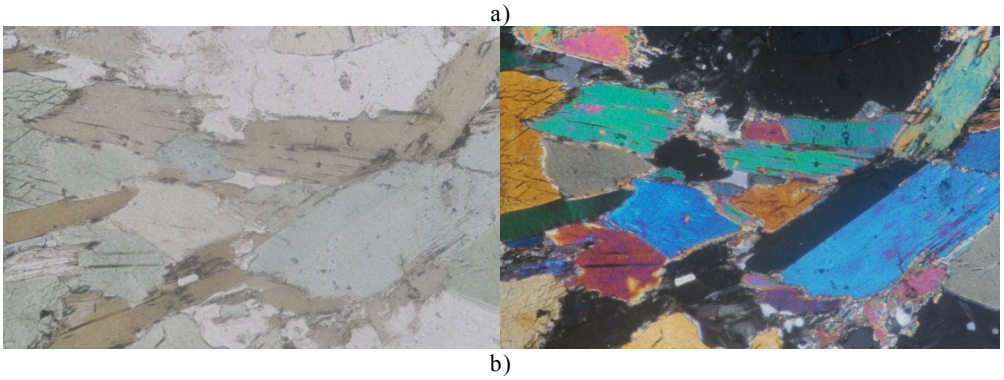

b)

Figure 4-40 – Photomicrographs of sample W13 under PPL (left) and XPL (right). a) magnification x2 (field of view ~7mm across) b) magnification x10 (field of view ~1.5mm across)

W-C Sample – Calcrete

Sample W-C is a calcrete sample, white in colour, collected from the surface in the same location as W13 (figure 4-39, figure 4-41). Calcrete was found in a number of locations throughout the Wailpally catchment, commonly occurring both as calcrete nodules on the surface as well as in layers within the weathered rock.

Sample W-C consists mostly of calcium carbonate which shows a layered/banded texture (figure 4-42). Within this matrix of calcite there are several small clasts of quartz, feldspar and the occasional epidote, biotite, zircon and titanite (identified under EM). Larger clasts are mostly plagioclase feldspar, alkali-feldspar and quartz, or a mixture of these three (figure 4-42).

Potentially F-bearing minerals include:

- W-C – calcite, biotite, epidote, titanite

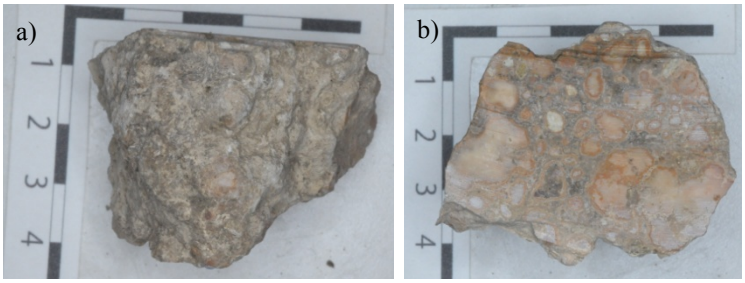

Figure 4-41 – a) sample W-C crust b) sample W-C cut section. For area of collection see W13.

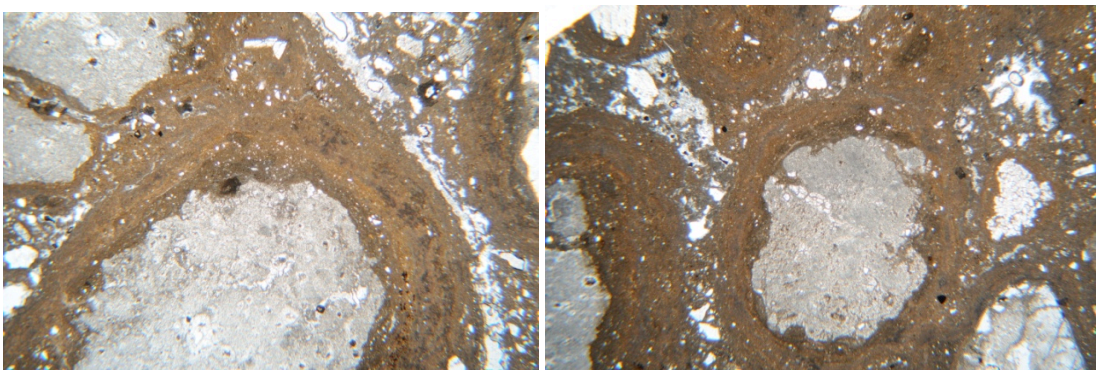

Figure 4-42 - Photomicrographs of W-C, PPL, magnification x2

4.4.4 Petrological Summary

The samples collected from Maheshwaram and Wailpally can be divided into the following sets based on grain size, colour and mineralogy (sample M2a (porphyritic biotite granodiorite) can be grouped with the porphyritic granites as well as the biotite granodiorite W16a):

- Pegmatites
    - W17a – Epidote quartz syenite (pegmatite)
- Porphyritic granites
    - M2a – Porphyritic biotite granodiorite
    - M6a – Porphyritic epidote chlorite granodiorite
    - W1a – Porphyritic chlorite monzogranite
    - W2a – Porphyritic epidote granodiorite
- Medium/coarse grained biotite granites:
    - M2a – Biotite granodiorite (porphyritic)
    - W16a – Biotite granodiorite (medium grained)
- Medium grained amphibole granites:
    - M4a – Amphibole monzogranite
    - W11a – Amphibole granodiorite
- Fine grained samples
    - M3a – Pink monzogranite
    - M7a – Grey monzogranite
    - W14a – Granodiorite
- Other samples
    - W13 – Mafic vein material
    - W-C – Calcrete

The main minerals present are quartz, K-feldspars, plagioclase feldspar, biotite, chlorite, titanite, epidote, epidote (var2) and fluorite as well as iron and titanium oxides. Primary titanite is observed only in M4, W1, W2, and fluorite is only observed in M3a, W1a and W14a (and possibly W16a).

Some of the samples show gneissic textures (e.g. M2a, M6a, W1a, and W2a).

4.5 X-Ray Diffraction

Three powdered fresh and weathered rock pairs from Maheshwaram were analysed with XRD (figure 4-43, figure 4-44 and figure 4-45). The main minerals identified are quartz, potassium feldspar, plagioclase feldspar (identified as albite, a sodium rich feldspar) and biotite as well as chlorite in fresh samples. Diffraction patterns at low values of 2Θ (up to 25°) are shown here as they give important information about micas, chlorite and clay minerals that are less easily seen in the rest of the diffraction pattern.

Diffraction patterns for the porphyritic biotite granodiorite samples M2a and M2b (figure 4-43) show a large amount of biotite mica in M2a (indicated by a large peak at ~10°), and much less in M2b. Chlorite is present in M2a in small amounts (peaks identified as clinochlore through the ICDD) but is not present in M2b. The broad and low peak at ~7° may be due to swelling clays that have formed from chlorite weathering. A clay band at ~23° is also seen in M2b but not in M2a.

Diffraction patterns of pink monzogranite samples M3a and M3b (figure 4-44) show chlorite present in fresh sample M3a removed in M3b, possibly altering to smectite (at ~7°). The clay band at ~23° is also measured in M3b but not M3a. Small amounts of mica are present in both M3a and M3b.

The diffraction pattern for grey monzogranite samples M7a and M7b (figure 4-45) is similar to that of M3, with a reduction in chlorite from M7a to M7b, an increase in clays, and a small amount of biotite mica in both samples.

Semi-quantitative abundances of the main minerals present in each sample (table 4-4) show very little difference between fresh and weathered samples in the quantities of albite and quartz. In all three sample pairs the proportion of K-feldspars increases slightly, and in two cases the proportion of quartz increases slightly (M2 and M7). High quantities of biotite are measured in M2a (16%), which decreases on weathering to M2b (10%). A decrease in biotite in comparison to the respective fresh samples is also observed in M3b and M7b, although the fresh samples do not contain large amounts of biotite to begin with (3%). Chlorite (as clinochlore) is only identified in fresh samples, and is absent in all weathered samples.

It was not possible to identify which clay minerals are present in the weathered samples or their abundances from the XRD analysis that was preformed, but their presence in the samples can be observed in the diffraction patterns. Further analysis of the clay minerals by XRD would require separation and alignment of minerals before analysis.

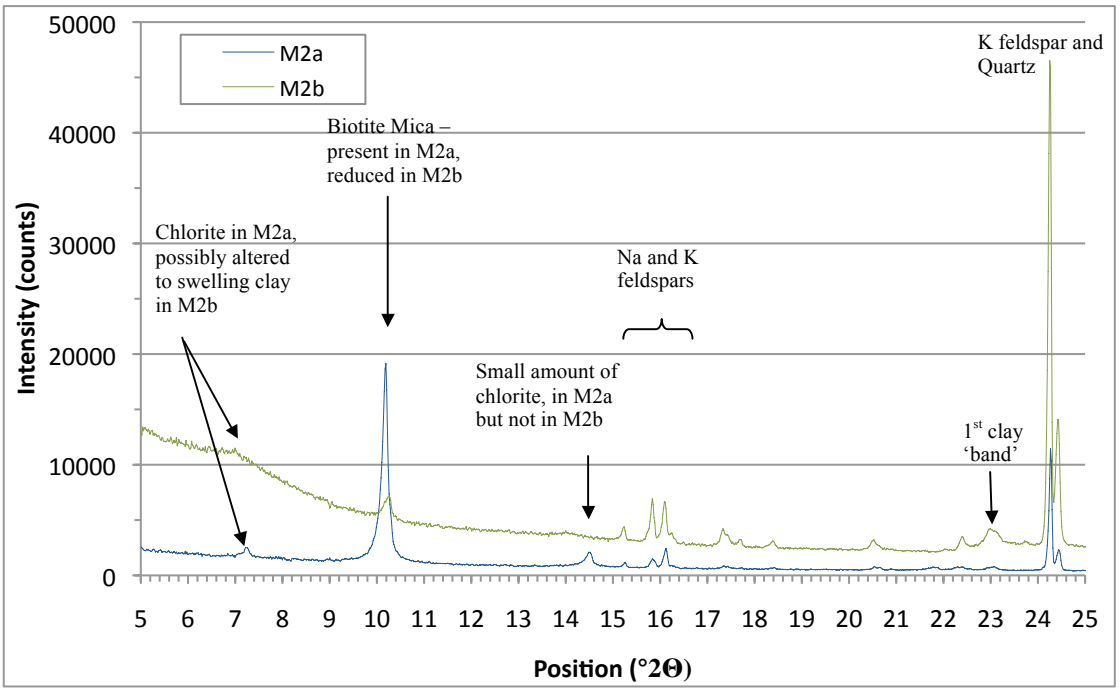

Figure 4-43 – XRD pattern for M2a and M2b up to position 25° 2Θ.

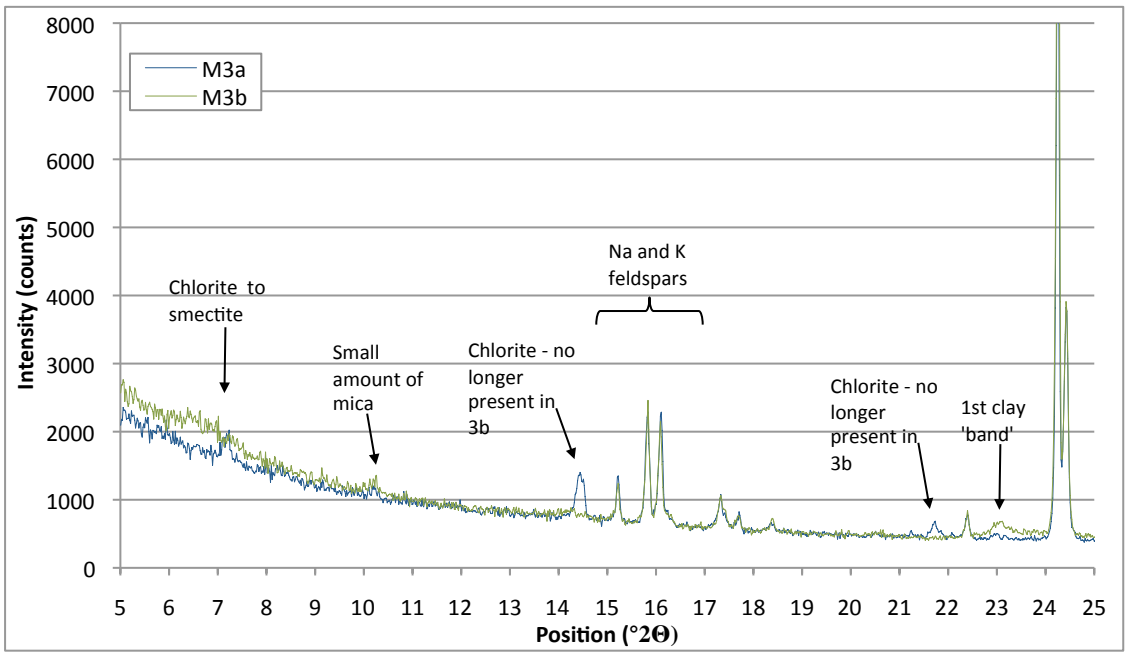

Figure 4-44 – XRD pattern for M3a and M3b up to position 25° 2Θ.

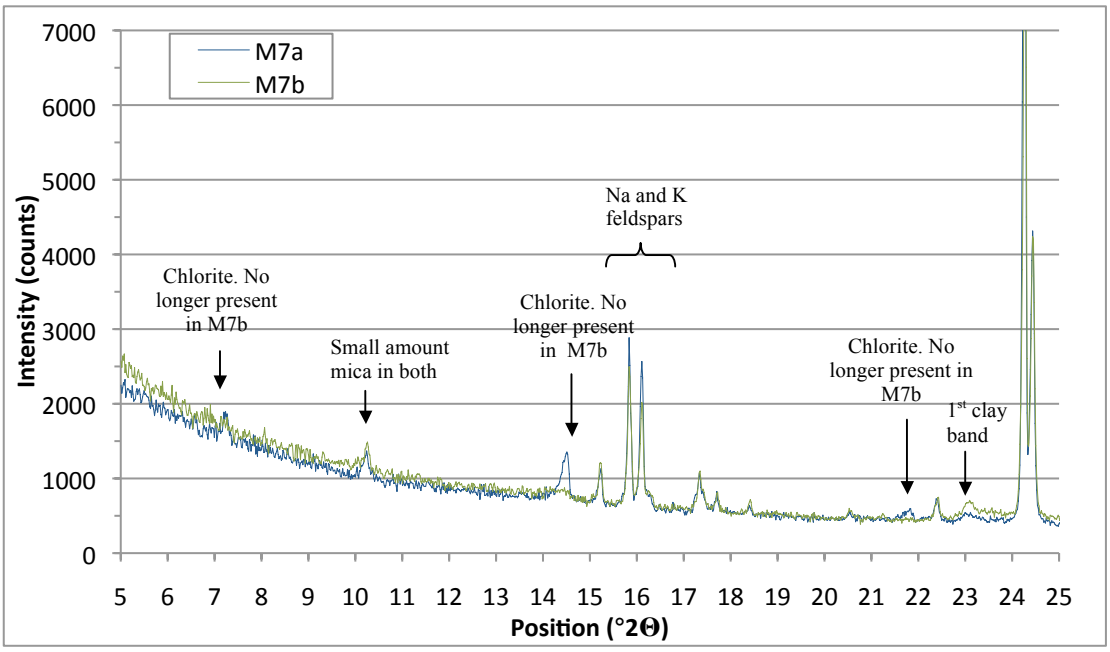

Figure 4-45 – XRD pattern for M7a and M7b up to position 25° 2Θ.

Table 4-4 – Semi-Quantitative abundances of primary minerals present in selected Maheshwaram samples

Mineral	Abundance %					
	M2a	M2b	M3a	M3b	M7a	M7b
K feldspar	22	25	36	39	40	42
Albite (sodium feldspar)	24	23	26	27	26	25
Quartz	36	42	33	33	30	32
Biotite	16	10	3	1	3	1
Clinochlore	3		2		2	

The abundances of minerals determined by XRD do not compare directly to estimates by point counting, as XRD only identifies the main minerals present in this sample, whereas less abundant minerals are also identified in point counting.

All samples analysed here would be classified as monzogranites according to the IUGS classification scheme, but from point counting, M2a is a granodiorite. Point counting also identifies high biotite in M2a and M2b compared to the other samples.

4.6 Electron Microprobe (EM) elemental analysis

The following minerals were identified to contain F:

- Fluorite
- Apatite
- Titanite
- Epidote var 2
- Titanium phosphate (present in sample W2b only)
- Biotite
- Amphibole
- Epidote
- Chlorite

Mineral F content is compared between samples using the students t-test (2 tailed, 2 sample unequal variance), and reported at the significance levels of 0.01 (1%) and 0.05 (5%).

4.6.1 Maheshwaram samples

The average F content of specific minerals in all samples analysed is given in figure 4-46 and table 4-5, and a summary of F analysis is given in figure 4-47 showing the minimum, maximum and average mineral F contents measured. Up to 22 measurements were made on any mineral. High F content was measured in a number of different minerals in pink monzogranite sample M3a and amphibole monzogranite sample M4a. In contrast, F was below detection limit in all minerals in weathered grey monzogranite sample M7c and in weathered M7b above detection limits only in apatite, biotite and chlorite (table 4-5).

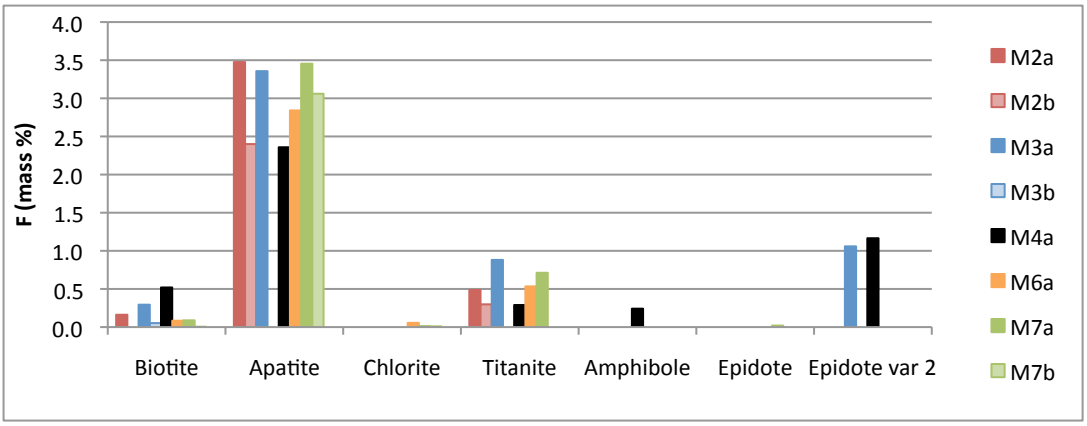

Figure 4-46 - Average F content of the principal F-bearing minerals in Maheshwaram samples

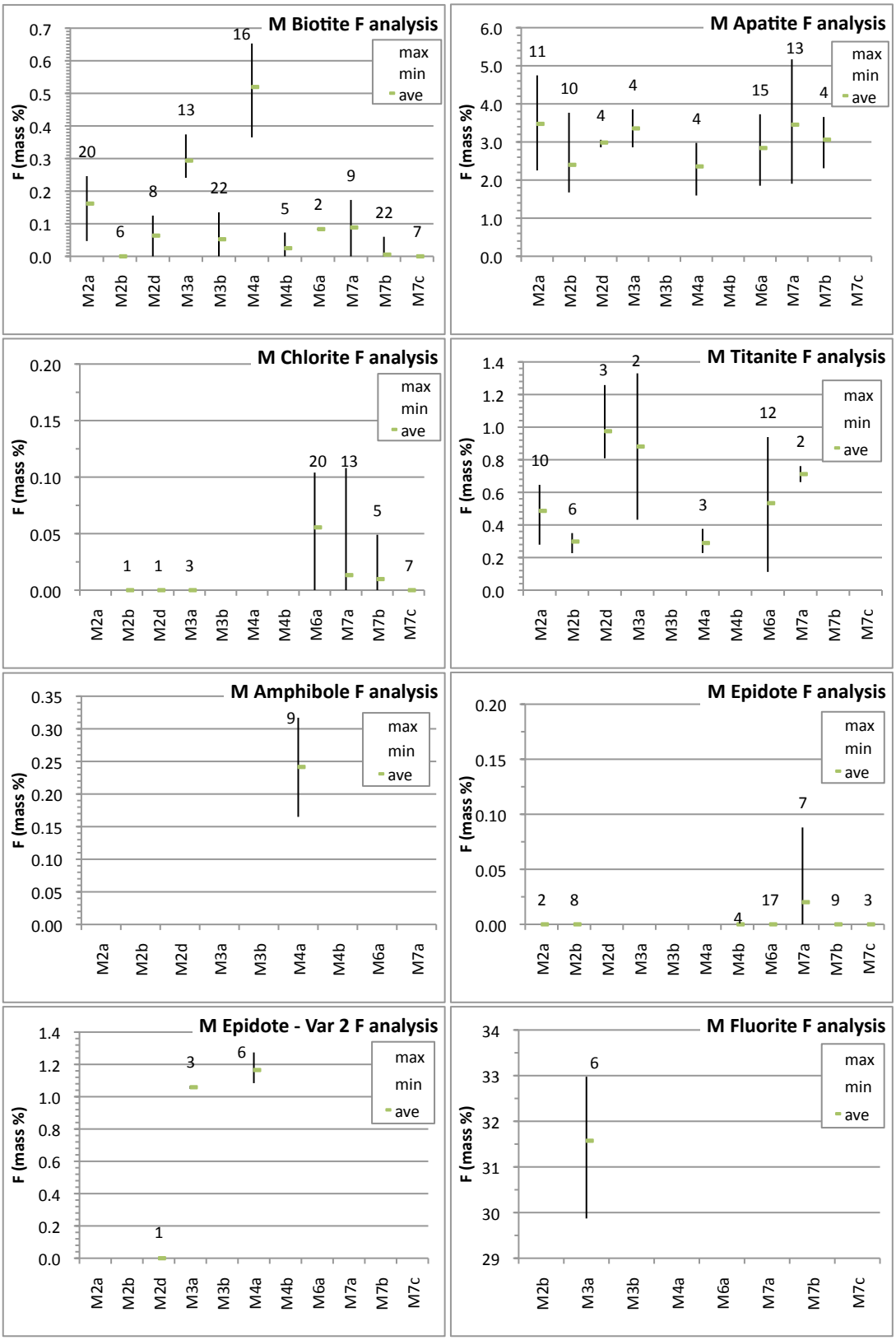

Figure 4-47 - Range and average F content of the main F-bearing minerals in Maheshwaram samples. Number of measurements given above each sample. Where no values are given, that mineral was either not present or not measured.

Table 4-5 - Average F content (mass %) of minerals in Maheshwaram samples. F=Fresh, W=Weathered. The two highest average mineral F concentrations for each sample in bold. Blank spaces indicate mineral not measured. Measurements below detection limit (0.05 mass % F) taken as zero for the purpose of average calculations.

	M2a	**M2b**	**M2d**	**M3a**	**M3b**	**M4a**	**M4b**	**M6a**	**M7a**	**M7b**	**M7c**
	F	**W**	**W**	**F**	**W**	**F**	**W**	**F**	**F**	**W**	**W**
Fluorite				**31.57**							
Apatite	**3.48**	**2.40**	**2.98**	**3.36**		**2.36**		**2.84**	**3.45**	**3.06**	
Titanite	**0.49**	**0.30**	**0.98**	0.88		0.29		**0.53**	**0.71**		
Epidote var 2			0.77	1.06		**1.17**					
Biotite	0.16	0	0.06	0.29	**0.05**	0.52	**0.03**	0.08	0.09	**0.01**	0
Amphibole						0.24					
Chlorite		0	0	0			0	0.06	0.01	0.01	0
Epidote	0	0						0	0.02	0	0
Iron oxide					0			0	0	0	
Ilmenite								0	0		0
K feldspar							0				
Na feldspar							0				
$CaCO_3$							0				

An example of the difference in F content between minerals within a sample is given in the EM-EDX element map in figure 4-48. Brighter areas of the maps indicate regions of higher F content. The mapped area includes K-feldspars and plagioclase feldspars, both of which show negligible fluorine. Biotite contains elevated F content, while brighter areas on the F-element map include titanite as a rim around the biotite (formed as an alteration product), apatite as long thin needles, as well as a very bright area of fluorite within the biotite. Weathering of biotite can be seen by the variation of K across the grain.

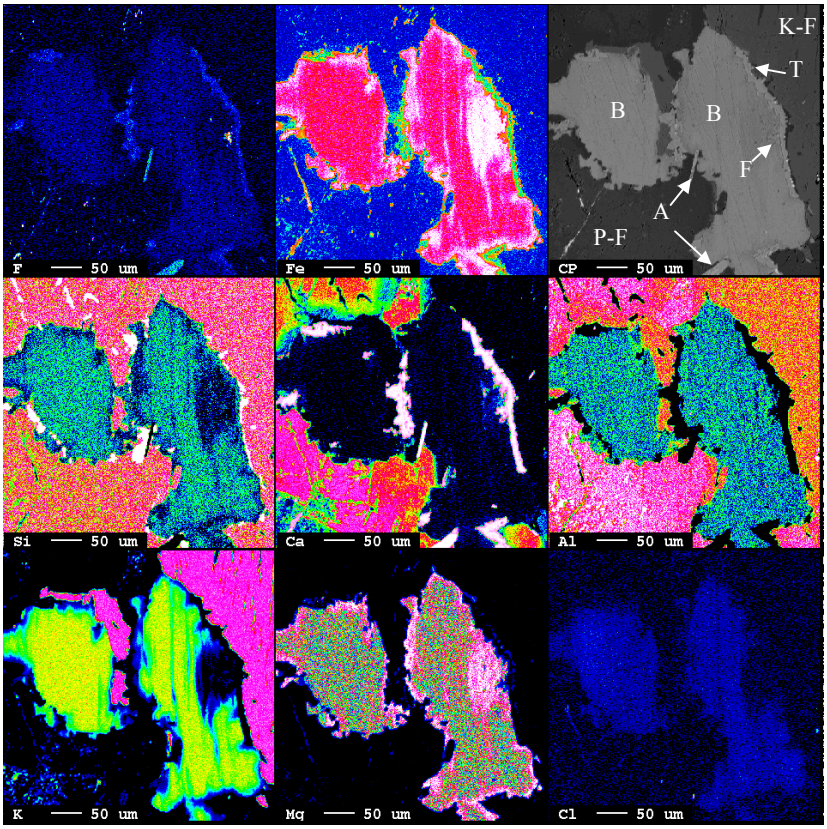

Figure 4-48 - Element mapping of an area of sample M3a produced by EM-EDX. Brighter areas indicate higher concentrations. Top right image is the backscattered electron (EBSD) image with mineral labels, A=apatite, B=biotite, F=fluorite, K-F=k-feldspar, P-F=plagioclase feldspar, T=titanite.

4.6.1.1 Biotite

Biotite is present in all Maheshwaram samples. The average F content of biotite in sample M4a (amphibole granite) is significantly higher at 0.52 mass % F than in all other samples (sig. at 1%). The next highest average biotite F concentration, 0.29 mass % F, is in sample M3a (pink monzogranite). Biotite in fresh grey monzogranite M7a and porphyritic epidote chlorite granodiorite M6a contain little F (average 0.09 and 0.08 mass % F, respectively) (figure 4-47).

Overall, biotite in fresh samples has significantly higher F content (average 0.27%) than in weathered samples (average 0.03%). This is also true in individual fresh-weathered pairs (all sig. at 1%). The weathering of biotite commences along the cleavages of the mineral resulting in the loss of interlayer potassium (K) ions, which may be used as a weathering indicator (see chapter 2, section 2.1.10). Despite much

individual scatter (figure 4-49) there is a positive relationship between average K_2O and F content in biotites (figure 4-50), linking loss of F in biotite to weathering.

Biotites in M2a have on average a higher K_2O but lower F content than other high K_2O biotites. This could indicate that biotite in this sample has naturally low F content. Low F and K_2O values in fresh sample M7a may be an indication that this sample has been subject to a higher degree of weathering than other fresh rock samples (recognised in sample descriptions, see table 4-1).

TiO_2 is also mobilised as biotite is weathered (figure 4-51). In many weathered samples titanite and titanium oxides are formed as weathering products.

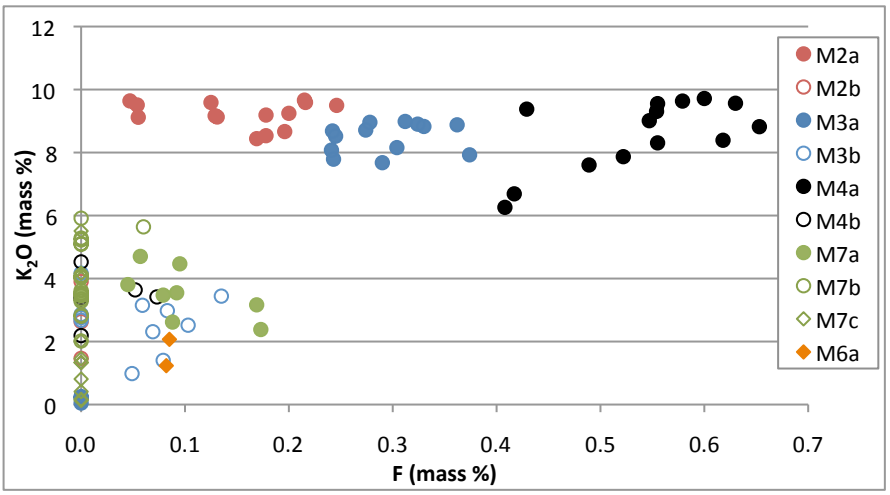

Figure 4-49 – F vs. K_2O (mass %) content in biotites in Maheshwaram samples. Fresh samples shown with solid markers, weathered samples shown with markers with no fill.

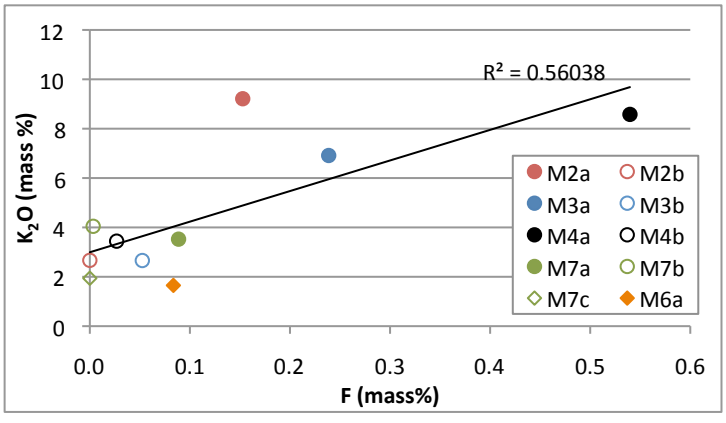

Figure 4-50 - Average K_2O and F in biotites in Maheshwaram samples. Fresh samples shown with solid markers, weathered samples shown with markers with no fill. Trend line and R^2 value shown.

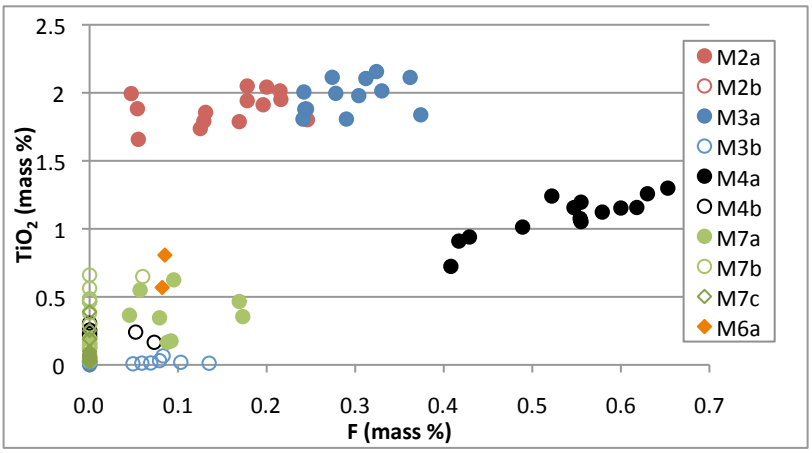

Figure 4-51 – F vs. TiO_2 (mass %) content in biotites in Maheshwaram. Fresh samples shown with solid markers, weathered samples shown with markers with no fill.

4.6.1.2 Chlorite

The F content of chlorite is low or below detection limit in Maheshwaram samples (figure 4-47). Chlorite was observed as an alteration product of biotite where F and K_2O have been removed but the structure of the biotite remains, and is present in all fresh samples and in weathered samples of M2 and M7. Chlorite in sample M6a (porphyritic epidote chlorite granodiorite) and M7a (grey monzogranite) have the highest F content measured (maximum 0.11 mass % F). Sample M6a also has a high chlorite content (8.4%). Several varieties of chlorite were identified using a chlorite classification spreadsheet (Tindle, 2009), including ripidolite (Mg-rich), brunsvigite (Fe-rich), pychnochlorite (Fe-Mg rich) and pseudothuringite (Al-Fe rich). There was no significant difference in F content between different chlorite types.

4.6.1.3 Titanite

Titanite is present in all fresh samples, and in weathered samples M2b and M2d (weathered porphyritic biotite granodiorite). High F content was measured in titanite in sample M2d and M3a (fresh pink monzogranite), and low F content in M4a (fresh amphibole monzogranite) and M2b (significantly lower to M2a, M6a, M7a and M2d at 5%) (figure 4-47). In sample M4a titanite is present as a primary mineral; in all other samples titanite is present as an alteration product, usually in association with biotite.

Partial substitution of Ti by Al in titanites is charge-compensated by fluoride-hydroxide anions substituting for oxygen in the structure (see chapter 2, section 2.1.5) (Malcherek et al. 1999) and so a correlation between Al substitution and F content would be expected (figure 4-52 and figure 4-53).

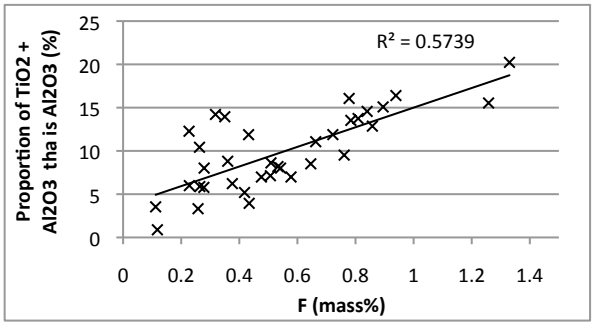

Figure 4-52 - Proportion of TiO_2 and Al_2O_3 that is Al_2O_3 (%) vs. F content in titanites in Maheshwaram samples

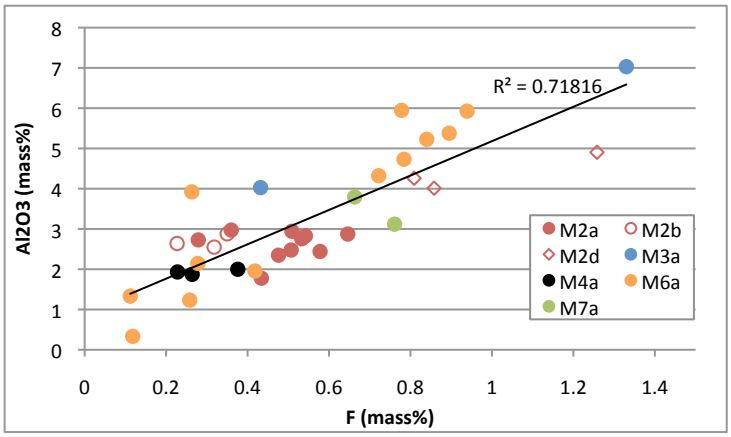

Figure 4-53 - F and Al_2O_3 content of titanites in Maheshwaram. Fresh samples shown with solid markers, weathered samples with markers with no fill

Overall there is no significant difference between the F content of fresh and weathered titanite, although the F content of titanite in fresh porphyritic biotite granodiorite sample M2a is significantly higher than in weathered sample M2b. Secondary titanite forming from alteration of biotite may incorporate some of the biotite F into its structure.

Figure 4-54 is an EM-EDX element map of sample M6a (porphyritic epidote chlorite granodiorite) showing chlorite and titanite with an ilmenite core. The chlorite has a low F content (average 0.06 mass % F by point analysis), whereas the titanite has a higher F content (average F 0.64 mass %). The F content of titanite varies across the mineral, with the right hand side of the mineral having a higher F content than the left

hand side of the mineral, which has been partly altered to ilmenite (F content below detection limit). Apatite is also present in the top right hand corner with a high F content (average F 2.64 mass %).

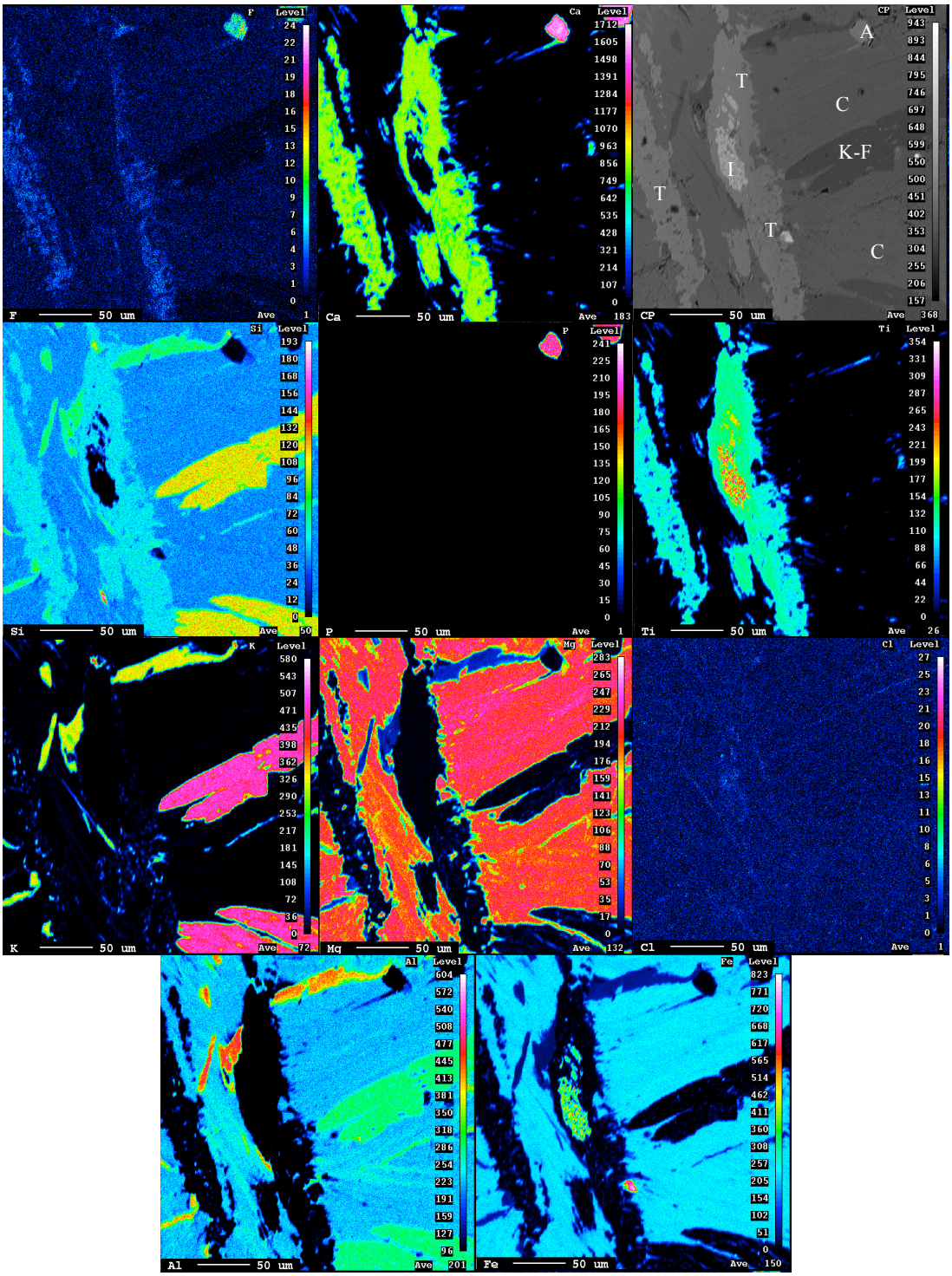

Figure 4-54 - Element mapping of titanite and chlorite in sample M6a produced by EM-EDX. Brighter areas indicate higher concentrations. Top right image is the EM-EBSD image with mineral labels, A=apatite, C=chlorite, I=ilmenite, K-F=K-feldspar, T=titanite.

4.6.1.4 Apatite

Apatite has the second highest average F content after fluorite in the Maheshwaram samples. All apatite samples measured are fluorapatite, with little variation in F content between fresh rock samples (figure 4-47), although sample M4a (amphibole monzogranite) has slightly lower apatite F content than other fresh rock samples. Overall, apatites in fresh samples (average 3.16 mass % F) have a higher F content than weathered samples (average 2.68%F) (significant at 5%).

4.6.1.5 Epidote (variety 1 and 2)

Two varieties of epidote (epidote and epidote var 2) were measured in Maheshwaram samples. Their average compositions are shown in table 4-6.

Table 4-6 - Average composition of epidote and epidote var 2 in Maheshwaram samples

	SiO_2	TiO_2	Al_2O_3	Cr_2O_3	FeO	MnO	MgO	CaO	Na_2O	K_2O	Cl	F	P_2O_5	Total
Epidote (Norm)	37.0	0.07	21.4	0.02	12.4	0.13	0.04	22.89	0.01	0.01	0.01	0.02	0.03	94.05
Epidote (var 2)	33.3	0.58	8.9	0.02	17.0	0.15	0.11	34.17	0.02	0.01	0.01	1.09	0.02	94.87

The F content of epidote in most samples is below detection limits (<0.05). Only two samples, the weathered amphibole monzogranite M4b and fresh grey monzogranite M7a, have epidote with measureable levels of fluoride (figure 4-47). No difference in F content of epidotes was seen between samples. Epidote var 2 has higher concentrations of F (figure 4-55), but few examples of this mineral were identified in thin section (figure 4-14 – d, page 99, shows a thin section photomicrograph of epidote var 2 in sample M4a).

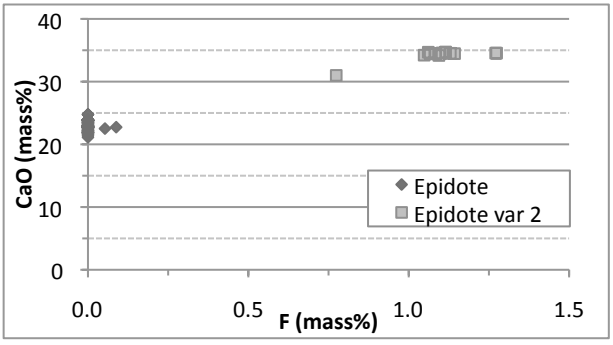

Figure 4-55 - CaO and F content of epidotes in Maheshwaram samples

Figure 4-56 shows an area of sample M4 consisting of biotite, amphibole, quartz, epidote, titanite and apatite. This biotite has slightly elevated F concentration

compared to quartz (this biotite has an average F concentration of 0.54% F), whereas the epidote is not noticeable on the F map due to low concentrations. Higher F concentrations are seen in apatite and in a titanite vein running across the biotite.

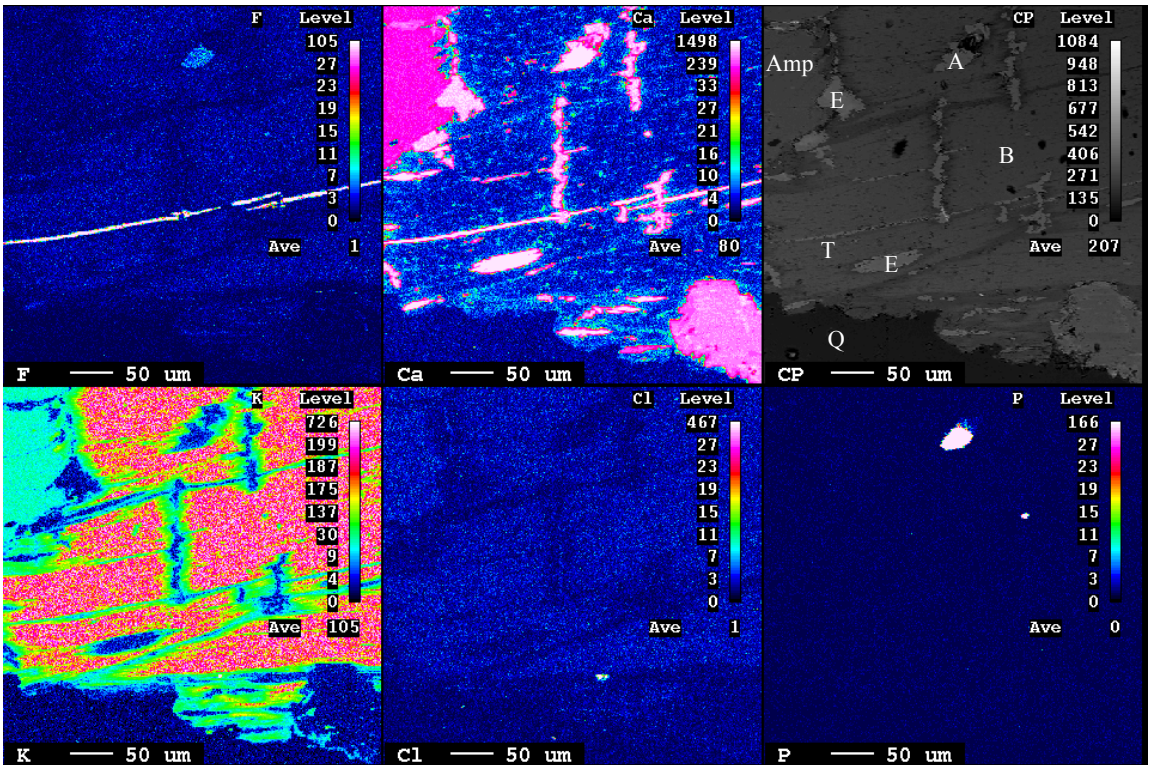

Figure 4-56 - Element mapping of an area of sample M4a produced by EM-EDX. Brighter areas indicate higher concentrations. Top right image is the backscattered electron (EBSD) image with mineral labels, A=apatite, Amp=amphibole, B=biotite, E=epidote, Q=Quartz, T=titanite.

4.6.1.6 Fluorite

Fluorite was observed in one sample, M3a (pink monzogranite), in small amounts (0.16%) in association with biotite (figure 4-11, page 97). EM-EDX point analysis of fluorite measured an average F content of 37.16% F. This is approximately ten times the F content of the more common F-bearing minerals such as apatite.

4.6.1.7 Amphiboles

One Maheshwaram sample, M4a (amphibole monzogranite), contained amphiboles. These were identified as magnesio-hornblende using an amphibole classification spreadsheet (Preston and Smith, 2002). The F content of magnesio-hornblende (average 0.24 mass % F) is lower than biotite, titanite, epidote var 2 and apatite in this sample. Amphiboles are usually easily weathered, releasing fluorine preferentially from their structure (Edmunds and Smedley, 2005).

4.6.2 Wailpally samples

The average F content measured by EM-EDX point analysis in all samples analysed is given in figure 4-57, figure 4-58 and table 4-7, and a summary in figure 4-59. Up to 18 measurements were made on any mineral. The porphyritic chlorite monzogranite (W1a), amphibole granodiorite (W11a), weathered granodiorite (W14b) and mafic vein sample (W13) have several minerals with a high average F content, whereas the F content of minerals in the pegmatite epidote quartz syenite sample (W17a) and weathered biotite granodiorite sample (W16b) is generally low. Fluorite has the highest F content, with apatite, titanite and epidote var 2 following.

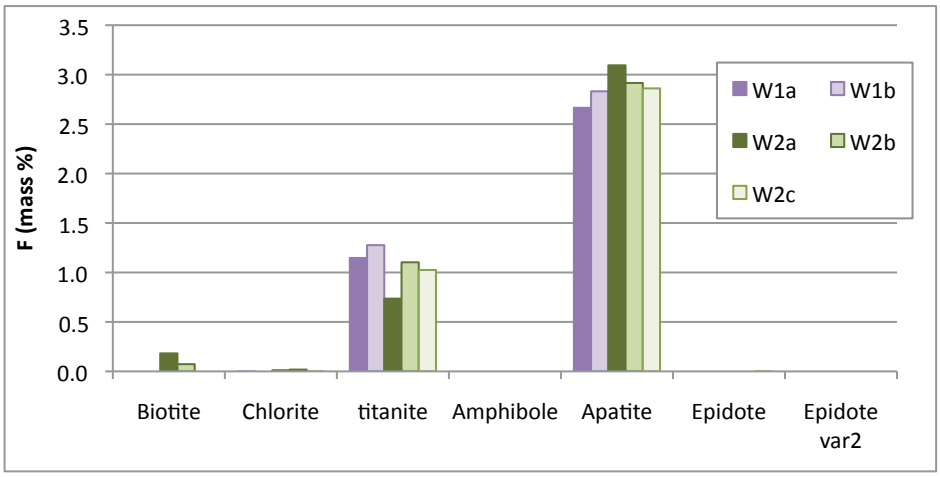

Figure 4-57 - Average F content of the principal F-bearing minerals in samples W1a (fresh), W1b (weathered), W2a (fresh), W2b (weathered), W2c (weathered)

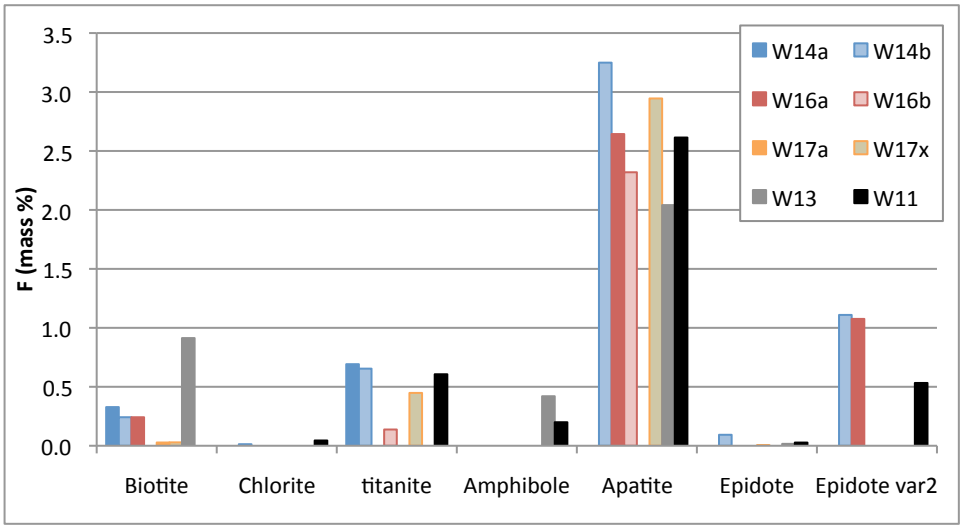

Figure 4-58- Average F content of the principal F-bearing minerals in samples W14a(fresh), W14b (weathered), W16a (fresh), W16b (weathered), W17a (fresh), W17x (weathered).

Table 4-7- Average F content (mass %) of different minerals in Wailpally samples. F=Fresh, W=Weathered. Sample C is a calcrete sample. The two highest average mineral F concentrations for each sample are in bold. Blank spaces indicate mineral not measured. Measurements below detection limit (0.05 mass% F) taken as zero for the purposes of average calculations

	W1a	W1b	W2a	W2b	W2c	W14a	W14b	W16a	W16b
F/W	**F**	**W**	**F**	**W**	**W**	**F**	**W**	**F**	**W**
Fluorite	**27.36**					**19.55**			
Apatite	**2.66**	**2.83**	**3.09**	**2.92**	**2.86**		**3.25**	**2.64**	**2.32**
Titanite	1.15	**1.28**	**0.74**	**1.10**	**1.03**	**0.69**	0.65		**0.14**
Epidote var2							**1.11**	**1.08**	
Ti Phosphate				0.38					
Biotite		0	0.18	0.07		0.33	0.24	0.24	0
Amphibole									
Chlorite	0		0.01	0.02	0	0	0.01		0
Epidote		0	0	0	0	0	0.09		
Epidote var 2									
Fe Oxide			0						
Ilmenite	0	0	0	0	0			0	
K feldspar								0	
Na feldspar		0							
Ti Oxide		0			0.07				0
Ca Oxide									
Quartz		0		0					

	W11a	W13	W-C	W17a	W17x
F/W	**F**	**F**	**N/A**	**F**	**W**
Fluorite					
Apatite	**2.61**	**2.04**			**2.95**
Titanite	**0.61**		**0.92**		**0.45**
Epidote var2	0.53				
Ti Phosphate					
Biotite		**0.91**	**0.13**	**0.03**	0.03
Amphibole	0.20	0.42			
Chlorite	0.04		0.06	0	0
Epidote	0.03	0.02	0	**0.01**	0
Epidote var 2		0.18		0	
Fe Oxide					
Ilmenite					
k feldspar					0
Na feldspar					0.03
Ti Oxide					
Ca Oxide			0.02		
Quartz			0		

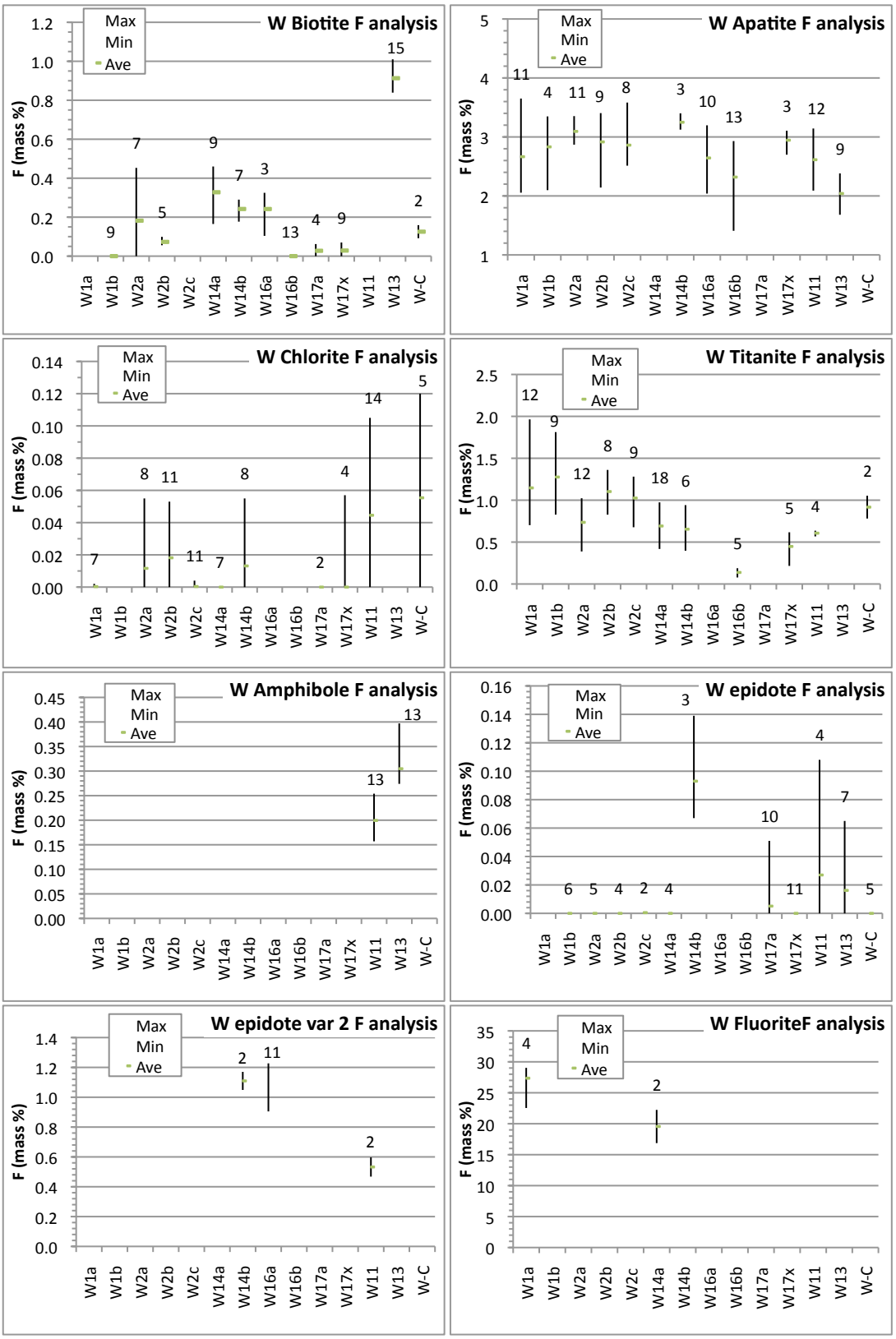

Figure 4-59 - Range and average F content of F-bearing minerals in Wailpally samples. Number of points measured shown above each sample.

4.6.2.1 Biotite

Biotite is present in all Wailpally samples except fresh samples W1a (porphyritic chlorite monzogranite) and W11a (amphibole granodiorite). The F content of biotite in mafic vein sample W13 (average 0.91 mass % F) is significantly higher than in all other samples (significant at 0.01 level) (figure 4-59). The next highest average biotite F content is 0.33 mass % F in sample W14a (granodiorite). Sample W17a (pegmatitic epidote quartz syenite) has the lowest fresh rock average biotite F content (0.03 mass % F), significantly lower than all other fresh rocks (significant at 0.05 level). Biotite F content in weathered samples W16b, W17b and W1b is also low (below, or close to the detection limit).

Overall, biotite F content in fresh samples is higher than in weathered samples (significant at 1%). This is observed in fresh-weathered rock pairs W2, W14 and W16 (figure 4-59). As discussed previously (section 4.6.1.1), biotite weathering is linked to K_2O content. In Wailpally samples, there is a positive relationship between K_2O and F content in biotite, both in individual and average values (figure 4-60 and figure 4-61). The K_2O and F content of biotite is high in sample W14b, suggesting that biotite in this sample has been little weathered. Loss of K_2O can also be observed within an individual mineral under EM-EBSD (see figure 4-68 on page 139).

Ti is also mobilised as biotite weathers, with a positive correlation between biotite F and TiO_2 content (figure 4-62).

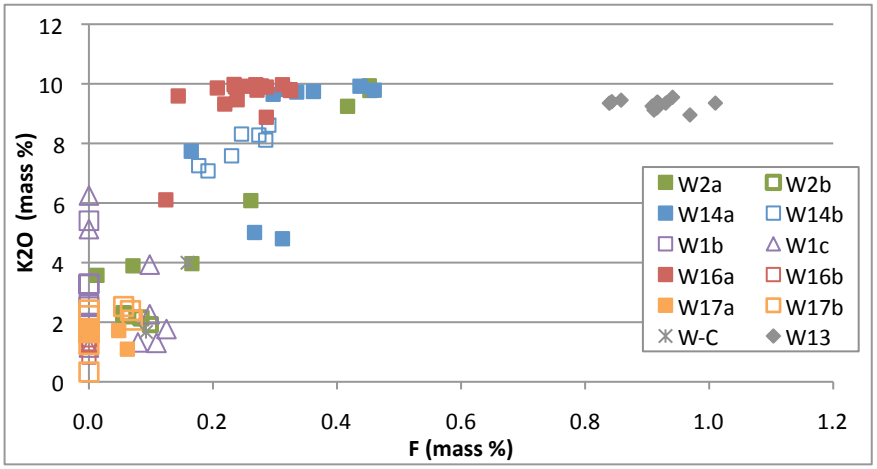

Figure 4-60- F vs. K2O (mass %) in biotite in samples from Wailpally (EM-EDX point analysis). Fresh samples shown with solid markers, weathered samples shown with markers with no fill.

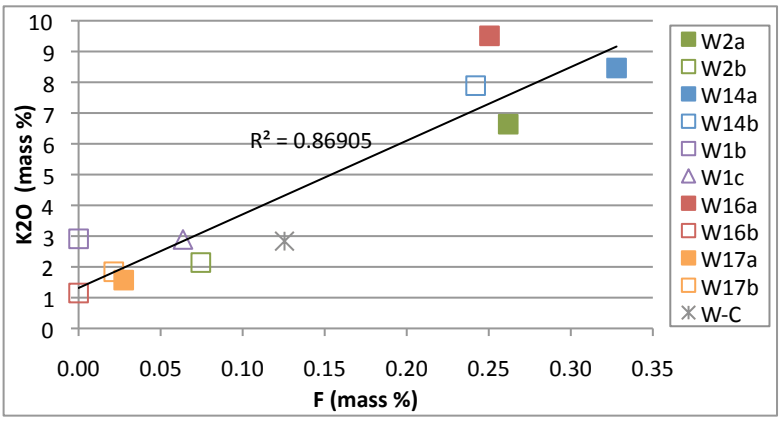

Figure 4-61 - Average K2O and F content of biotites in Wailpally samples (EM-EDX point analysis). Sample W13 not included

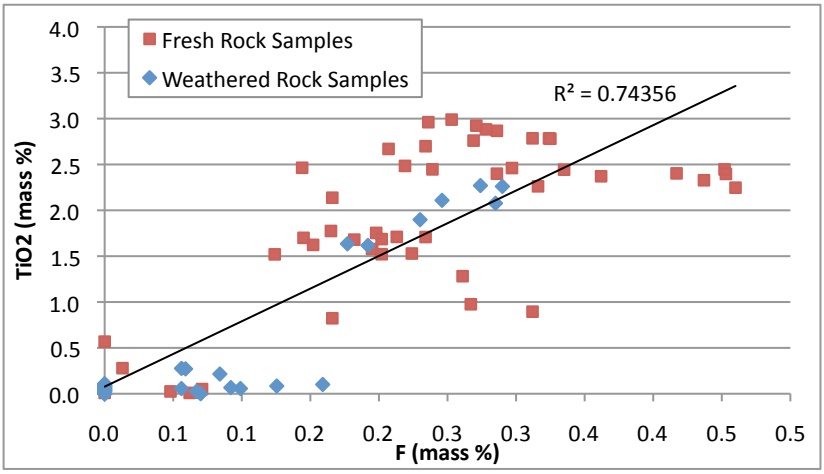

Figure 4-62 - F vs. TiO2 (mass %) in biotite in fresh and weathered rock samples from Wailpally (EM-EDX point analysis). Sample W13 not included in this figure.

4.6.2.2 Chlorite

Chlorite F content is low in all samples measured (figure 4-57 to figure 4-59). Chlorite in calcrete sample W-C and amphibole granodiorite sample W11a have a higher average F content (0.06 and 0.05 mass % F) than other samples, however these values are still very low (close to the detection limit) (figure 4-59). Ripidolite (Mg-rich chlorite), brunsvigite (Fe-rich), pychnochlorite (Fe-Mg rich) and some diabantite (Mg-rich) were identified using a chlorite identification spreadsheet (Tindle, 2009). Pychnochlorite has a higher average F content than ripidolite or brunsvigite (figure 4-63). Only two samples of diabantite were measured, both with high F content.

In many cases chlorite may be present as a weathering product of biotite.

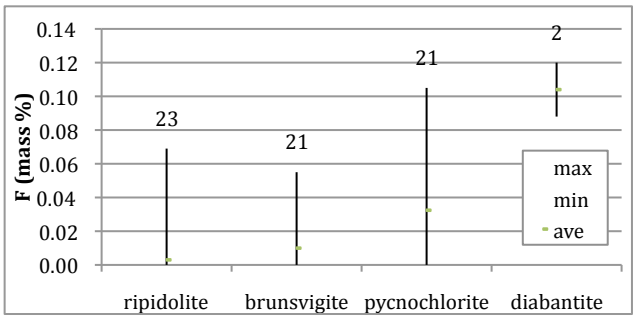

Figure 4-63 - Minimum, maximum and average F content in chlorites in Wailpally samples. Number of points measured shown above each mineral.

4.6.2.3 Titanite

The F content of titanite is high compared to many other F-bearing minerals (figure 4-57 to figure 4-59). In a large proportion of Wailpally samples titanite is present as an alteration product, however in fresh and weathered porphyritic samples (W1&b and W2&b) titanite is also present as a primary mineral. Titanite is not present in fresh biotite granodiorite (W16a), the mafic vein sample (W13), or the pegmatite sample (W17a). The average titanite F content varies little between fresh and weathered samples, apart from samples from W2 (porphyritic epidote granodiorite). Here the weathered samples W2b and W2c have a higher titanite F-content than their fresh rock counterpart W2a (significant at 1%). Secondary titanite forming from biotite may incorporate some of the biotite F into its structure.

A weak positive relationship is seen between Al_2O_3 and F (figure 4-64). Substitution of Al and Fe for Ti in titanite may often be charge-compensated by fluoride-hydroxide ions (see chapter 2, section 2.1.5) as demonstrated in Maheshwaram samples (section 4.6.1.3).

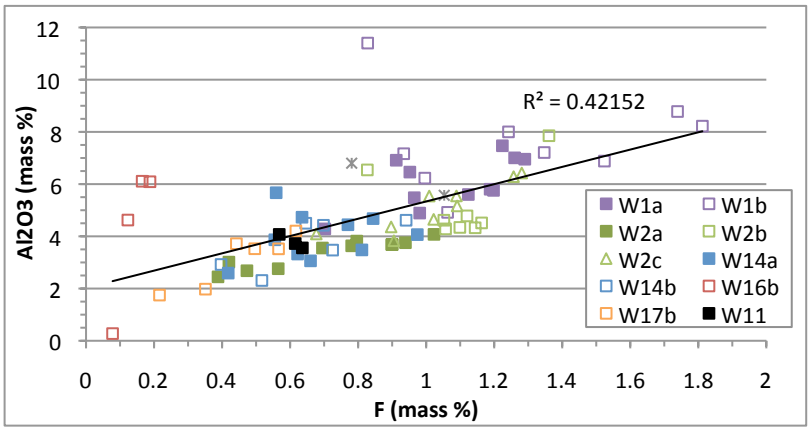

Figure 4-64 - F and Al2O3 in Titanite in WP samples. Fresh rock samples shown as solid markers, weathered rock samples as markers with no fill.

Element mapping of titanite in sample W1b (weathered porphyritic chlorite monzogranite) is shown in figure 4-65. Here a large titanite crystal has been altered to iron oxides and titanium oxides. Elevated F content is mapped in the titanite (average F 1.67% in this area by point analysis) and a small apatite grain (average F 2.10% in this apatite), but F is below detection limit in Fe and Ti oxides. The titanite present shows spatial variations in composition (in both Ti and Al content).

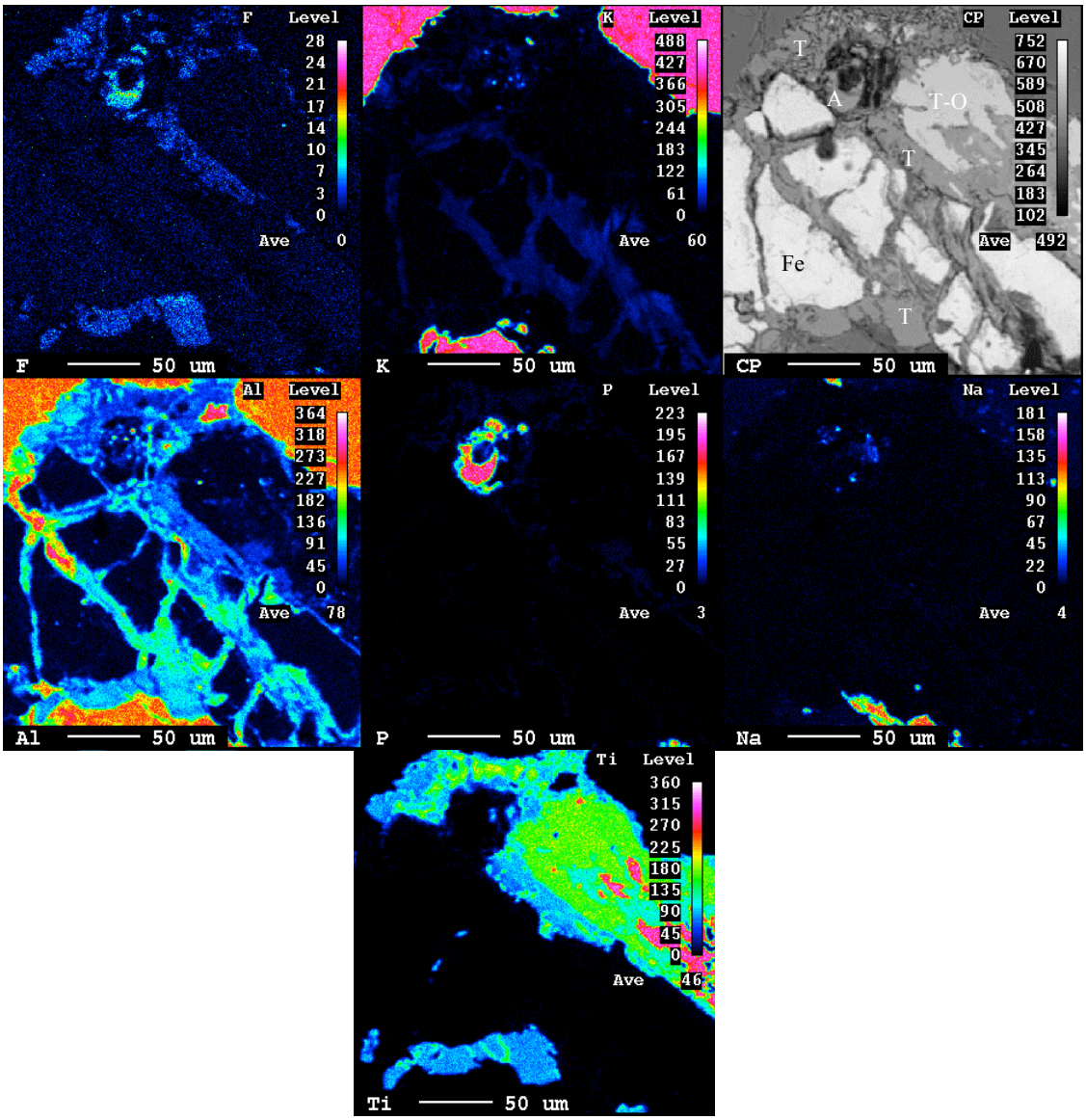

Figure 4-65 - Element mapping of an area of sample W1b produced by EM-EDX. Brighter areas indicate higher concentrations. Top right image is an EM-EBSD image with mineral labels, A=apatite, Fe=iron oxide, T=titanite, T-O=titanium oxide.

4.6.2.4 Apatite

Apatite has the highest average F content after fluorite in the Wailpally samples (average 2.71 mass % F) and is present in all samples apart from W14a and W17a. The F content of apatite is similar between all samples, apart from mafic vein sample W13 which has a low average apatite F content (2.04 mass % F) (figure 4-59). The F content of apatite does not change significantly between fresh samples and their weathered equivalents.

Element mapping (EM-EDX) of a large apatite crystal surrounded by biotite, titanite and epidote is given in figure 4-66. High F content is measured in apatite (average 3.45 % F in this area) with little variation across the crystal. Weathered chlorite (average 0.00% F in this area) and titanite (average 0.95% F in this area) are present as well as some epidote (figure 4-66).

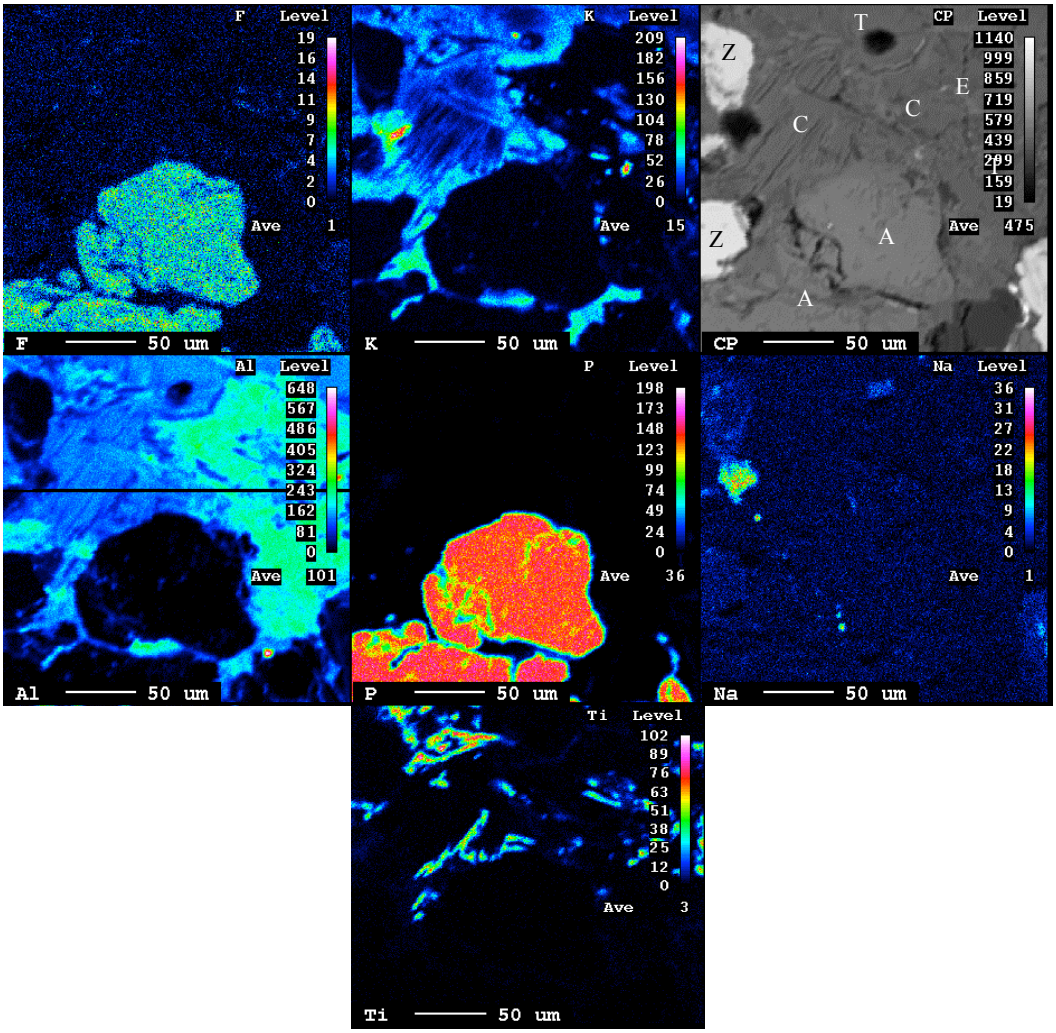

Figure 4-66 – W2c element map (EM-EDX). Brighter areas indicate higher concentrations. Top right image is the EM-EBSD image with mineral labels, A=apatite, C=chlorite, E=epidote, T=titanite, Z=zircon.

4.6.2.5 Epidote (variety 1 and 2)

Two varieties of epidote (epidote and epidote var 2) were measured in Wailpally. Table 4-8 shows their average composition. Epidote has a low F content in all samples (below detection limit in most measurements). Epidote var. 2 (high Ca) has a higher F content (average 1.01 mass % F) (table 4-6, figure 4-67), however is less common (see point counting). Epidote var. 2 in W11a has a lower F content than other samples (figure 4-59).

Table 4-8 - Average composition of epidote varieties in Wailpally samples

	SiO_2	TiO_2	Al_2O_3	Cr_2O_3	FeO	MnO	MgO	CaO	Na_2O	K_2O	Cl	F	P_2O_5	Total
Epidote Normal	36.6	0.08	22.6	0.04	13.0	0.15	0.21	22.6	0.03	0.03	0.02	0.01	0.02	95.3
Epidote (Var. 2)	34.1	1.58	9.8	0.01	15.7	0.16	0.05	34.6	0.02	0.02	0.03	1.01	0.01	97.0

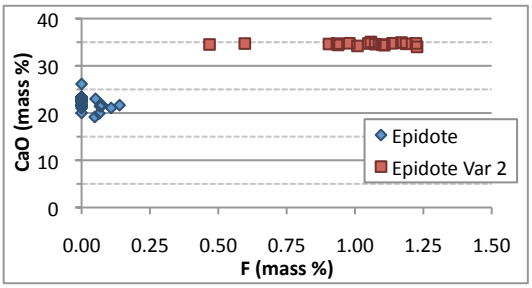

Figure 4-67- CaO and F content of epidote in Wailpally samples

4.6.2.6 Fluorite

Fluorite was identified and measured in fresh rock samples W1a (porphyritic chlorite monzogranite) and W14a (granodiorite). A small amount of fluorite was observed in W16a (biotite granodiorite), but this was not confirmed under EM and due to its small size cannot be confirmed as fluorite from optical petrology alone. Fluorite was not found in any weathered samples. The F content of fluorite is much higher than in other F-bearing minerals, with F as a major component of the structure (CaF_2). In sample W14a, fluorite (average 19.6 mass % F) was located within biotite, closely associated with an aluminium oxide (figure 4-68). Fluorite in sample W1a (average 27.4 mass % F) was found within chlorite as a mass of fluorite and titanite with a centre of high CaO and low fluorine. Where fluorite is present this is a potentially significant source of F to water. As Fluorite was not found in the weathered rock samples this may indicate that the fluorite has been removed upon weathering.

Fluorite within biotite was mapped in fresh granodiorite sample W14a (figure 4-68 and figure 4-69). The biotite here has varying composition, as seen by the variation in K_2O and TiO_2 content shown in the element map (figure 4-69), and shown by the alternating light (high K_2O) and dark (low K_2O) 'stripes' in figure 4-68. A small amount of F is also measured in biotite (average F 0.32% in this area) and titanite (average F 0.81% in this area) (figure 4-69), although this is masked in the element map by the high F content of fluorite.

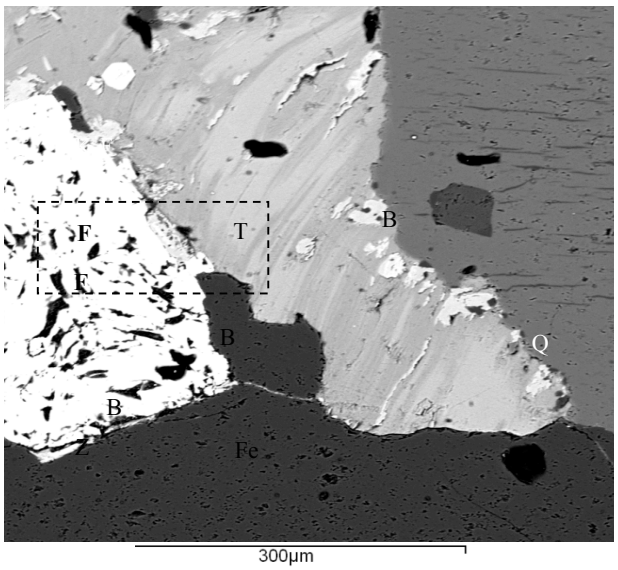

Figure 4-68 – EM-EBSD image of biotite with titanite and fluorite in sample W14a. B=biotite, F=fluorite, Fe=iron oxide, K-F=potassium feldspar, Q=quartz, T=titanite, Z=zircon. Dashed box shows area mapped in figure 4-69.

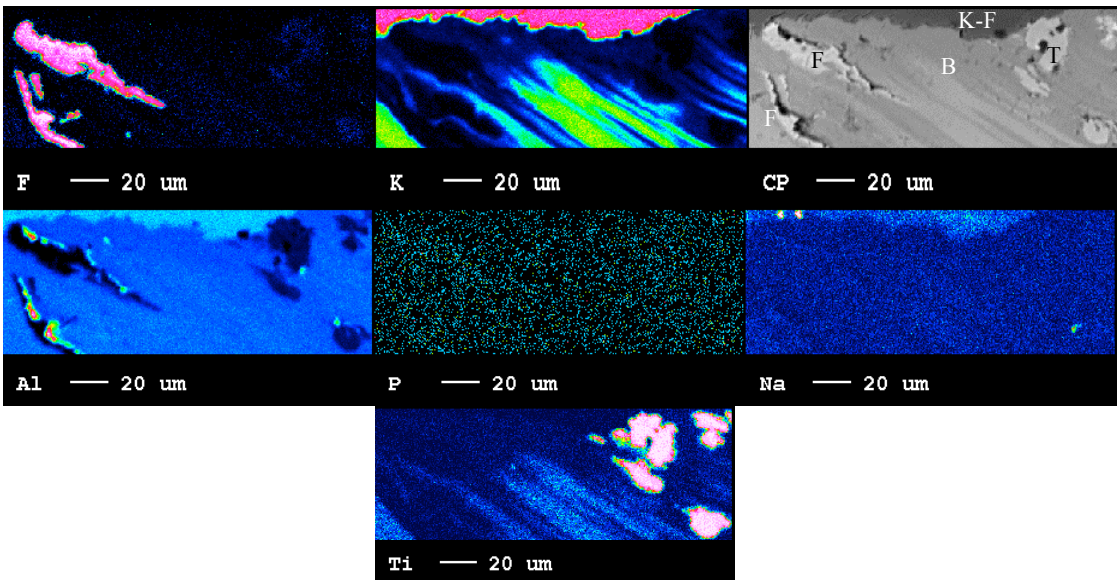

Figure 4-69 - Element mapping of an area of sample W14a produced by EM-EDX. Brighter areas indicate higher concentrations. Top right image is the EM-EBSD image with mineral labels, B=biotite, F=fluorite, K-F=potassium feldspar, T=titanite.

4.6.2.7 Amphiboles

Amphiboles are present in two samples, W13 (mafic vein material) and W11a (amphibole granodiorite). Amphiboles in sample W13 are calcic amphiboles, mainly magnesio-hornblende, with some actinolite also. In sample W11a the amphibole is also a calcic amphibole, ferro-edenite. The F content of amphiboles in W13 is higher than in sample W11a (average 0.30 and 0.20 mass % F respectively, difference significant at 1%) (figure 4-59). Amphiboles with a higher MgO content and lower Fe content have a higher F content (figure 4-70 and 4-71).

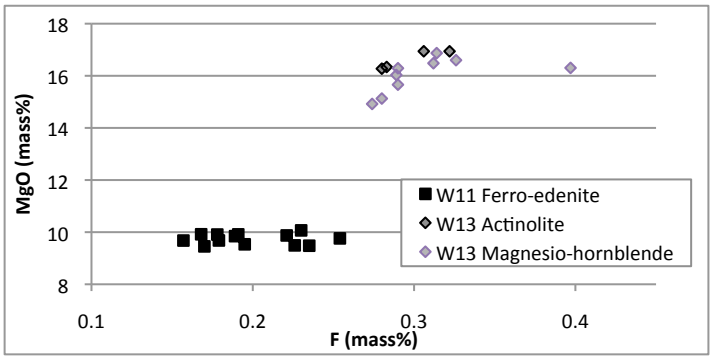

Figure 4-70 - F vs. MgO (mass %) in amphiboles in samples W11a and W13

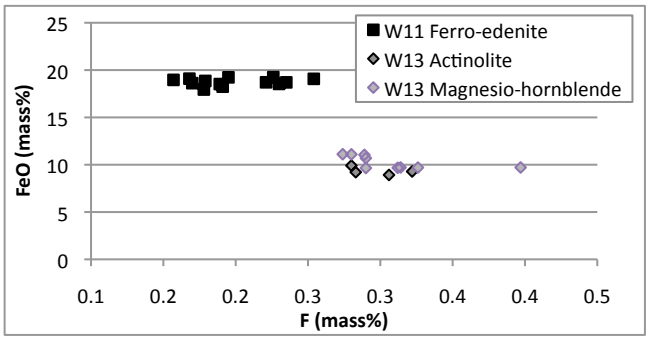

Figure 4-71 - F vs. FeO in amphiboles in samples W11a and W13

4.6.2.8 Other minerals

The F content of iron oxides, ilmenite and titanium oxides were below detection limits in almost all measurements. Two exceptions included a titanium oxide in sample W2c (composition 50-70% TiO_2, 1.5-2.5% SiO_2, 4-6.5% FeO and a range of 0.06-0.07% F), and a titanium phosphate in W2b (composition 63-65% TiO_2, 4-5% FeO, 6-9% P_2O_5 and average of 0.38% F).

The F content of calcite in sample W-C (calcrete) was in most cases either below or close to the detection limit, with an average (over 11 measurements) of 0.02 mass %

F. As this sample is largely made up of calcite this may form an important source of F.

All measurements of quartz, plagioclase feldspar and alkali feldspar had F content below detection limits (quartz measured in 3 samples, alkali feldspar in 2 samples and plagioclase feldspar in 2 samples). This was expected as these minerals do not often contain fluorine.

4.6.3 Comparison and Summary of Mineral F Content in Maheshwaram and Wailpally

Table 4-9 shows the F-bearing minerals present in the research catchments, their occurrence and average F content, and table 4-10 shows the average F content of F-bearing minerals in fresh and weathered samples.

Of the F-bearing minerals present in the research catchments, fluorite and apatite have the highest average F content (average 28.95 and 2.96 mass % F respectively), and chlorite and epidote have the lowest average F content (average 0.03 and 0.01 mass % F respectively). Biotite and apatite are common in both catchments, whereas amphiboles, primary titanite and fluorite are present only in particular samples. Epidote and chlorite are common minor minerals in many samples, but do not have high F content. Mafic vein (W13) biotite and amphiboles have an F content higher than that of any other sample measured, with averages of 0.91 and 0.42 mass % F respectively. The abundance of these minerals in W13 and their high F content makes this an important source of F within the fresh rock.

Fluorite, with a high F content (17-32 mass % F) is rare, and where present it is a trace mineralogical constituent contributing less than 0.2% of the total sample (point counting) (table 4-9). Fluorite was usually found in association with biotite or chlorite. No fluorite was found in weathered samples.

Apatite, with the second highest F content after fluorite, has a higher average F content in fresh samples in Maheshwaram than Wailpally (3.16 and 2.63 mass % F respectively, difference significant at 1%). Maheshwaram fresh samples also have a higher apatite F content than Maheshwaram weathered samples (table 4-10). Apart from this, little variation was seen between individual samples.

Titanite is present in many samples as an alteration product, and in some samples as a primary mineral with large crystals that are in most cases severely weathered. In both catchments, titanite has a high F content, higher on average in Wailpally samples than in Maheshwaram samples (table 4-10). Titanite in both catchments showed a positive linear relationship between F content and Al_2O_3 content (although a stronger correlation is shown in Maheshwaram samples).

In both catchments, biotite F content is higher in fresh samples than weathered samples, showing a positive relationship between K_2O and F content indicating F loss upon weathering. Biotite F content is high in the mafic vein sample W13, the amphibole monzogranite M4a, and the granodiorite sample W14a (average 0.91, 0.52 and 0.33 mass % F, respectively) (figure 4-72) and low in the weathered samples and in fresh grey monzogranite sample M7a, porphyritic epidote chlorite granodiorite sample M6a and pegmatitic epidote quartz syenite sample W17a (average 0.09, 0.08 and 0.03 mass % F, respectively). Biotite in Wailpally weathered samples has a higher average F content than in Maheshwaram weathered samples, possibly due to Maheshwaram biotite samples being further weathered, as suggested by K_2O content.

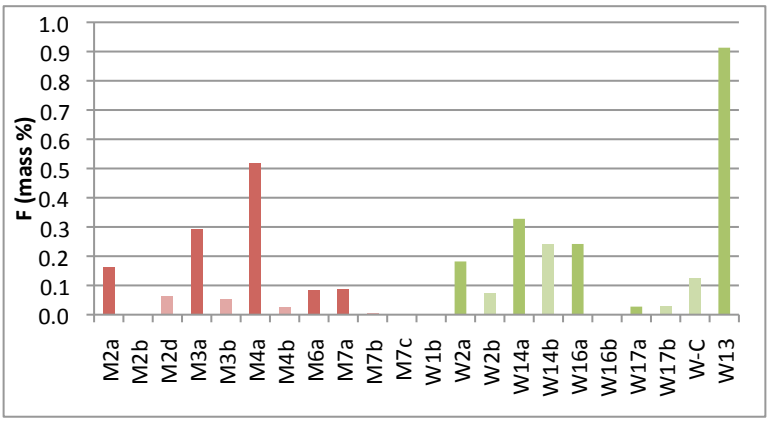

Figure 4-72 - Average F content of biotite in Maheshwaram and Wailpally samples. Weathered samples are shown as faded bars.

Three samples contain amphiboles (M4, W11, W13, including magnesio-hornblende, actinolite, and ferro-edenite). Amphiboles in sample W13 have significantly higher F content (0.30 mass % F) than in M4 and W11a (significant at 1%), which have similar F contents (0.24 and 0.20 mass % F respectively). No amphiboles were seen in weathered samples. Amphiboles are fairly easily weathered and on weathering release fluorine preferentially from their structure.

Table 4-9– The occurrence of F-bearing minerals and the average F content in Maheshwaram (M) and Wailpally (W) fresh rock samples

Mineral	Occurrence	Average F content in fresh rocks (mass %)		Notes
		M	W	
Fluorite 	Rare. When present, only in small quantities (<0.2%). Pink monzogranite (M3) porphyritic chlorite monzogranite (W1) granodiorite (W14)	31.57	26.33	Removed upon weathering (not found in weathered samples).
Apatite 	Present in most samples. Abundance from 0.1-1.2 %.	3.16	2.75	Average F content less in weathered samples than fresh samples in M. Similar F content in all W samples.
Epidote Var 2 	Not common. Present in 5 fresh samples and 2 weathered. Abundance 0.1-0.7%	1.13	0.99	
Titanite 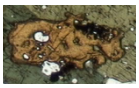	Common as an alteration mineral. Present as a primary mineral only in amphibole monzogranite (M4), porphyritic chlorite monzogranite (W1) and porphyritic epidote granodiorite (W2).	0.53	0.79	Average F content higher in W samples than M samples. Secondary titanite may retain F from the weathering of biotite.
Biotite 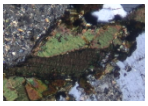	Common. Abundance ranges 0-22%	0.27	0.25	Loses F upon weathering as indicated by correlation with K_2O. Biotite in fresh samples has a higher F content than weathered samples. Biotite in the Amphibole monzogranite (M4a), Granodiorite (W14a) and mafic vein material (W13) has a higher F content than other samples.
Amphiboles 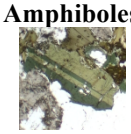	Present only in amphibole monzogranite (M4a), amphibole granodiorite (W11a) and mafic vein material (W13). Abundance within these samples ranges 7-37%	0.24	0.20	Removed upon weathering (not found in weathered samples).
Chlorite 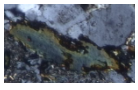	Present in most samples. Abundance 0-9%	0.03	0.02	F content low or below detection limit in all samples.
Epidote 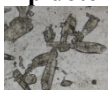	Present in many samples. Usually with a low abundance, but in some samples this is up to 14%	0.00	0.01	F content low or below detection limit in all samples.

In both catchments chlorite and epidote F content is near to or below detection limits (table 4-10). Several varieties of chlorite were identified, with a higher average F-content in pychnochlorite than in ripidolite and brusvigite in Wailpally samples. Two varieties of epidote were measured, with epidote (var 2) having a higher F content than epidote (normal) (table 4-9).

XRD results show clays to be present in the weathered samples measured (samples M2b M3b and M7b). It was not possible to observe these minerals in point counting and EM-EDX, however they may be an important source of F in the weathered rock (see chapter 2, section 2.1.13)

Table 4-10 - Average F content in F-bearing minerals in Maheshwaram and Wailpally (sample W13 given separately)

Mineral	In Fresh/Weathered Samples	Average F (mass %)	
		Maheshwaram	Wailpally
Biotite	Fresh	0.27	0.25
	Weathered	0.03	0.07
	W13	-	0.91
Chlorite	Fresh	0.03	0.03
	Weathered	0.00	0.03
Titanite	Fresh	0.53	0.79
	Weathered	0.52	0.92
Apatite	Fresh	3.16	2.63
	Weathered	2.68	2.76
Fluorite	M3a	31.57	-
	W1a	-	22.54
	W14a	-	16.87
Amphiboles	M4a	0.24	-
	W11a	-	0.20
	W13	-	0.42

4.6.4 Comparison of Mineral F Content with other Published Mineral F Content

Table 4-11 shows published F content of F-bearing minerals, as well as the average measured F content from fresh Maheshwaram and Wailpally samples. The average mineral F contents from mafic vein sample (W13) are also given for comparison. In most cases measured F contents are within or similar to the published F content range. The published F content for fluorite is higher than the measured F content of

fluorite in both Maheshwaram and Wailpally. This may be due to the small mineral size of fluorite in thin section making analysis difficult, or due to the formation of fluorite as a secondary mineral within biotite giving a lower F content. Epidote var 2 has a high F content compared to epidote, although no published values of epidote F content are given.

Table 4-11 – Comparison of average mineral F content in Maheshwaram and Wailpally with published ranges. *formula for magnesio-hornblende. **formula for ripidolite. ($^{+}$)Epidote var 2 samples. Values in italics from Correns (1956). Other published values from Deer et al. (1992). Average F content for W samples not including W13.

Mineral	Formula	Published F content (mass %)	F content M (fresh)	F content W (fresh)	F content W13 Mafic vein
Amphiboles	$Ca_2(Mg,Fe)_4Al[Si_7AlO_{22}](OH)_2$*	0-2.69 *0.027-2.9*	0.24	0.20	0.42
Apatite	$Ca_5(PO_4)_3(OH,F,Cl)$.	0.16-5.60 *1.35-2.56*	3.16	2.75	2.04
Biotite	$K_2(Mg,Fe)_4(Fe,Al)_2[Si_6Al_2O_{20}](OH)_2(F,Cl)_2$	0-0.91 *0.095-3.5*	0.27	0.25	0.91
Chlorite	$(Mg,Fe,Al)_6(Si,Al)_4O_{10}(OH)_8$.**	Not given	0.03	0.02	N/A
Epidote	$Ca_2(Fe^{3+},Al)Al_2O.OH.Si_2O_7.SiO_4$	Not given	0.01 (1.13^{+})	0.01 (0.99^{+})	0.02
Fluorite	CaF_2	*51.33*	31.57	26.33	N/A
Titanite	$CaTi[SiO_4](O,OH,F)$	0.61	0.53	0.79	N/A

4.7 Whole Rock Fluorine Analysis (WRF)

The whole rock fluorine (WRF) content of each sample was measured using the Ingram (1970) method with slight adaptations (for full method see appendix 2). Samples were prepared and measured using a fluorine ISE in two runs. Repeat measurements were taken of all sample solutions and each measurement converted to ppm F values using the two adjacent calibrations. Where possible, samples were prepared in duplicate. The values of duplicates and repeats are presented in addition to average values. WRF values for profile samples are given in chapter 5, section 5.2.

WRF content is compared between samples of equivalent lithology, between fresh and weathered rocks and with other mineralogical results.

USGS geological reference standard G2 was used to test the accuracy of analysis. This is a powdered and homogenised sample of granite from Rhode Island, USA. Two samples of G2 were analysed, the WRF value of which should be 1280 ± 80 ppm F. In both cases the WRF value measured for G2 was low, with averages of 1001 and 958 ppm F (table 4-12). Low values could be due to deficiencies in the method of extraction of F from the solid sample into solution, or due to low ISE sensitivity and accuracy. Low values may also be due to solution matrix effects as the fluorine ISE only measures free fluoride ions and not complexed fluorine (Stecher, 1983). A list of other potential sources of error is given in appendix 2. Repeat solution measurements at close intervals, calibrated with the same standard set give different F values (table 4-12), showing the accuracy of ISE measurement to be low. A slow drift in measured mV value is observed in readings of standard calibration solutions, with values decreasing slightly throughout the measurement period, although this drift is less than the differences in measurements taken (see appendix 2 for details). The standard deviation of measurements in this study is 75.6, and can be cited as ±7.6%, whereas a precision of ±2% has been reported as achievable (Stecher, 1983).

Fluorine has been measured in several international standards using the Ingram (1970) method with a fluorine ISE by Stecher (1983) where it was also found that this method gives consistently low results, but that accuracy can be improved by

decreasing the ratio of sample weight to dissolved volume, or by combining this calibration method with the method of standard additions (as by Troll et al. (1977)) which gives consistently high results. Either of these approaches would be recommended for further experiments.

Table 4-12 Whole rock fluorine measurements of reference material G2 (1280 ± 80 ppm F). Two separate sample preparations are given, G2 and G2 repeat. WRF values for each sample are calculated from multiple ISE readings of the same solution.

Sample	WRF (ppm F)	Average F of each sample	Average F	Standard Deviation
G2	1035	1011	992	75.6
	873			
	1001			
	941			
	1031			
	1142			
	1061			
G2 - repeat	1003	958		
	974			
	945			
	908			

The low F value of G2 obtained, as well as the accuracy of repeat ISE readings should be considered when interpreting sample results. As most of the samples are the same type of material as G2 (i.e. granite) it may be assumed that the proportion of F extracted during sample preparation is similar and therefore that analytical results can be compared between samples. Most sample solutions were measured two to three times allowing for comparison of repeat ISE readings.

4.7.1 Results

ISE Calibration

Electrode calibration using standard solutions gives a regression line with a good fit (R^2 = 0.98-0.99) and shows a suitable range between mV readings for the majority of calibration sets (the guideline difference in mV readings for solutions with a decade difference in F concentration is 54-59mV). The decade difference at low F values is lower in both runs (between 52 and 53 mV difference in run 1, between 32 and 57 mV difference in run 2) indicating a lower accuracy at low F values. Standard

solutions drift gradually over the measurement period so regular re-calibration is necessary (see appendix 2).

Where samples are out of calibration range, results are given as 'below x', where 'x' is the equivalent WRF value of the lowest F standard solution. Only samples within calibration range are used for averages. Details of standard solutions are given in appendix 2. Repeat samples give similar results, indicating an adequate precision (table 4-13 and table 4-14).

Maheshwaram

Sample M2a (porphyritic biotite granodiorite) has the highest WRF value (1749 ppm F), with M4a (amphibole monzogranite) following (1159 ppm F) (figure 4-73, table 4-13). The high WRF value of M2a is due to the abundance of biotite and apatite in this sample, and the high WRF value of M4a is due to the abundance of hornblende and high F content of biotite. These two samples have by far the highest WRF values, with all other samples below 500 ppm F.

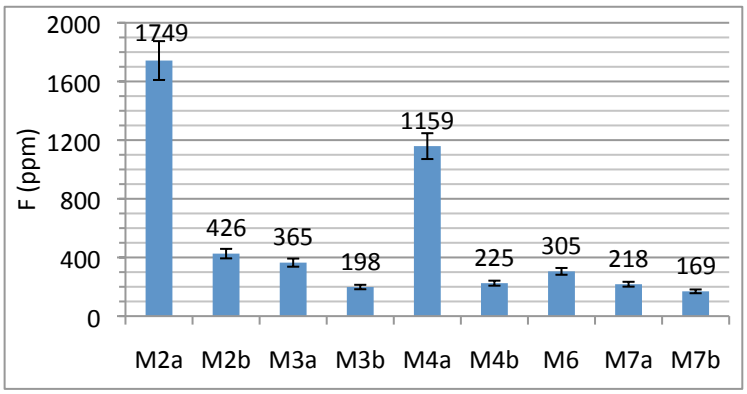

Figure 4-73 – Maheshwaram average Whole Rock Fluorine content in each sample. Value given above each sample. Error bars (7.6%) shown.

Low WRF values are measured in weathered samples and in fresh samples M3a (pink monzogranite), M6a (porphyritic epidote chlorite granodiorite) and M7a (grey monzogranite) (figure 4-73). Sample M3a contains fluorite with a high F content, however fluorite is only a trace mineralogical constituent (0.2%) and therefore does not contribute a large amount to total rock F. Samples M6a and M7a have low mineral F content and/or a low abundance of F-bearing minerals.

In all sample pairs, the fresh rock sample has a higher WRF value than their weathered equivalent. This is to be expected from mineralogical results as the fresh samples have a greater abundance of F-bearing minerals, often also with a higher F content.

Table 4-13 – Maheshwaram Whole Rock Fluorine (WRF) values. WRF values are calculated from ISE readings using the two adjacent calibration sets, giving two values for each reading. Repeat ISE readings are also given. Repeat samples prepared are indicated by an 'r' by the sample name.

Sample	Rock Type	WRF value (ppm F)		Average (ppm F)
		Initial Readings	Repeat Readings	
M2a	Porphyritic biotite granodiorite	1725	1814	1749
M2a (r)		1801	1657	
M2b	Weathered sample	447	406	426
M3a	Pink monzogranite	436	394	365
M3a (r)		340	289	
M3b	Weathered sample	213	184	199
M4a	Amphibole monzogranite	1256	1267	1159
M4a (r)		1117	997	
M4b	Weathered sample	221	194	225
M4b (r)		251	246	
M4b (r)		202	234	
M6	Porphyritic epidote-chlorite granodiorite	343	297	305
M6 (r)		275		
M7a	Grey monzogranite	236	199	218
M7b	Weathered sample	169	<100	169

Wailpally

The measured WRF values for Wailpally are given in table 4-14, figure 4-74 and figure 4-75. Sample M13 (mafic vein material) has the highest WRF value measured (5536 ppm F), over five times higher than the highest WRF value measured in Wailpally (W1a, 1102 ppm F). This sample is mostly biotite mica and amphiboles and is expected to have high total F content from previous mineralogical investigations (see section 4.6.3).

Of the fresh rock samples, W1a (porphyritic chlorite monzogranite) has the highest WRF value (1102 ppm F). This sample contains apatite and titanite both with high F content (average 2.66 and 1.15 mass % F respectively) as well as small amounts of fluorite. Samples W16a (biotite granodiorite), W17x (weathered monzodiorite) and W11a (amphibole granodiorite) follow close behind, with 930, 863 and 824 ppm F

respectively (figure 4-75). Fresh pegmatite sample W17a has a very low F content, with levels below the detection limit in all measurements. This sample has few F-bearing minerals (chlorite and epidote) with low F content.

In fresh-weathered rock pairs, WRF is higher in the fresh sample than the weathered equivalent (table 4-14, figure 4-75). This is expected from mineralogical studies where fresh samples generally have more F-bearing minerals and higher mineral F content than weathered samples.

Of the weathered samples, W17x (weathered epidote quartz monzodiorite) has the highest WRF (930 ppm F), higher than fresh rock samples W11a and W16a. Sample W11b also has a high WRF value (632 ppm F). This is discussed further in chapter 5, section 5.2 with the other profile samples. Other weathered samples W1b, W16b and W-C have low WRF values. Sample W-C has few F-bearing minerals, but contains F in calcite (average 0.02 mass % F), which, as this makes up most of the sample, may contribute a significant amount to WRF.

Table 4-14 – Wailpally Whole Rock Fluorine (WRF) values. WRF values are calculated from ISE readings using the two adjacent calibration sets, giving two values for each reading. Repeat ISE readings are also given. Repeat samples prepared are indicated by an 'r' by the sample name.

Sample	Rock Type	WRF value (ppm F)		Average (ppm F)
		Initial Readings	Repeat Readings	
W1a	Porphyritic chlorite monzogranite	1071		1102
W1a (r)		1133		
W1b	Weathered sample	<250	172	172
W16a	Biotite granodiorite	867	994	930
W16b	Weathered sample	195	237	233
W17a	Pegmatitic epidote quartz syenite	<250		<100
W17a (r)		<100	<100	
W17x	Weathered monzodiorite	863		863
W11a	Amphibole granodiorite	824		824
W11b	Weathered sample (profile sample 7m)	649	597	623
W13	Mafic vein material	5537	5539	5536
W13 (r)		5532		
WC	Calcrete	292	253	272

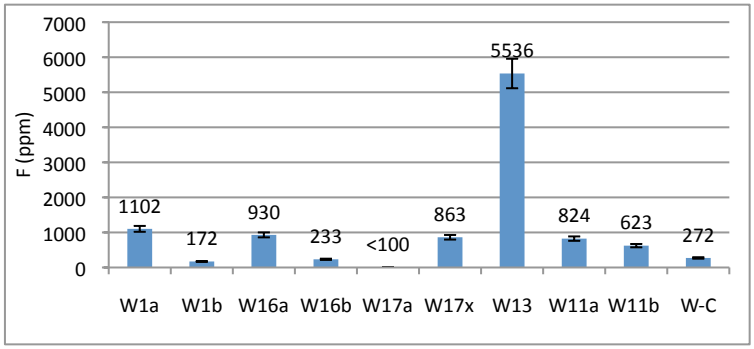

Figure 4-74 - Wailpally average measured WRF values. Values given above each sample. Weathered sample W11b is profile sample at 7m depth. Error bars (7.6%) shown.

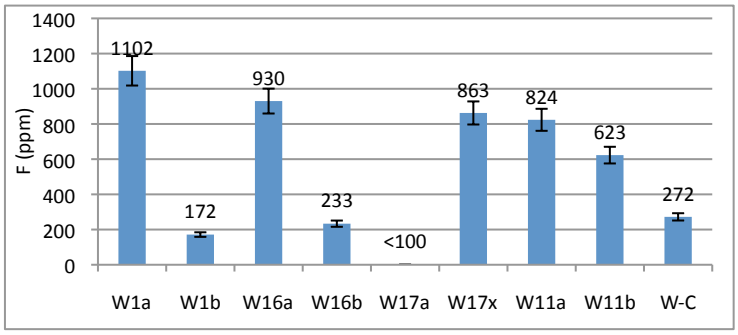

Figure 4-75 - Wailpally average measured WRF values (not including sample W13).Values given above each sample. Sample W11b is profile sample at 7m depth. Error bars (7.6%) shown.

4.7.2 Summary and Discussion

Higher WRF values are measured in fresh rocks than in their weathered equivalents. This is because more F-bearing minerals are present, usually with a higher F content (section 4.6). The range of WRF values for fresh rocks and weathered rocks in both catchments is similar (table 4-15). The two highest fresh rock WRF values measured are in Maheshwaram, however there are a greater number of high F (>800ppm) fresh rocks in Wailpally.

Table 4-15 - Range of WRF values for fresh and weathered rocks in Maheshwaram and Wailpally (W13 not included – 5536 ppm F)

	Fresh rock WRF range (ppm F)	**Weathered rock WRF range (ppm F)**
Maheshwaram	218 - 1742	169-426
Wailpally	<100 - 1102	171 - 863

The highest fresh rock WRF values in both catchments are found in gneissic porphyritic granites (although these have very different compositions). In Maheshwaram this is a biotite granodiorite (M2a), and in Wailpally it is a chlorite

monzogranite (W1a) (figure 4-76). In the Maheshwaram catchment this lithology makes up a large proportion of the catchment (~70%), whereas in Wailpally the high F lithology is found in the western region only (~10% of the catchment).

The amphibole monzogranite in Maheshwaram (M4a) also has a high WRF content (1159 ppm F). Although the two highest WRF measurements are Maheshwaram samples, a greater number of Wailpally samples have a high WRF value (above 800 ppm F, W11a, W16a and W17x). The majority of the Wailpally catchment is underlain by pink and grey granites, which are here represented by samples W16a (biotite granodiorite), W11a (amphibole granodiorite) and W14a (granodiorite, WRF value not measured).

The highest WRF value overall was measured in mafic vein sample W13 (5536 ppm F), which has an abundance of F-bearing biotite and amphiboles. Therefore, where present mafic veins may be a significant source of F to groundwater.

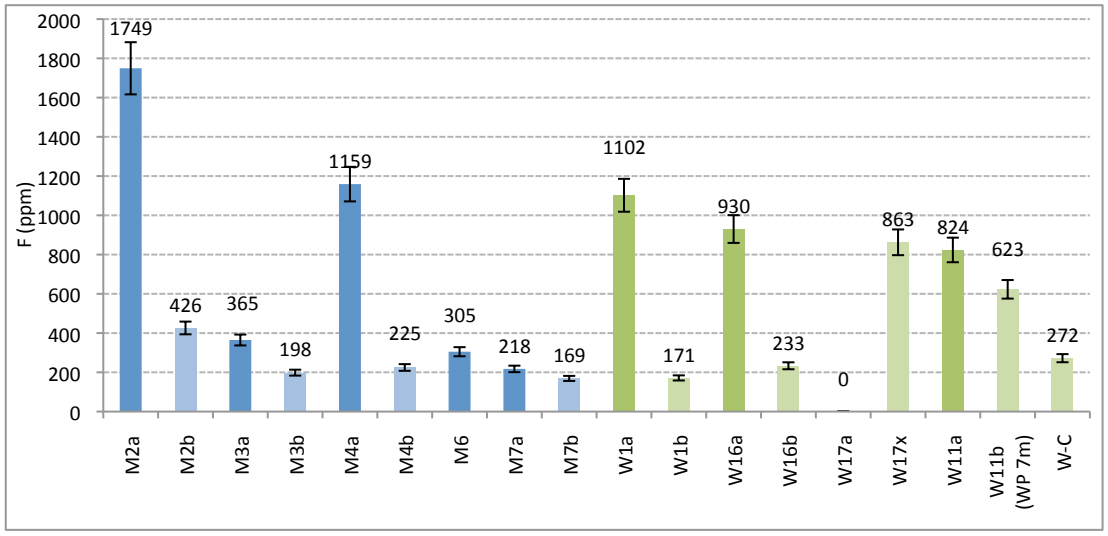

Figure 4-76 - Average WRF values for Maheshwaram and Wailpally. Values given above bars (ppm F). Sample W13 (5536 ppm F) not included. Weathered samples shown as faded bars. Error bars (7.6%) shown.

Comparison with Published WRF Values

Granite rocks typically have between 200 and 2000 ppm F (Jeffery and Hutchinson, 1986). The WRF values measured here are within this range. Table 4-16 gives a selection of WRF measurements of granites in Andhra Pradesh.

Previous work in Maheshwaram by Atal (2008) gave WRF values, using X-Ray Fluorescence (XRF), of 329 ppm F for biotite granite (this study 1742 ppm F, sample M2a), 122 ppm F for leucocratic granite (this study 365 ppm F, sample M3a and 218 ppm F, sample M7a) and 720 for intermediate granite (this study 1159 ppm F, sample M4a).

Previous WRF measurements in Wailpally by Reddy et al. (2009) (using XRF) give values of between 242 and 990 ppm F (table 4-16), with the highest F concentrations in the porphyritic pink granite (similar to sample W1a (1102 ppm F) – which in this study also has the highest WRF value in Wailpally). The lowest values of F were measured in grey granite from the east of Wailpally (similar to sample W14a and W16a - 930 ppm F). Reddy et al. (2009) also measured F in calcretes with values ranging 440-1160 ppm F. This is higher than the calcrete sample measured in this study (W-C, 272 ppm F).

WRF measurements in Maheshwaram and Wailpally by Atal (2008) and Reddy et al. (2009) using XRD are lower than WRF measurements of samples from similar locations in this study using the ISE Ingram (1970) method, and are in some cases at the lower end of the range given by Jeffery and Hutchinson (1986). The low published WRF values may be due to the method used, Atal (2008) and Reddy et al. (2009) used XRF, in which elements lighter than sodium (Z=11) can be difficult to analyse. Comparisons are difficult as detailed sample descriptions and F measurements of standard materials are not given in either study.

WRF values measured in this study are similar to those measured by Natarajan and Mohan Rao (1974) and Natarajan and Murthy (1974) (table 4-16), although in some cases there are large differences. Natarajan and Mohan Rao (1974) measured high WRF content in porphyritic granites in the region south of Antampet (near sample sites W1 and W2), with an average of 3,300 ppm F. The range in WRF measurements was from 250 (grey and pink granites-possibly similar to W11a) to 3,300 (porphyritic granites) (table 4-16). Biotite rich inclusions within grey granite gneiss (equivalent to W13) were measured to have a F content of only 250 ppm F, much lower than W13 values (although specific mineralogy of the biotite rich inclusions in Natarajan and Mohan Rao (1974) are not known).

Measurement of fluorine in geological standard G2 show that analysis in this study gives low results, therefore the WRF values measured here are likely to be low compared to their true WRF values. Future WRF work should take into account the suggestions by Stecher (1983) to improve results.

Table 4-16– Whole rock fluorine measurements of granites in Andhra Pradesh, and comparison with similar/equivalent samples measured in this study in Maheshwaram (M) and Wailpally (W). All values are averages unless given as a range. All values from this study are from Set 2 analyses unless specified.

Location	Reference	Rock Type	WRF (ppm F)	Method	WRF values obtained for similar/equivalent samples in this study	
					WRF (ppm)	Sample
Andhra Pradesh - Wailpally Catchment	Reddy D. et al. (2010)	Grey Granite	242	XRF	930	W16a
		Pink Porphyritic Granite	990		1102	W1a
		Calcrete	440 to 1160		272	W-C
Andhra Pradesh - Nalgonda district	Natarajan and Mohan Rao (1974) and Natarajan and Murthy (1974)	Grey and pink granites	250	Not given	824	W11a
		Grey granite	400		930 1159 218	W16a M4a M7a
		Grey granite gneiss	600		930 1742	W16a M2a
		Pink granites	600		365	M3a
		Pegmatites	600		<100	W17a
		Porphyritic granite	3300		1102 1742 305	W1a M2a M6a
		Dolerite dykes	250		-	-
		Biotite rich inclusions	250		5536	W13
		Epidote veins	400		-	-
		Quartz veins	500		-	-
	Mondal et al. (2009)	Granites and Gneiss	460 - 1709	XRF	Range 218-1742	
Andhra Pradesh Nalgonda district and Hyderabad	Rao (1993)	Granites (Nalgonda)	325- 3200 (ave 1400)	ISE	Range (W) <100-1102	
		Granites (Hyderabad)	270		Range (M) 218-1742	
Andhra Pradesh Maheshwaram catchment	Atal (2008)	Biotite granite	329	XRF	1742	M2a
		Leucocratic granite	122		365 218	M3a M7a
		Intermediate granite	720		1159	M4a
Andhra Pradesh Antampur district	Rao and Devadas (2003)	Granitic gneiss and gneissic granites	500-725	Not given	Range 218-1742	

4.8 Whole Rock Chemical Analysis (WRC)

Samples were analysed for major elements using lithium metaborate fusion and ICP-AES analysis at the NHM (see appendix 2 for method). Results are given in table 4-17 and table 4-18. Results for profile samples are given in chapter 5, section 5.2. Low totals (<98%) may be due to the presence of carbonate, water or other volatiles. Total iron is given as Fe_2O_3.

Table 4-17 - Bulk Chemical Compositions of Maheshwaram samples (weight %). F=fresh sample, W=weathered sample. DL=detection Limit. < indicates less than detection limit

Weight %	M2a	M2b	M3a	M3b	M4a	M4b	M7a	M7b	DL
	F	W	F	W	F	W	F	W	
Al_2O_3	14.41	13.67	12.70	12.77	13.21	9.10	12.75	13.15	0.01
CaO	2.41	1.55	0.77	0.95	3.36	23.60	0.68	0.46	0.05
Fe_2O_3	3.61	3.88	1.52	1.47	4.44	2.09	1.53	1.62	0.01
K_2O	4.55	4.56	5.61	5.60	2.70	3.30	5.77	5.80	0.05
MgO	1.14	0.91	0.24	0.26	2.44	0.63	0.23	0.19	0.005
MnO	0.04	0.05	0.03	0.01	0.09	0.02	0.02	0.03	0.001
Na_2O	3.11	2.40	2.97	2.56	3.73	1.23	2.70	2.26	0.005
P_2O_5	0.19	0.20	<	<	0.12	<	<	<	0.05
SiO2	66.49	66.18	74.13	71.75	66.57	38.25	72.31	71.97	0.01
TiO_2	0.49	0.51	0.18	0.20	0.38	0.20	0.21	0.19	0.01
totals	96.44	93.90	98.15	95.56	97.05	78.43	96.21	95.67	-

Table 4-18 - Bulk Chemical Compositions of Wailpally samples (weight %). F=fresh sample, W=weathered sample. DL=detection Limit. < indicates less than detection limit

Weight %	W1a	W1b	W16a	W16b	W17a	W17x	W11a	W13	W-C	DL
	F	W	F	W	F	W	F	Vein	Calcrete	
Al_2O_3	12.3	12.7	13.8	13.6	17.6	8.14	14.2	9.3	1.78	0.5
CaO	1.41	0.41	2.05	0.94	1.12	5.09	3.27	5.09	45.14	0.05
Fe_2O_3	2.86	1.59	3.34	1.73	0.80	5.26	4.13	7.25	0.50	0.01
K_2O	4.87	6.10	3.81	5.48	11.4	0.27	3.56	5.04	0.51	0.05
MgO	0.54	0.12	1.02	1.15	0.08	2.49	1.83	11.1	0.57	0.01
MnO	0.036	0.014	0.042	0.015	0.008	0.085	0.063	0.190	0.019	0.001
Na_2O	2.79	2.49	3.44	2.66	2.17	0.12	3.53	0.64	0.16	0.05
P_2O_5	<	<	<	<	<	<	<	<	<	0.2
SiO_2	69.7	73.0	67.5	70.5	64.0	71.5	66.8	55.6	9.66	0.1
TiO_2	0.50	0.19	0.33	0.28	0.03	0.55	0.29	0.23	0.06	0.01
Total	95.0	96.6	95.4	96.4	97.2	93.5	97.6	94.4	58.4	-

Maheshwaram WRC

Weathered samples have a lower Na_2O content than fresh samples due to the weathering of albite feldspar while K_2O values remain similar due to the retention of K-feldspars. Weathered porphyritic biotite granodiorite sample M2b and weathered amphibole monzogranite sample M4b have much lower MgO than their fresh counterparts due to the weathering of biotite and amphiboles respectively. Fresh pink and grey monzogranites (M3a and M7a) do not contain large amounts of either of these minerals and so have a lower MgO content that remains similar in the weathered rock. The percentage of TiO_2 increases slightly in most samples due to retention of Ti in titanite, titanium oxides and titanium iron oxides (e.g. ilmenite).

A large difference is noted between amphibole monzogranite samples M4a and M4b. SiO_2 and Al_2O_3 are much lower, and CaO higher in the weathered equivalent, corresponding to a large reduction in aluminosilicate minerals and an increase in calcite seen in thin section. The low total of M4b may be due to the presence of calcium carbonate.

Wailpally WRC

Paired porphyritic chlorite monzogranite samples (W1) and biotite granodiorite samples (W16) show a large decrease in CaO and smaller decrease in Na_2O between fresh and weathered samples due to the loss of plagioclase feldspars. K_2O increases in the weathered samples due to the retention of K-feldspars. SiO_2 also increases in weathered samples due to the retention of quartz and other resilient silicate minerals. A large decrease in TiO_2 content is measured between W1a and weathered equivalent W1b. In W1a large amounts of titanite are present as a primary mineral, while in W1b Ti is primarily located in secondary titanite and titanium oxides. A smaller decrease in TiO_2 content is observed between fresh weathered pair W16, where in both samples TiO_2 is present in secondary titanite and titanium oxides. MgO is low in W1a and W1b due to a lack of biotite or amphiboles in this sample. An increase in MgO content is seen between W16a and W16b possibly due to the retention of some biotite and chlorite, or in clays.

Pegmatite sample W17a has a much higher K_2O content than the other fresh rock samples, due to the large proportion of K-feldspar that make up this sample. The sample contains little MgO due to lack of major Mg bearing minerals.

Mafic vein sample W13 has a very high MgO content as it is primarily formed of amphiboles and biotite, with a low Al_2O_3, SiO_2 and Na_2O content compared to fresh rock samples due to a lack of quartz and feldspars. Fe_2O_3 is also high due to the iron content of amphiboles and biotite.

The weathered epidote quartz monzodiorite sample (W17x) has low Al_2O_3, K_2O and Na_2O content and high CaO, Fe_2O_3, MgO compared to other weathered samples. This could be due to high quantities of epidote and plagioclase feldspar, with less K-feldspar.

Calcrete sample W-C has a high CaO content and low analysis total due to its high calcium carbonate content.

4.9 Chapter Summary

The mineralogical and chemical analyses have determined the occurrence and F content of the principal F-bearing minerals in each catchment, and the differences between the granitic lithologies and between the fresh and weathered equivalents. Both similarities and differences are evident between the two catchments. The following minerals are found to contain F (in approximate order of high to low F content):

- Fluorite (present only in samples M3a, W1a and W14a)
- Apatite
- Titanite
- Epidote var 2
- Titanium phosphate (present only in sample W2b)
- Biotite
- Amphibole (present only in samples M4a, W11a and W13)
- Epidote
- Chlorite

The mineral F content is in most cases similar between catchments, but with different abundances. Mineral loss of F upon weathering is indicated in biotite F content analysis in both catchments and in apatite F content in Maheshwaram samples. Mineral F content is similar in most cases between samples, although some variation is seen (e.g. M4a has a higher than average biotite F content). Biotite and amphiboles in sample M13 have significantly higher F content than other samples.

Fresh samples have a higher WRF content than their weathered equivalents, with the highest fresh rock WRF content in each catchment in gneissic porphyritic granites (M2a and W1a). Whole rock chemistry analysis show differences in composition between sapls, with the differences in WRC measurements between fresh and weathered samples indicating the weathering of various minerals.

The data enables the mass balance of F to be developed for each catchment as described in the following chapter.

Chapter 5. Fluorine Mass Balance and Weathering Profiles

Fluoride mass balances were calculated for fresh and weathered samples from Maheshwaram and Wailpally by combining results from petrological point counting, electron microprobe energy dispersive X-ray detection (EM-EDX) mineral F analysis and whole rock F analysis. The mass balances were established to determine the relative mineralogical contributions to the total F content of the rock, to determine F distribution within the weathering profile, and to quantify F removal and redistribution upon bedrock weathering and regolith development (section 5.1).

The weathering profile was further investigated by analysis of one profile from each catchment, including sample description, chemistry and whole rock fluorine with depth (section 5.2).

5.1 Fluorine Mass Balance

5.1.1 Methodology

Results from optical petrography, point counting and EM-EDX point analysis were combined to assess the relative mineralogical contributions to the total F content of rock samples, and hence to describe mineralogical contribution to a mass balance of fluorine. The mineral abundance from point counting was converted to a 'weight percentage' using median mineral density values from Deer et at. (1992). The contribution of each mineral is calculated by:

$$A_M \times F_M \times 100 = C_{M\,(ppm)}$$

where A_M is the Mineral M abundance as a % (calculated from point counting and mineral densities), F_M is the Mineral M fluorine content from EM-EDX analysis (mass % F) and C_M is the F contribution by mineral M to rock F content (in ppm). An illustration of the method used to develop the fluorine mass balance is given in figure 5-1.

The difference between F mass balance calculations of fresh samples and their weathered equivalent indicates the total F lost through weathering and the relative contribution to loss from different minerals.

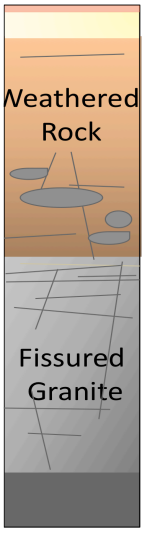

	F-bearing minerals	Abundance (%)	F content (EM-EDX) mass%	Contribution to total F content (in ppm F)	Total F content (ppm F)
Weathered	**Biotite**	5 %	0.06	5×0.06×100 = 30	Sum of the contribution of each mineral 30+125= **155 ppm F**
	Apatite	0.5 %	2.5	0.5×2.5×100= 125	
Fresh	**Biotite**	10 %	0.1	10×0.1×100 = 100	Sum of the contribution of each mineral 100+350= **450 ppm F**
	Apatite	1 %	3.5	1×3.5×100= 350	

Figure 5-1 - Illustrative mass balance and fluoride distribution in fresh and weathered rocks in a profile, for two F-bearing minerals

For each mineral, the F lost through weathering can be calculated from the loss of that mineral from the sample (F_1) and the difference in F content between the fresh and remnant weathered mineral (F_2) using:

$$F_{lost} = F_1 + F_2$$

where the F loss through the removal of an F-bearing mineral upon regolith development (F_1) can be calculated by:

$$F_{1\,(ppm)} = (A_{\,M\text{-}F(r)} - A_{\,M\text{-}W(r)}) \times F_{\,M\text{-}F\,(ppm)}$$

where $A_{M\text{-}F(r)}$ is the relative abundance of mineral M in the fresh rock as a ratio (e.g. 1.6% would be 0.016), $A_{M\text{-}W(r)}$ is the abundance of mineral M in the weathered rock as a ratio, and $F_{M\text{-}F(ppm)}$ is the F content of mineral M in the fresh rock in ppm (e.g. 0.09% F is the equivalent of 900 ppm F).

The loss of F reflected in the decrease in F content of a mineral that remains in the weathered sample (F_2) is calculated using:

$$F_{2\,(ppm)} = (F_{\,M\text{-}F(ppm)} - F_{\,M\text{-}W(ppm)}) \times A_{\,M\text{-}W(r)}$$

Where $F_{M\text{-}F(ppm)}$ is the F content of mineral M in the fresh rock (in ppm), $F_{M\text{-}W(ppm)}$ is the F content of mineral M in the weathered rock (in ppm) and $A_{M\text{-}F(r)}$ is the abundance of mineral M in the weathered rock (as a ratio). Alternatively the total F lost and weathered (F_{loss}) may be calculated from the difference in total mineral F in fresh and weathered minerals, rather than by calculating the different F losses (F_1 and F_2). This can be done using the equation below:

$$F_{loss\ (ppm)} = (A_{M\text{-}F(r)} \times F_{M\text{-}F(ppm)}) - (A_{M\text{-}W(r)} \times F_{M\text{-}W(ppm)})$$

This methodology provides an estimate of the loss of F from individual mineral sources present and allows for comparison of F loss between difference samples.

The F mass balance assumes all F to be located within minerals observed in thin section, and does not account for F that may be located within the profile either in clay minerals or sorbed to mineral surfaces. The point counting analysis is also assumed to be a fair and complete representation of the minerals present in the sample. In some cases a mineral that is present in point counting analysis has not been measured in EM-EDX for that sample; in this case an average F content for that mineral from other fresh or weathered samples is used. In other cases a mineral may be present only in very small amounts, with F content measured in EM-EDX, but the mineral is not counted in point counting. Here the mineral is given an abundance of half of the lower resolution for point counting. This does not usually have a large impact the mass balance results, although in the case of high F minerals such as fluorite, this could significantly change calculated rock F content.

5.1.2 Maheshwaram

Mineralogy of F in bedrock and the equivalent regolith

Calculated fluoride mass balances for Maheshwaram samples are summarised in table 5-7 (page 187) and figure 5-2 below. In all cases the majority of F is located in the fresh rock, in minerals such as biotite, apatite, fluorite and amphiboles. The total rock F content is lower in the weathered samples, where the fewer F-bearing minerals that remain usually have a lower F content. The percentage contribution of each mineral to total sample F is given in table 5-1.

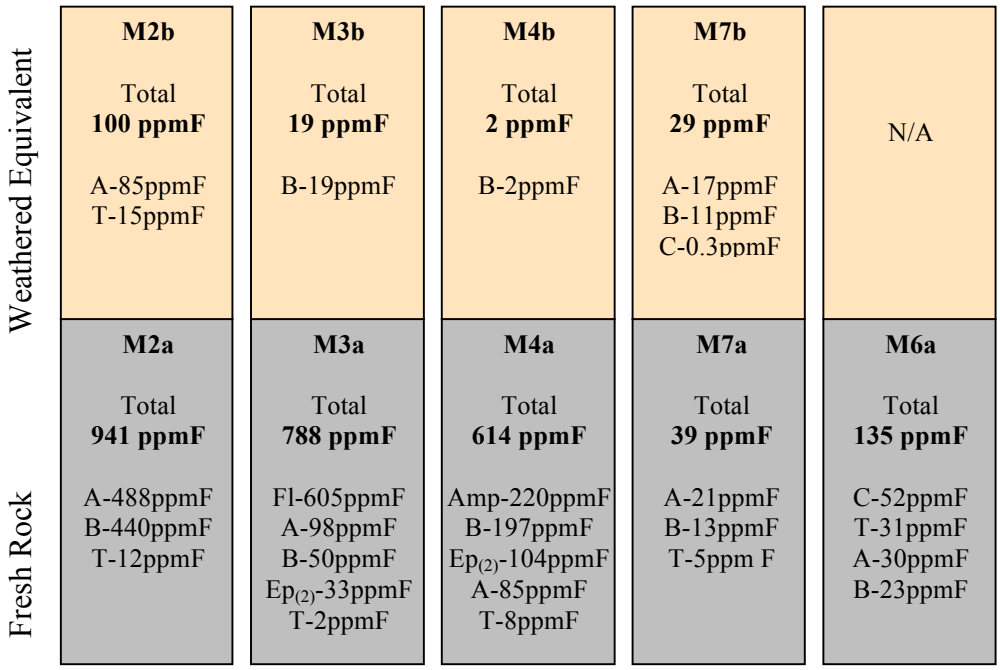

Figure 5-2 - Maheshwaram mass balance results. Total F and mineral F contribution. A=Apatite, Amp= Amphibole, B=Biotite, C=Chlorite, $Ep_{(1)}$=Epidote, $Ep_{(2)}$=Epidote var 2, Fl=Fluorite, T=Titanite. N/A: Not Available. Values are rounded to nearest whole number.

Sample M2a and b - Porphyritic Biotite Granodiorite

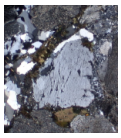

In the fresh rock sample M2a, >99% of F is located in apatite and biotite (table 5-1). The average F content of biotite is low in M2a (average 0.16 mass % F) compared to M3a and M4a (average 0.29 and 0.53 mass % F, respectively). However, as biotite is abundant in this sample (27 wt. %) the contribution to total sample F from biotite is high. Chlorite and epidote do not contribute to the F content of the rock. In the weathered equivalent M2b, biotite and apatite have a lower abundance (a third and a quarter of the original, respectively) and all minerals have a lower F content (significant at 5%; see chapter 4, section 4.6.1). All F has been removed from the biotite that remains. Titanite, precipitated as a product of biotite weathering, is more abundant in the weathered sample. The total F content of the rock is greatly reduced as a result of weathering, from 941 ppm F in M2a to 100 ppm F in M2b (figure 5-2).

Sample M3a and b – Pink Monzogranite

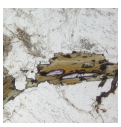

Most fluorine in fresh sample M3a is located in fluorite, which contributes 77% of the total rock F despite being a trace mineralogical constituent at <1% of the total mass (table 5-7). Apatite (12%), biotite (6%), epidote (4%) and titanite (<1%) also contribute F, however in smaller amounts (table 5-1). F

in chlorite is below detection limit and biotite is only a minor mineralogical constituent. In the weathered equivalent M3b, no fluorite was observed, suggesting its removal on weathering. Weathering also decreases the F content of biotite, but in the absence of fluorite, apatite, and titanite, biotite is the sole repository for F in the weathered sample. The total F content of the fresh rock is much higher (788 ppm F) than in the weathered equivalent M3b (19 ppm F) (figure 5-2).

Sample M4a and b - Amphibole Monzogranite

In fresh rock sample M4a, F is located mainly in amphiboles (36%) and biotite (32%), with epidote (var 2) and apatite also contributing to total F (17% and 14%, respectively) (table 5-1). Titanite contributes a small amount (1%) to total F. There is a large difference in the total F calculated for M4a (614 ppm) and M4b (2 ppm). In the weathered equivalent M4b, there is very little F (99% less than fresh sample M4a). No amphiboles were observed in the weathered sample, and a lower abundance of biotite (a quarter of the original), with a reduced F-content.

Sample M7a and b - Grey Monzogranite

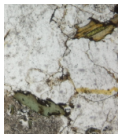

In fresh sample M7a, F-bearing minerals are scarce, contributing only 1.8% of the total sample mineralogy. The F content of these minerals is similar to other samples, apart from biotite, which here has a low average F content (0.09 mass % F). Apatite and biotite are the main contributors to total F (53 and 33% of the total F, respectively), with titanite (12%) and epidote (2%) contributing small amounts. However, due to the low abundance of these minerals the total F content of this sample is small (39 ppm F) compared to other fresh rock samples (70-95% lower). The weathered equivalent M7b also has a low total F (29 ppm F). There is little difference between the two samples, with similar F contributions from apatite, biotite and chlorite. The F content of apatite and chlorite is not significantly different between the two samples. No titanite or epidote was observed in M7b, and the contribution to F from biotite calculated to be slightly lower than that of the fresh sample.

Sample M6 - Porphyritic Epidote Chlorite Granodiorite

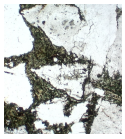

F in fresh sample M6 is primarily located in chlorite (38%), titanite (23%), apatite (22%), and biotite (17%). The total F for this sample is

low, at 135 ppm. Chlorite has a low F content in most Maheshwaram samples (near or below detection limit) although the average F content of chlorite in M6a is 0.06 mass % F, and with a high proportion of chlorite in this sample (9.3%) this leads to a large contribution to total F. Biotite in this sample has a low F content (0.08 mass % F), and there is a low abundance of other F-bearing minerals such as apatite.

Table 5-1 - Percentage contribution of each mineral to total sample F. Contributions over 25% in bold and red. A=apatite, B=biotite, C=chlorite, T=titanite, Ep=epidote, Ep(2)=epidote var 2, Amp=amphibole, F=fluorite, CaO=calcite.

Mineral	% Contribution of each mineral to total F content of sample								
	M2a	M2b	M3a	M3b	M4a	M4b	M6a	M7a	M7b
A	**52**	**85**	12		14		22	**53**	**60**
B	**47**		6	**100**	**32**	**100**	17	**33**	**39**
C							**38**		1
T	1	15	0.5		1		23	12	
Ep								2	
Ep(2)			4		17				
Amp					**36**				
F			**77**						
Total	100	100	100	100	100	100	100	100	100

Comparison with Whole Rock Fluoride concentrations

Calculations of rock F content by mineralogical mass balance differ from chemical analysis of whole rock fluorine (WRF) (table 5-2, figure 5-3) due to the different focus of each method. Whole rock chemical analysis by the Ingram method aims to measure the total fluorine content of the sample, whereas the mass balance calculations aim to find the total mineralogical F from EM-EDX and point counting analysis. The conversion of point counting area % to weight % using density values was done in order to reduce differences in calculations of percentage contribution. The weight percent mass balance calculations give higher total F content than mass balance calculations using point counting abundances only (e.g. M2a calculated total F from mass balance using area % is 816 ppm F, however taking into account mineral density, total calculated F from mass balance using weight % is 941 ppm F).

In most cases the mass balance calculations give a much lower total F content than the chemical WRF method, in one case with a difference of 99% (M4b). While there may be a systematic under-estimation of F content by the mineralogical mass balance, the difference between mass balance total mineralogical F and Ingram WRF is higher

in weathered rock samples (76-99%) than in the fresh rock samples (46-82%) (table 5-2). This difference is likely to be due to an additional source of F that is more abundant in the weathered samples but is not identified through point counting and EM analysis. This is probably one or more clay minerals, which may have a high F content, and which are identified in weathered samples in XRD analysis (chapter 4, section 4.5), but are not observed in thin section as they are removed or destroyed in the process of thin section preparation. F may also be sorbed to Al or Fe oxides, which have been found to occur in soils and weathered materials (Harrington et al., 2003), or sorbed to calcite that may be precipitated in Ca rich waters (Jacks and Sharma, 1995).

Table 5-2 – Total fluorine, measured using Ingram Whole Rock Fluorine (WRF) chemical method, and calculated from mass balance.

Sample	**Average WRF** (ppm F)	**Total F from Mass Balance** (ppm F)	**Difference** (WRF-Mass Balance)	**Difference** (as % of WRF value not 'measured' in mass balance)
M2a	1749	941	808	46
M2b	426	100	326	76
M3a	365	788	-423	-116
M3b	198	19	179	90
M4a	1159	614	545	47
M4b	225	2	223	99
M6	305	135	170	56
M7a	218	39	179	82
M7b	169	29	140	83

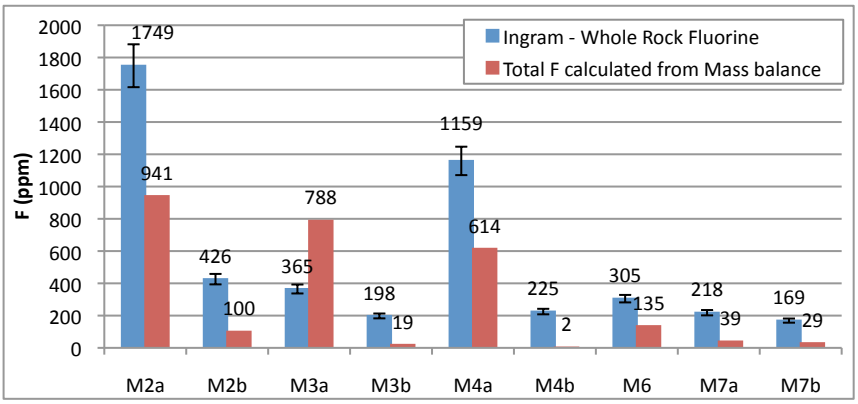

Figure 5-3 – Maheshwaram Total Fluorine measured using the Ingram Whole Rock Fluorine method and calculated from mass balance. Error bars on Whole Rock Fluorine are RSD (7.6%).

In sample M3a the mass balance methods give a higher total F than measured in WRF (423 ppm higher). This may be due to the presence of fluorite, which dominates the mineralogical F mass balance, but may not be representative at a larger volume scale.

In both calculations the fresh porphyritic biotite granodiorite sample M2a has the highest total F content, and M2b (the weathered equivalent) has the highest total F content of the weathered samples (figure 5-3).

Fluoride lost through weathering

The difference between the mineralogical mass balances for F in the fresh rocks and their weathered equivalents can be used to estimate mineral F loss through bedrock weathering, and hence establish the primary mineralogical sources for F lost to groundwater on weathering. A summary is given in figure 5-4, with details of the calculations in figure 5-5.

In all samples the fresh rock has a higher calculated total F than its weathered equivalent. The largest difference between samples is from the fresh porphyritic biotite granodiorite sample M2a (total 941 ppm F) and its weathered equivalent M2b (total 100 ppm F), which is attributed primarily to biotite and apatite F loss (figure 5-4). All F is removed from the biotite that remains in the weathered rock (although some of this F may be retained in secondary titanite formed), and the apatite remaining has a lower abundance and F content than in the fresh sample (significant at the 5% level).

The difference in F content between the fresh pink monzogranite sample M3a and its weathered equivalent M3b (769 ppm F) is primarily due to the loss of fluorite, corresponding to almost 80% of total F lost. Although fluorite is only a trace mineralogical constituent in the fresh sample (abundance is 0.19%) it contributes over 75% of the fresh sample's total F, and its absence in the weathered equivalent M3b results in a large difference in total F (figure 5-4). F is also lost upon the removal of apatite, titanite and epidote (these minerals are absent in the weathered equivalent) and through the decrease in F content of biotite (containing >80% less F).

F lost between the fresh amphibole monzogranite sample M4a and its weathered equivalent M4b (612 ppm F) is due to the absence of amphiboles in the weathered sample (corresponding to 36% of total F lost) and the reduction in biotite F content

and abundance (corresponding to 32% of total F lost). F is also lost through the absence of apatite, titanite and epidote var 2 in the weathered sample.

The difference in total F between the fresh grey monzogranite sample M7a and its weathered equivalent M7b is small, with similar mineralogical contributions of F in both samples (total F loss 10 ppm F). No titanite or epidote was observed in the weathered sample, and the mineralogical F content of biotite reduced (from 0.09 to 0.03 mass % F) which accounts for the small difference in total F content.

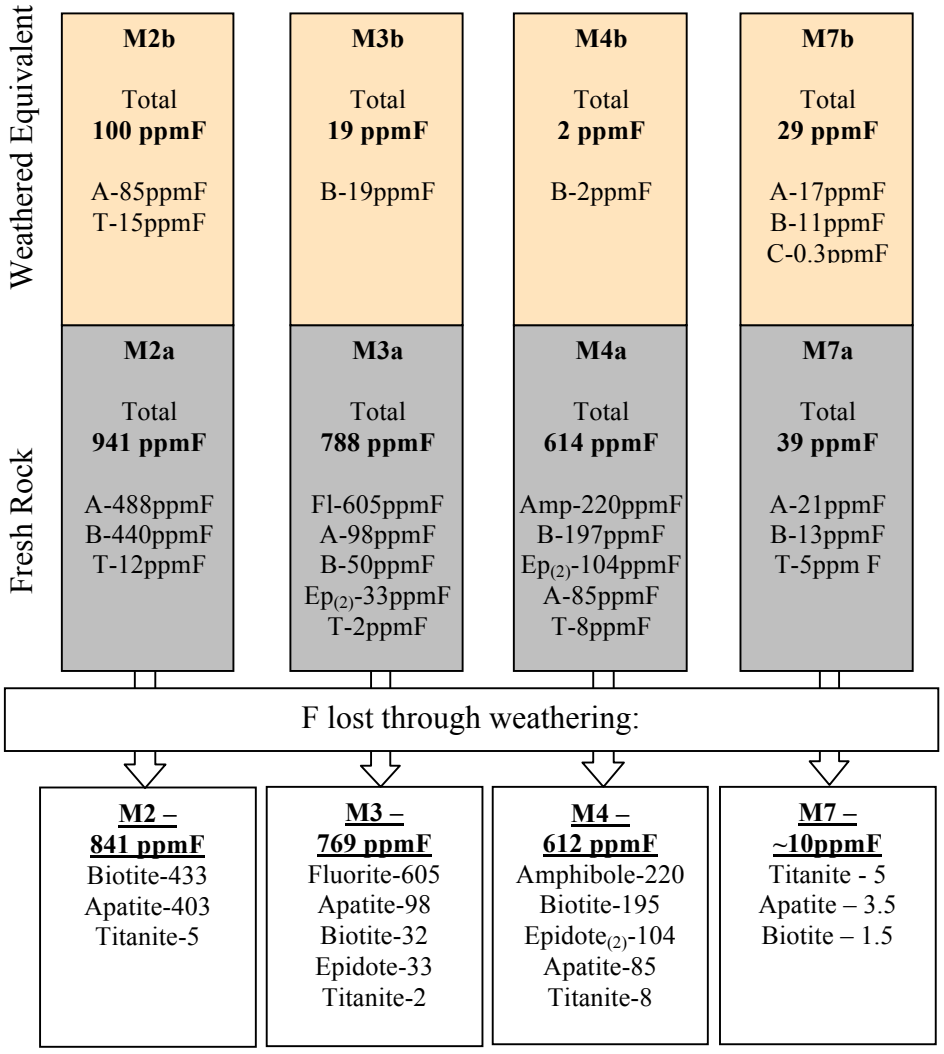

Figure 5-4 - Contribution of F-bearing minerals to total F in fresh and weathered rocks of Maheshwaram, and F lost upon weathering (total F lost underlined, mineral F loss listed below). A: Apatite, Amp: Amphibole, B:Biotite, C: Chlorite, Ep(1): Epidote, Ep(2): Epidote var 2, Fl: Fluorite, T: Titanite. Values given are rounded.

The mineralogical F loss calculated by mass balance differs from the F loss calculated from the difference in chemical WRF measurements, again due to the scope of the methods used. F loss calculated by both methods is given in table 5-3.

Calculated F loss is higher using the Ingram WRF values, indicating additional sources of F present in the fresh rock that are lost upon weathering. In sample M3a however, F loss is higher by mass balance calculations. This is because mass balance also calculates a higher total F than measured using WRF, but may also indicate that a higher proportion of F released on weathering of the fresh bedrock is re-precipitated in the weathered rock. The percentage F lost from fresh rocks gives the highest percentage loss from M4 and lowest form M7 in both methods.

Table 5-3 - Total F difference between fresh and weathered Maheshwaram samples calculated from mass balance and measured chemically with the Ingram WRF method

	Ingram – WRF (chemical method)		Mass Balance (calculation)	
Sample	F difference between fresh and weathered (ppm)	% of fresh rock F lost	F difference between fresh and weathered (ppm)	% of fresh rock F lost
M2	1323	76 %	732	89 %
M3	166	46 %	642	98 %
M4	934	81 %	512	99.7 %
M7	49	22 %	8	26 %

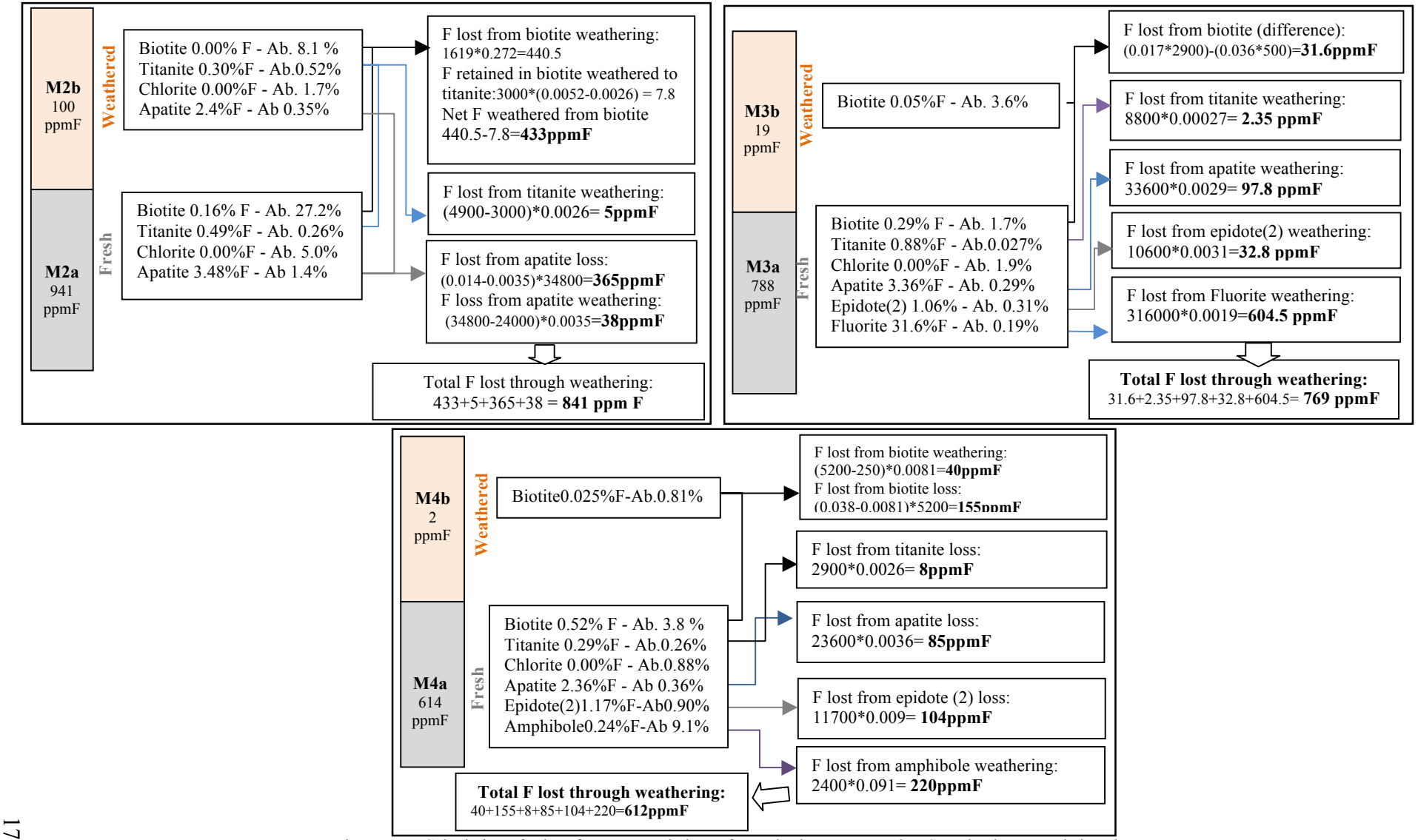

Figure 5-5– Calculation of F loss from F mass balance for Maheshwaram samples. Stated values rounded to show a minimum of two significant figures, calculated values based on full numbers. Ab: Abundance (wt. % from point counting and mean published density values). F content as average mass % F from EM-EDX.

5.1.3 Wailpally

Mineralogy of F in bedrock and the equivalent weathered regolith

Calculated fluoride mass balances for Wailpally are given in table 5-8 (page 188) and summarised in figure 5-6 (below). In all cases fresh samples have higher total F than their weathered equivalent, with F primarily located in fluorite, apatite, titanite, amphiboles and in some cases biotite and epidote. The percentage contribution of each mineral to total sample F is given in table 5-4.

Sample W1a and b – Porphyritic Chlorite Monzogranite

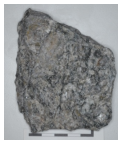

In fresh rock sample W1a, total F content is from fluorite, apatite and titanite (present as a primary mineral), all of which contribute an approximately equivalent proportion (36%, 32% and 32%, respectively) (table 5-4). The total contribution of F from epidote is less than 1%. In the weathered equivalent W1b, no fluorite was found suggesting the mineral has been lost upon weathering. In W1b, apatite and titanite are the principal contributors to total F, with their mineralogical F content similar to that in fresh sample W1a, although with a lower abundance (both reduced to approximately 1/5th of original abundance). Epidote (var 2) also contributes to total F in W1b, with a high F content (1.01 mass % F).

Sample W2a and c – Porphyritic Epidote Granodiorite

In fresh rock sample W2a, the majority of F is located in titanite (present as a primary mineral), epidote var 2 and apatite (contributing 38%, 29% and 28% of total F, respectively). Biotite (4%) and chlorite (2%) also contribute small amounts of F. The total F in the fresh sample W2a (667 ppm F) is higher than that of the weathered equivalent W2c (207 ppm F). While apatite largely retains its F in the weathered equivalent W2c, epidote var 2 and biotite both lose F on weathering, with some biotite altered to chlorite (as observed in petrological observations). Titanite is less abundant in the weathered sample, but with a higher F content (0.74 mass % F in W2a, 1.03 mass % F in W2c).

Sample W14a and b – Granodiorite

Mass balance calculations give a small total F content for fresh rock sample W14a (total 250 ppm), all of which is located in fluorite (54%), biotite (24%) and titanite (22%). Fluorite is only a trace mineralogical

component in this sample (<0.1%), although its high F content (22.2 mass % F) makes it an important F-bearing mineral. However, the overall low abundance of fluorite, biotite and titanite, and the lack of other F-bearing minerals such as apatite and epidote lead to a low total F content. In the weathered equivalent W14b, no fluorite was observed, suggesting the loss of this mineral on weathering. F in weathered sample W14b is primarily located in biotite (42%) and apatite (25%), with epidote var 2 (18%), titanite (11%), epidote (3%) and chlorite (1%) also contributing. F content of titanite is similar in the fresh and weathered samples, although in lower abundance, and biotite has a lower F content and abundance. Epidote in W14b contributes a small amount to total F, whereas in the fresh sample it does not contribute at all. Due to the low F content of the fresh sample W14a, the difference between the fresh sample and weathered equivalent is low (92 ppm F difference).

Sample W16a and b - Biotite Granodiorite

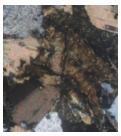

F in fresh sample W16a is located primarily in apatite (47% of total F) and biotite (35%). The total F content is higher in the fresh sample (387 ppm F) than in the weathered equivalent (67 ppm F). In the weathered equivalent W16b, the majority of F is located in apatite (80%), with biotite containing no F, and a small amount of F located in epidote var 2 (19%) and titanite (1%). The absence of F in biotite in the weathered sample suggests that it has been removed on weathering, with some F being retained in the weathering product titanite. Apatite has a similar F content in both samples (not significantly different), although there is less apatite in weathered sample W16b (reduced by ~65%).

Sample W17a – Pegmatitic Epidote Quartz Syenite

Due to a scarcity of F-bearing minerals, fresh sample W17a has a very low total F content of 10 ppm F. F-bearing minerals present include epidote (var 2) (contributing 7 ppm F) and epidote (contributing 3 ppm F) and biotite (less than 1 ppm F).

Sample W17x – Weathered Epidote Quartz Monzodiorite

F in this weathered sample is primarily located in apatite (68%) with the remainder in titanite (26%) and biotite (6%). The total F for this sample is similar to other weathered rock samples (150 ppm F).

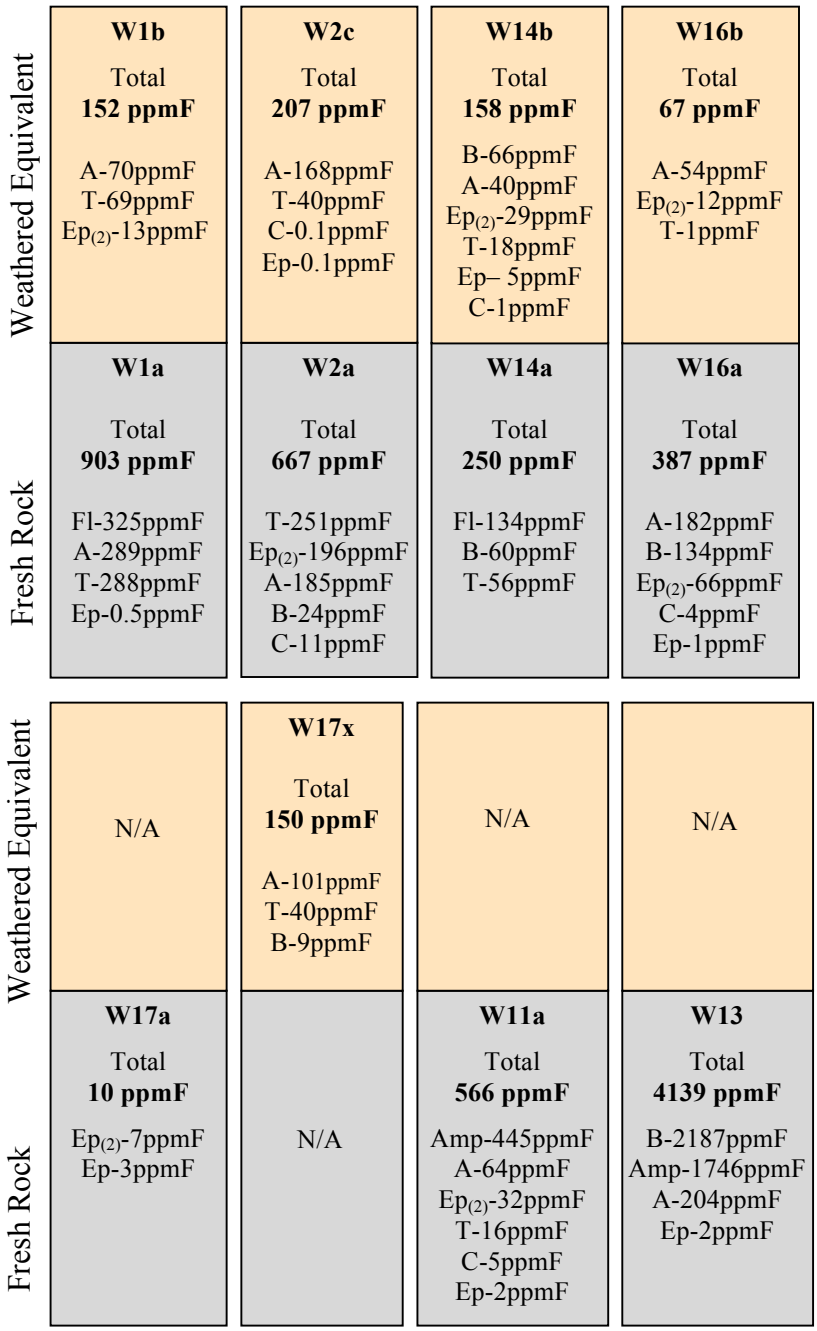

Figure 5-6 – Wailpally mass balance results. Total F and mineral F contribution. Numbers rounded. A: Apatite, Amp: Amphibole, B:Biotite, C: Chlorite, Ep(1): Epidote, Ep(2): Epidote var 2, Fl: Fluorite, T: Titanite. N/A: Not Available

Sample W11 – Amphibole Granodiorite

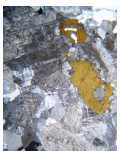

F in fresh sample W11a is mainly located within amphiboles (79% of total F), with smaller contributions from apatite (11%), epidote var 2 (6%), titanite (3%), chlorite (1%) and epidote (<1%). Amphiboles are a major F-

bearing mineral in this sample, making up 22% of the sample, with an average F content of 0.20 mass% F. The total F content of this sample is 566 ppm F (figure 5-6).

Sample W13 – Mafic Vein Material

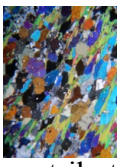

Fresh sample W13 has an abundance of biotite and amphiboles, both of which have high F content and contribute large amounts to the sample total F (2,187 ppm F and 1,746 ppm F, respectively) (figure 5-6). Apatite also contributes F (204 ppm F), as does epidote (2 ppm F) in smaller amounts. This sample has a very large total F content of 4,139 ppm F.

Sample W-C – Calcrete

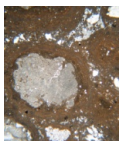

The calcrete sample W-C has only a small proportion of F-bearing minerals, with apatite, biotite and titanite together making up only 0.29% of the sample. The majority of the sample is calcite (92%) which contains a small amount of F (average 0.02 mass % F), therefore contributing a significant amount of F to the total F content (81% of the total 214 ppm F). Mass balance calculations for this sample are shown in table 5-8 (page 188).

Table 5-4 - Percentage contribution of each mineral to total sample F. Contributions over 25% in bold and red. A=apatite, B=biotite, C=chlorite, FeO=iron oxide, T=titanite, Ep=epidote, Ep(2)=epidote var 2, Amp=amphibole, F=fluorite, CaO=calcite.

Mineral	% Contribution of each mineral to total F content of sample												
	W1a	**W1b**	**W2a**	**W2c**	**W14a**	**W14b**	**W16a**	**W16b**	**W17a**	**W17x**	**W11a**	**W13**	**WC**
A	**32**	**46**	**28**	**81**		**25**	**47**	**80**		**68**	11	5	15
B			4		24	**42**	**35**			6		**53**	<1
C			2	<1		1	1				1		<1
T	**32**	**45**	**38**	19	22	11		1		**26**	3		3
Ep	<1			<1		3	<1		**29**		<1	<1	
Ep(2)		9	**29**			18	17	19	**71**		6		
Amp											**79**	**42**	
F	**36**				**54**								
CaO													**81**
TOTAL	**100**	**100**	**100**	**100**	**100**	**100**	**100**	**100**	**100**	**100**	**100**	**100**	**100**

Comparison with Whole Rock Fluoride concentrations

Calculations of rock F content by mineralogical mass balance for Wailpally samples differ from WRF measurements (figure 5-7, table 5-5), giving lower results. The largest difference (83%) between measurements is for weathered epidote quartz monzodiorite sample W17x. Both methods of calculation show W13 (mafic vein material) and W1a (porphyritic chlorite monzogranite) to have the highest total F and W17a (pegmatite sample), W16b (weathered biotite granodiorite) and W1b (weathered porphyritic chlorite monzogranite) to have the lowest (see figure 5-7).

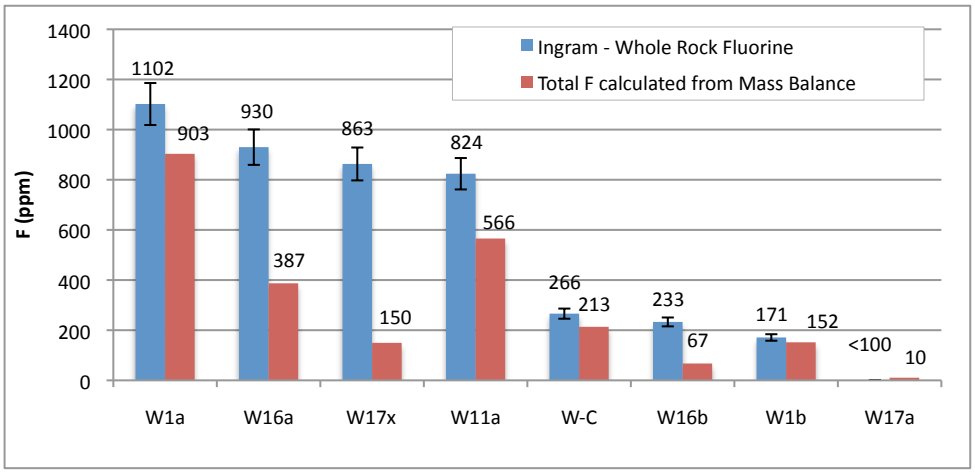

Figure 5-7 - Total fluoride calculated by mass balance and measured by WRF-ISE in Wailpally (not including W13). Error bars on Whole Rock Fluorine are RSD (7.6%).

Table 5-5 - Measured Ingram WRF values for Wailpally samples compared with mass balance calculated F values

Sample	**Average WRF** (ppm F)	**Total F from Mass Balance** (ppm F)	**Difference** (WRF-Mass Balance)	**Difference** (as % of WRF value not 'measured' in mass balance)
W1a	1102	903	199	18
W1b	171	152	19	11
W16a	930	387	543	58
W16b	233	67	166	71
W17a	<100	10	n/a	n/a
W17x	863	150	713	83
W13	5536	4139	1397	25
W11a	824	566	258	31
W11b	623	n/a	n/a	n/a
W-C	266	214	52	20

The calcrete sample (W-C), mafic vein material (W13) and fresh and weathered porphyritic chlorite monzogranite (W1a&b) have a smaller difference between

methods of calculation. In W13 and W-C this is probably due to the sample F mineralogy, with W13 mostly biotite and amphibole and W-C mostly calcite, which are more easily quantified during point counting. Smaller differences in W1a and W1b suggest a smaller proportion of F located in additional F sources within the rock. Large differences in other samples (weathered and fresh biotite granodiorite, W16a&b, weathered epidote quartz monzodiorite, W17x, and amphibole granodiorite W11a) suggest large contributions from an additional source of F that has not been included in the mass balance calculations (e.g. clays or F sorbed to Al or Fe oxides as discussed earlier).

Fluoride lost through weathering

The difference between the mineralogical mass balance for F in the fresh rocks and their weathered equivalents is used to estimate mineral F loss through weathering and the primary mineralogical sources of F lost to groundwater on weathering. A summary of F loss is given in figure 5-8 and the details of calculations in figure 5-9.

In all samples the fresh sample has a higher calculated total F than its weathered equivalent (figure 5-8). The largest difference between a fresh and weathered sample pair is between the porphyritic chlorite monzogranite samples, W1 a&b (752 ppm F difference), and the smallest difference between the granodiorite samples W14 a&b (92 ppm F difference). In both of these samples F is principally lost from fluorite (figure 5-8).

In fresh sample W1a fluorite contributes a large proportion of F (36%) and is absent from the weathered equivalent suggesting its removal upon weathering (F loss from fluorite 325 ppm F). Both apatite and titanite also contribute a large amount of F in the fresh sample (289 and 288 ppm F, respectively), and are greatly reduced in abundance in the weathered equivalent (although not in mineral F-content), therefore reducing their contribution to total F (to 70 and 69 ppm F, respectively).

F loss between granodiorite samples W14a and W14b (92 ppm F) is also primarily due to fluorite, which in fresh sample W14a contributes 54% of the total F content, but is not observed in W14b suggesting its removal upon weathering. F is also lost from titanite, which has a lower abundance in W14b (although a similar mineral F content). EM-EDX point analysis gives a high K_2O and F content of biotite in W14b compared to other weathered sample biotites, suggesting that biotite in this sample

has been little weathered. F is retained in the weathered sample in biotite as well as in epidote, epidote var 2 and chlorite. The difference in F between the fresh sample and weathered equivalent is therefore low (92 ppm F).

The F loss between porphyritic epidote granodiorite samples W2a and W2c (total 442 ppm F) is primarily due to the reduction in abundance of titanite (211 ppm F lost) and the loss of epidote var 2 (196 ppm F lost), with biotite loss also contributing a smaller amount (24 ppm F lost) (figure 5-8). Apatite has a similar mineral F content in both samples, as well as a similar abundance, therefore does not contribute to F loss.

F loss between biotite granodiorite samples W16a and W16b (320 ppm F) is due to the loss of F from biotite, the F content of which was below detection limits in sample W16b (although some biotite F is potentially retained in titanite), and due to the reduction in abundance of apatite in the weathered equivalent, although both samples have a similar F content (figure 5-8). A smaller amount of F is also lost from epidote var 2 and chlorite.

As the total F calculated from mass balance differs to that measured using the Ingram WRF chemical method, the F loss calculated by the two methods is also different (table 5-6). In W1 and W16 F loss is smaller when calculated through mass balance. This is because the total F calculated in mass balance is lower in both fresh and weathered samples, indicating further possible sources of F in the fresh rock, not all of which are retained in the weathered rock. The percentage F loss, however, is similar using both methods.

Table 5-6 - Total F difference between Wailpally fresh samples and their weathered equivalents calculated from mass balance and measured with WRF chemical analysis

	Ingram WRF (chemical method)		Mass Balance (calculation)	
Sample	F difference between fresh and weathered (ppm)	% of fresh rock F lost	F difference between fresh and weathered (ppm)	% of fresh rock F lost
W1	931	84	752	83
W2	-	-	442	66
W14	-	-	92	37
W16	697	75	320	83

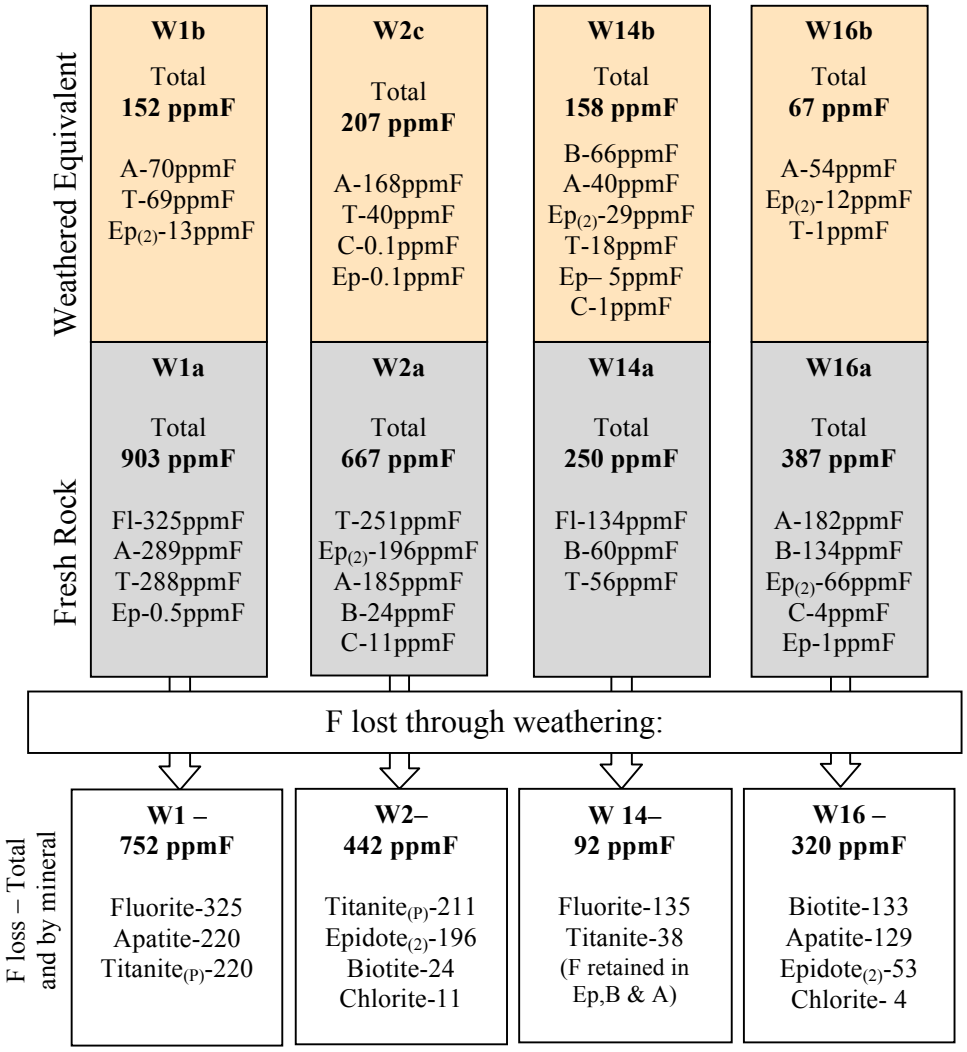

Figure 5-8 - The contribution of F-bearing minerals to total F in fresh and weathered rocks of Wailpally, and F lost upon weathering (total F lost underlined, mineral F loss listed below). Numbers rounded. A=Apatite, Amp=Amphibole, B=Biotite, C=Chlorite, Ep=Epidote, $Ep_{(2)}$=Epidote var 2, Fl=Fluorite, T=Titanite , $Titanite_{(P)}$=Primary Titanite

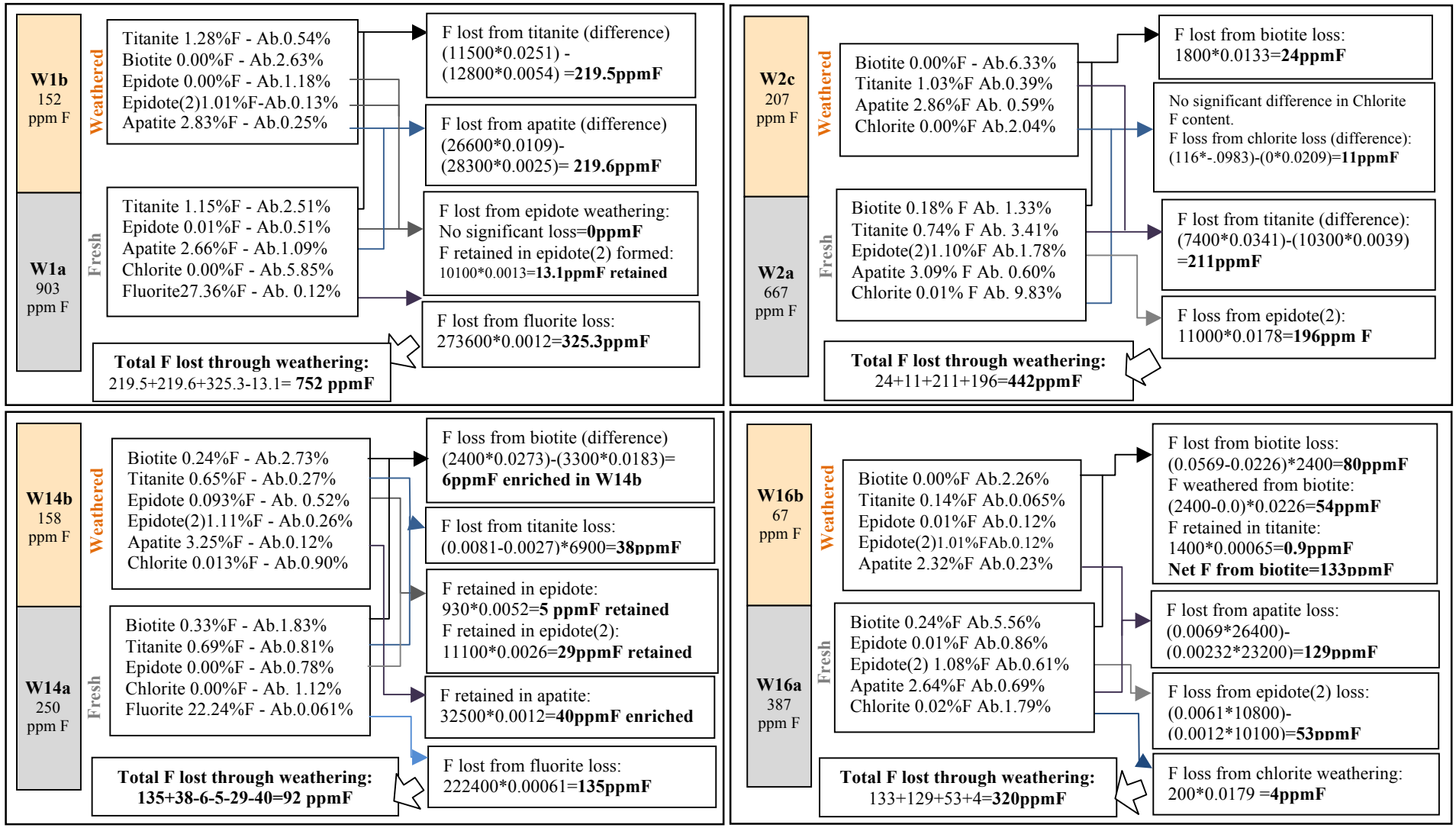

Figure 5-9 - Calculation of F loss from F mass balance for Wailpally samples. Stated values rounded to show a minimum of two significant figures, calculated values based on full numbers. Ab: Abundance (wt. % from point counting and mean published density values). F content as average mass % F from EM-EDX.

5.1.4 Discussion of the Mineralogical Distribution of F in Maheshwaram and Wailpally, and the Principal Sources of F to Groundwater on Weathering

A summary of the catchment-wide mineralogical F occurrence and sources of F to groundwater upon weathering calculated by mass balance are shown in figure 5-10. The relative importance of each mineral is calculated using mass balance results and the relative distribution/abundance of each lithology within each catchment (calculations are weighted depending on the abundance of each sample lithology) and does not take into account any variations in hydrological conditions or groundwater flow. Percentage contributions show the relative importance of each mineral calculated from weighted averages. As no mineralogical F loss has been calculated for sample W11 (the primary amphibole-bearing lithology of the Wailpally catchment) due to lack of thin section for point analysis, an estimation of amphibole F loss for this sample has been included in the catchment wide summary. This estimation assumes that all F is lost from amphiboles upon regolith formation, as observed in sample M4a (amphibole monzogranite) in Maheshwaram.

Mass balance calculations for Maheshwaram profiles indicate that total F content is higher in the fresh rock than the weathered rock, with F located in apatite and biotite, as well as fluorite and amphiboles where present (figure 5-10). In some samples epidote (var 2), secondary titanite and chlorite also contain F. Sample M2a (porphyritic biotite granodiorite) has the highest total F content (941 ppm F by mass balance) due to the abundance of F-bearing minerals (primarily biotite and apatite), and sample M7a (grey monzogranite) the lowest fresh rock F content due to a lack of F-bearing minerals. This is consistent with WRF measurements where sample M2a (1749 ppm F) also has the highest F content, and M7a a low F content (218 ppm F). Although sample M3a (pink monzogranite) contains fluorite, it has a lower F content than M2a.

Maheshwaram samples show mineralogical F loss from biotite, apatite, fluorite and amphiboles in the process of weathering and regolith development (figure 5-10), with the greatest loss from sample M2a porphyritic biotite granodiorite and smallest loss from sample M7a grey monzogranite. Fluorite is completely destroyed upon

weathering and regolith development. However, fluorite is only found in one sample (M3a), so may not be a large source of F to groundwater over the whole region. Biotite is thoroughly but not completely destroyed to release F. Apatite is less easily weathered but contains relatively high F.

In Wailpally, F content is consistently higher in the fresh rock than the weathered equivalents, although the regolith retains a higher proportion of F than in Maheshwaram. The primary F-bearing minerals in Wailpally fresh samples are amphiboles and apatite, with titanite and fluorite and biotite and epidote var 2 contributing to total F in some samples (e.g. W13, W16a and W2a) (figure 5-10). Mafic vein sample W13 has very high total F, located primarily in biotite and amphiboles, which have high F content and also are in abundance in the sample. Sample W1a (porphyritic chlorite monzogranite), has the highest calculated fresh rock total F (903 ppm F from mass balance), with high F contributed from fluorite, apatite and primary titanite. The lowest calculated total F in a fresh rock sample is in the pegmatite sample, W17a which has few F-bearing minerals. Mass balance total F values are lower than those measured by WRF but have a similar order of abundance within the Wailpally samples.

The principal mineralogical F loss calculated in Wailpally is from amphiboles, fluorite and apatite (figure 5-10). In the porphyritic granites (W1 and W2) titantite and epidote (var 2) also contribute a large amount to F loss, and in biotite granodiorite sample (W16a) biotite contributes significantly to F loss. Biotite is only a major contributor to total sample F in W13 (mafic vein sample) and W16a (biotite granodiorite), and is not as commonly occurring throughout the samples as it is in Maheshwaram. Primary titanite, which is not found in the Maheshwaram samples, and fluorite, which is less common in the Maheshwaram samples, are important F-bearing minerals and important sources of F to groundwater where present in Wailpally.

The relative abundance of particular F-bearing minerals is commonly different between fresh and weathered samples. Where fluorite and/or amphiboles are important F-bearing minerals in fresh samples (e.g. M3a, M4a, and W1a), these minerals are not present in the weathered equivalents. In Maheshwaram, apatite and biotite are still major F-bearing minerals in the weathered rock, although they

contribute a lower amount of F. In Wailpally apatite and titanite often remain major F-bearing minerals in weathered samples (again with a smaller total F). In some cases the proportion of total F from biotite is greater in the weathered sample than in the fresh rock equivalent (e.g. W14b).

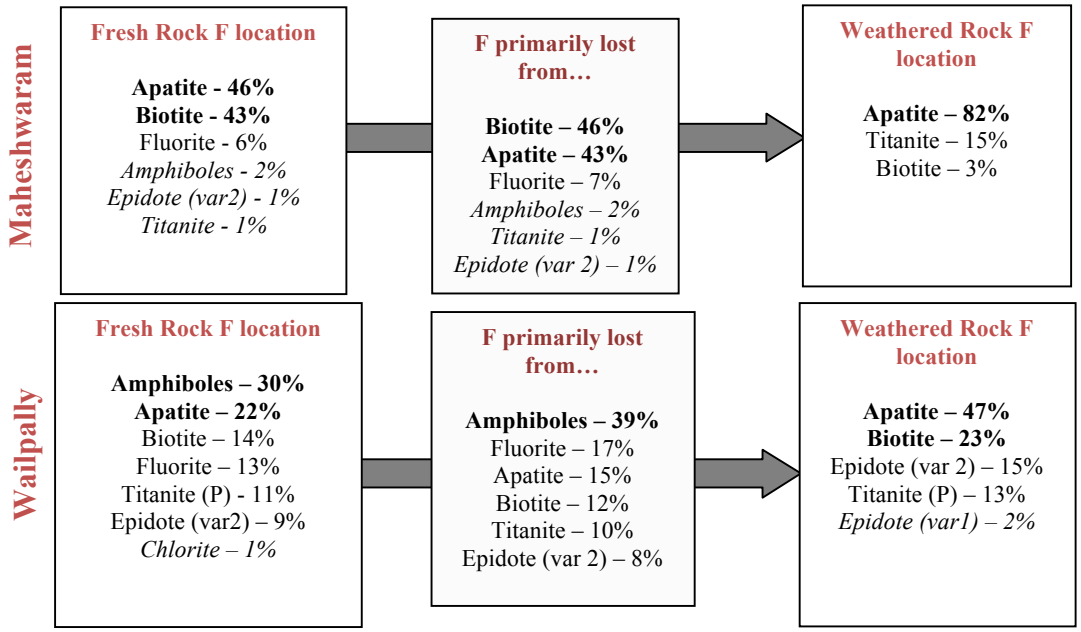

Figure 5-10 – Summary of F distribution and F loss with minerals listed in order of importance with catchment wide contributions given as percentages. Minerals shown in bold contribute most to F catchment wide, and in italics the least. As no weathered equivalents of samples containing amphiboles were available for EM-EDX or point analysis in the Wailpally samples it is uncertain as to their contribution to sample F loss. Sample W13 is not included in the Wailpally summary calculatons.

In both catchments, samples with a higher fresh rock F content lose a larger proportion of their F content on weathering (figure 5-11). This is observed both when using mineralogical F calculations from mass balance and when using whole rock F measurements from Ingram WRF. High percentage F loss is calculated from the porphyritic biotite granodiorite (M2a) and the amphibole monzogranite (M4a) in Maheshwaram and from the porphyritic chlorite monzogranite (W1) and biotite granodiorite (W16) in Wailpally. F loss from these samples is primarily biotite and apatite in M2 and W16, from amphiboles and biotite in M4 and from fluorite, apatite and titanite in W1.

F loss and the availability of F for release to groundwater are further investigated in batch leaching experiments in Chapter 6.

The total sample F calculated through mass balance is lower than that measured chemically through WRF in the majority of samples. This may indicate additional

sources of F that are not observed through point counting or EM analysis. In the case of the weathered rocks this is likely to include clays (as observed through XRD in Maheshwaram samples), and may also include F sorbed onto Al or Fe minerals. XRD analysis shows clay minerals to be present in Maheshwaram weathered samples (M2b, M3b and M7b - no other samples were analysed). F^- ions can replace OH^- ions in the clay mineral structure. Clays that often have a high F content include illite, palygorskite, kaolinite and montmorillonite (Savenko, 2001). Clay minerals are not identified in EM analysis or point counting and are therefore not included in the F mass balance calculations. The large differences in weathered sample's total F calculated by mineralogical mass balance and determined chemically (WRF) are likely to be in part due to the presence of F-bearing clays.

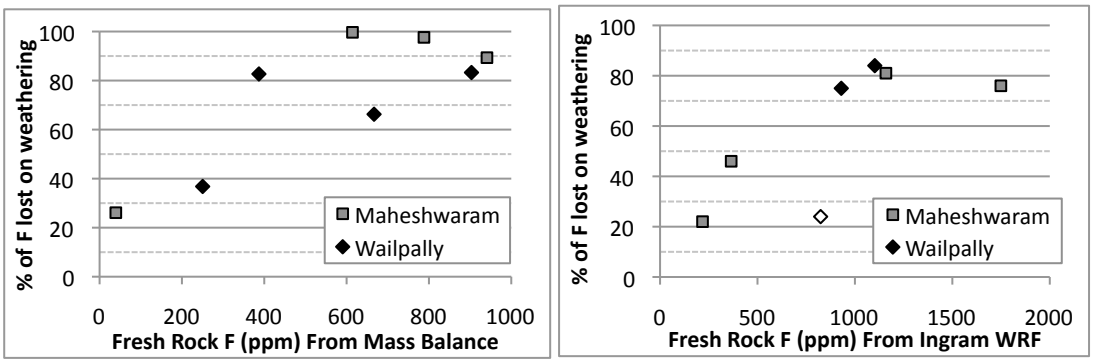

Figure 5-11 – Fresh rock F content and proportion of F lost on weathering (calculated from difference in F content between fresh samples and their weathered equivalent). The % F loss for sample W11a is calculated using a profile sample (7m depth) and is shown as a marker with no fill.

Geological Occurrence and Distribution

Figure 5-12 shows a map of the Maheshwaram catchment showing WRF content and primary F-bearing minerals (contributing over 25% of total F in mass balance calculations) present in the samples representing each area. Mass balance F loss (classed as high: >700, medium: >200 and low: <200) is also shown.

The majority of the Maheshwaram catchment is classed as biotite granite, represented in this study by sample M2a (gneissic porphyritic biotite granodiorite), the fresh sample of which has the highest WRF content of the Maheshwaram samples (1749 ppm F) and the highest calculated F loss from mass balance (figure 5-12). The mineral sources of F in fresh rock M2a are apatite (contributing 52%), biotite (contributing 47%) and titanite (contributing 1%) (mass balance calculation). In the

weathered equivalent, the contribution to total F is from apatite (85%) and titanite (15%) only, with apatite and biotite as the principal contributors to F in groundwater on weathering. As this lithology is representative of a large area of the catchment, the weathering of these minerals is important in the mobilisation of F to groundwater. The porphyritic epidote chlorite granodiorite (M6a) was also collected from within this area, although this lithology is thought to have localised occurrence only, and not be widespread throughout the catchment. The remaining area of the Maheshwaram catchment is divided into Leucogranite (10% of the area, represented here by samples M3 and M7) and Intermediate Granite (20% of the area, consisting of biotite granite, leucogranite and pegmatites, and from which sample M4 was collected) (figure 5-12). Exactly how representative the research samples, defined by the available of geological materials, are of each area has not been tested. The amphibole monzogranite (M4a) also has a high WRF value (1159 ppm F), primarily due to F-bearing magnesio-hornblende and biotite, with these two minerals also the principal source of F loss, although this lithology has a restricted occurrence in the catchment. Pink monzogranite (M3a) has a WRF value of 365 ppm F, with fluorite as the principal F-bearing mineral (and source of F loss). The grey monzogranite (M7a) has a low WRF content (218 ppm F), fewer F-bearing minerals and low calculated F loss by mass balance.

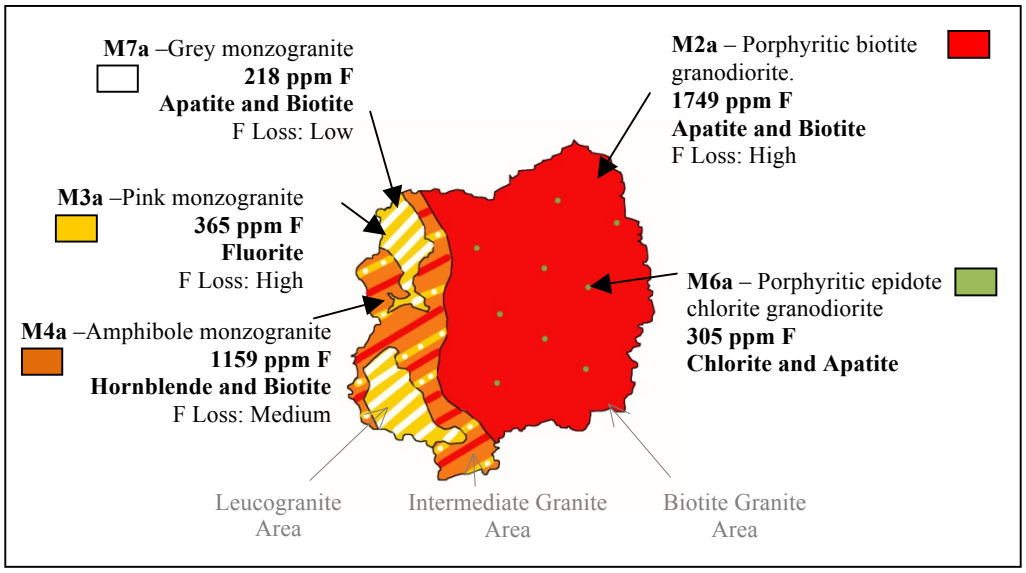

Figure 5-12 – Map of Maheshwaram with sample WRF content and principal F-bearing minerals from mass balance. Where the exact spatial distribution of a sample is unknown, they are represented by stripes (M3a, M4a, M7a) or dots (M6a). F Loss as calculated by mass balance shown as High (>700 ppm F), Medium (>200 ppm F) or Low (<200 ppm F).

Overall, the centre and east of the catchment have rocks with higher F, with low F samples distributed throughout this area in small amounts (porphyritic epidote chlorite granodiorite - M6a). Lithologies with lower WRF content and F loss are present in the west of the catchment (leucogranite areas, pink monzogranite M3a and grey monzogranite M7a), with a mixture of high, low and medium WRF lithologies in the intermediate area (including amphibole monzogranite M4a).

Figure 5-13 is a map of Wailpally showing the different lithologies collected, their WRF value and principal F-bearing minerals calculated from mass balance. Mass balance calculated F loss is also shown. The exact distribution of the amphibole granodiorite, biotite granodiorite and granodiorite is unknown, yet these make up a large proportion of the area.

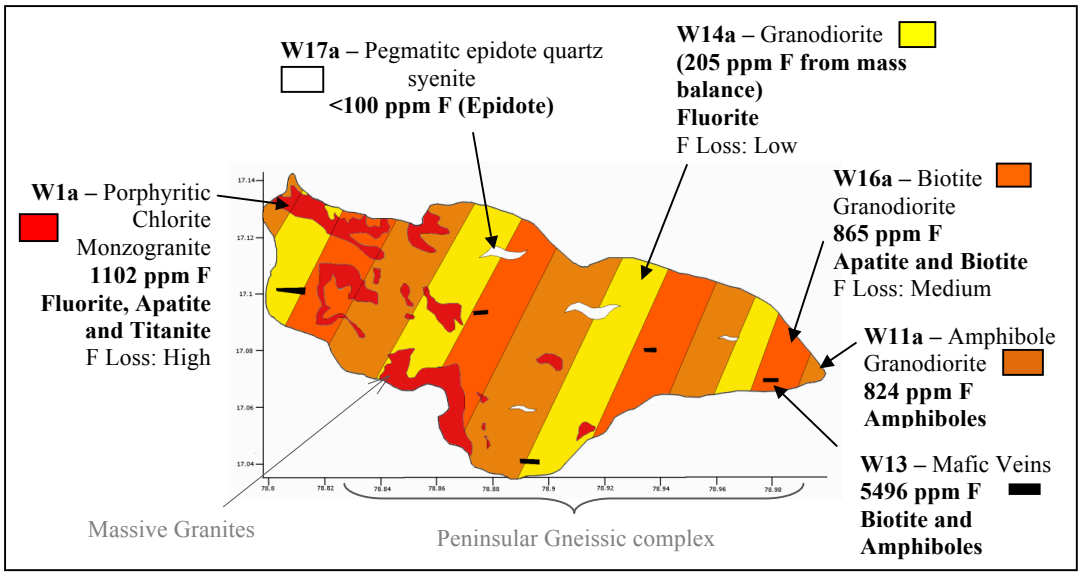

Figure 5-13 - Map of Wailpally with sample WRF content and principal F-bearing minerals marked. Where the distribution of a sample is unknown they are represented by stripes (W11a, W14a, W16a) or throughout the catchment as for W17a and W13. F loss as calculated by mass balance shown as High (> 700ppm F), Medium (> 200ppm F) or Low (< 200ppm F).

The geology of the Wailpally catchment is predominantly pink and grey granites, with porphyritic granites in the western hill regions and calcrete and pegmatite veins throughout the catchment. The pink and grey granites are here represented by samples W11a (amphibole granodiorite), W14a (granodiorite) and W16a (biotite granodiorite), the WRF content of which ranges from 824 ppm F (in W11a) to 930 ppm F (in W16a) (figure 5-13). This is lower than the WRF content of the predominant Lithology of Maheshwaram (M2a, 1749 ppm F). The principal F-

bearing minerals in these samples are amphiboles (W11a), fluorite (W14a), and apatite and biotite (W16a).

The highest WRF values in Wailpally are from the porphyritic granites (W1a porphyritic chlorite monzogranite and W2a porphyritic epidote granodiorite) with a WRF value of 1102 ppm F (W1a) and high mass balance total F (903 ppm F in W1a and 667 ppm F in W2a) and which are representative of the western hill regions (figure 5-13). The principal F-bearing minerals in these samples are fluorite (W1a only), apatite, titanite and epidote var 2 (W2a only). Mafic vein material (W13), with a high absolute F content (5536 ppm F from WRF and 4139 ppm F from mass balance) due to F-bearing biotite and amphiboles, is located throughout the catchment and has been observed at locations W1, W14 and W16. Pegmatite samples (W17a) have a low F content (<100 ppm F) and few F-bearing minerals and are therefore not a major source of F in the catchment.

In both catchments the porphyritic granites (M2 in Maheshwaram and W1 in Wailpally) have the highest fresh rock total F content (measured by WRF and calculated by mass balance) of the catchment. These samples also both have the highest calculated F loss upon weathering from mass balance. In Maheshwaram this lithology makes up a large proportion of the area (~70%), whereas in Wailpally this lithology is found in the western hill regions only (approximately 10% of total catchment area). Rainfall recharge in Wailpally is thought to mainly occur in the western hill regions (Reddy et al., 2009), with groundwater flow from west to east in the catchment, therefore the high F content of these samples could impact the groundwater F content of recharged groundwater. This is discussed further in chapter 7.

Table 5-7–Fluoride mass balance for Maheshwaram. '%'=abundance (weight percentage, calculated from point counting and mineral densities), 'F-Mass%'= average F content from EM-EDX, 'ppm F'=total F contributed from that mineral in the sample. Quartz and feldspar contain no detectable F and are omitted. Numbers in red = not determined. *value estimated (mineral seen but not counted, point counting abundance given as half of lower 'detection limit') $^{+}$value estimated (mineral present but no ED-EMS F analysis. Value given as average for fresh/weathered samples from Maheshwaram).

	M2b			M3b			M4b			M7b					
	%	F-Mass %	ppm F	%	F-Mass %	ppm F	%	F-Mass %	ppm F	%	F-Mass %	ppm F			
Apatite	0.35	2.40	85	0	0	0	0	0	0	0.06*	3.06	17.4			
Biotite	8.11	0	0	3.59	0.05	18.8	0.81	0.03	2.02	3.81	0.03^{+}	11.4			
Chlorite	1.73	0	0	0	0	0	0	0	0	0.31	0.01	0.3			
FeO	8.06	0	0	5.87	0	0	3.36	0	0	9.26	0	0			
Titanite	0.52	0.30	15	0	0	0	0	0	0	0	0	0			
Epidote	0	0	0	0	0	0	0.46	0	0	0	0	0			
Epidote (var 2)	0	0	0	0	0	0	0	0	0	0	0	0			
Amphibole	0	0	0	0	0	0	0	0	0	0	0	0			
Fluorite	0	0	0	0	0	0	0	0	0	0	0	0			
TOTAL:			**100**			**19**			**2**			**29**			
	M2a			**M3a**			**M4a**			**M7a**			**M6**		
	%	**F-Mass %**	**ppm F**	**%**	**F-Mass %**	**ppm F**	**%**	**F-Mass %**	**ppm F**	**%**	**F-Mass %**	**ppm F**	**%**	**F-Mass %**	**ppm F**
Apatite	1.40	3.48	487.9	0.29	3.36	97.8	0.36	2.36	85.0	0.06*	3.45	20.8	0.10	2.84	29.7
Biotite	27.2	0.16	440.5	1.72	0.29	50.4	3.80	0.52	197.4	1.46	0.09	12.9	2.73	0.08	22.8
Chlorite	5.03	0	0	1.87	0	0	0.88	0	0	0.11	0.01	0.1	9.29	0.06	51.6
FeO	1.14	0	0	3.71	0	0	0	0	0	6.48	0.00	0	3.07	0	0
Titanite	0.26	0.49	12.5	0.03*	0.88	2.3	0.26	0.29	7.1	0.07*	0.71	4.7	0.57	0.53	30.7
Epidote	2.49	0	0	0.31	0	0	0.90	0	0	0.39	0.02	0.8	6.47	0	0
Epidote (var 2)	0	0	0	0.31	1.06	32.8	0.90	1.17	104.3	0	0	0	0	0	0
Amphibole	0	0	0	0	0	0	9.11	0.24	220.0	0	0	0	0	0	0
Fluorite	0	0	0	0.19	31.57	604.5	0	0	0	0	0	0	0	0	0
TOTAL:			**941**			**788**			**614**			**39**			**135**

Table 5-8 – Fluoride mass balance for Wailpally. '%'=abundance (wt. %, calculated from point counting and mineral densities), 'F-Mass%'= average F content from EM-EDX, 'ppm F'=total F contributed from that mineral in the sample. Quartz and feldspar contain no detectable F and are omitted. Numbers in red = not determined. *value estimated (mineral seen but not counted, point counting abundance given as half of lower 'detection limit') $^{+}$value estimated (mineral present but no ED-EMS F analysis. Value given as average for fresh/weathered samples from Wailpally).

Mineral	W1b			W2c			W14b			W16b			W17x						WC					
	%	F-mass %	ppm F	%	F-mass %	ppm F	%	F-mass %	ppm F	%	F-mass %	ppm F	%	F-mass %	ppm F				%	F-mass %	ppm F			
Apatite	0.3	2.83	69.6	0.59	2.86	167.8	0.12	3.25	39.8	0.23	2.32	53.7	0.34	2.95	101.5				0.12	2.76^{+}	32.9			
Biotite	2.6	0	0	6.33	0	0	2.73	0.24	66.1	2.26	0	0	2.99	0.03	8.6				0.06*	0.13	0.7			
Chlorite	0	0	0	2.04	0	0.1	0.90	0.01	1.2	0.74	0	0	1.79	0	0				0.05*	0.06	0.3			
FeO	1.0	0	0	3.05	0	0	2.19	0	0	7.54	0	0	0.56	0	0				0.19	0	0			
Titanite	0.5	1.28	68.8	0.39	1.03	39.6	0.27	0.65	17.6	0.06*	0.14	0.9	0.88	0.45	39.5				0.07*	0.92	6.0			
Epidote	1.2	0	0	1.50	0	0.1	0.52	0.09	4.9	0.12	0	0	17.61	0	0				0	0	0			
Epidote (2)	0.1	1.01^{+}	13.2	0	0	0	0.26	1.11	28.9	0.12	1.01^{+}	12.5	0	0	0				0	0	0			
Amphibole	0	0	0	0	0	0	0	0	0	0	0	0	0	0	0				0	0	0			
Fluorite	0	0	0	0	0	0	0	0	0	0	0	0	0	0	0				0	0	0			
CaO				0	0	0	0			0	0	0							91.8	0.02	173.7			
TOTAL:			152			207			158			67			150						214			

Mineral	W1a			W2a			W14a			W16a			W17a			W11a						W13		
	%	F-mass %	ppm F	%	F-mass %	ppm F	%	F-mass %	ppm F	%	F-mass %	ppm F	%	F-mass %	ppm F	%	F-mass %	ppm F				%	F-mass %	ppm F
Apatite	1.1	2.66	289.2	0.6	3.09	184.7	0	0	0	0.69	2.64	182.3	0	0	0	0.24	2.61	64.0				1.00	2.04	204.2
Biotite	0	0	0	1.3	0.18	24.3	1.83	0.33	59.9	5.56	0.24	135.4	0.04	0.03	0.1	0	0	0				23.95	0.91	2189.9
Chlorite	5.9	0	0	9.8	0.01	11.4	1.12	0	0	1.79	0.02^{+}	3.6	0.06	0	0	1.19	0.04	5.5				0	0	0
FeO	1.0	0	0	0.4	0	0	1.20	0	0	1.12	0	0	0.43	0	0	0.40	0	0				0	0	0
Titanite	2.5	1.15	288.4	3.4	0.74	250.6	0.81	0.69	55.9	0	0	0	0	0	0	0.27	0.61	16.3				0	0	0
Epidote	0.5	0.01^{+}	0.5	7.0	0	0	0.78	0	0	0.86	0.01^{+}	0.9	5.94	0.01	3.0	0.87	0.03	2.3				1.16	0.02	1.9
Epidote (2)	0	0	0	1.8	1.1^{+}	195.8	0	0	0	0.61	1.08	65.8	0.07	0.09^{+}	7.3	0.61	0.53	32.2				0	0	0
Amphibole	0	0	0	0	0	0	0	0	0	0	0	0	0	0	0	22.32	0.2	445.2				41.58	0.42	1746.3
Fluorite	0.1	27.36	325.3	0	0	0	0.06 *	22.24	134.6	0	0	0	0	0	0	0	0	0				0	0	0
CaO	0	0	0	0	0	0	0			0	0	0	0	0	0	0	0	0						
TOTAL:			903			667			250			387			10			566						4139

5.2 Samples with depth through the weathering profile

Samples were collected with depth through the weathering profile of both catchments in June 2009. This was done in wide diameter dug-wells with access via steps made in the side of the well. Fresh rock samples were collected from the same location for comparison. These samples were analysed in hand specimen, and some were selected for whole rock chemistry, whole rock fluorine and batch leaching experiments.

5.2.1 Maheshwaram Profile

Profile samples were collected from the sample site M2 (in the same location as sample M2b, which was collected at 10m depth). This is a large (8-10m wide) and deep (10m) dry dug-well with steps. The dug-well was near a road, and surrounded by vegetation (figure 5-14, figure 5-15). Samples were collected using a geological hammer, at intervals of 0.5m from the base of the well. Size and sorting may be influenced by method of collection of samples (hammering), although field observations showed all samples to be inequigranular. The saprolite was fairy hard, with large feldspars and quartz crystals visible. Some thin mafic veins were present, as well as an abundance of fractures with 'fill' material.

The Maheshwaram profile can be divided into four sections from field observations and sample descriptions (table 5-9, figure 5-16):

- Soil samples (0-2m depth) - Soft material, increasing organic matter towards the top. Light brown to yellowy-brown.
- Sandy saprolite (2-3m depth) - Shallow samples with few mafics and feldspars, and more quartz. Orange/brown in colour.
- Saprolite - mid depth samples (3-5.5m) - with pink feldspars, biotite, quartz. Grey/Yellow/Orange/Pink in colour. Many fractures visible.
- Saprolite - deep samples (6-10m) - with large pink feldspars, white feldspars, quartz, platey biotite (in varying sizes). Hard samples, greyish/yellow in colour.

Within these sections are fractures filled with clay rich and carbonate rich material (e.g. at 8.8m, 6m, 4.5m and 2m depth) (table 5-9, figure 5-15, figure 5-16).

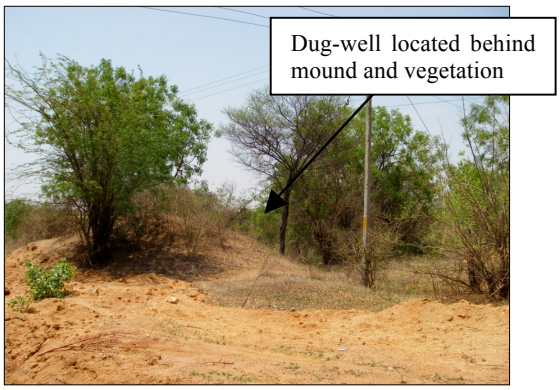

Figure 5-14 – Location of Maheshwaram Dug-well

Figure 5-15 – Side of dug-well where Maheshwaram profile samples were taken. Fractures preserved in the weathered rock are highlighted. Photos were taken from the bottom of the well. The tape measure on the bottom section is at 4m length, and at the top section 5m.

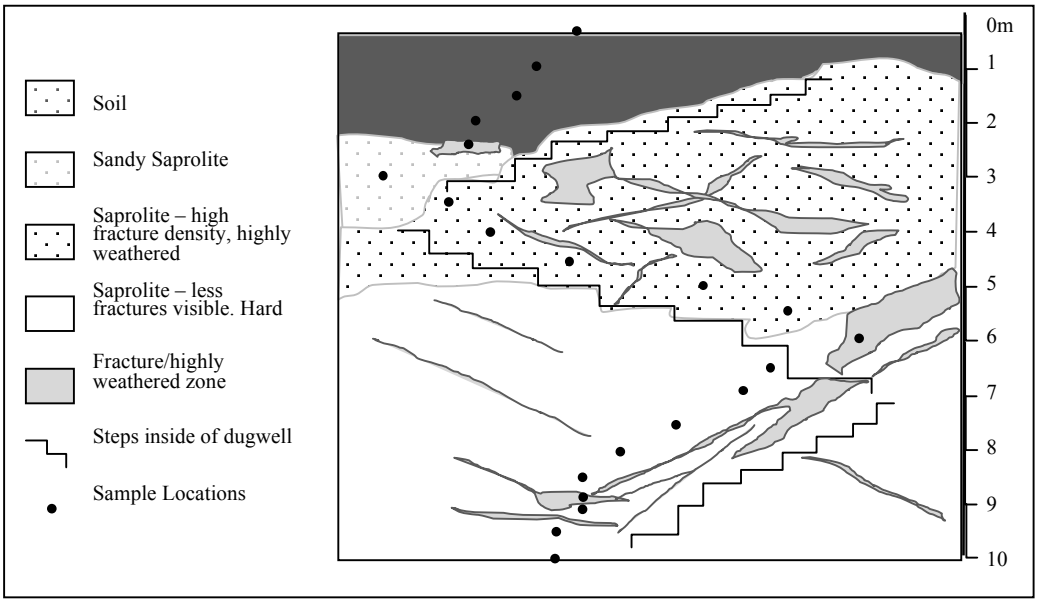

Figure 5-16 – Diagram of Maheshwaram dug-well with locations of profile samples and depth. Diagram is not to scale horizontally.

Table 5-9 - Description of Maheshwaram Profile samples. Abbreviations: Shape: Ang = Angular, PrisA = Prismoidal-Angular, Sph =Spherical, SphS =Spherical-Subrounded, SubA=Sub-Angular, SubAP = Sub-Anuglaur Prismoidal, SubD = Sub-Discoidal, SubP-SR = Sub-Prismoidal, Sub-rounded, SubR =Sub-Rounded, SubRS= Subrounded-spherical. Identifiable minerals: Feldsp =feldspar, Qtz =Quartz. Photographs taken at the same magnification, shutter speed and aperture with scale bar in cm.

Sample Image	Depth (m)	Size	Shape	Colour	Identifiable Minerals/Notes
	**0**	Variations in size	Soil	Light brown	Organic matter present. Brown coating on everything. Pink and white feldsp, carbonate.
	0.5	Equi-granular ~0.5cm	Soil	Moderate yellowish brown	Organic matter present. Pink feldsp, white feldsp, qtz
	1	More Equi-granular ~0.5cm	Soil	Light Brown	Organic matter present. Pink feldspars, white feldsp, qtz
	1.5	Blocky texture (up to 8cm)	Soil	Dark yellowish orange	Organic matter present. Pink feldspar, biotite mica, white feldsp, carbonate (few), qtz (small)
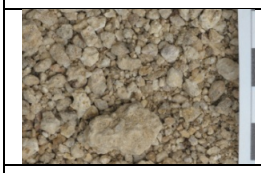	**2 Fill**	Sandy Fill material	Sandy Sap	Very pale orange	Carbonate (fizzes with 10% HCl – large amount ~40%), quartz, pink feldsp (few).
	2.5		Sandy sap	Light Brown	Everything coated in brown/red powder. Carbonate (fizzes with 10% HCl). Mainly qtz,

Sample Image	Depth (m)	Size	Shape	Colour	Identifiable Minerals/Notes
					some pink feldsp & biotite. Hard to identify due to brown/red covering.
	**3**	Fine-1.5com	SubR-SubS	Moderate orange pink	Pink feldsp (some v dark bright pink patches), white feldsp, mafics including biotite mica (few), qtz
	3.5	Fine-2cm	SubP-Ang	Moderate orange pink	Pink feldsp, biotite mica (some in large pieces that break up easily along lines of mica cleavage, leaving a bright orange stain), white feldsp, iron staining, qtz
	**4**	V fine-2cm	SubP-A	Very pale orange	Pink Feldsp (make up most of larger pieces), white feldsp, biotite (some in large pieces), qtz, white/red iron staining
	4.5 Fracture Fill	V fine-1.5cm	A-subP	Moderate orange pink	Carbonate (~2% fizzes with 10% HCl), pink feldsp (~40%), biotite mica (~10%), white feldsp, qtz, iron staining
	**5**	V fine-1cm	Sph-Ang	Moderate orange pink	Pink feldsp (make up most of larger pieces), biotite (sometimes large), white feldsp, Fe staining, qtz
	5.5	V fine-1.5cm	SubP-Ang	Greyish orange pink	Pink feldsp (make up most of the larger pieces), biotite (sometimes large), qtz, Fe staining, hard.
	**6 Fracture Fill**	V fine-1cm	SubP-SubA	Moderate orange pink	White carbonate (~20% fizzes with 10% HCl) some minerals in a carbonate 'cement', pink feldsp (<20%), qtz (few), red Fe staining (few)
	6.5	V fine-4cm	SubA-SubP	Moderate orange pink	Pink feldsp (make up most of the larger pieces), white feldsp, biotite, iron staining, qtz
	7	V fine – 2cm	SubP-SubR	Moderate orange pink	Pink feldsp (make up most of the larger pieces), biotite (as larger pieces & in smaller fragments), qtz, white feldsp.

Sample Image	Depth (m)	Size	Shape	Colour	Identifiable Minerals/Notes
	7.5	V fine-3cm	SubP-subR	Moderate orange pink	Pink feldsp (make up most of the larger pieces), white feldsp, biotite, qtz, (biotite and qtz are mostly smaller pieces). Red/orange iron staining. Mafics.
	**8**	Fine-1cm	SubAS-SubP-SR	Moderate orange pink	Pink feldsp (make up most of the larger pieces), qtz, biotite (make up some of the larger pieces), white feldsp, unidentified mafic mineral, iron staining
	8.5	Fine-1cm	SubRS-SubAP	Moderate orange pink	Pink and white feldsp, qtz, biotite (small platey pieces), iron staining
	8.8 Fracture Fill	Fine-1.5cm	SphS-PrisA	Moderate orange pink	Pink and white feldsps (less white feldsp than before), increase in qtz, biotite, iron staining, white carbonate mineral (<5%), mafic red mineral unidentified
	9	Powder-1.5cm	SubA-SubD	Moderate orange pink	Pink and white feldsp, qtz, biotite, red iron staining
	9.5	Powder-1.3cm	Sph-subA	Moderate orange pink	Pink and white feldsp (make up most of the larger pieces), biotite, qtz, red/orange iron staining
	**10**	Powder-4cm	SubA-subP	Moderate orange pink	Pink feldsps (make up most of the larger pieces), white feldsp, platey biotite (intact), qtz, red/orange iron staining. In the field the sample was very hard.

The corresponding fresh rock sample (M2a) is a gneissic porphyritic biotite granodiorite, with microphenocrysts of feldspar, and a smaller mass of quartz, biotite, chlorite, epidote, zircon, titanite and apatite (mineral composition and abundance in table 5-10). This sample was taken from adjacent to the dug well from which the profile samples come.

Table 5-10 – Mineral composition and abundance in fresh rock sample M2a, and weathered profile sample M2b (~10m depth). Mineral formulas calculated from EM-EDX analysis. * indicates no EM analysis available, general formula given.

Mineral	Mineral formula in M2a fresh rock sample from EM analysis	%	
		M2a	M2b
Quartz	SiO_2*	21.4	17.9
Microperthite	-	0.2	
Plagioclase	$NaAlSi_3O_8$ - $CaAl_2Si_2O_8$*	31.5	19.3
K-Feldspar	$KAlSi_3O_8$*	13.6	47.7
Apatite	$Ca_{4.91}\ Al_{0.03}Fe_{0.01}K_{\ 0.01}\ (P_{0.85}O_4)_3\ (OH_{0.55}F_{0.45})$	1.2	0.3
Biotite	$(Na_{0.01}K_{0.90})\ (Al_{0.37}Fe_{1.43}Ti_{0.11}Mg_{0.93}Mn_{0.02})\ (Si_{2.73}Al_{1.27})\ (Cl_{0.01}F_{0.04}OH_{1.96})$	24.0	7.4
Chlorite	$(Fe, Mg, Al)_6(Si, Al)_4O_{10}(OH)_8$*	4.7	1.6
Iron Oxide	FeO - Fe_2O_3 - Fe_3O_4*	0.6	4.2
Titanite	$Ca_{1.04}\ (Ti_{0.87}Al_{0.08}Fe_{0.02})SiO_4(F_{0.22}OH_{0.78})$	0.2	0.4
Epidote	$(Ca_{2.15}\ Mg_{0.06})\ (Al_{2.22}Fe_{0.34})(Si_{3.54}O_{24})(OH)_2$	2.0	0.7
Zircon	$Zr[SiO_4]$*		0.1
Calcite	$CaCO_3$*		0.5
	Total:	100	100

Whole Rock Chemistry

Whole rock chemistry (WRC) results are given in table 5-11 and figure 5-17. The distribution of elements within the weathering profile compared to the fresh rock sample (M2a) is illustrated in figure 5-18 to figure 5-20.

Table 5-11 – Whole Rock Chemistry (by lithium metaborate method) of Maheshwaram profile samples. All Fe given as Fe_2O_3

%	M2a	Profile samples										
depth	**-**	**10m**	**9m**	**8m**	**7m**	**6m**	**5m**	**4m**	**3m**	**2m**	**1m**	**0m**
Al_2O_3	14.4	13.44	14.2	14.4	14.0	13.4	13.6	14.3	13.71	11.40	13.70	13.89
CaO	2.41	1.76	1.45	1.52	1.69	4.16	1.65	2.15	1.42	11.57	0.95	1.17
Fe_2O_3	3.61	3.82	2.71	3.01	2.79	2.64	2.85	3.96	3.53	2.49	3.04	3.27
K_2O	4.55	4.48	5.81	5.53	5.08	5.63	5.05	5.03	4.96	3.58	5.03	5.17
MgO	1.14	0.90	0.65	0.68	0.74	0.76	0.79	0.98	0.76	0.71	0.46	0.54
MnO	0.04	0.04	0.03	0.03	0.03	0.01	0.04	0.04	0.03	0.02	0.02	0.03
Na_2O	3.11	2.58	2.58	2.89	2.80	2.15	2.72	3.07	2.98	1.85	1.43	1.87
P_2O_5	0.19	0.22	0.15	0.15	0.15	0.09	0.14	0.20	0.18	0.10	0.08	0.10
SiO2	66.5	67.84	67.0	70.7	68.7	66.3	67.9	66.8	68.54	51.85	64.94	65.48
TiO_2	0.49	0.55	0.39	0.42	0.35	0.30	0.41	0.55	0.48	0.32	0.36	0.37
Total	96.4	95.6	94.9	99.4	96.3	95.4	95.2	97.1	96.6	83.9	90.0	91.9

Many elements are lower in concentration in the saprolite compared to the fresh sample, are then fairly consistent through the saprolite, and lower again in the soil zone (1-2m) (table 5-11 and figure 5-18). Some elements, for example CaO and

NaO, show overall decreasing trends towards the surface as seen in figure 5-18 and figure 5-19, likely due to the progressive weathering of plagioclase. CaO increases at 2 and 6m depth (figure 5-20) are associated with fracture fill material. MgO and P_2O_5 also decrease overall towards the surface, with MgO decreases likely to result from biotite weathering and P_2O_5 from apatite weathering (with fluorapatite more easily weathered than other apatites). Mass balance calculations give biotite and apatite as the principal mineralogical sources of F loss from M2a (Section 5.1.2).

K_2O is enriched in all samples above 10m (close to bedrock concentration); K-bearing potassium feldspars are more resilient to weathering than other silicate minerals present. The decrease in Na_2O/K_2O ratio (from 0.7 to 0.4) is likely to be due to the preferential weathering of plagioclase compared to K-feldspar. EM analysis shows that K is lost from biotite upon weathering (chapter 4, section 4.6.1), and K may also be retained in clay minerals, although these will make up a small portion of the sample total K content.

Fe_2O_3 is enriched at 10m and 4m, and otherwise slightly depleted. On weathering of biotite, chlorite and epidote, Fe^{2+} may be mobilised, and redistributed irregularly as FeOOH precipitates. Al_2O_3 and SiO_2 are consistent by contrast through the profile except at the level of fracture fill; Al is largely insoluble and would be expected to remain in the solid phase (figure 5-19). Ti, Al and Fe^{3+} are usually considered to be immobile elements (the later under oxidising conditions only), whereas Ca, Na and Mg are readily mobilised to groundwater solution (Middelburg et al., 1988; Nesbitt and Young, 1984; Loughnan, 1969).

Fracture fill materials at 2 and 6m depth have high CaO. At 2m CaO is very high, and a decline in all other elements is measured as well as a low analytical total (table 5-11). At 6m depth, Ca is not as high, and corresponds to a decrease in MnO, P_2O_5, TiO_2, Na_2O and Fe_2O_3, and an increase in K_2O. Fractures at 2 and 6m are very different, with a clear fracture present at 6m (figure 5-15), and only a slight distinction from surrounding material within the sandy saprolite at 2m depth. The material in these fracture fills is likely to be mainly clay minerals (which may retain K_2O, Al_2O_3) and disseminated calcium carbonates.

The sample at 4m depth has relatively high concentrations of many elements such as Al_2O_3, Fe_2O_3, MgO, MnO, Na_2O, P_2O_5 and TiO_2. This sample may be enriched in minerals such as biotite, titanite, iron oxides, and apatite.

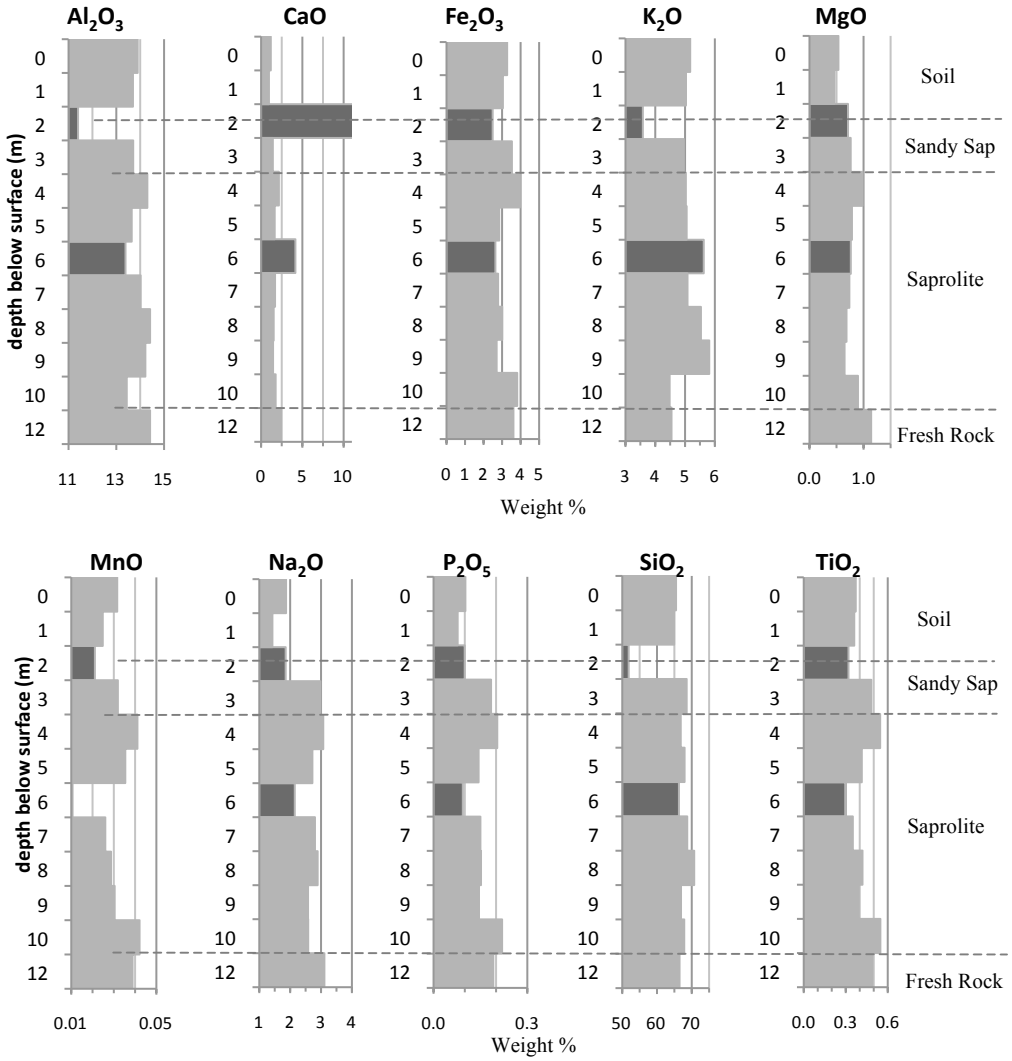

Figure 5-17 – Maheshwaram element profiles through the weathered rock from surface soil (0m depth) to bedrock (12m depth – this is not the actual depth of bedrock). Fracture fill samples indicated by darker bars (at 2 and 6m depth). Element analysis part of whole rock chemical analysis using lithium metaborate fusion. All results are in wt. %.

Petrological observations show that weathered sample M2b (collected from ~10m depth in this profile) has less biotite, chlorite, apatite, plagioclase and epidote than fresh sample M2a (table 5-10) which correlates to the element losses seen in the profile (MgO loss from biotite and chlorite, P_2O_5 loss from apatite, CaO and Na_2O loss primarily from plagioclase). Enrichment of K_2O corresponds to the relative enrichment of K-feldpsar in the weathered sample as observed in point counting. Sample M2b also has a higher percent of iron oxides visible (table 5-10). Biotite and

many plagioclase feldspars in M2b are also seen to be heavily weathered. XRD results from sample M2a and M2b show reduced biotite and chlorite content in the weathered sample, as well as the presence of clay minerals (chapter 4, section 4.5).

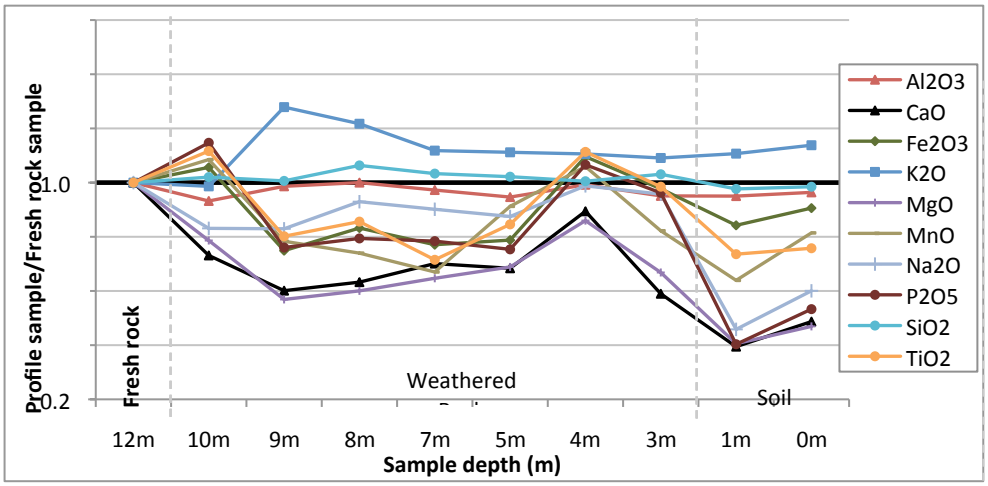

Figure 5-18 - Fresh rock (M2a) normalised diagram of element abundance with depth (B=fresh rock sample M2a). Values <1 indicate element loss, values >1 indicate element enrichment. Fresh rock sample M2a included at depth 12m. Infill material at 2m and 6m depth is not included.

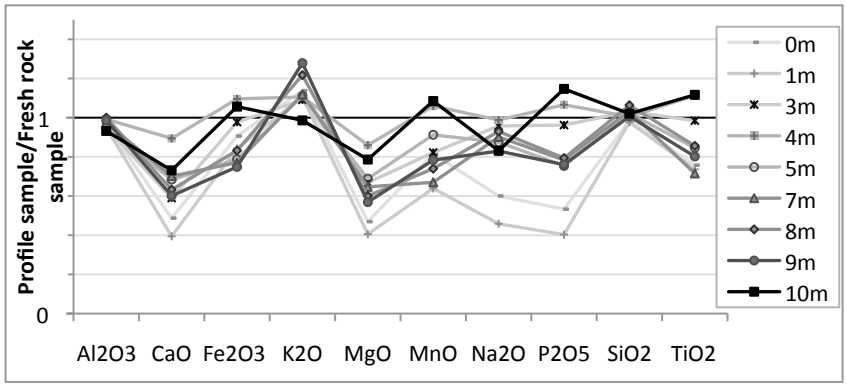

Figure 5-19 - Fresh rock normalised diagram of the Maheshwaram weathering profile. Values >1 indicate element enrichment, values <1 indicate element loss. Infill material at 2m and 6m depth is not included.

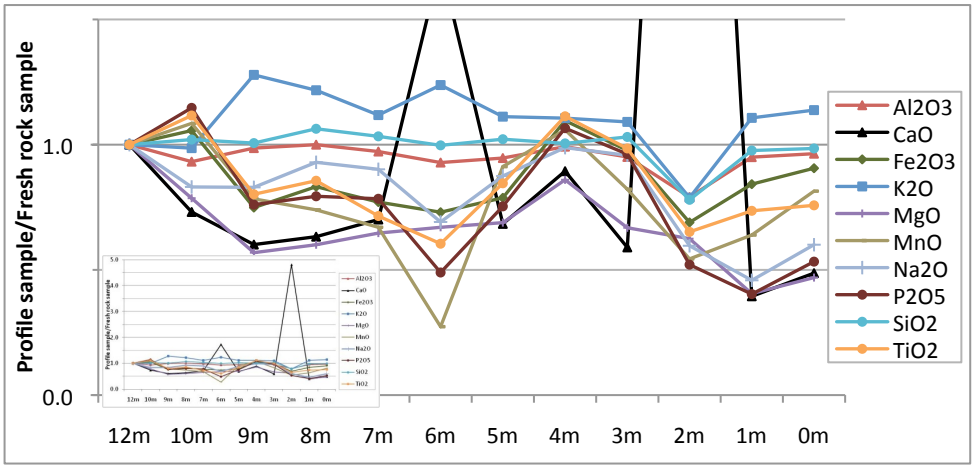

Figure 5-20 - Fresh rock (M2a) normalised diagram of element abundance with depth (B=fresh rock sample M2a). Values <1 indicate element loss, values >1 indicate element enrichment. Fresh rock sample M2a included at depth 12m. Infill material at 2m and 6m depth.

The degree of weathering can be assessed by the Chemical Index of Alteration (CIA), which increases as weathering proceeds (see chapter 2, section 2.2.2). The value of CaO used in calculating should be from silicates only, and therefore fracture fill material is not included. Calculated CIA values are shown in figure 5-21.

The CIA is highest in shallow samples of the soil zone (at 0 and 1m), and lowest in the fresh rock sample at 12m. Throughout the majority of the regolith the state of weathering is relatively constant, as it has similar CIA values.

The similarity in the state of weathering for the majority of the regolith indicates chemical weathering intensities being alike at all depths, with initial changes from partly weathered rock to saprolite occurring rapidly, and subsequent changes being much slower (e.g. Stolt et al., 1992).

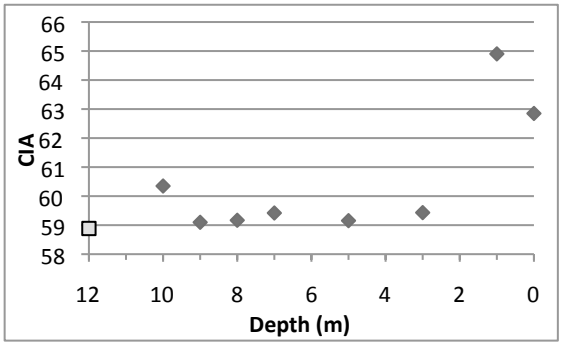

Figure 5-21 – The Chemical Index of Alteration (CIA) through the depth profile in the Maheshwaram catchment. Not including samples at 2, 4 and 6m. The fresh rock sample M2a, CIA 58.89, is indicates as a □ at a depth of 12m.

Whole Rock Fluorine

Details of the whole rock fluorine (WRF) method are given in chapter 4 and appendix 2.

The lowest WRF values are measured in the soil zone (328 ppm F at 0m), and the highest measured in the fresh rock (1749 ppm F in M2a) (table 5-12, figure 5-22). Of the weathered rock samples between these, low values of F are measured at 6m depth (in fracture fill material) and high values at 4m (enriched layer). WRF values do not show a straightforward increase with depth, supporting the similarity in weathering state calculated from CIA above and suggesting there may be accumulation of F in parts of the weathered regolith (e.g. 4m). Samples with a lower K_2O and higher MgO

content (implying less weathering and/or increased biotite content) have higher WRF values (figure 5-23).

The profile of F concentration (low at 0m and 6m, high at 4m and in the fresh sample) (figure 5-22) is similar to the element profiles of MnO, Na_2O, Fe_2O_3, MgO, P_2O_5 and TiO_2 (figure 5-17).

Table 5-12 - Maheshwaram Profile whole rock fluorine measurements.

Sample Depth	WRF measurement (ppm F)		Average F (ppm)
	Initial readings	Repeat readings	
M2a Fresh rock sample	1725	1814	1749
	1801	1657	
8	521	549	535
6 (fill)	403	444	423
4	717	788	753
0 (soil)	315	341	328

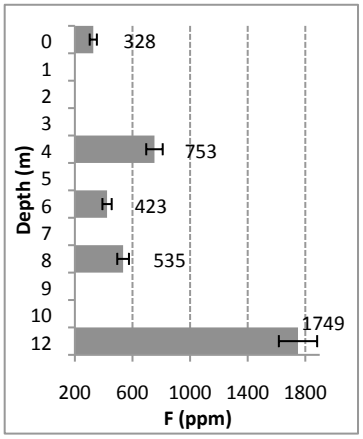

Figure 5-22 - WRF with depth in the Maheshwaram profile. WRF measured at 0, 4, 6,and 8m. Fresh rock sample is indicated at 12m depth (not actual depth).

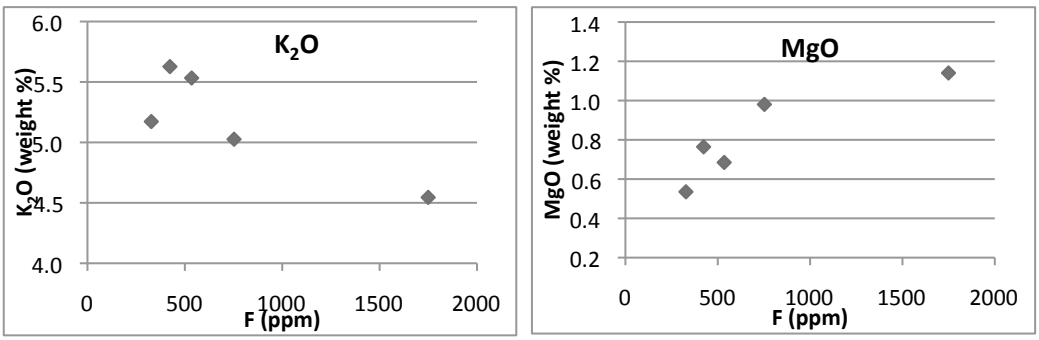

Figure 5-23 – Maheshwaram sample F content vs K_2O content and MgO content.

5.2.2 Wailpally Profile

Wailpally profile samples were collected from a wide dugwell with steps for access (figure 5-24, figure 5-25) at location W11 (see map in chapter 4, section 4.2). The top of the well is supported by brick work on one side, which is higher than the opposite side. Sample depths are measured from the vegetation surface on the north side of the well (left hand side of figure 5-25). The weathering profile here is not as thick as the Maheshwaram profile, with fresh rock observed at the bottom of the well (~9-10m depth). Fresh rock sample W11 was taken from the bottom of the well, and saprolite samples taken from the sides of the well using a geological hammer at intervals of 1m. Size and sorting may be influenced by the method of sample collection (hammering). Sample descriptions are given in table 5-13 and approximate sample locations in figure 5-26.

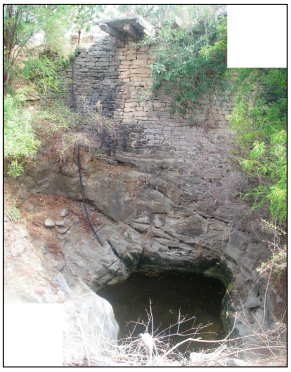

Figure 5-24 - Photograph of Wailpally dug well

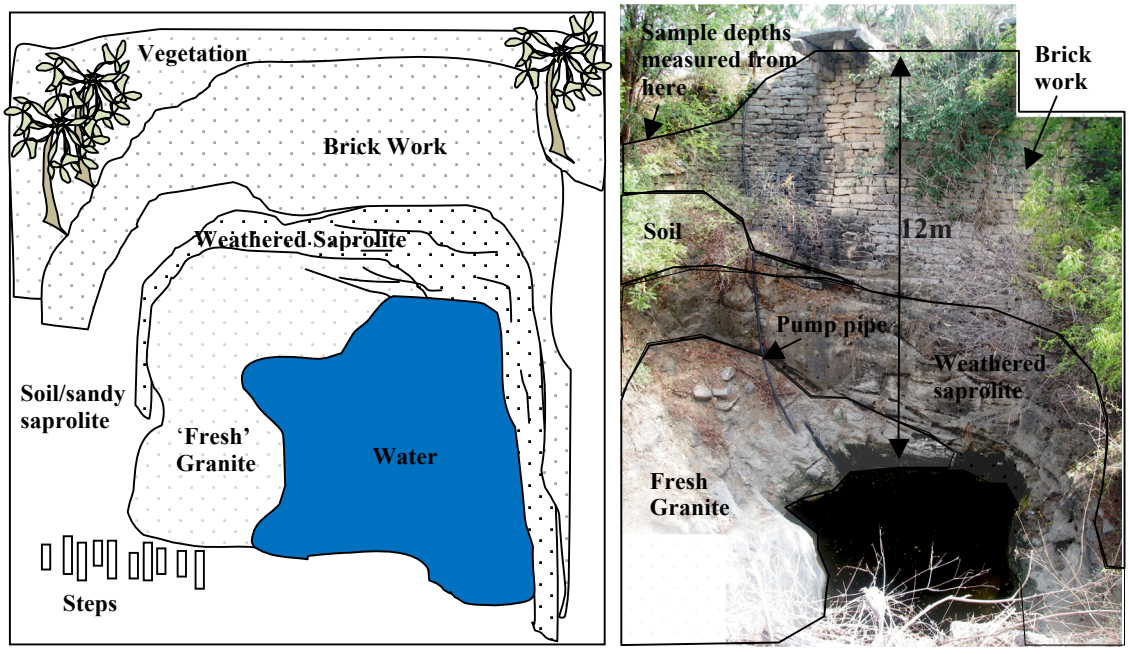

Figure 5-25. Diagram of Wailpally profile well (left) with overlay on photo (right)

Samples have an overall increasing mafic concentration with depth as well as an increasing grain size and hardness (table 5-13). All samples contain pink and white feldspars, quartz and mafics with many samples containing small amounts of carbonate (e.g. samples at 3m and 5m). The profile sample at 2m is taken from the sandy saprolite and has more quartz, less mafics and a smaller grain size.

Table 5-13 - Descriptions and photos of Wailpally Profile samples. Abbreviations: Shape: PrisA = Prismoidal-Angular, Sph=Spherical, SubA=Sub-Angular, SubP= Sub-Prismoidal, Sub-rounded, SubR =Sub-Rounded. Identifiable minerals: Feldsp=feldspar, Qtz =Quartz. Photographs taken at the same magnification, shutter speed and aperture with scale bar in cm.

Sample Image	Depth (m)	Size	Shape	Colour	Identifiable Minerals/Notes
	**2 Sandy Sap**	V fine to 1cm	SubP-SubA	Greyish orange pink	Pink and white feldspars (make up the larger pieces), qtz, some Fe staining. No carbonate, less mafics
	**3**	V fine to 1cm	SubP-SubA	Very pale orange	White feldsp, less mafics, qtz, small amount pink feldsp, carbonate coating/cement on many minerals
	**4**	V fine to 1.5cm	SubR-SubP	Very pale orange	High quantity mafics, white feldsp, some pink feldsp, qtz, fe staining, few carbonates present
	**5**	V fine to 4.5cm	SubR-SubP	Very pale orange	Very large white felsp, high quantity mafics, qtz, some fe staining, carbonate.
	**6**	V fine to 2cm	Pris-SubA	Moderate orange pink	High quantity of mafics, greenish chlorite, qtz, white feldsp, orange carbonate.
	**7**	V fine to 5cm	SubA-Sph	Greyish orange pink	High quantity mafics, white feldsp, qtz, orange carbonate, fe staining, pink feldsp

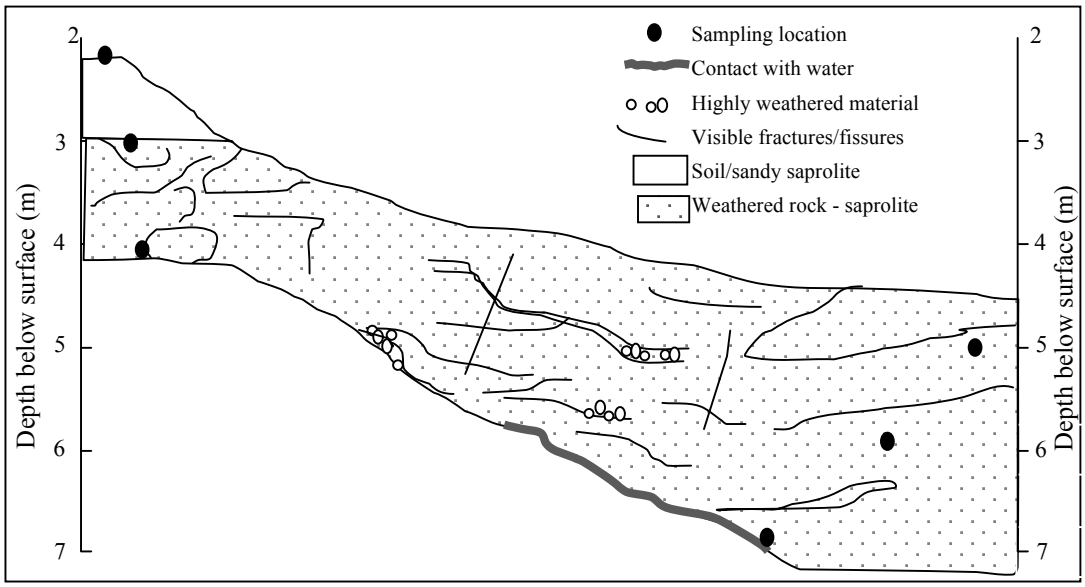

Figure 5-26 – Flattened view of saprolite in the Wailpally dug-well profile showing approximate location of sampling points.

Fresh rock sample W11a was taken from the bottom of the well and is an amphibole granodiorite, medium to coarse grained with quartz, feldspars and amphiboles, and minor chlorite, apatite and epidote (see chapter 4, section 4.4.3). Amphiboles are identified as ferro-edenite and chlorite of pycnochlorite through EM-EDX analysis with mineral classification spreadsheets (Preston and Smith, 2002; Tindle, 2009). Mineral composition and abundances are given in table 5-14.

Table 5-14 – Mineral composition and abundance in fresh rock profile sample W11a. Mineral formulas calculated from EM-EDX analysis. * indicates no EM analysis available, so general formula given.

Mineral	**Mineral formula**	**%**
		W11
Quartz	SiO_2*	14.7
Microperthite	-	1.0
Plagioclase	$NaAlSi_3O_8$ - $CaAl_2Si_2O_8$*	44.2
K-Feldspar	$KAlSi_3O_8$*	18.4
Apatite	$(Ca,Al_{0.01})_5\ (P_{0.84}Si_{0.01}O_4)_3\ (F_{0.7}OH_{0.3})$	0.2
Chlorite	$(Mg_{0.42}\ Fe^{2+}_{0.34}Fe^{3+}_{0.01}Mn_{0.01}Al_{0.19})_{12}\ [(Si_{0.74}Al_{0.26})_8\ O_{20}]$ $(Cl_{0.02}F_{0.07}OH_{15.91})$	1.1
Iron Oxide	FeO - Fe_2O_3 - Fe_3O_4	0.2
Titanite	$Ca_{0.93}(Ti_{0.85}Al_{0.16}Fe_{0.06}Mg_{0.04})SiO_4(F_{0.25}OH_{0.75})$	0.2
Epidote	$(Ca_{2.00}Mn_{0.02})\ (Al_{2.35}Fe_{0.85})(Si_{3.12}O_{24})(OH)_2$	0.7
Epidote var 2	$(Ca_3Mg_{0.02}Mn_{0.02})\ (Al_{0.896}Fe_{1.14}Ti_{0.03})(Si_{2.96}Al_{0.39}O_{24})(F_{0.27}OH_{1.73})$	0.5
Amphibole	$(Na_{0.21}K_{0.18})\ (Ca_{0.92}Na_{0.08})_2\ (Mg_{2.37}Fe^{2+}_{1.67}Fe^{3+}_{0.52}Al_{0.27}Ti_{0.10}Mn_{0.07})$ $(Si_{0.85}Al_{0.15})_8\ O_{22}\ (OH,F,Cl)_2$	18.7
	Total:	100

Whole Rock Chemistry

The concentrations of elements in the weathering profile are given in table 5-15 and figure 5-27. Comparisons to fresh rock sample W11a are given in figure 5-28 and figure 5-29.

Table 5-15 – Whole rock Chemical analysis of Wailpally profile samples and fresh rock W11a (given at 9m depth). '<' indicates lower than detection limit

Composition (wt. %)	W11a	Sample Depth (m)					
		7	6	5	4	3	2
Al_2O_3	14.15	14.28	13.79	14.07	14.07	13.92	13.72
CaO	3.27	3.36	3.54	3.55	2.79	2.66	2.05
Fe_2O_3	4.13	3.84	3.25	2.95	3.11	2.33	2.19
K_2O	3.56	4.04	3.67	3.31	3.61	3.30	3.77
MgO	1.83	1.49	1.52	1.33	1.63	1.00	0.88
MnO	0.06	0.06	0.05	0.04	0.03	0.03	0.02
Na_2O	3.53	3.49	3.43	3.69	3.52	3.72	3.50
P_2O_5	<	0.11	0.10	0.09	0.09	0.07	0.08
SiO2	66.79	68.17	66.10	66.61	66.94	69.53	69.86
TiO_2	0.29	0.28	0.29	0.24	0.28	0.22	0.22
F (ppm)	823.7	657.8			715.5		561.1

Overall, concentrations of MgO, P_2O_5, Fe_2O_3, MnO, and TiO_2 decrease towards the surface. Lower concentrations of P_2O_5 are likely to result from apatite weathering, of MgO from amphibole (and potentially chlorite) weathering and of TiO_2 from titanite weathering. The decrease in Fe_2O_3 towards the surface is indicative of an increase in weathering (Stolt et al., 1992), and may result from the loss of Fe from minerals such as chlorite, epidote and amphiboles. The overall decrease in CaO towards the surface is likely to result from plagioclase weathering. This is usually also associated with a decrease in Na_2O, however this is not the case in this profile. The average CaO content of the Wailpally profile samples is higher than the Maheshwaram profile samples (apart from fracture fill material). This is seen in the profile material, with many samples containing small amounts of carbonate, and in the high plagioclase and amphibole content of the fresh rock samples in Wailpally

SiO_2, Al_2O_3, Na_2O and K_2O change little through the profile, with a slight decrease in Al_2O_3 and increase in SiO_2 towards the surface (figure 5-28). SiO_2 enrichment is likely to be due to the removal of other elements while SiO_2 remains and K_2O is primarily located in potassium feldspars, which are more resistant to weathering than other silicate minerals.

No samples were taken of fracture fill material, although samples at 3m and 5m depth were noted to have increased carbonate visible. The sample at 4m depth is enriched in MgO, Fe_2O_3, TiO_2 and K_2O relative to adjacent samples and may correspond to an amphibole (or chlorite) rich layer.

Mass balance F calculations show most F in sample W11a to be located in amphiboles with smaller amounts in apatite, epidote (var 2), and titanite, and very small amounts in chlorite and epidote (section 5.1.3). Amphibole weathering is therefore likely to be important in the release of F to groundwater.

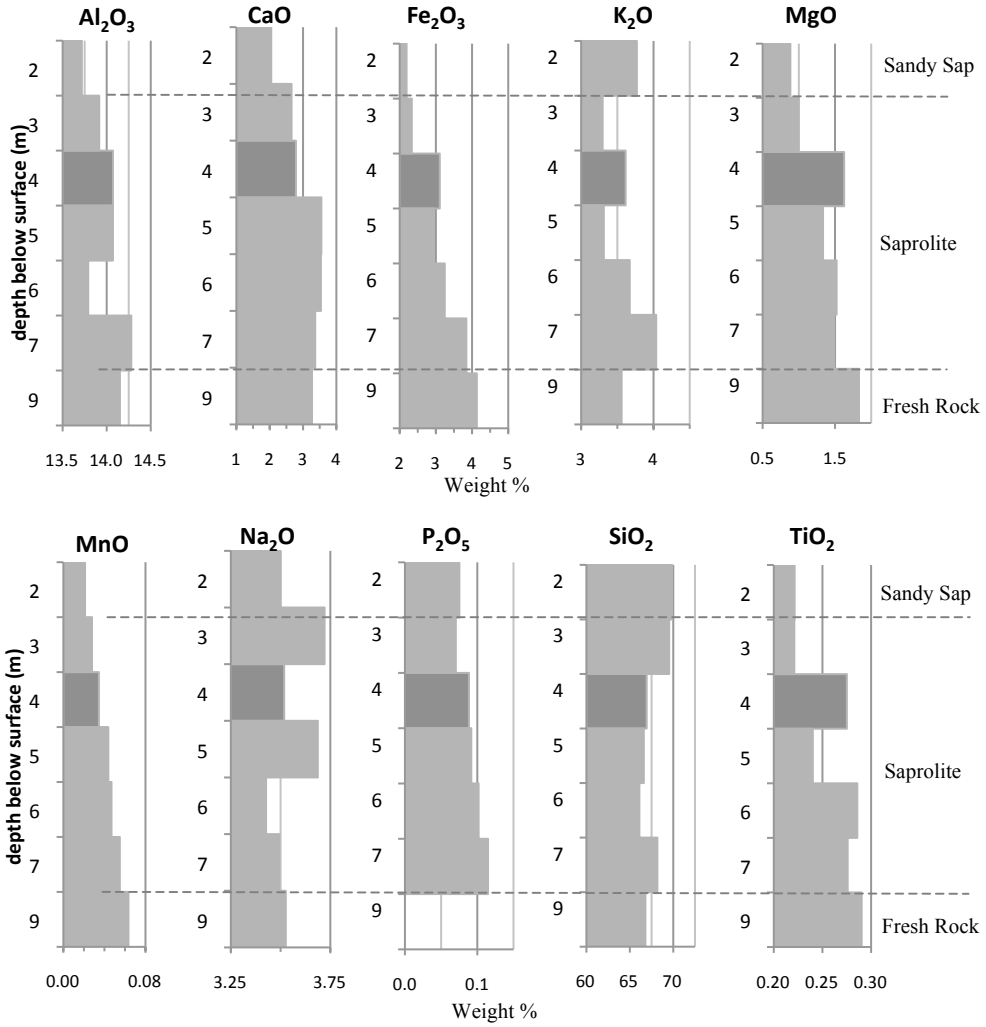

Figure 5-27 – Wailpally element profiles through the weathered rock from surface soil (0m depth) to bedrock (9m depth – this is not actual depth of bedrock). P_2O_5 was not measured in fresh rock sample W11a. All results are in wt. %. Dark bar at 4m due to a potentially amphibole rich layer.

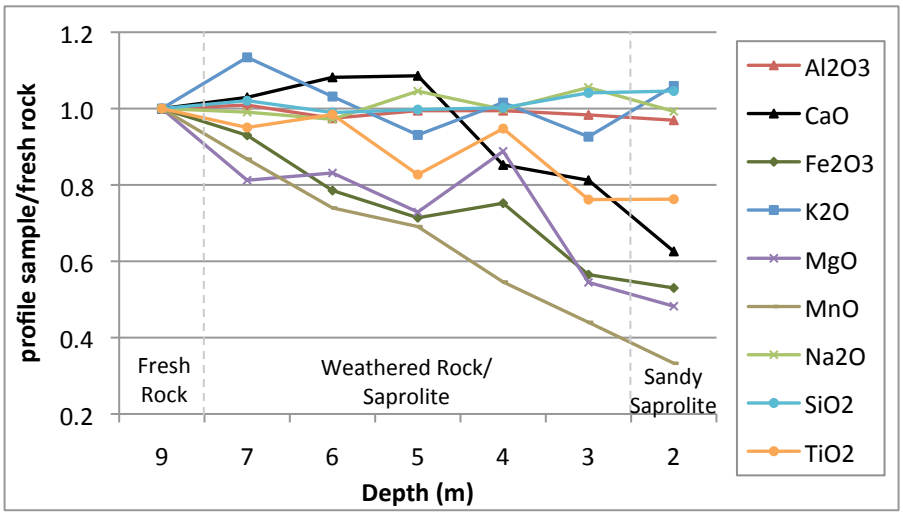

Figure 5-28 - Fresh rock normalised diagram element abundance with depth. Values >1 indicate element enrichment compared to fresh sample W11a, values <1 indicate element loss. Fresh sample W11a included at depth 9m.

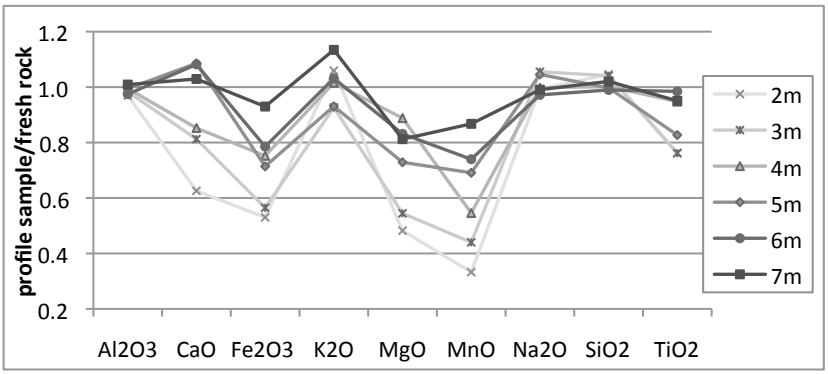

Figure 5-29 - Fresh rock normalised diagram of the Wailpally weathering profile. Values >1 indicate element enrichment compared to fresh sample W11a, values <1 indicate element loss.

The weathering trends seen here with depth (including MgO, P2O5, Fe_2O_3, CaO, MnO, and TiO_2) suggest an increase in weathering towards the surface. Calculated CIA supports this, with a strong correlation (R^2=0.907) between sample depth and CIA. However the fresh sample W11a has a high CIA value compared to deep saprolite samples (figure 5-30).

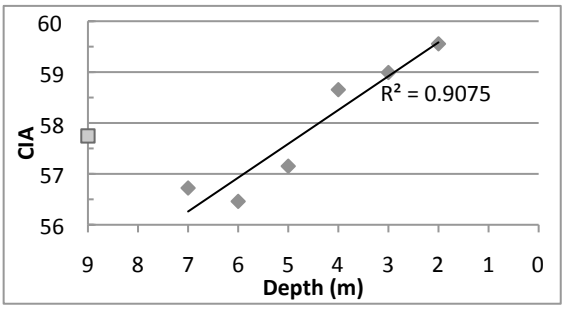

Figure 5-30 – Chemical Index of Alteration (CIA) for Wailpally Profile samples. Fresh rock sample W11a shown at 9m depth (not actual depth) as a □, with a CIA value of 57.7.

Whole Rock Fluorine

The highest whole rock F (WRF) value measured is in fresh rock sample W11a (834 ppm F) (figure 5-31). WRF content decreases towards the surface in samples at 7 and 2m (623 and 530 ppm F, respectively) (table 5-16 and figure 5-31). The sample at 4m has a higher WRF measurement compared to the other weathered samples (716 ppm F). This could be due to the higher concentration of mafics at this depth as noted in profile descriptions and whole rock chemistry results.

Samples with a higher Fe_2O_3, MgO, and TiO_2 content and with lower SiO_2 content have a higher WRF content (figure 5-32). The higher content of these elements and a lower SiO_2 content imply a higher proportion of F-bearing minerals such as amphiboles and titanite and a lower degree of weathering.

Table 5-16 - Wailpally Profile whole rock fluorine measurements

Sample Depth	WRF measurement (ppm F)		Average F (ppm)
	Initial readings	Repeat readings	
W11a Fresh Rock sample	824		824
7	649	597	623
4	716		716
2	569	491	530

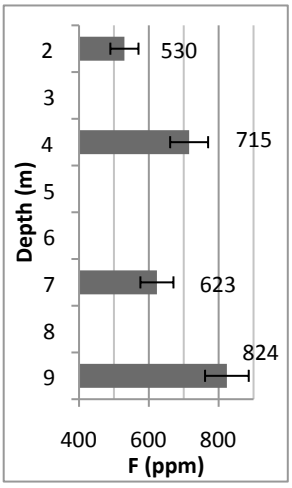

Figure 5-31 - Whole rock fluoride values with depth in the Wailpally weathering profile. Fresh rock sample given at 9m depth (not actual depth).

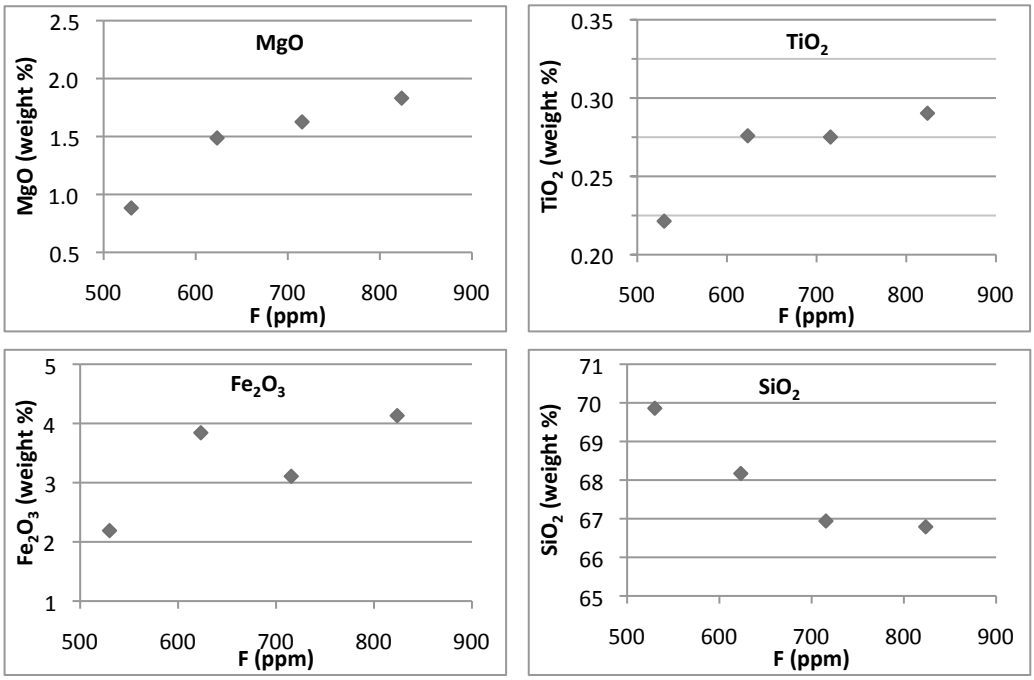

Figure 5-32 – Wailpally sample F content vs MgO, TiO_2, Fe_2O_3 and SiO_2 content.

5.2.3 Profile Summary

The Maheshwaram profile includes soil samples (0-2m), sandy saprolite (2-3m), and saprolite with increasing hardness and mafics with depth (up to 10m). Multiple fractures with clay and disseminated carbonate are present which have a low WRF content (e.g. at 6 and 2m depth), as well as layers with a higher concentration of F-bearing minerals with a high WRF content (e.g. at 4m). The fresh rock sample is a gneissic porphyritic biotite granodiorite also containing epidote, apatite and titanite.

Element profiles with depth show many elements to be lower in concentration in the saprolite compared to the fresh sample, fairly consistently through the saprolite, and lower again in the soil zone. Sample F content is highest in the fresh rock sample (1749 ppm F) and lowest in the soil sample (328 ppm F) with F values within the saprolite varying between 423 and 753 ppm F. Figure 5-33 shows the profile with WRF values.

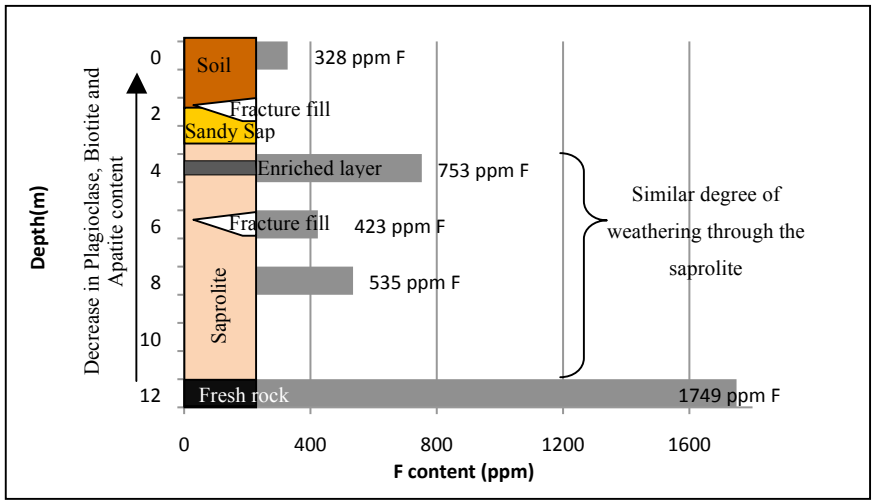

Figure 5-33 – Weathering profile and whole rock fluorine content at location M2 in the Maheshwaram catchment

The weathering of plagioclase feldspar, apatite, and biotite is noted in the element profiles as well as in sample mineralogy. Weathering of these minerals is important in the profile mass balance calculations, where the primary loss of F from the profile is calculated to be from apatite and biotite. Soil samples at 0 and 1m (the soil zone) are most weathered and fresh rock sample M2a is the least weathered, however

throughout the majority of the regolith the state of weathering is relatively constant. This may be due to chemical weathering rates and intensities being similar at all depths, with initial changes from partly weathered and fractured rock to saprolite occurring rapidly, and subsequent changes being much slower (e.g. Stolt et al., 1992).

The Wailpally weathering profile is not as thick as the Maheshwaram profile and includes a hard saprolite with decreasing grain-size and decreasing concentration of mafics towards the surface. The top 2-3m of the Wailpally profile are softer sandy saprolite. The main minerals present include pink and white feldspars, quartz and amphiboles as well as calcium carbonates. The fresh rock sample is an amphibole granodiorite which also contains chlorite, apatite and epidote. Figure 5-34 shows the profile with WRF values.

Element profiles show a decrease towards the surface in MgO, P_2O_5, Fe_2O_3 and TiO_2 and may reflect the weathering of plagioclase feldspar, amphiboles and titanite. Mass balance calculations show amphiboles to be the primary F-bearing mineral in the fresh rock sample, and therefore the weathering of amphiboles is important in F release to groundwater. The highest WRF value was measured in the fresh rock sample (824 ppm F) and the lowest in the sandy saprolite sample at 2m (530 ppm F). The sample at 4m depth is enriched in MgO, Fe_2O_3, TiO_2 and K_2O relative to adjacent samples, with a high WRF content (715 ppm F) and may correspond to an amphibole (or chlorite) rich layer. The degree of weathering increases towards the surface with shallower samples more weathered than deeper samples.

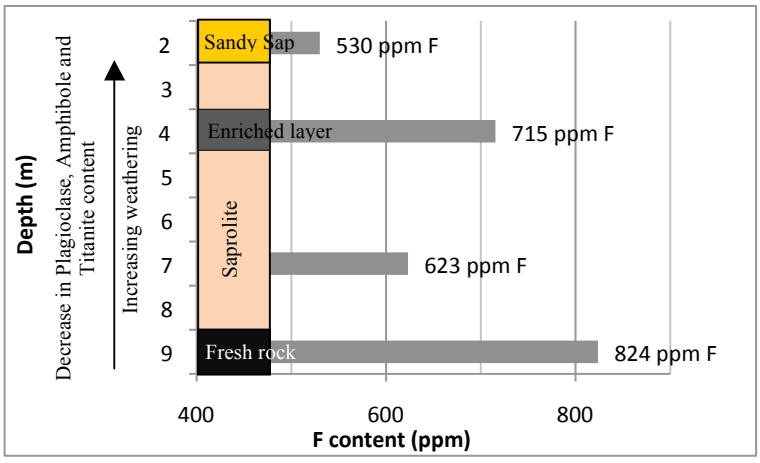

Figure 5-34 - Weathering profile and whole rock fluorine content at location W11 in the Wailpally catchment

The differences in profile structure, depth and chemistry at W11 in the Wailpally catchment compared to at M2 in the Maheshwaram catchment are due to the different mineralogy of the parent rock, and may also relate to the differing locations of the profiles in their respective catchments, including catchment differences in topography and weathering. The Maheshwaram profile fresh rock is gneissic porphyritic biotite granodiorite, with many preserved fissures in the saprolite later, whereas the Wailpally profile bedrock is amphibole granodiorite with few preserved fissures. Both profiles have layers of increased F content, due to a higher proportion of F-bearing minerals. The Maheshwaram profile is located in the south of the Maheshwaram catchment, where the water table and topography is slightly higher. Groundwater flow in Maheshwaram is typically south to north, although the hydraulic gradient is low. The Wailpally profile however, is located at the base of the catchment in the plain, near the discharge region in the east where the weathering profile is thinner. As the Wailpally profile is more evolved it may be older than the Maheshwaram profile.

Chapter 6 – Experimental Observations of F Leaching to Aqueous Solutions

6.1. Introduction

The F content of the bedrock and regolith, and their constituent minerals in the Maheshwaram and Wailpally catchments has been investigated in chapter 4. The mineralogical sources of F released to groundwater on regolith development have been identified by mass balance comparison between fresh rock and their weathered equivalents in chapter 5. The release of F into groundwater depends on the nature of the water-rock interaction. These processes have been investigated through batch leaching experiments, described in this chapter, with the objective of investigating the relative mobility of F to solution from bedrock lithologies and regolith equivalents, and the mobilisation of F from weathered samples at different depths in the regolith profile. Leaching experiments may also give an indication of F presence in clay minerals or adsorbed to Al or Fe minerals that are not identified through the mineralogical mass balance approach.

A semi-quantitative 'F-source strength' has been determined with rankings derived for groups of lithological types in each catchment.

Batch leaching experiments were conducted using both fresh and weathered samples from Maheshwaram and Wailpally following the general approach of Chae et al (2006), who investigated the sources of F and [F^-] evolution resulting from water rock interaction using a granite sample from South Korea and a separated biotite fraction of this granite. Chae et al (2006) reacted a range of size fractions with pure water for up to 1,200 hours (50 days). [F^-] was found to be limited by fluorite saturation. Chae et al (2006) concluded that fluoride in groundwater in granitic bedrock originates from the dissolution of biotite and that the behaviour and concentration of F^- in solution is controlled by fluorite saturation, which in turn depends on the evolving Ca^{2+} concentration.

Short duration leaching experiments in the Wailpally catchment have been carried out by Reddy D. et al. (2010) on soil and calcrete samples, reacted with water (1:1 ratio)

for 2 hours, and for 1 week. Results showed higher concentrations of F^- (up to 7.6mg/l in 2 hours) leached from weathered calcrete than from fresh calcrete. Fluoride concentrations from fresh calcrete increased over 1 week, whereas little change was seen in weathered calcrete.

6.2. Method

The method used in this study was adapted from Chae et al (2006). The samples (table 6-1) were crushed to a uniform grain size and sieved to achieve the size fraction 0.5-2mm. One set of fresh and weathered rock (M2a and M2b) were also crushed to <65μm for a small grain size experiment. Forty grams of sample were added to 200ml of de-ionised water to give a rock-water ratio of 1:5 in a plastic bottle. The bottle was placed on a roller for continuous movement at room temperature. Four ml of liquid was extracted at regular intervals, filtered, and split into two containers for analysis; one left un-acidified for analysis of anions by IC and one acidified with concentrated nitric acid (70%) for analysis of cations by ICP-AES. Acidified samples were also diluted with deionised water to increase the volume available for analysis. Experiments were conducted at the UCL Wolfson Laboratory in sets of 7 samples and at the Natural History Museum in a set of 11 samples (Wailpally profile samples). Repeats were run for the majority of samples. A blank was run with every set of experiments consisting of 200ml of deionised water in a bottle. Further details of the method are given in appendix 3.

Due to the constant movement of samples in the rollers, sample attrition and physical breakdown may occur over time, decreasing the sample size and exposing fresh surfaces to the leaching water. This will affect the concentration of leached elements in solution and should be taken into account when interpreting results.

A correction was applied to account for the removal of water during the sampling procedure (equation below).

$$C_{cor} = [(C_{mes}-C_{prev}) * (V_s/V_o)] + C_{prev}$$

Where:

V_s = Volume in reaction vessel when sampled (ml)

V_o = Original volume in the reaction vessel (ml)

C_{cor} = Corrected Concentration of element C (mg/l)

C_{mes} = Measured Concentration of element C (mg/l)

C_{prev} = Corrected concentration of previous sample of element C (mg/l)

The correction assumes that the change in volume does not change the amount of element C that is brought into solution between sampling, and calculates what the concentration of that element would be in the original volume of solution.

The standard error of F measurements using the IC (in the Wolfson Laboratory at UCL) is 0.117 (this is the standard deviation (SD) of repeat analyses (n=8) of a standard solution with a F^- concentration of 1.09 mg/l). The relative standard deviation (RSD) is 4%. The precision as SD is shown in the results presented as error bars.

Samples Used

Samples of the principal lithologies of interest were selected from Maheshwaram and Wailpally (table 6-1). Sample mineralogy, whole rock chemistry (WRC) and whole rock fluorine (WRF) have been previously determined (see chapter 4) and are given in table 6-2 and table 6-3. Batch leaching experiments using depth profile samples are discussed separately in section 6.5.

Treatment of Results

Repeat runs were compared to determine any anomalous results or strong deviations. In most cases repeat samples were very similar. Where F^- concentrations differ in repeat runs, both results are shown. Results from blank runs gave indications of background concentrations and potential contamination, and in most cases were close to zero in all elements measured. There were some cases of apparent contamination in the IC measurements; these results have been removed, and the explanation for the contamination is discussed in appendix 3.

Table 6-1 – Summary of samples used for batch leaching experiments and experiment and analysis details.

Sample	Sample Geology	Size fraction used	Total time (hrs)	Cations analysed	Anions analysed
M2a	Porphyritic biotite granodiorite	<65um	7,824	Ca,K,Mg,Na	F,Cl
M2b	Weathered sample	<65um	7,824	Ca,K,Mg,Na	F,Cl
M2a	Chlorite biotite granodiorite	0.5-2mm	4,750	Ca,K,Mg,Na	F,Cl
M2b	Weathered sample	0.5-2mm	4,750	Ca,K,Mg,Na	F,Cl
M3a	Monzogranite	0.5-2mm	4,750	Ca, K, Mg, Na	F,Cl
M3b	Weathered sample	0.5-2mm	4,750	Ca, K, Mg, Na	F,Cl
M7a	Grey monzogranite	0.5-2mm	770	Ca,Fe,K,Mg,Na,P	F,Cl
M7b	Weathered sample	0.5-2mm	525	Ca,Fe,K,Mg,Na,P	F,Cl
W1a	Porphyritic chlorite monzogranite	0.5-2mm	503	Ca,Fe,K,Mg,Na,P	F,Cl
W1b	Weathered sample	0.5-2mm	503	Ca,Fe,K,Mg,Na,P	F,Cl
W16a	Biotite granodiorite	0.5-2mm	506	Ca,Fe,K,Mg,Na,P	F,Cl
W16b	Weathered sample	0.5-2mm	504	Ca,Fe,K,Mg,Na,P	F,Cl
W17a	Epidote quartz syenite (pegmatite)	0.5-2mm	503	Ca,Fe,K,Mg,Na,P	F,Cl
W17x	Weathered epidote quartz monzodiorite	0.5-2mm	503	Ca,Fe,K,Mg,Na,P	F,Cl
W11a	Amphibole granodiorite	0.5-2mm	509	Ca,Fe,K,Mg,Na,P	F,Cl
W-C	Calcrete	0.5-2mm	503	Ca,Fe,K,Mg,Na,P	F,Cl
W-S	Soil	0.5-2mm	382	Ca,Fe,K,Mg,Na,P	F,Cl
W13	Mafic vein	0.5-2mm	502	Ca,Fe,K,Mg,Na,P	F,Cl
Blank 1	-	-	1,825	Ca,Fe,K,Mg,Na,P	F,Cl
Blank 6	-	-	502	Ca,Fe,K,Mg,Na,P	F,Cl

The final leached [F^-] of each experiment (taken at 500 hours) is first presented to give an overall view of leachable F^- in both catchments. Following this, further details of F^- and other elements leached over time are presented and implications for the potential sources of F^- to aqueous solution are discussed.

Correlations between the concentration of leached F^- and other elements were determined using SPSS and a two tailed spearman rank correlation coefficient.

PHREEQC was used to determine the saturation index (SI) in relation to fluorite. The measured concentrations of cations and anions from IC and ICP-AES from each sample were input into the model (in units of ppm). Standard pure water (with a density of 1kg/l) was applied in PHREEQC as the liquid phase. Other inputs used

were; room temperature (25°C), pH 7 (default), pe 4 (default – not specified), and the amount of water in the experiment. A formal charge balance was not possible as pH and HCO_3 were not determined in the leachates.

Table 6-2 – Mineral abundances (%) from point counting, with minerals and general mineral formula. $^{+}$magnesio/ferro hornblende formula. F=fresh sample, W=weathered sample. *present but not counted –abundance given as half of the point counting resolution.

Mineral and Formula (general)	**M 2a**	**M 2b**	**M 3a**	**M 3b**	**M 7a**	**M 7b**	**W 1a**	**W 1b**	**W 16a**	**W 16b**	**W 17a**	**W 17x**	**W 11**	**W 13**
	F	**W**	**F**	**W**	**F**	**W**	**F**	**W**	**F**	**W**	**F**	**W**	**F**	**F**
Quartz – SiO_2	21.4	17.9	28.1	36.3	40.4	30.3	14.4	31.4	29.8	21.4	7.7	5.0	14.7	13.2
Microperthite	0.2		4.3	1.6	21.6	0.6	14.5	0.7	19.6	0.1	2.9		1.0	
Plagioclase – $NaAlSi_3O_8$-$CaAl_2Si_2O_8$	31.5	19.3	31.4	27.7	15.7	27.7	29.4	40.0	31.1	43.7	12.7	53.3	44.2	5.3
K-Feldspar – $KAlSi_3O_8$	13.6	47.7	30.2	25.8	17.3	31.4	32.6	23.5	10.7	27.8	71.8	20.7	18.4	18.8
Apatite - $Ca_5(PO_4)_3(OH,F,Cl)$	1.2	0.3	0.2			0.4	0.9	0.2	0.6	0.2		0.3	0.2	0.9
Biotite – $K_2(Mg,Fe)_4(Fe,Al)_2[Si_6Al_2O_{20}]OH_2(F,Cl)_2$	24.0	7.4	1.5	3.1	1.3	3.4		2.3	4.9	2.1		2.8	0.1	23.6
Chlorite – (Fe, Mg, Al)6(Si, Al)4O10(OH)8	4.7	1.6	1.7		0.1	0.3	5.3		1.6	0.7	0.1	1.7	1.1	
Iron Oxides – FeO-Fe_2O_3-Fe_3O_4	0.6	4.2	1.9	2.9	3.3	4.7	0.5	0.5	0.6	3.9	0.3	0.3	0.2	
Titanite - $CaTi[SiO_4](O,OH,F)$	0.2	0.4	*0.02**				1.9	0.4		*0.05**		0.7	0.2	
Epidote - $Ca_2Al_2(Fe^{3+};Al)(SiO_4)(Si_2O_7)O(OH)$	2.0	0.7	0.2	0.1	0.3	1.1	0.4	0.9	0.7	0.1	4.6	14.4	0.7	1.0
Epidote var2			0.2					0.1	0.5	0.1			0.5	
Amphibole – $Ca_2(Mg,Fe)_4Al[Si_7AlO_{22}](OH)_2^{+}$													18.7	37.2
Fluorite – CaF_2			0.2				0.1							
Zircon – $Zr[SiO_4]$		0.1		0.1								0.8		
Calcite - $CaCO_3$	0	0.5	0	2.4	0	0								
Total:	100	100	100	100	100	100	100	100	100	100	100	100	100	100

Table 6-3- Bulk chemical composition of Maheshwaram and Wailpally samples, including whole rock chemical analysis (WRC) values in weight %, and whole rock fluorine analysis (WRF) in ppm. < indicates less than detection limit (F detection limit 100 ppm, P_2O_5 detection limit for Maheshwaram samples = 0.05, for Wailpally samples = 0.2)

		Al_2O_3	CaO	Fe_2O_3	K_2O	MgO	MnO	Na_2O	P_2O_5	SiO_2	TiO_2	F
M2a	F	14.4	2.41	3.61	4.55	1.14	0.04	3.11	0.19	66.5	0.49	1749
M2b	W	13.7	1.55	3.88	4.56	0.91	0.05	2.4	0.2	66.2	0.51	426
M3a	F	12.7	0.77	1.52	5.61	0.24	0.03	2.97	<	74.1	0.18	365
M3b	W	12.8	0.95	1.47	5.6	0.26	0.01	2.56	<	71.8	0.2	198
M7a	F	12.8	0.68	1.53	5.77	0.23	0.02	2.7	<	72.3	0.21	218
M7b	W	13.1	0.46	1.62	5.8	0.19	0.03	2.26	<	72	0.19	169
W1a	F	12.3	1.41	2.86	4.87	0.54	0.036	2.79	<	69.7	0.5	1102
W1b	W	12.7	0.41	1.59	6.1	0.12	0.014	2.49	<	73	0.19	171
W16a	F	13.8	2.05	3.34	3.81	1.02	0.042	3.44	<	67.5	0.33	930
W16b	W	13.6	0.94	1.73	5.48	1.15	0.015	2.66	<	70.5	0.28	233
W17a	F	17.6	1.12	0.8	11.4	0.08	0.008	2.17	<	64	0.03	<
W17x	W	8.14	5.09	5.26	0.27	2.49	0.085	0.12	<	71.5	0.55	863
W11a	F	14.2	3.27	4.13	3.56	1.83	0.063	3.53	<	66.8	0.29	824
W13	F	9.3	5.09	7.25	5.04	11.1	0.19	0.64	<	55.6	0.23	5536
W-C	W	1.78	45.14	0.5	0.51	0.57	0.019	0.16	<	9.66	0.06	272

6.3. Batch Leaching Results – Catchment Samples

6.3.1. Overview of leached [F^-]

The final [F^-] in leached solution at the end of the experiments (~500 hours) and the initial [F^-] in leached solution (at 1-2 hours) for comparison are shown in figure 6-1 and figure 6-2.

Mafic vein material from Wailpally has the highest final [F^-] (3.72 mg/l, figure 6-1). The next two highest final [F^-] are also from Wailpally samples, the porphyritic chlorite monzogranite (sample W1a, 2.83 mg/l) and the calcrete (sample W-C, 2.69 mg/l). The lowest [F^-] was leached from the weathered pink monzogranite in Maheshwaram (M3b) and the pegmatitic epidote quartz syenite (W17a) in Wailpally. The remaining Wailpally and Maheshwaram samples have similar final F^- concentrations, with the highest Maheshwaram final [F^-] leached from the grey monzogranite (M7a - 1.30 mg/l) and the weathered sample M2b (1.12 mg/l).

Initial leached [F^-] is highest from the calcrete sample (W-C). A high initial [F^-] is also leached from weathered samples M2b (porphyritic biotite granodiorite) and M7b

(grey monzogranite) (figure 6-2), with the majority of paired samples also showing a higher initial [F^-] from the weathered rock than the fresh rock equivalents (apart from W1). This reverses with time, with the final [F^-] leached higher from fresh rock samples than from their weathered equivalents. One exception to this is the porphyritic biotite granodiorite from Maheshwaram (M2a and M2b), where the weathered sample gives a higher initial and final [F^-].

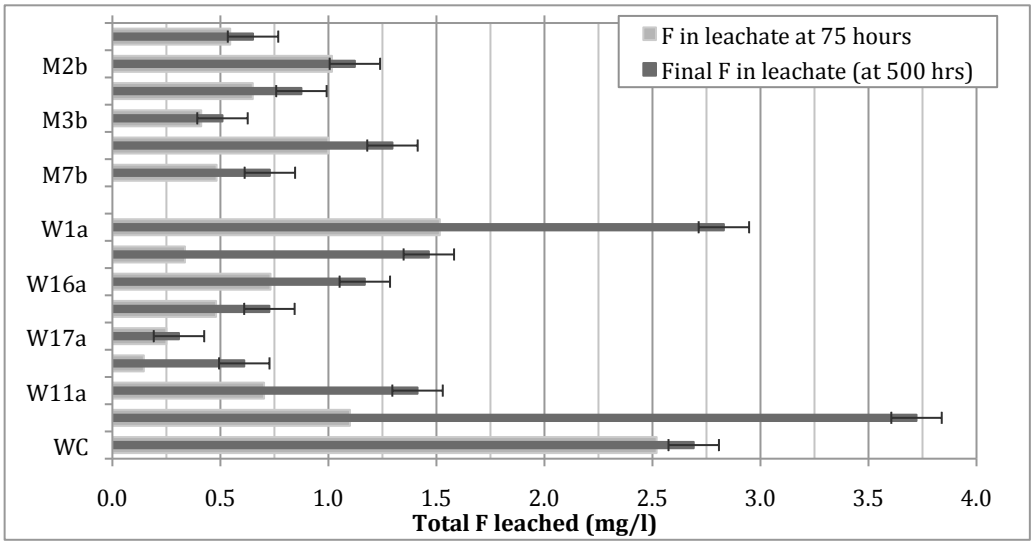

Figure 6-1 – Final Concentration of fluoride leached at ~500 hours and at ~75 hours. Concentration of fluoride leached at approx 75 and 500 hours. All M samples at 71-75hrs (except M7a at 117hrs, and M3b at 56hrs), and at 482 hrs (except M7b at 525hrs and M7a at 431hr). All W samples at 72-79hrs (except W1b at 25hours and W1a at 50hrs), and at 502-509hrs.

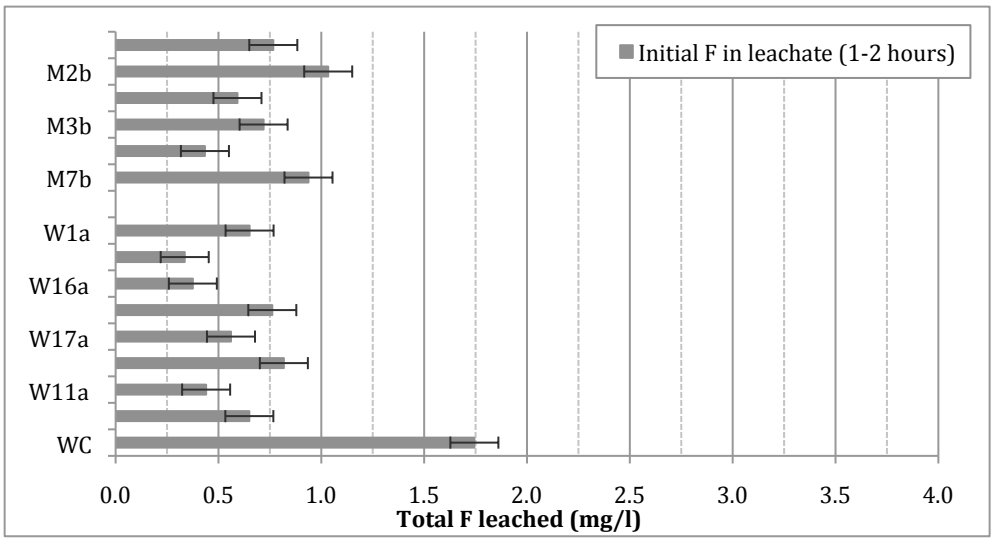

Figure 6-2 – Initial concentration of fluoride leached at 1-2 hours. All samples are taken at 1-2 hours, apart from sample W11a (taken at 6 hours) and W1b (taken at 25 hours).

Figure 6-1 also shows [F^-] in solution at 75 hours. In several samples this is similar to the final F^- concentration (e.g. in the calcrete sample W-C, and in both porphyritic

biotite granodiorite samples M2a and M2b). Where the [F^-] in solution is much lower at 75 hours (e.g. mafic vein sample W13 and the porphyritic chlorite monzogranite W1a), the release of F^- to water is more gradual. Due to the constant movement of samples in the rollers, sample attrition and physical breakdown may occur over time, decreasing the sample size and exposing fresh surfaces to the leaching water. This mechanical attrition will affect the concentration of leached elements in solution with time.

Figure 6-3 and figure 6-4 show sample WRF content verses the final leached F^- concentration. Wailpally fresh rocks show a positive trend of increasing F^- leached from samples with higher WRF content. No such correlation is seen in the Wailpally weathered samples, neither in the Maheshwaram fresh samples where the sample with the highest WRF (M2a, porphyritic biotite granodiorite) has the lowest fresh rock final [F^-].

The percentage of total F content (WRF) that is lost to water upon leaching in batch leaching experiments is shown in figure 6-5. Samples with a high percentage of F lost are generally weathered samples (e.g. W-C, W1b) and samples with low WRF values (e.g. M7a). A higher proportion of F within these samples may therefore be readily leachable or more loosely bound. Samples with higher WRF content lose a smaller percentage of total F (e.g. M2a, W13, and W17x). Although the final [F^-] leached from these samples is high in some cases (in W13), a higher proportion of F present may be less accessible to water-rock interaction or more strongly secured in minerals that are not as easily weathered.

Further detail of the water rock interaction process can be obtained by analysis of the elements leached over time, as described in the next section.

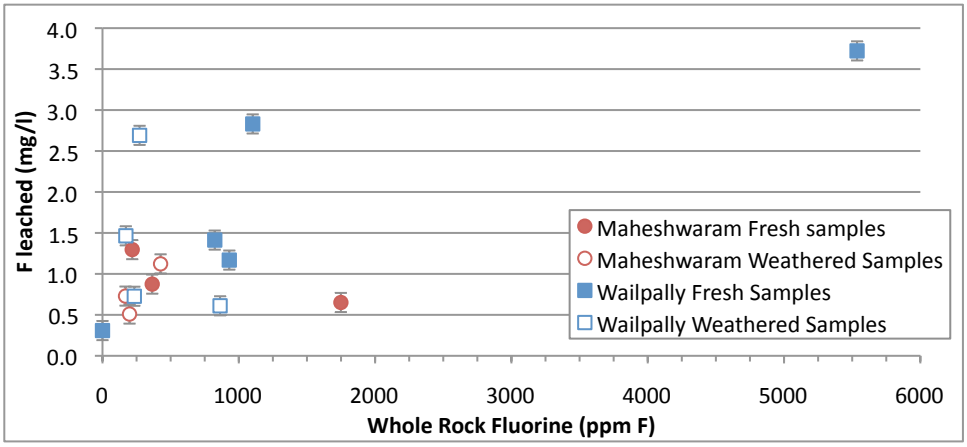

Figure 6-3 - Whole Rock Fluorine (WRF) and final concentration of F^- leached.

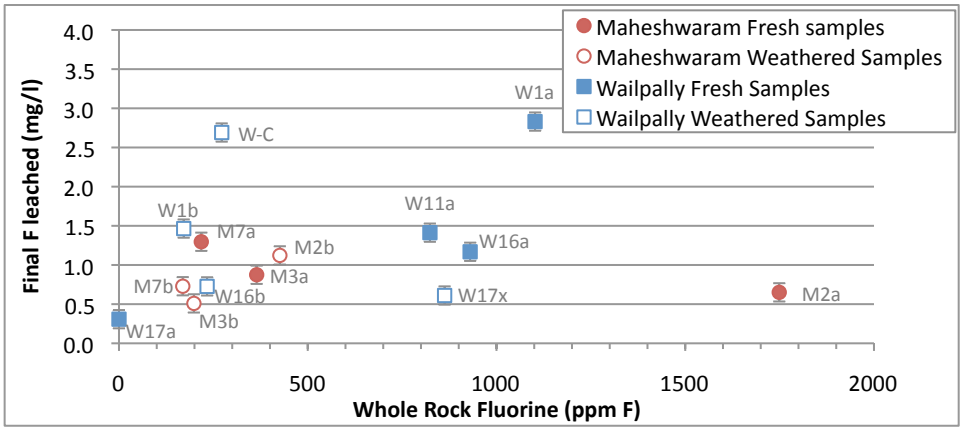

Figure 6-4 – Whole Rock Fluorine (WRF) and final concentration of F^- leached. Not including sample W13 (WRF=5536 ppm F, Final F^- leached=3.72mg/l).

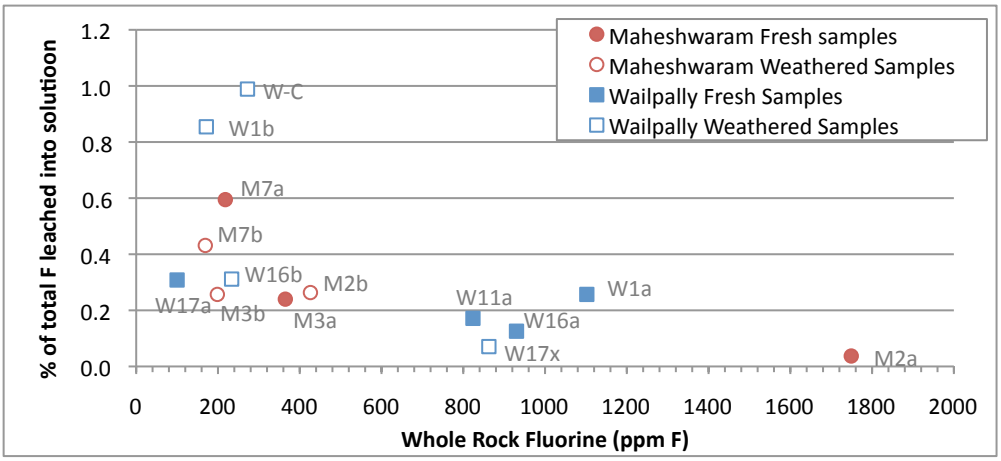

Figure 6-5 - The percentage of sample whole rock fluorine (WRF) removed to water upon leaching (using the final F^- concentration in leached solution at 500 hours as F removed to water). Sample W13 not shown (WRF=5536, percentage of total F^- leached=0.07)

The results of Maheshwaram batch leaching experiments are given in figure 6-6 to figure 6-18, and the results of Wailpally batch leaching experiments in figure 6-20 to figure 6-31.

6.3.2. Maheshwaram Catchment

Fluoride leaching

In all samples the initial increase in F^- concentration, by the time the first sample was taken, was to between 0.4 and 1.1 mg/l (figure 6-6). In the porphyritic biotite granodiorite samples (M2), a higher [F^-] was leached from the weathered sample (M2b) than the fresh sample. In both of these samples, [F^-] in leached solution slowly increases throughout the experiment (figure 6-6). In the pink monzogranite (M3) and grey monzogranite (M7), the initial (0-10 hours) [F^-] leached from weathered rocks is slightly higher than from fresh rocks, however [F^-] leached from weathered samples then either decreases or remains constant, while [F^-] in fresh sample leachate increases. In the grey monzogranite (M7a) the increase in [F^-] from the fresh sample occurs at ~100 hours, whereas in the pink monzogranite (M3a) leached F^- does not significantly increase until ~400 hours (figure 6-6).

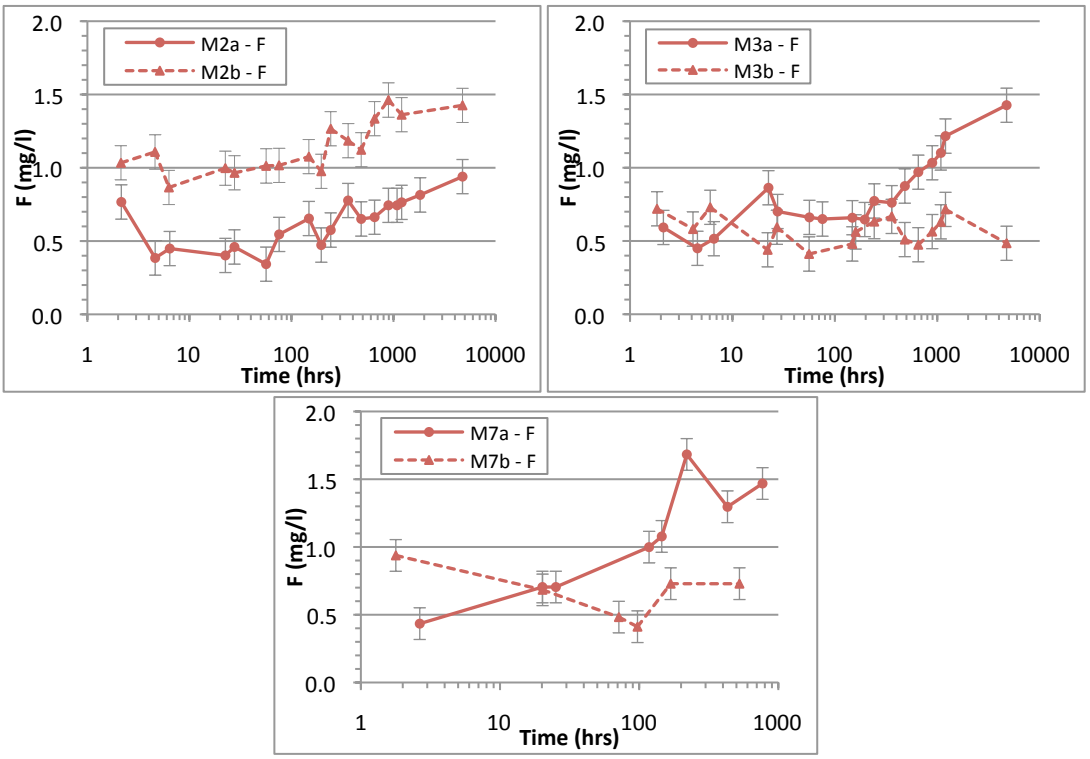

Figure 6-6 – Fluoride concentrations in leached solution from Maheshwaram fresh samples and their weathered equivalents

Of the three fresh rock samples, the highest [F^-] was leached from the grey monzogranite (M7a), with F^- leached from the pink monzogranite (M3a) and the porphyritic biotite granodiorite (M2a) following (figure 6-7). The increase in [F^-] in the grey granite (M7a) occurs earlier than the increase seen in the pink monzogranite

(M3a). In the weathered samples, the highest [F^-] was leached from the weathered porphyritic biotite granodiorite (M2b), with the pink and grey monzogranites following (M3b and M7b).

In all coarse experiments (0.5-2mm) the aqueous solution remains under-saturated with respect to fluorite indicating that this is not a limiting factor on F^- in solution (figure 6-8).

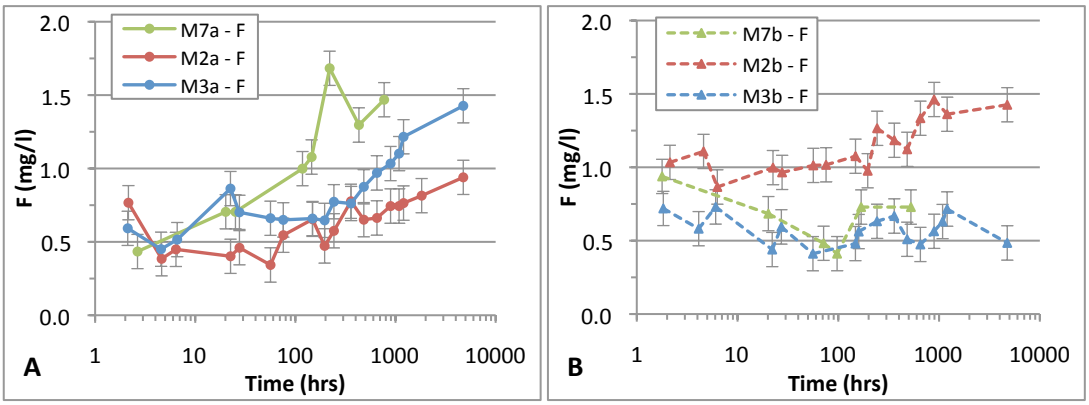

Figure 6-7 – Fluoride concentrations in leachate from Maheshwaram fresh (A) and weathered (B) samples

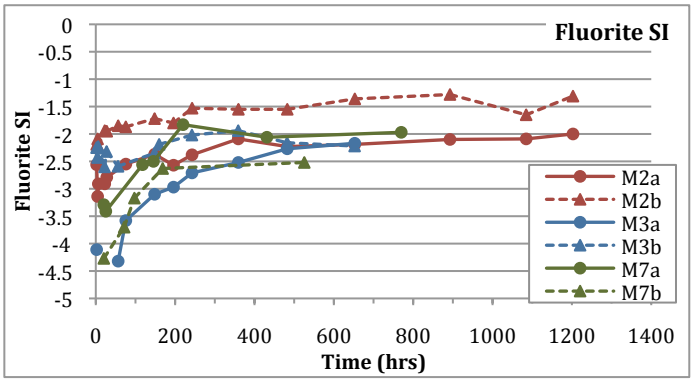

Figure 6-8 – Fluorite saturation indices (SI) determined by PHREEQC for Maheshwaram coarse experiments.

The initial increase in [F^-] at the start of the experiments may indicate that F is loosely bound (e.g. in clays, or sorbed to Al or Fe minerals) and a larger amount of F appears to be loosely bound in weathered material and more easily removed than in fresher rock, resulting in the slightly higher initial [F^-] leached from weathered samples. The higher WRF content in the fresh rock is likely to be more strongly secured in primary mineral phases, resulting in an increase in leached F^- later in the experiment as weathering progresses (as seen in the grey and pink monzogranites). Increased physical breakdown of samples due to the rolling movement of sample mixing may also contribute to later increases in leached F^-. However the [F^-] leached from the

weathered porphyritic biotite granodiorite (M2b) remains higher than the fresh sample equivalent (M2a) in both fine and coarse experiments.

Experiments using finely crushed (<65um) porphyritic biotite granodiorite (M2a-fine and M2b-fine) give much higher leached [F^-] than experiments with coarse material (figure 6-9). The initial increase in [F^-] by the time the first sample taken is high (M2a to 2.13mg/l F and M2b to 3.68mg/l F), after which [F^-] are fairly constant until ~2700 hours when [F^-] in leached solutions again increases (M2a to 4.68mg/l F and M2b to 7.63mg/l F) and afterwards again decrease (final F^- concentration of 2.98mg/l in M2a and 5.36mg/l in M2b). Both fine experiments show this large increase, whereas the coarse experiments do not (figure 6-9). Calculation of fluorite SI show solutions to be under-saturated with respect to fluorite at the beginning of the experiment, with both solutions approaching steady state as time progresses (figure 6-10). Solution M2b (fine experiment) reaches super-saturation by 1500 hours. This corresponds to the late-stage increase and decrease in solution [F^-], with [F^-] decreasing once fluorite saturation is exceeded and it is likely that fluorite precipitates out of solution.

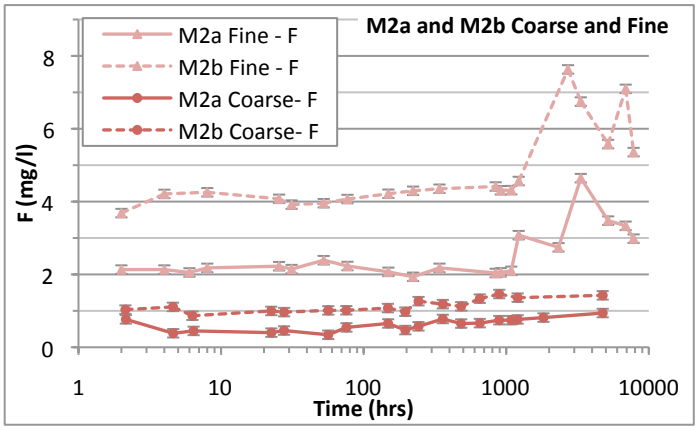

Figure 6-9 – Fluoride concentrations in leachate from M2a and M2b fine (<0.65µm) material. Error bars are SD.

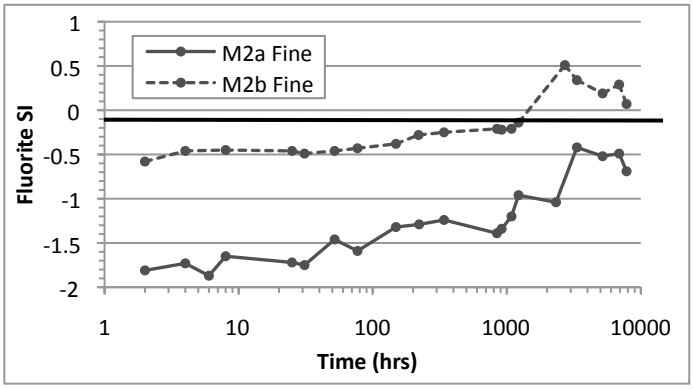

Figure 6-10 – Saturation Indices calculated using PHREEQC for Fluorite in M2a and M2b Fine (<65µm) experiments

Other Elements

Elements leached with time are given in figure 6-11 to figure 6-18. The concentration of most elements in solution increases with time, although some elements show a more erratic behaviour with small sharp increases and decreases (e.g. Cl, figure 6-13 and figure 6-16).

The concentration of Ca and Mg increases rapidly in the first stage of the experiment (0-500 hours) in all samples (apart from the fresh grey monzogranite sample M7a, figure 6-15). The increase is later less rapid and in some cases reaches a plateau (figure 6-14 to figure 6-15). In the pink and grey monzogranites (M3 and M7) the increase in $[Ca^{2+}]$ and $[Mg^{2+}]$ is delayed (increasing after ~75 hours in the pink monzogranite M3a and after ~100 hours in the grey monzogranite M7b) (figure 6-13 and figure 6-15). In all fresh and weathered pairs, a higher concentration of Ca and Mg is leached from the weathered sample. High Ca concentrations are leached from the porphyritic biotite granodiorite samples (M2a and M2b) and in the weathered pink monzogranite (M3b) (end concentrations of 7.31, 13.58 and 12.09 mg/l respectively).

The concentration of K in solution also increases (although more gradually) with time in all samples apart from weathered samples M2b and M7b. The $[K^{+}]$ leached from the porphyritic biotite granodiorite (M2a) is higher than from the pink and grey monzogranites (M3a and M7a).

Finely crushed experiments of porphyritic biotite granodiorite (M2a and M2b) show a similar pattern to coarser fractions with an initial increase in concentration of most elements (up to 200 hours), but with a higher concentration of each element leached (figure 6-17 and figure 6-18). This is expected due to the larger surface area available for reaction. Both samples also have a late-stage increase, M2a at 2500 hours, and M2b at 1500 hours, with a peak in element concentrations followed by a decrease to values higher than pre-peak concentrations.

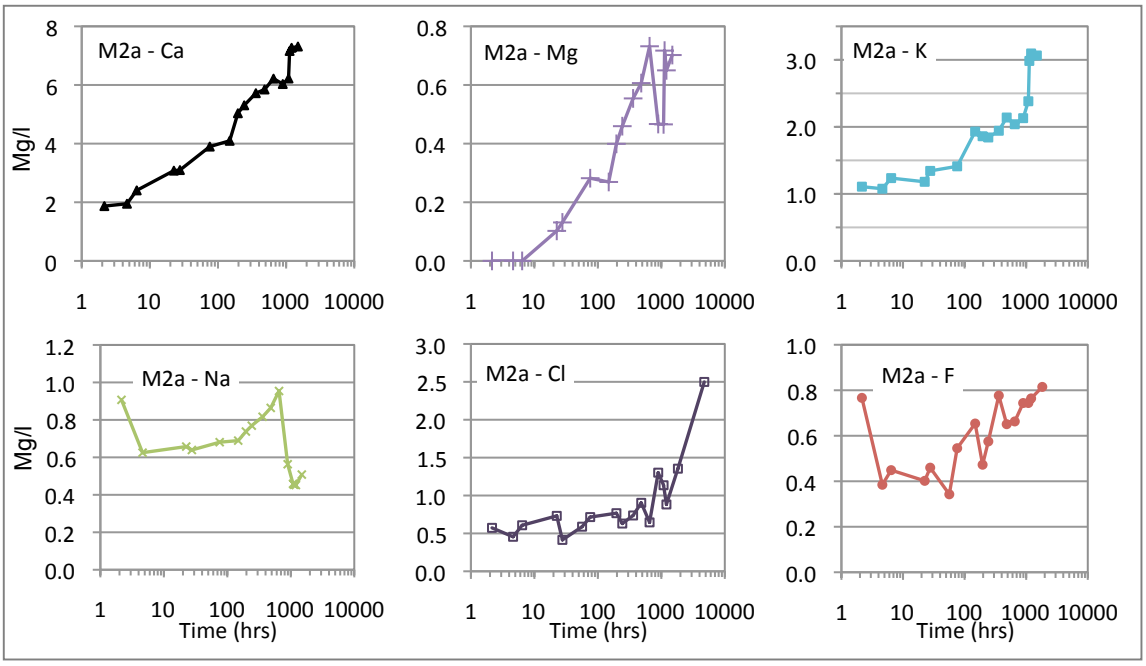

Figure 6-11 – Fresh porphyritic biotite granite sample M2a batch leaching. Element concentration (mg/l) in solution with time (hours).

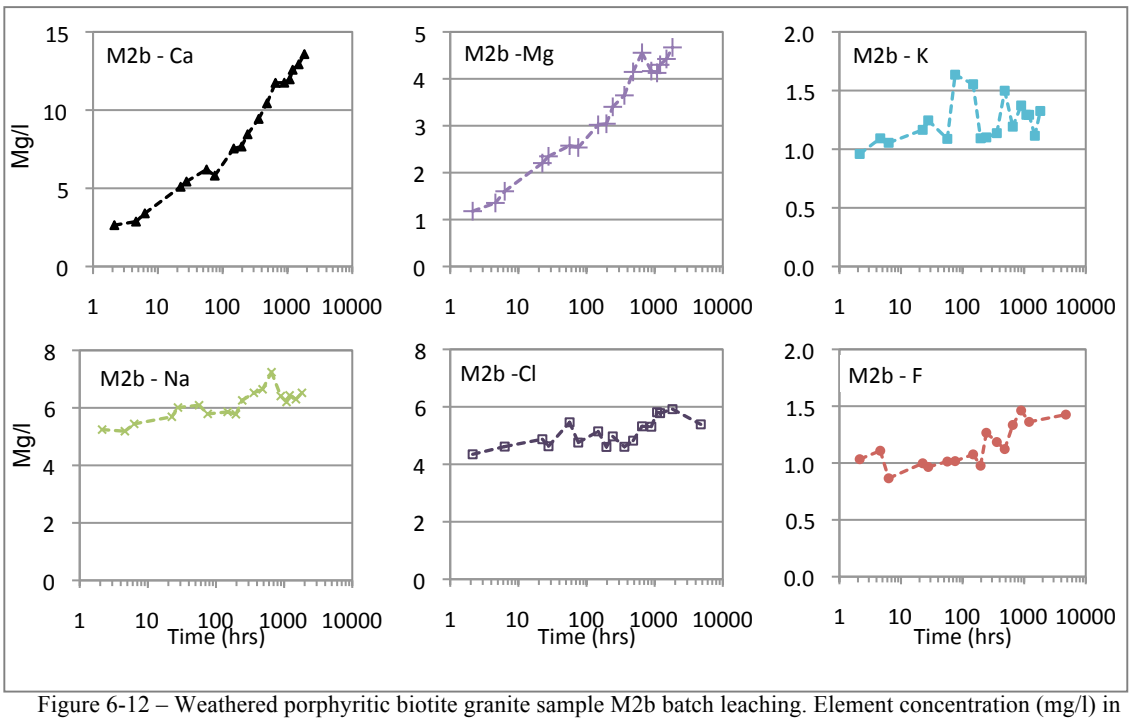

Figure 6-12 – Weathered porphyritic biotite granite sample M2b batch leaching. Element concentration (mg/l) in solution with time (hours).

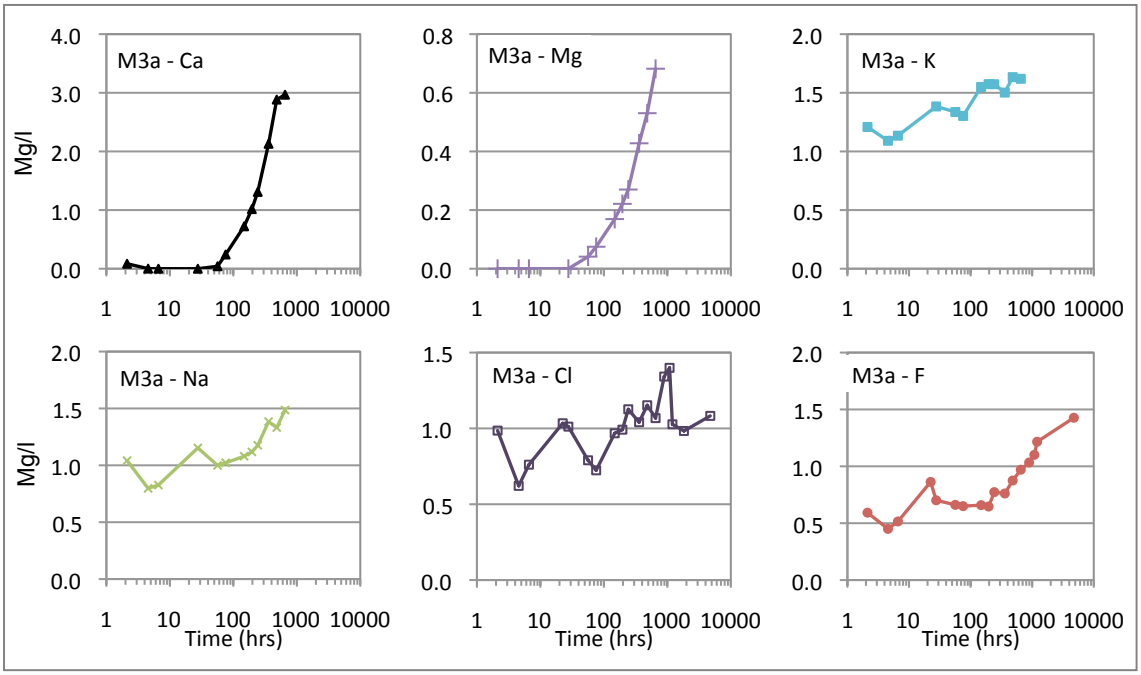

Figure 6-13 – Fresh pink monzogranite sample M3a batch leaching. Element concentration (mg/l) in solution with time (hours).

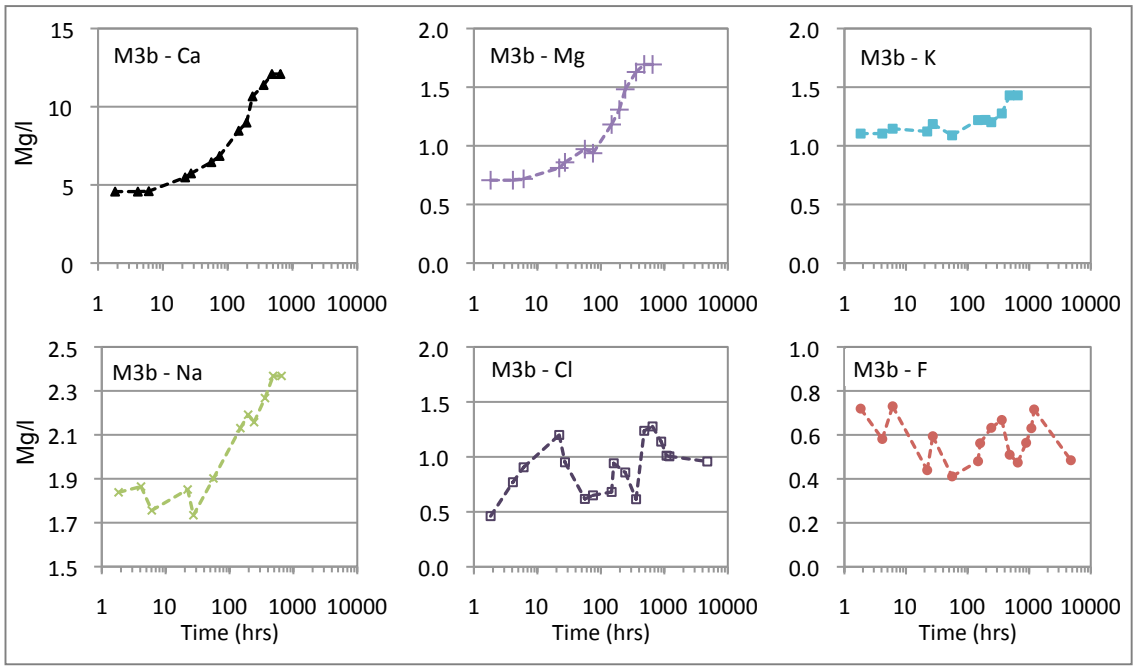

Figure 6-14 – Weathered pink monzogranite sample M3b batch leaching. Element concentration (mg/l) in solution with time (hours).

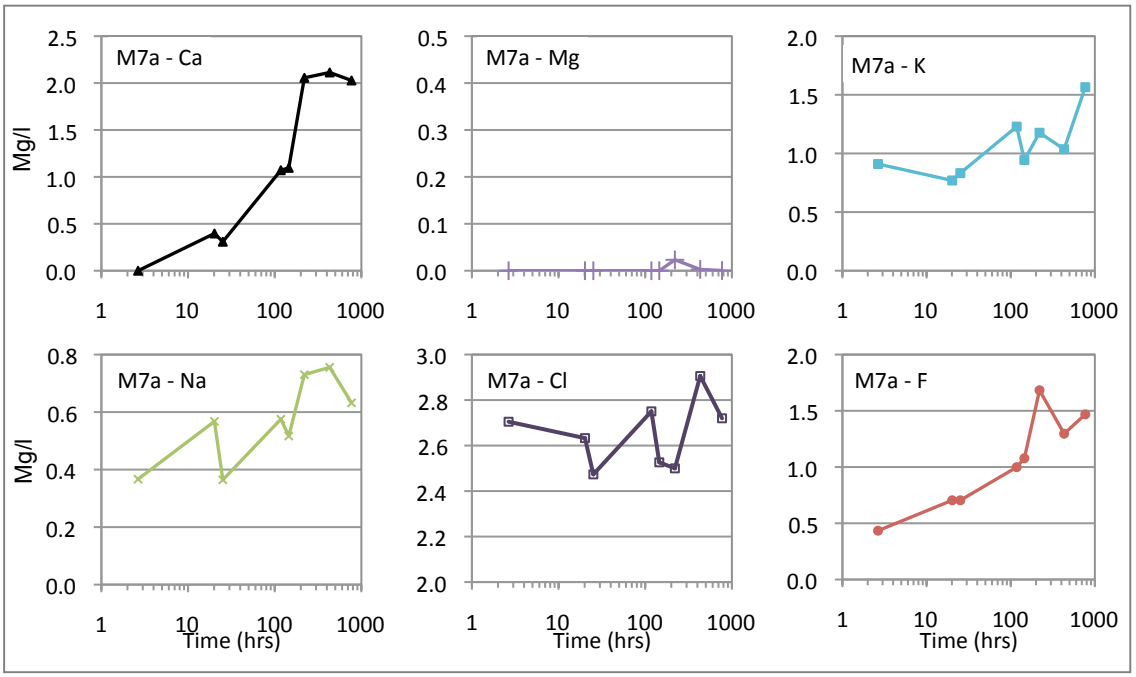

Figure 6-15 – Fresh grey granite sample M7a batch leaching. Element concentration (mg/l) in solution with time (hours).

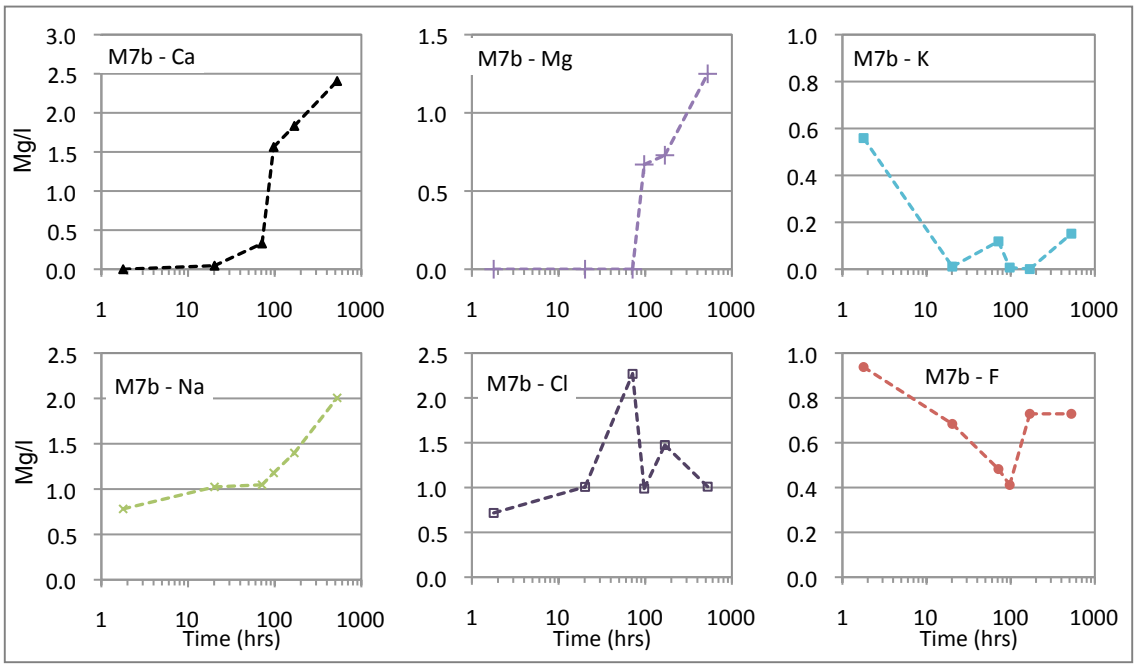

Figure 6-16 - Weathered grey granite sample M7b batch leaching. Element concentration (mg/l) in solution with time (hours).

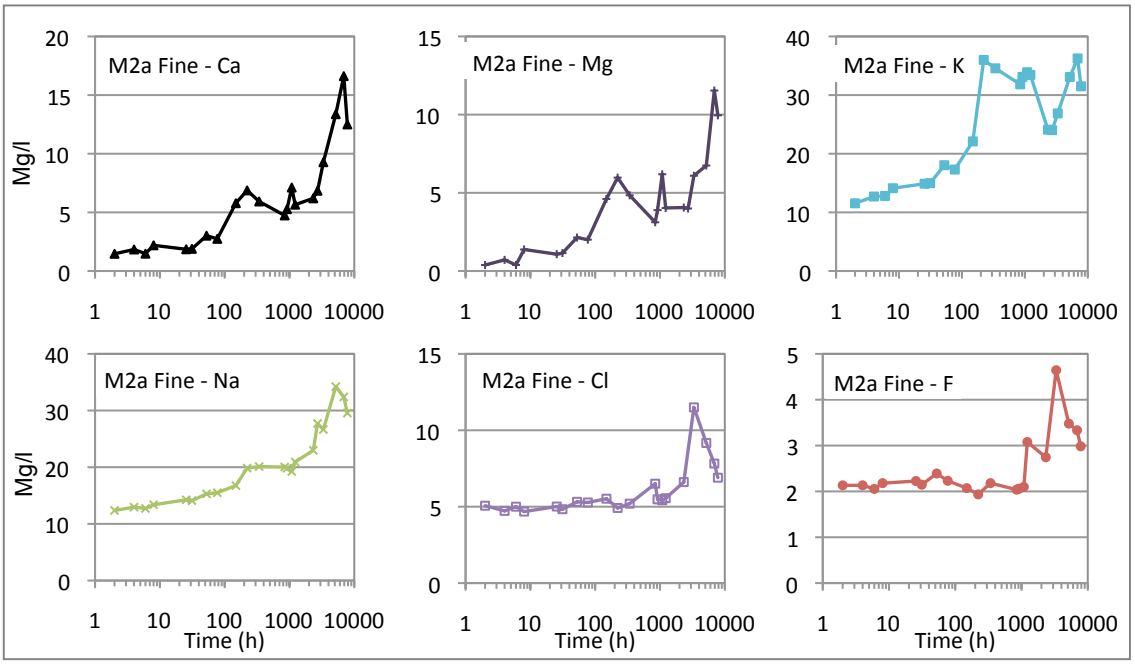

Figure 6-17 – Finely crushed (<65µm) fresh porphyritic biotite granite sample M2a batch leaching. Element concentration (mg/l) in solution with time (hours).

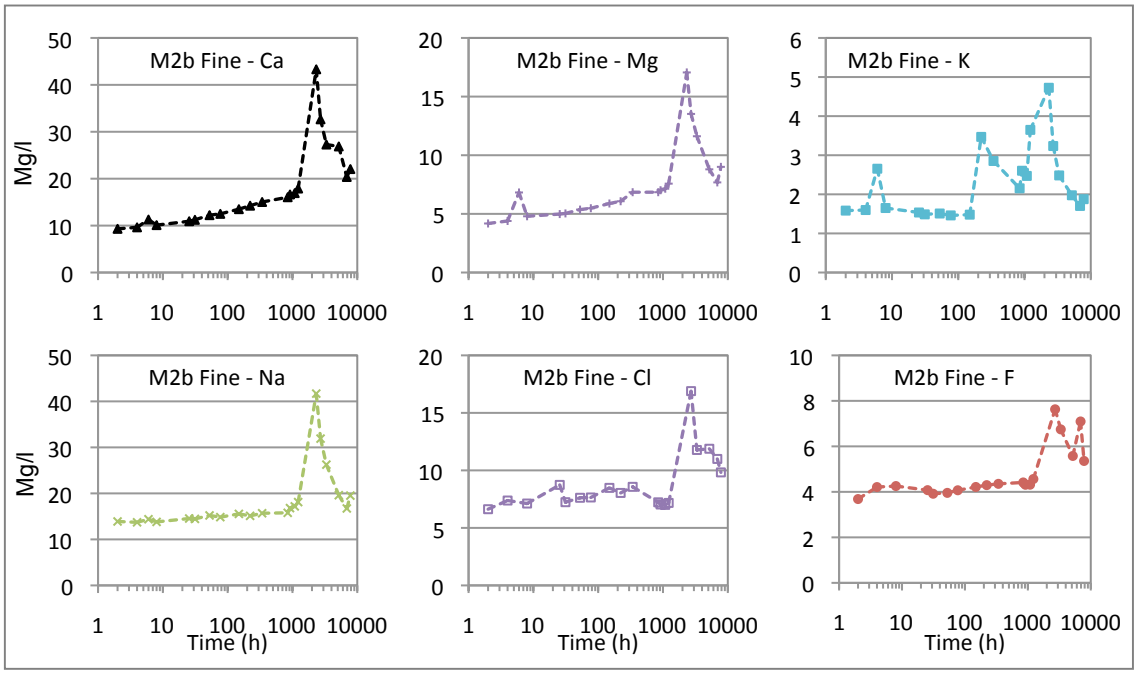

Figure 6-18 - Finely crushed (<65µm) weathered porphyritic biotite granite sample M2b batch leaching. Element concentration (mg/l) in solution with time (hours).

Potential Sources of Leached Fluoride - Maheshwaram

The correlation coefficients between leached [F^-] and other elements are given in table 6-4 with the F^- concentration with other elements in solution plotted in figure 6-19. A strong correlation may indicate that elements are being released from the same mineral. Fluoride shows a strong correlation (significant at 0.05 or lower) with Ca in most experiments and also with K, Mg and Na in many of the experiments (table 6-4, figure 6-19). A weak correlation may be due to low leached [F^-] or may indicate that a number of different sources are contributing to F^- in solution. In the weathered grey and pink monzogranites (M3b and M7b) F has a weak correlation with other elements.

A strong correlation between Ca and F may be due to fluorite, calcrete-carbonate, apatite, epidote or titanite weathering (although many of these minerals are considered insoluble). A strong correlation between F and Mg (and K) may derive from biotite weathering. The correlation between F and Ca in M2b (fine) is reflected in the fluorite saturation of the solution, as once this is reached, [F^-] and [Ca^{2+}] decrease with fluorite likely to be precipitating out of solution.

Delayed increases in Ca and Mg concentrations in M3a and M7a may be linked to the late increases in [F^-] in both of these samples (figure 6-13, figure 6-15). This is supported by a strong correlation between F and Ca concentrations in M7a and M3a, and between F and Mg in M3a.

Magnesium in solution is likely to originate from the breakdown of biotite. The high K and Mg concentration in leached solutions from the fresh porphyritic biotite granodiorite (M2a - fine and coarse experiments) may be due to weathering of biotite, which is abundant in this sample (24%). A strong correlation between [F^-] and [Mg^{2+}] and [K^+] in M2a (coarse) and M2b (coarse and fine) suggests biotite as a source of F to the leached solution.

Leached solution from the fresh pink monzogranite sample (M3a) also shows a strong correlation between [F^-] and [Mg^{2+}] and [K^+]. Correlation between F and Ca concentrations may also indicate fluorite weathering from this sample.

Table 6-4 – Spearman Rank Correlation Coefficient (R) for elements in Maheshwaram batch leaching solutions. *indicates that correlation is significant at the 0.05 level, **indicates that correlation is significant at the 0.01 level (also shown in bold). The number of points correlated ranges from 12-18 apart from in M7a and M7b where the number of points ranges from 6-8.

Sample	F-Ca	F-Mg	F-K	F-Na	F-Cl	F-Fe	F-P
M2a	0.567*	0.589*	0.619*	0.167	**0.654****		
M2b	0.586*	**0.667****	0.343	**0.642****	0.449		
M3a	**0.719****	**0.814****	**0.839****	**0.898****	**0.694****		
M3b	-0.273	-0.301	-0.021	-0.329	-0.312		
M7a	**0.946****	0.581	0.731*	**0.802***	0.108	0.731*	-0.581
M7b	-0.116	0.123	0.462	-0.116	-0.232	-0.406	0.123
M2a fine	0.450*	0.403	0.128	0.555*	0.567*		
M2b fine	**0.909****	**0.906****	**0.693****	**0.842****	0.563*		

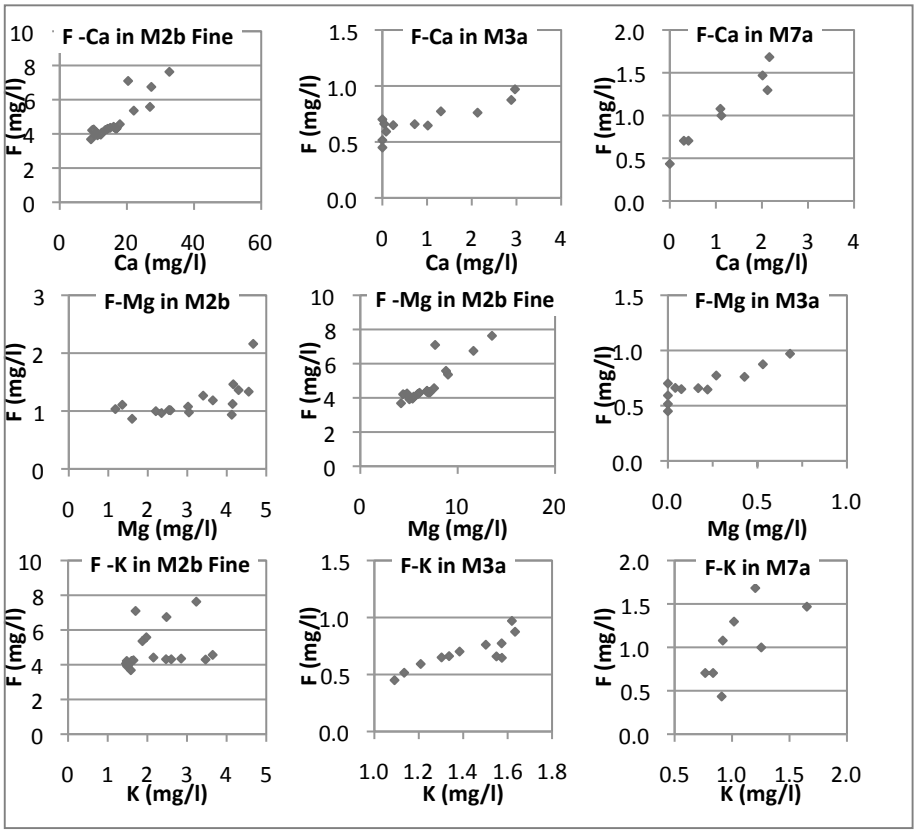

Figure 6-19 – Scatter plots of concentration of F vs. Ca, Mg or K in leaching solutions where a strong correlation (significant at 0.01 level) is present (see table 6-4).

The identification of the sources of leached fluoride would be aided by further information such as solution pH and bicarbonate concentration. Initial increases in element concentration in solution may be due to surface defects produced by crushing aiding mineral dissolution or due to the presence of very fine material not removed by sieving. Increasing the physical breakdown of minerals by attrition may lead to a

further increase in elements leached. This may be the cause of a late-stage increase in element concentration in the fine experiments and M3a and M7a.

6.3.3. Wailpally Catchment

Batch leaching results for Wailpally samples are shown in figure 6-20 to figure 6-31.

Fluoride leaching

In the majority of experiments, leached [F^-] from fresh rocks increases with time, whereas the weathered rock experiments show less change in [F^-] with time, and in some cases [F^-] remains similar for the duration of the experiment (figure 6-21).

Leached [F^-] is highest from the mafic vein sample (W13) and the porphyritic chlorite monzogranite rock sample (W1a), both of which have a similar leached [F^-] up to 400 hours, after which leached [F^-] from the mafic vein material continues to increase, and [F^-] from the porphyritic chlorite monzogranite increases less (end concentrations W13=3.72mg/l, W1a=2.89mg/l) (figure 6-21). Fluoride leached from W13 may have continued to increase had the experiment been run for longer whereas W1a seems to have reached a plateau. The high [F^-] leached from mafic vein material W13 and porphyritic chlorite monzogranite W1a is linked to the sample's high whole rock fluorine content (W13=5536 ppm F, W1a=1102 ppm F) and abundance of F-bearing minerals.

The pegmatitic epidote quartz syenite (W17a), with a low WRF (<100 pm F) and a scarcity of F-bearing minerals, leaches very little F^-. The weathered epidote quartz monzodiorite (W17x) and weathered biotite granodiorite (W16b) samples also leach low concentrations of F^-, with [F^-] changing little from start to finish. The amphibole granodiorite (W11a) and biotite granodiorite (W16a) have a similar leached F concentration for most of the experiment (figure 6-21).

Of the weathered samples, the highest [F^-] is leached from the calcrete sample (W-C), with a concentration of 2.5 to 3mg/l F in the leached solution from 25 hours onwards. The [F^-] leached from other weathered samples is lower, with both the weathered biotite granodiorite and monzodiorite (W16b and W17x) remaining low (<1mg/l) throughout (figure 6-21). A soil sample (W-S) from near site W1 was also included in

the batch leaching experiments, although for a shorter duration. This sample also has a low [F^-] leached.

Within the fresh and weathered pairs (W1a&b, W16a&b), a higher [F^-] is leached from fresh rock samples than from their weathered equivalents. The difference between F^- leached from W1a and W1b (porphyritic chlorite monzogranite) is large compared to the difference between W16a and W16b (biotite granodiorite) (figure 6-20).

The final F^- leached from Wailpally fresh rocks fits well with WRF values (see section 6.3); however this is not so for the weathered rock samples (figure 6-3 and figure 6-4). For example, leached solution from sample W17x (weathered epidote quartz monzodiorite) has a low final leached [F^-] (0.61 mg/l F) although it has a high WRF value (863 ppm F), whereas calcrete sample W-C has a low WRF value (272 ppm F) but high final [F^-] leached (2.68 mg/l F). This is due to the location of F within the sample, with F in less readily leached samples located in minerals where it is bonded more strongly. In the calcrete sample (W-C) most F is held either as fluorite or as F^- bound to the surface of calcite, which may be more readily leached to water.

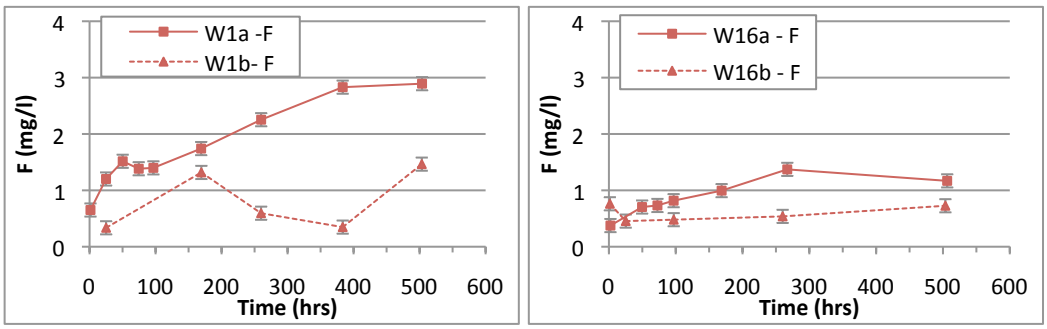

Figure 6-20 – Concentration of F in paired fresh and weathered Wailpally batch leaching solutions.

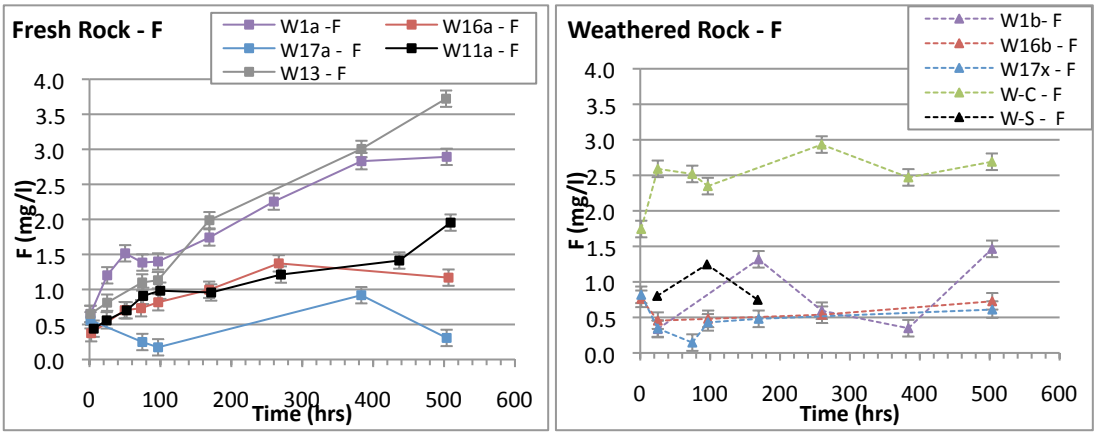

Figure 6-21 – F leached from fresh and weathered samples from Wailpally

All solutions were under-saturated with respect to fluorite. Fluorite saturation is therefore not a limiting factor on [F^-] in solution (figure 6-22).

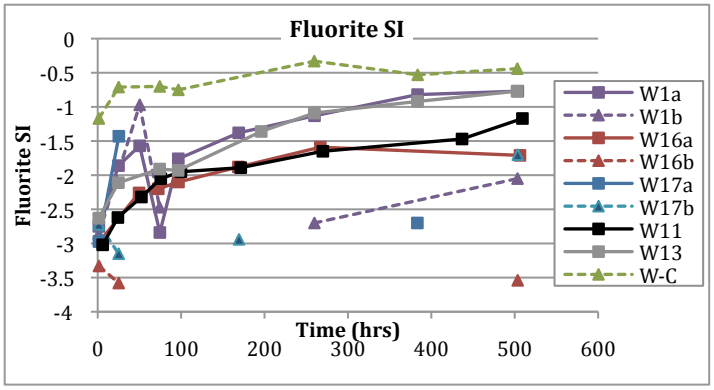

Figure 6-22 - Fluorite saturation indices (SI) determined by PHREEQC for Wailpally experiments.

Other Elements

Elements leached over time for each sample are given in figure 6-23 to figure 6-31. The concentration of many elements in leached solution increases with time, although in some samples an increase followed by a decrease is also observed.

In paired fresh-weathered rock samples (W1 - porphyritic chlorite monzogranite and W16 - biotite granodiorite), higher concentrations of Ca and F are leached from fresh rock and higher concentrations of Fe are leached from weathered rock. In the biotite granodiorite (W16), higher concentrations of K and Cl are leached from the fresh rock compared to the weathered rock, whereas similar concentrations of K and Cl are leached from the fresh and weathered porphyritic chlorite monzogranite samples (W1). The fresh rock samples have a higher Ca and F content than the weathered rock samples (from WRC analysis, table 6-2) which may explain the higher concentrations leached into solution. Fresh rock samples also have higher whole rock Fe than the weathered samples, however more Fe is leached from weathered samples possibly due to differing forms and location of Fe within the weathered samples.

An increase in concentration with time is measured for Ca (apart from W1b, W16b, and W17a) and for Mg (apart from W1a, W1b, W16b and W17x). In several samples Ca and Mg concentrations reach a maximum and then remain level for the remainder of the experiment (such as in W16a biotite granite, W17x weathered epidote quartz

monzodiorite, and W13 mafic vein material (figure 6-25, figure 6-28 and figure 6-30).

High Ca concentration is likely to be due to the weathering of plagioclase feldspar or calcite (and potentially titanite, hornblende, or epidote). Leached [Ca^{2+}] is highest from the calcrete sample W-C (max 27.08mg/l) as the sample is predominantly calcium carbonate. Low [Ca^{2+}] is leached from the weathered porphyritic chlorite monzogranite (W1b), the weathered biotite granodiorite (W16b) (both of which have low total Ca content), and the fresh pegmatitic epidote quartz syenite (W17a).

A high [Mg^{2+}] leached may be due to weathering of biotite or amphiboles where present (W13 and W11a). K is also leached from biotite and K-feldspars (although these are less easily weathered), and in some samples an increase in [K^{+}] leached with time is also measured (e.g. W16a and W13).

The concentration of Fe increases with time in many experiments (W1b, W16a, W16b and W17a), and in some cases increases and then decreases again (W11a - figure 6-29). All sample leachate is supersaturated with respect to several Fe phases from the start of the experiment (calculated using PHREEQC), which will affect the concentrations of Fe in solution.

Leachate from pegmatitic epidote quartz syenite sample (W17a) has a low concentration of most elements (Ca, Na, Fe and Mg). This is due to the sample composition, containing mostly potassium feldspars, and little of the above mentioned elements in WRC analysis (table 6-2). The highest concentration of any element leached in W17a is K, although this is not particularly high compared to other samples.

Leachate concentrations from the mafic vein sample (W13) are high (figure 6-30), the concentration of K leached, for example, reaching 16.72 mg/l. This sample has a high total K contentfrom WRC analysis compared to other samples (7.25 weight %; table 6-2) and consists primarily of amphiboles (mostly magnesio-hornblende with some actinolite) and biotite, which may also contribute to K leached. This sample also has a very high total Mg content (11.1 weight %, table 6-2), although leached Mg reaches only 1.5mg/l (similar to Mg leached from W11a, W16b and lower than Mg leached

from W17b and W-C). This may indicate that K is lost more easily than Mg from biotite, and that Mg is also not easily lost from amphiboles.

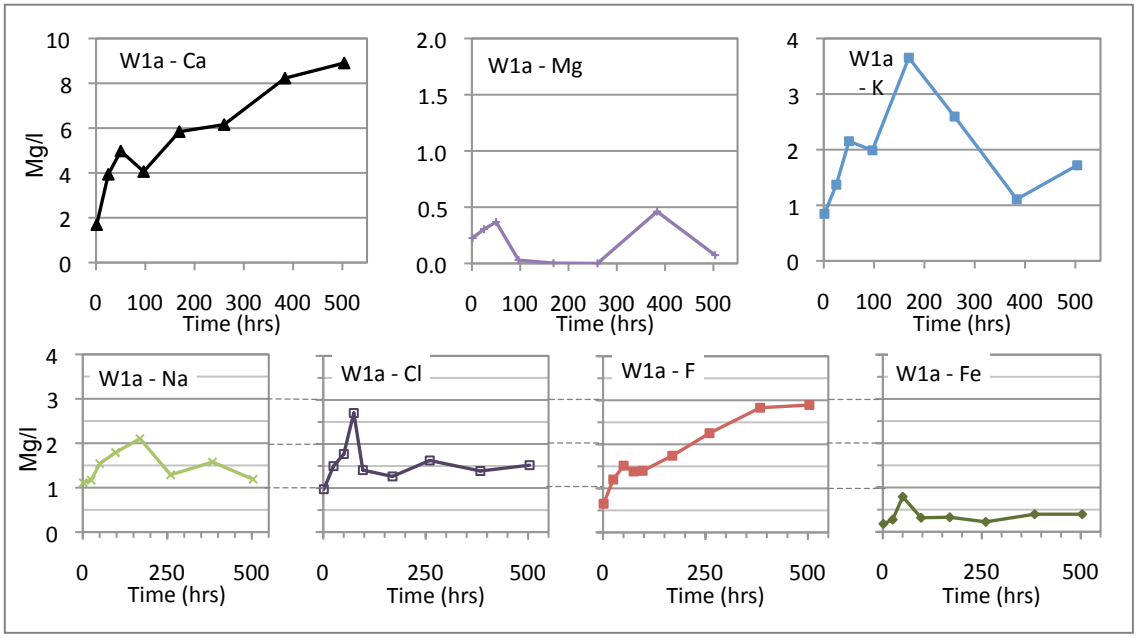

Figure 6-23 - Fresh porphyritic chlorite monzogranite sample W1a batch leaching. Element concentration (mg/l) in solution with time (hours).

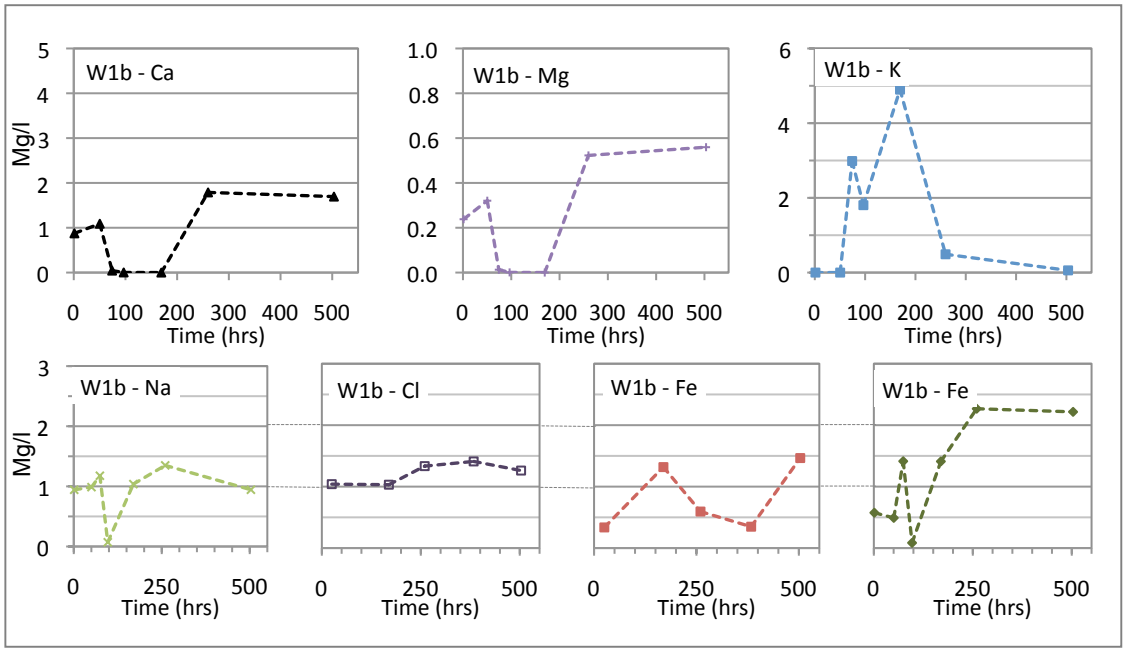

Figure 6-24 - Weathered porphyritic chlorite monzogranite sample W1b batch leaching. Element concentration (mg/l) in solution with time (hours).

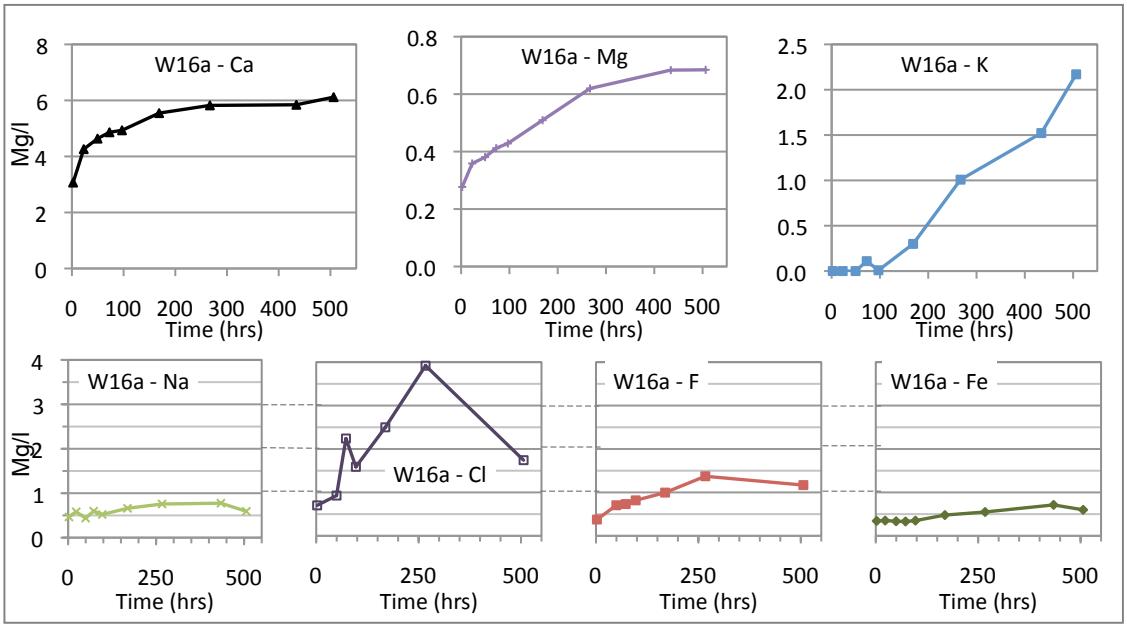

Figure 6-25 – Fresh biotite granodiorite sample W16a batch leaching. Element concentration (mg/l) in solution with time (hours).

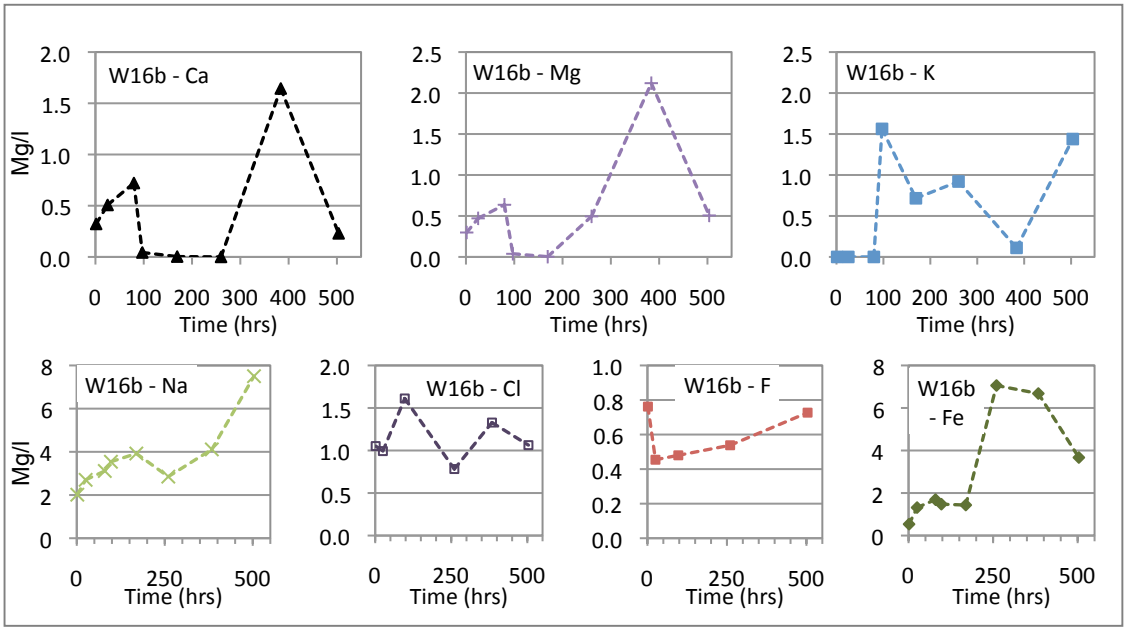

Figure 6-26 – Weathered biotite granodiorite sample W16b batch leaching. Element concentration (mg/l) in solution with time (hours).

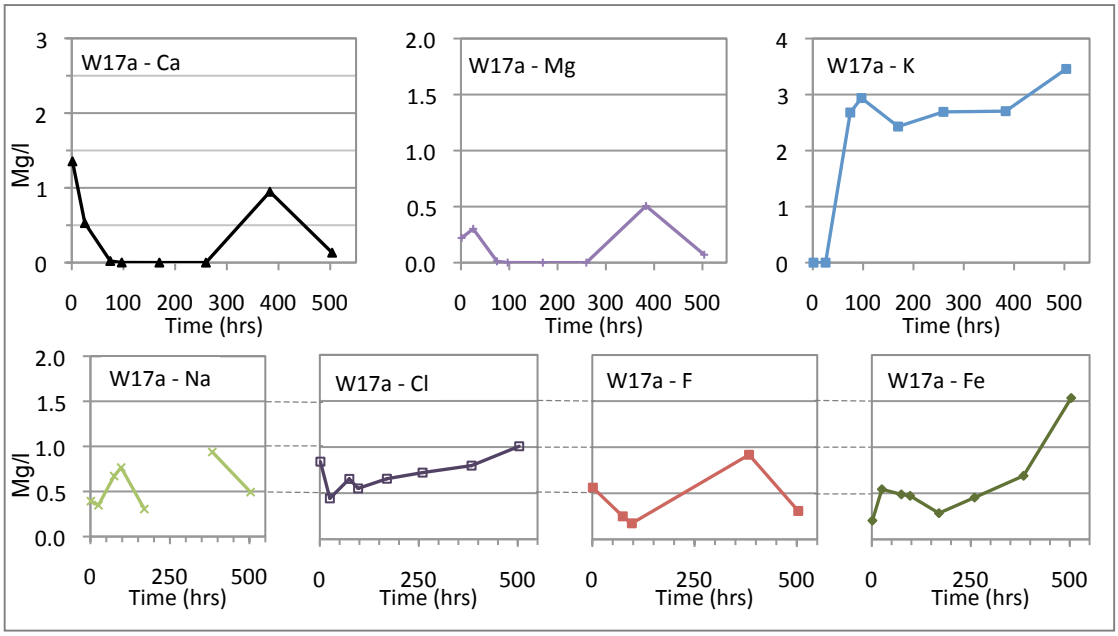

Figure 6-27 – Fresh pegmatitic epidote quartz syenite sample W17a batch leaching. Element concentration (mg/l) in solution with time (hours).

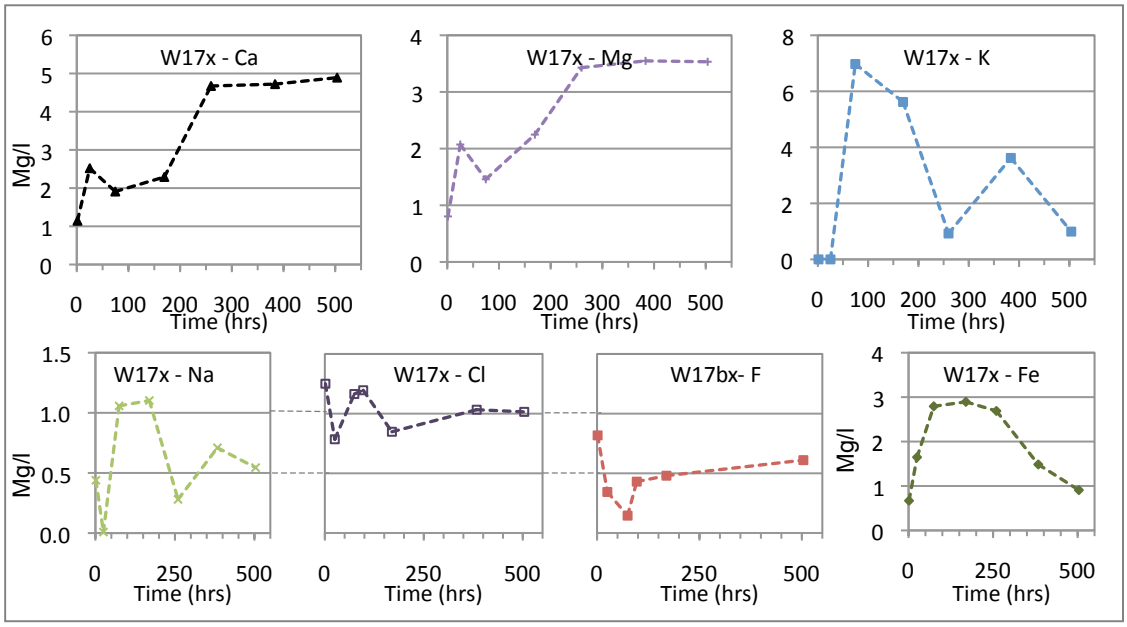

Figure 6-28 – Weathered epidote quartz monzodiorite sample W17x batch leaching. Element concentration (mg/l) in solution with time (hours).

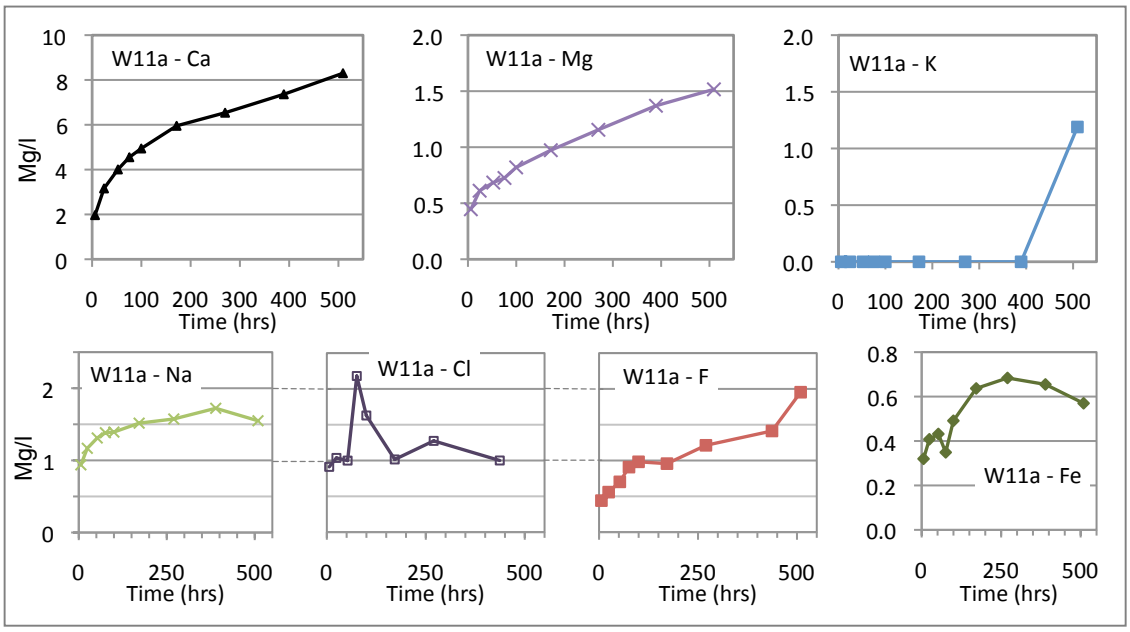

Figure 6-29 – Fresh amphibole granodiorite sample W11a batch leaching. Element concentration (mg/l) in solution with time (hours).

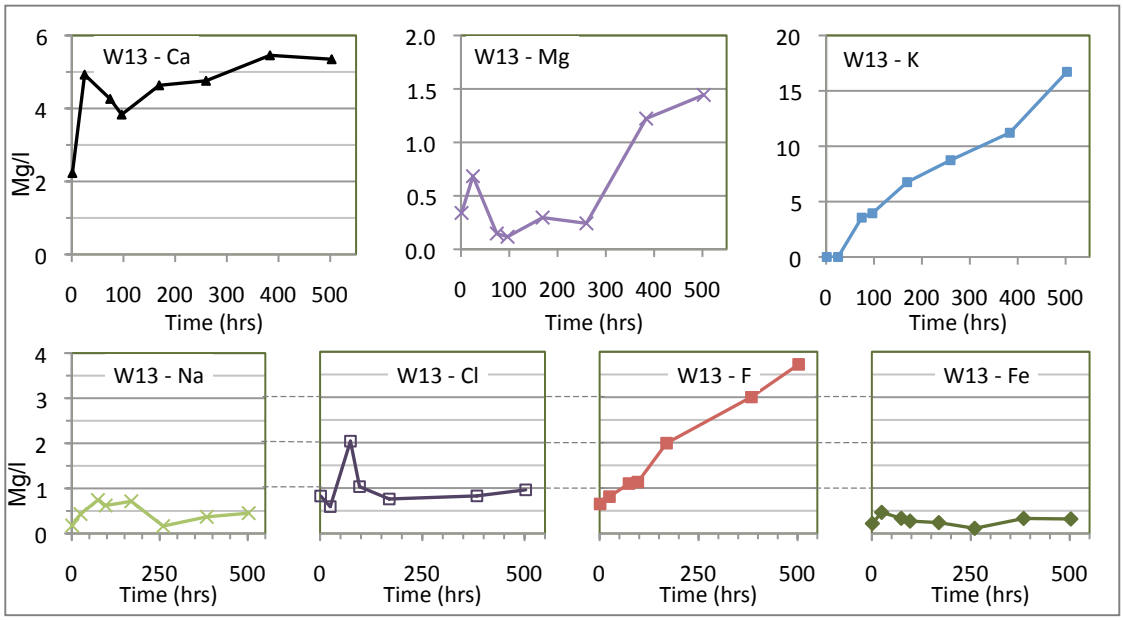

Figure 6-30 - Fresh mafic vein sample W13 batch leaching. Element concentration (mg/l) in solution with time (hours).

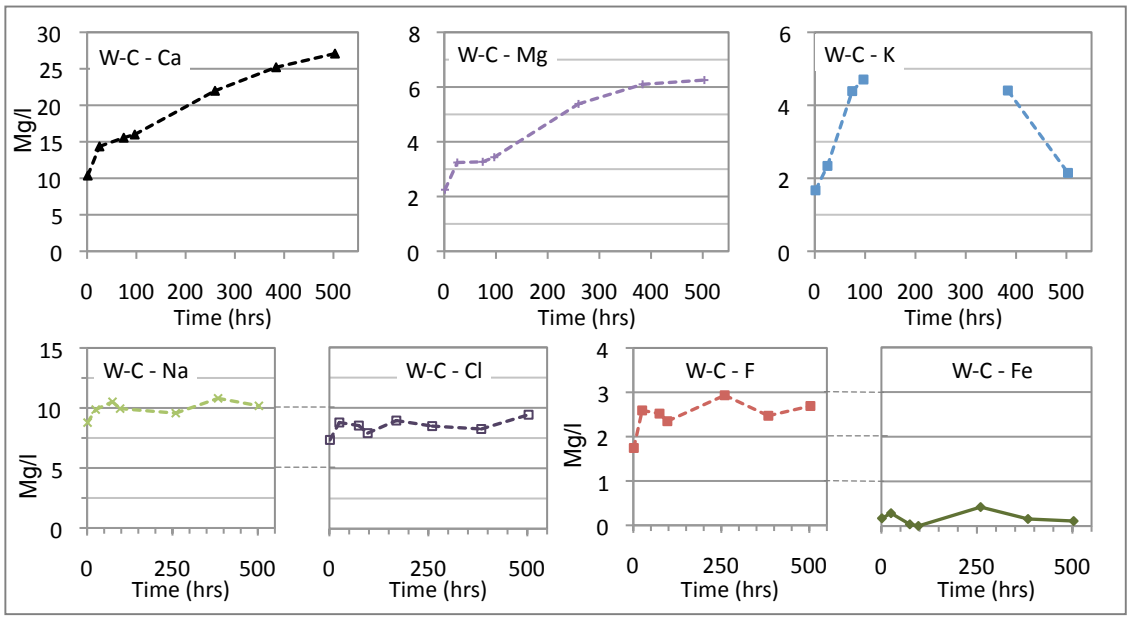

Figure 6-31- Calcrete sample W-C batch leaching. Element concentration (mg/l) in solution with time (hours).

Potential Sources of Leached Fluoride - Wailpally

The correlation coefficients between leached fluoride and other elements in solution are given in table 6-5 and scatter plots of F and other elements in leached solution in figure 6-32.

A strong correlation is seen between F and K in the mafic vein sample W13 (R=0.976, see also figure 6-32), indicating that these two elements may have originated from the same mineral (biotite). However, the correlation between F and Mg and Ca is not as strong in this sample. This may indicate that despite both biotite and amphiboles containing high F in this sample (average 0.91 mass % in biotite and 0.30 mass % in amphiboles), the source of water soluble F is likely to be biotite. A weak correlation between F and Mg release to solution may also be due to the preferential release of F from the amphibole structure or due to Mg loss from two different minerals (biotite and amphiboles). Amphibole granodiorite sample W11a also contains amphiboles (ferro-edenite, average 0.20 mass % F) but no biotite, and has a very strong correlation between F and Ca, Mg and Fe, but a weaker correlation with K (see table 6-5, and figure 6-32). In this case leached F is likely to be from amphiboles.

In the fresh biotite granite W16a, there is a strong correlation between F and K, Mg, Ca, and Fe. Possible sources of leached F may include biotite, apatite and epidote (var 2).

Two samples (biotite granodiorite W16a and amphibole granodiorite W11a) have a strong correlation between F and Fe, suggesting a common source (such as biotite) or F sorbed to Fe oxides present in the sample and facilitating Fe dissolution (although this is less common than Al oxide dissolution from F sorption – see chapter 2, section 2.1.15).

Samples with a strong correlation between F and Ca include the porphyritic chlorite monzogranite W1a, the biotite granodiorite W16a and the amphibole granodiorite. In W1a, the correlation is very strong (R=1.0, see figure 6-32), and could be related to fluorite, apatite or titanite dissolution. These are the principal F-bearing minerals in this sample (as seen in optical petrology, EM point analysis and mass balance calculations). A strong correlation between [F^-] and [Ca^{2+}] indicate that apatite weathering may also be a source of F in W16a and W11a.

No significant correlations are identified for the pegmatitic epidote quartz syenite sample (W17a), the weathered epidote quartz monzodiorite sample (W17x) or the weathered biotite granodiorite sample (W16b). This may be due to low F^- leached from the sample (as shown in figure 6-21).

In the calcrete sample (W-C), F may be present either as fluorite co-precipitated with calcite, or as F^- adsorbed to the calcite surface. The weak correlation between [F^-] and [Ca^{2+}] in leached solution (R=0.5) indicates the primary source of F^- to solution to be from desorbed F^- from the calcite surface (rather than fluorite dissolution). This agrees with EM point analysis of calcite which identifies the sample to be primarily composed of calcite, with a small amount of F, rather than containing the mineral fluorite. The solution remains under-saturated with respect to fluorite throughout the experiment.

Table 6-5– Spearman Rank Correlation Coefficient for F and other elements in Wailpally samples. * indicates the correlation significant at the 0.05 level, and ** indicates the correlation significant at the 0.01 level (these are in bold). The number of points correlated ranges from 5-11 in most cases. In W1b this is 3-5 points, and W-S, 3-4 points.

Sample	F-Ca	F-Mg	F-K	F-Na	F-P	F-Cl	F-Fe
W1a	**1.000****	-0.08	0.29	0.33	-0.44	0.13	0.56
W1b	-0.50	0.50	-0.50	**-1.000****	-0.50	-0.20	-0.50
W16a	**0.964****	**0.964****	**0.919****	**0.847***	-0.15	**0.821***	**0.847***
W16b	-0.56	-0.56	0.56	0.10	-0.56	-0.10	0.50
W17a	-0.11	-0.07	-0.36	0.11	-0.33	0.32	-0.36
W17b	-0.10	0.00	-0.56	-0.20	0.40	0.37	-0.70
W11a	**0.976****	**0.976****	0.58	**0.952****	0.49	**0.673***	**0.810***
W13	0.71	0.43	**0.991****	0.21	-0.38	0.25	0.09
W-S	0.40	0.20	-0.40	-0.40	-0.40	**1.000****	0.20
W-C	0.50	0.50	-0.46	0.04	0.20	**0.786***	0.43

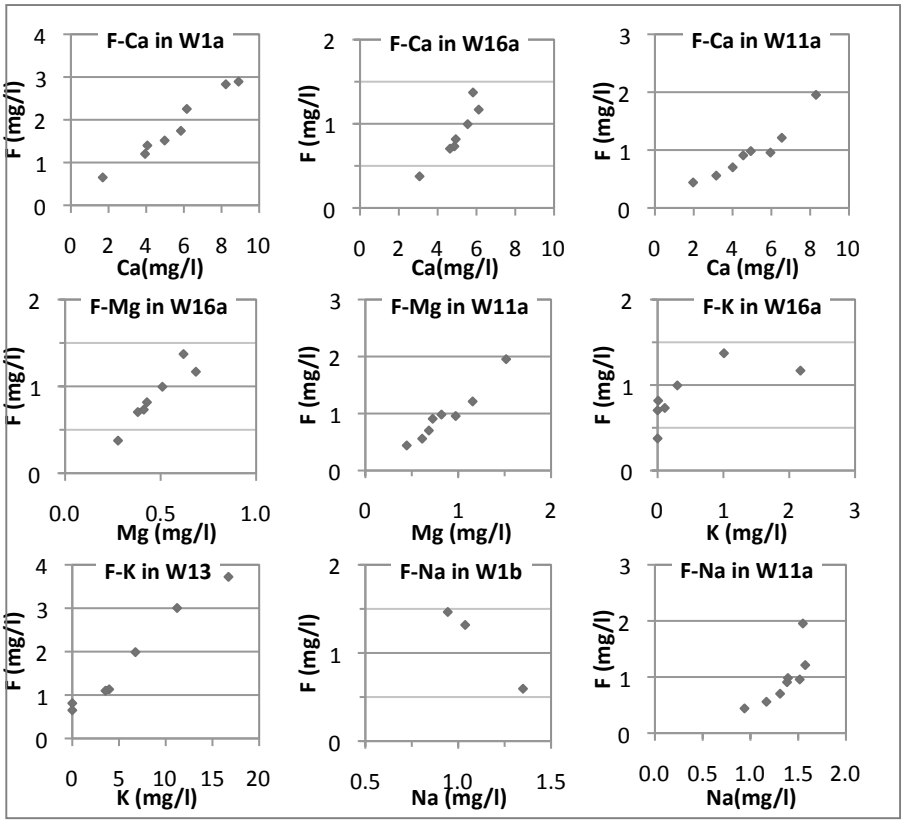

Figure 6-32 – Scatter plots of concentration of F in solution vs. Ca, Mg, K and Na in leaching solutions where a very strong correlation (significant at 0.01 level) is present (table 6-5).

6.4. Batch Leaching Results - Profile Samples

Profile samples at regular depth intervals from one site in each of the Maheshwaram and Wailpally catchments were chosen for batch leaching experiments (table 6-6). Sample whole rock chemistry (WRC) and whole rock fluorine (WRF) values are given in table 6-7. Experiments were conducted at the Wolfson laboratory at UCL and at the EMMA laboratories at the NHM. The method used was the same in both laboratories, except for a shaker being used at the NHM rather than a roller. This reduces the amount of agitation and movement of the sample, and so reduces sample breakdown through attrition. The different sample mixing methods may affect the results, and are therefore discussed separately, although some comparisons may still be made.

The fresh rock sample for the Maheshwaram profile is porphyritic biotite granodiorite sample M2a, and for the Wailpally profile is amphibole granodiorite sample W11a.

Table 6-6– Profile samples used for batch leaching experiments and experiment and analysis details. * Indicates samples placed in a shaker and analysed at the NHM. All other samples places on rollers and analysed at UCL.

	Sample Depth (m)	Notes	Size Fraction Used	Total Time (hrs)	Cations Analysed	Anions Analysed
Maheshwaram	0	Soil	0.5-2mm	506	Ca,Fe,K,M,Na,P	F,Cl
	2	Fracture fill	0.5-2mm	504	Ca,Fe,K,M,Na,P	F,Cl
	4	Mafic rich	0.5-2mm	503	Ca,Fe,K,Mg,Na,P	F,Cl
	6	Fracture fill	0.5-2mm	506	Ca,Fe,K,Mg,Na,P	F,Cl
	8		0.5-2mm	503	Ca,Fe,K,Mg,Na,P	F,Cl
	10		0.5-2mm	501	Ca,Fe,K,Mg,Na,P	F,Cl
	M2a	Fresh	0.5-2mm	4,750	Ca,K,Mg,Na	F,Cl
Wailpally	2*		0.5-2mm	360	Ca,Fe,K,Mg,Na,P,Si	F,Cl
	3*		0.5-2mm	360	Ca,Fe,K,Mg,Na,P,Si	F,Cl
	4*	Amphibole rich	0.5-2mm	361	Ca,Fe,K,Mg,Na,P,Si	F,Cl
	7*		0.5-2mm	360	Ca,Fe,K,Mg,Na,P,Si	F,Cl
	2		0.5-2mm	525	Ca,Fe,K,Mg,Na,P	F,Cl
	4	Amphibole rich	0.5-2mm	501	Ca,Fe,K,Mg,Na,P	F,Cl
	7		0.5-2mm	525	Ca,Fe,K,Mg,Na,P	F,Cl
	W11a	Fresh	0.5-2mm	509	Ca,Fe,K,Mg,Na,P	F,Cl
Blank 3			-	503	Ca,Fe,K,Mg,Na,P	F,Cl
Blank 4			-	360	Ca,Fe,K,Mg,Na,P,Si	F,Cl

Table 6-7 – Profile samples whole rock chemical analysis (WRC), as weight %, and whole rock fluorine (WRF) content as ppm. Fresh samples are M2a (porphyritic biotite granodiorite) and W11a (amphibole granodiorite) with no depth given

Weight %	Maheshwaram – Sample Depth (m)							Wailpally- Sample Depth (m)				
	M2a	10	8	6	4	2	0	W11a	7	4	3	2
Al_2O_3	14.41	13.44	14.41	13.38	14.30	11.40	13.89	14.15	14.28	14.07	13.92	13.72
CaO	2.41	1.76	1.52	4.16	2.15	11.57	1.17	3.27	3.36	2.79	2.66	2.05
Fe_2O_3 (t)	3.61	3.82	3.01	2.64	3.96	2.49	3.27	4.13	3.84	3.11	2.33	2.19
K_2O	4.55	4.48	5.53	5.63	5.03	3.58	5.17	3.56	4.04	3.61	3.30	3.77
MgO	1.14	0.90	0.68	0.76	0.98	0.71	0.54	1.83	1.49	1.63	1.00	0.88
MnO	0.04	0.04	0.03	0.01	0.04	0.02	0.03	0.06	0.06	0.03	0.03	0.02
Na_2O	3.11	2.58	2.89	2.15	3.07	1.85	1.87	3.53	3.49	3.52	3.72	3.50
P_2O_5	0.19	0.22	0.15	0.09	0.20	0.10	0.10	<	0.11	0.09	0.07	0.08
SiO2	66.49	67.84	70.71	66.31	66.83	51.85	65.48	66.79	68.17	66.94	69.53	69.86
TiO_2	0.49	0.55	0.42	0.30	0.55	0.32	0.37	0.29	0.28	0.28	0.22	0.22
F (ppm)	1749		535	423	753		328	824	623	715		530

The Ion Chromatography (IC) detection limit for fluoride for samples run at the NHM is 0.02 mg/l F. As no replicate samples were measured for F on the IC, a precision of 10% is assumed to be adequate (this is higher due to the low F values measured).

The precision of the UCL IC F measurements is 0.117 (the SD of repeat measurements), which can also be given as 4%.

Repeat runs were carried out for the majority of samples. Repeat experiments give very similar patterns of element concentration in solution, and similar overall end values in most cases. The end concentrations of leached F^- vary by ~0.5mg/l in Maheshwaram samples at 0, 4, 6 and 8m depth, although the concentrations of F at the start of the experiments are more similar. Final [F^-] in Wailpally NHM repeat experiments are within measurement error. The final [F^-] of repeat samples are shown in figure 6-33 and figure 6-34 to show this variation.

6.4.1. Overview of Leached [F^-]

The final [F^-] in profile batch leaching experiments is given in figure 6-33 (including repeat experiments). Experiments run at the NHM give substantially lower F^- concentrations than those run at UCL. This is due to the nature of sample mixing (with samples placed on rollers at UCL experiencing more agitation and physical breakdown than those on shakers at the NHM). The difference between the UCL and

NHM experiments indicate that sample attrition and physical breakdown do play a large role in the [F^-] in leached solution in the UCL experiments.

Overall, the final leached [F^-] is higher from the Maheshwaram profile samples than from the Wailpally profile samples (UCL experiments, figure 6-33). When comparing fresh rock samples however, a higher final [F^-] is leached from the Wailpally fresh rock (W11a) than the Maheshwaram fresh rock (M2a). In the Maheshwaram profile, the highest final [F^-] is from the sample at 6m depth (consisting of fracture fill material), with the fresh sample (M2a) having the lowest final [F^-] leached, similar to [F^-] leached from the soil sample at 0m (figure 6-33). The Wailpally profile shows a different pattern, with the highest [F^-] leached from the fresh sample (W11a), and little variation between leaching of other profile samples.

The Wailpally NHM batch leaching experiments include all profile samples (but not fresh sample W11a) (figure 6-33). The highest leached [F^-] is from the sample at 7m depth, and the lowest at 3m depth. Leaching of the sample at 4m depth (amphibole rich layer) also gives a high final [F^-].

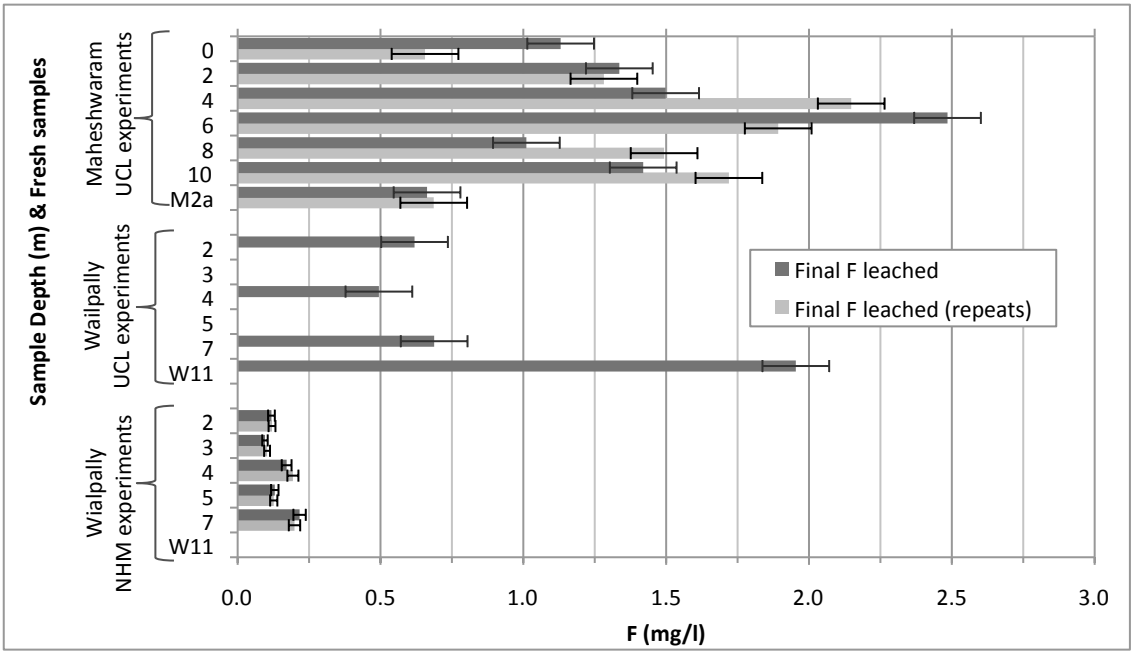

Figure 6-33 – Final [F^-] leached from Profile batch leaching experiments (including repeats and fresh samples M2a and W11a). Maheshwaram profile final [F^-] leached taken at ~500hours, Wailpally final [F^-] leached taken at ~360 hours (apart from repeats at 3 and 5m in NHM experiments, taken at 220 hours).

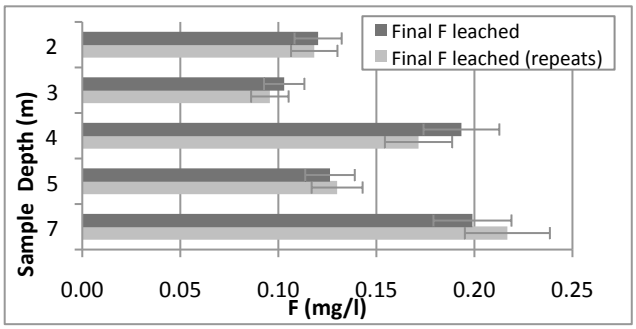

Figure 6-34 – Final [F^-] leached from Wailpally profile batch leaching experiments at the NHM. Final F concentration taken at ~360 hours apart from repeat samples at 3 and 5m depth, taken at 220 hours.

The relationship between final [F^-] in leaching experiments and sample WRF is shown in figure 6-35 and figure 6-36. In the UCL batch leaching experiments there is no obvious relationship between sample WRF and final [F^-] (figure 6-35). The fresh rock Maheshwaram sample (M2a) with the highest WRF value has a low final [F^-] leached. In the NHM experiments, the Wailpally samples show a rough increase in [F^-] leached as sample WRF increases, although this is only across three samples (figure 6-36).

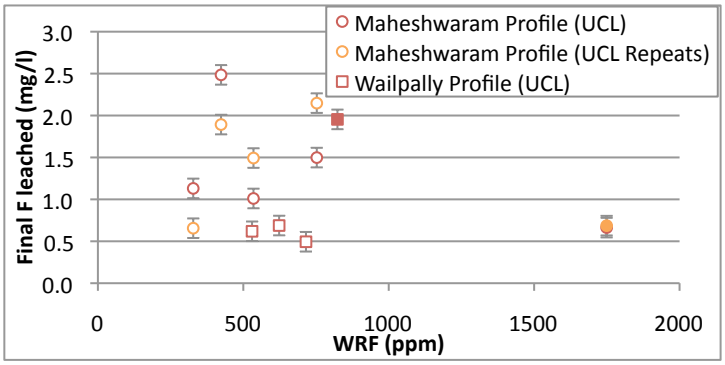

Figure 6-35 – Profile samples final F leached and WRF (UCL experiments). Samples with solid fill are fresh rock samples.

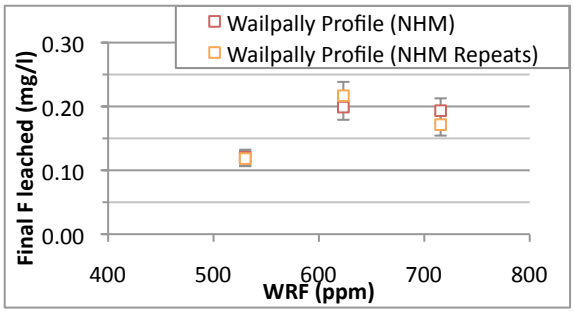

Figure 6-36 – Wailpally Profile samples final F leached and WRF (NHM experiments).

6.4.2. Maheshwaram Profile

Fluoride leaching

The [F^-] in leached solution with time in Maheshwaram profile samples is given in figure 6-37 and figure 6-38. There is an initial increase in [F^-] by the time the first sample is taken, followed in some samples by a sharp decrease at ~40 hours (0m, 10m) (figure 6-37). Other samples show little change in [F^-] with time (e.g. 2m, 8m, and M2a) (figure 6-38). The highest [F^-] leached is from the sample at 6m depth (fracture fill material, final [F^-] 2.48 mg/l). The soil sample at 0m also starts with a high [F^-] leached, although this decreases sharply at ~40 hours. The lowest [F^-] leached is from the fresh sample M2a (figure 6-37).

Overall a coarse trend may be seen of higher [F^-] leached from the shallower samples (2m and 4m) and lower [F^-] leached from the deeper samples (10m and M2a), with the exception of high F leached from 6m. However, at many points the [F^-] leached from different samples is very similar, with similar end [F^-] in samples at 4m, 10m, 2m and 0m (figure 6-37).

All sample solutions are under-saturated with respect to fluorite (figure 6-39), and super-saturated with respect to several Fe phases from the beginning of the experiment.

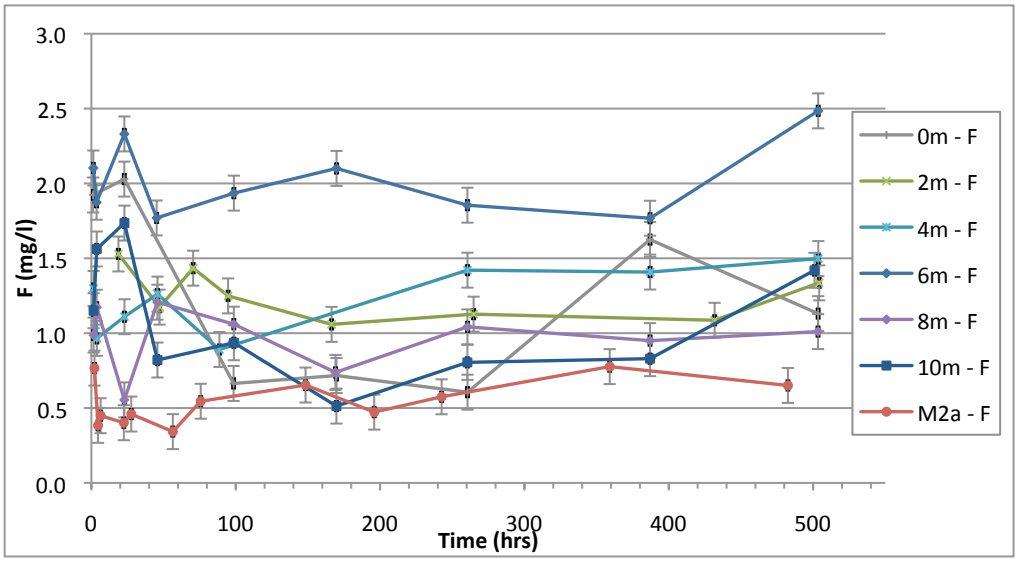

Figure 6-37 - F concentration in Maheshwaram Profile batch leaching solutions with time (experiments conducted at UCL).

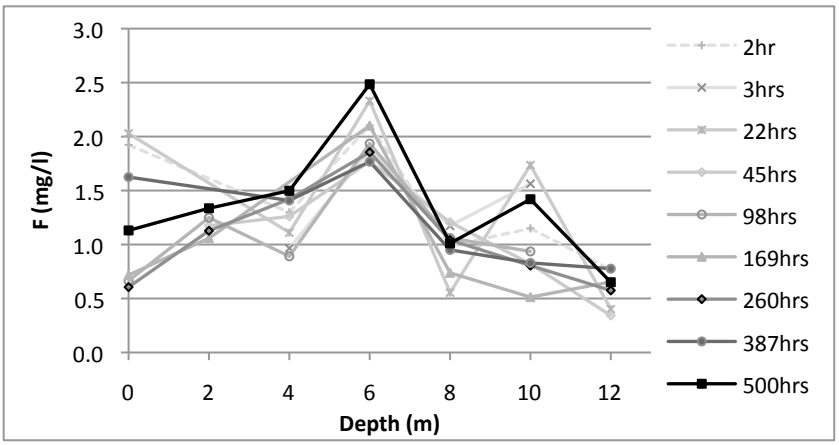

Figure 6-38 – Maheshwaram Profile samples: F concentration at time intervals with depth. Fresh rock sample M2a given at 12m depth (not actual depth)

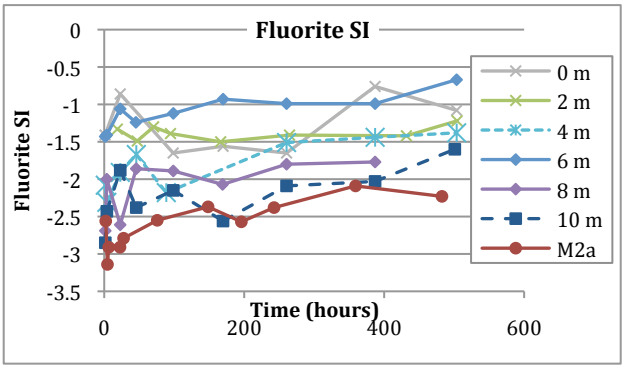

Figure 6-39 – Fluorite saturation indices (SI) determined by PHREEQC for Maheshwaram Profile experiments

Other Elements

Concentrations of Ca, Mg, Na and K leached with time are given in figure 6-40. All samples show an increase in the concentration of Ca and Mg with time. Profile sample WRC shows little change between 3 and 10m depth in most elements (see table 6-7 and chapter 5, section 5.2), therefore little difference may be expected between samples (apart from fracture material at 2m and 6m). However, variation between leached solutions is seen (figure 6-40). The concentration of elements leached is low in fresh sample M2a compared to other samples (apart from K leached, where all samples have low concentrations leached apart from the sample at 0m). The soil sample at 0m leached high concentrations of Ca and K due to its composition and the availability of K for release from readily available soil minerals (including clay minerals and on clay exchange sites). Fracture fill samples at 2m and 6m have high Mg and Ca leached. Samples at 4, 6 and 8m have similar Ca, K and Na leached.

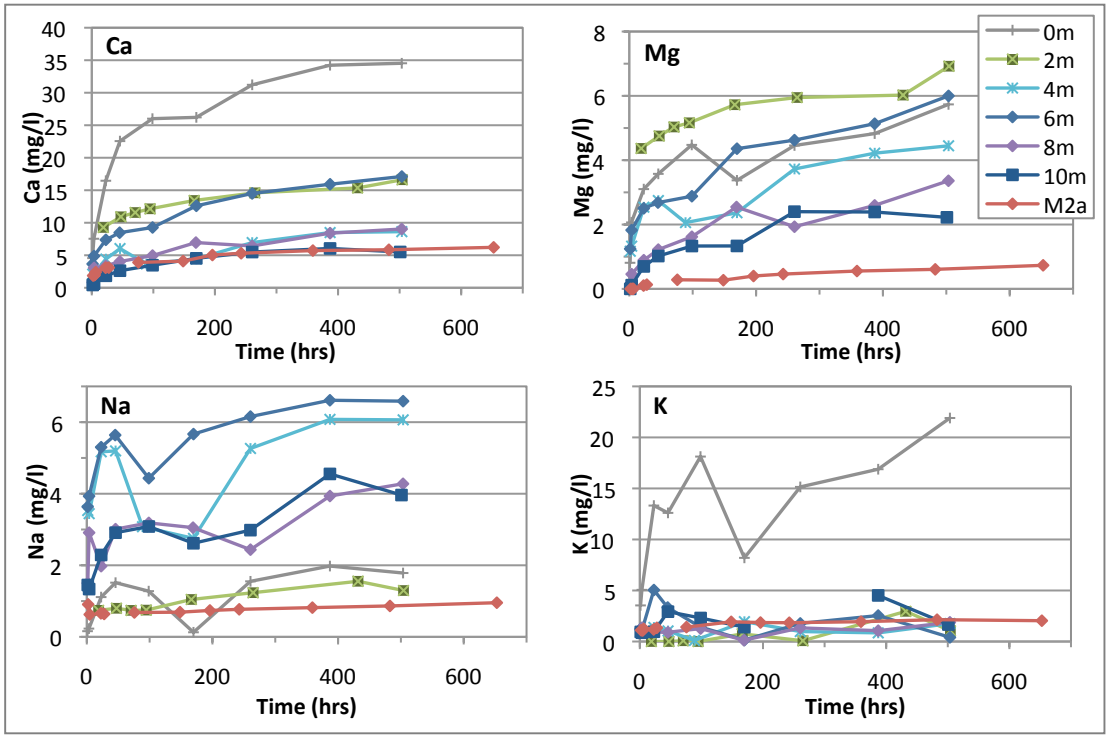

Figure 6-40 – Maheshwaram profile samples elements leached with time.

Potential Sources of Leached Fluoride – Maheshwaram Profile

Correlation coefficients for Maheshwaram profile samples show a weak correlation between F and all other elements measured in most samples. Significant correlation was only found in leached solution from the sample at 4m, between F and Ca (R=0.71), and F and Mg (R=0.71) (both significant at 0.05 level) and between F and Na (R=0.86, significant at 0.01 level). The sample at 4m has a high quantity of mafic minerals. The correlation between F and Mg may therefore suggest F from biotite weathering from this layer as a source of F^- to solution. Leachate from fresh sample M2a showed only a positive correlation between F and Cl (R=0.64, table 6-4).

The higher [F^-] leached from profile samples (with low WRF) than from the fresh sample (with high WRF) indicates that there is more F that is readily available. This may include desorption of F from clay minerals, Al and Fe oxides or calcite, whereas F^- located in fresh sample M2a is less easily leached into solution (more firmly held within silicate minerals). This is also supported by the lack of change of [F^-] with time in many samples (also indicating that available F is quickly brought into solution and therefore located where it is easily de-sorbed or in minerals easily dissolved).

Higher [F^-] leached from saprolite samples have implications for the sources of F^- to groundwater in this profile. The weathering of the fresh rock sample may result in the re-distribution of F in more 'mobile' locations within the saprolite, which may then later be flushed by recharging waters. Models of F release to groundwater based on this profile are further developed in Chapter 7.

The high [F^-] leached from fracture fill material at 6m is likely to be due to the high proportion of clay minerals and disseminated carbonate minerals present, which can contain readily water soluble F. Water infiltrating through the weathering profile will primarily flow through fractures as they have a higher permeability that the matrix of the saprolite. The high [F^-] leached from this fracture fill material may therefore be an important source of F to groundwater through recharging water. The other fracture fill sample at 2m depth has a lower [F^-] leached, possibly due to compositional differences (the sample at 2m has a higher CaO and lower K content than the sample at 6m, see WRC in table 6-7), of differences in F content (unknown), or due to differences in sample mineralogy and forms of F present (i.e. the clay content may be different, or more F may be precipitated with calcite as fluorite) or due to the location within the profile (the sample at 2m depth is nearer the surface, within the sandy saprolite, and therefore may be more weathered).

6.4.3. Wailpally Profile

Fluoride Leaching

Concentrations of F^- in leached solution with time are given in figure 6-41 to figure 6-43. Calculations using PHREEQC show all experiments to be under-saturated with respect to fluorite (figure 6-44).

UCL Wailpally leaching experiments:

In the UCL batch leaching experiments, [F^-] leached from the fresh sample (W11a) is low (<0.75 mg/l) at the start of the experiment (0-50 hours) and similar to the [F^-] leached from the shallowest profile sample at 2m (figure 6-41). In contrast [F^-]

leached from profile samples at 4m and 7m depth are high at the start of the experiment (0-25 hours) (1.04 and 1.25 mg/l F respectively).

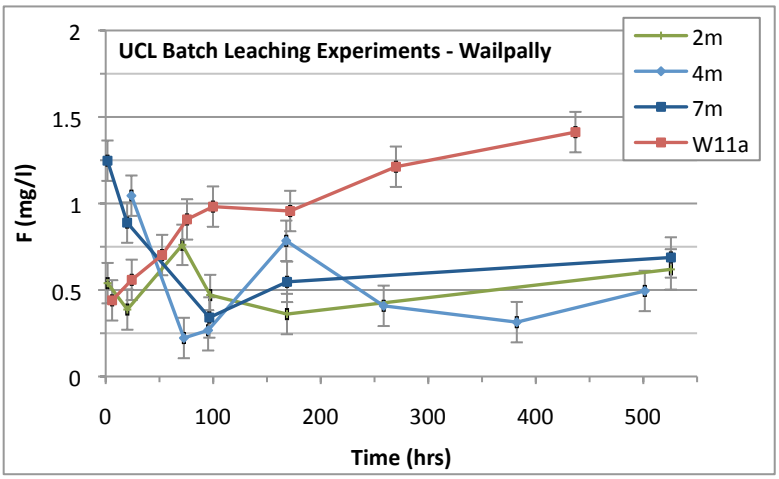

Figure 6-41 – F leached from Wailpally Profile samples with time (UCL experiments). Error bars are S.D.

However, the [F^-] leached from the fresh sample (W11a) increases throughout the experiment, and is higher than the [F^-] leached from the profile samples from ~75 hours onwards, reaching a final concentration of 1.41 mg/l F. The [F^-] leached from profile samples at 4m and 7m decreases after the initial high concentration, and then remains low (below 0.75 mg/l) for the remainder of the experiment. The [F^-] leached from the shallow sample at 2m is also low for the duration of the experiment, with a slight increase at ~75 hours.

NHM Wailpally leaching experiments:

The NHM leaching experiments include all profile samples and so give a full view of the relative mobility of F to water from different depths (figure 6-42). However, they do not include the fresh rock sample W11a. UCL leaching experiments show the [F^-] leached from fresh sample W11a to be higher than [F^-] leached from profile samples. This can be taken into account when interpreting NHM profile experiments.

The [F^-] in leached solution increases with time in all experiments (figure 6-42, figure 6-43). Overall a higher [F^-] is leached from deeper samples (7m) and from the amphibole rich layer at 4m (with a high WRF value), and lower [F^-] leached from mid to shallow samples (2m, 3m and 5m) (figure 6-42).

Wailpally profile samples are increasingly weathered towards the surface, with a higher WRF content in the fresh sample and the enriched layer at 4m depth. Here, higher WRF content and sample weathering is somewhat related to the mobility of F^- from the sample, with deeper samples and those with higher WRF leaching higher concentrations of F^- to water.

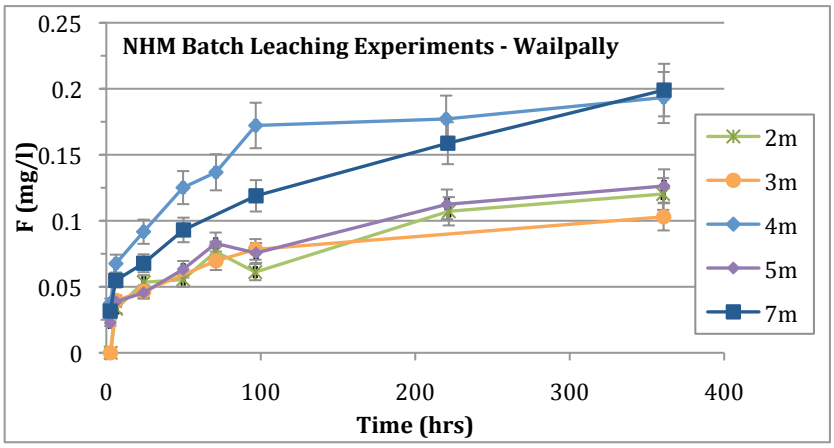

Figure 6-42 – F leached from Wailpally Profile samples with time (NHM experiments) Error bars are S.D.

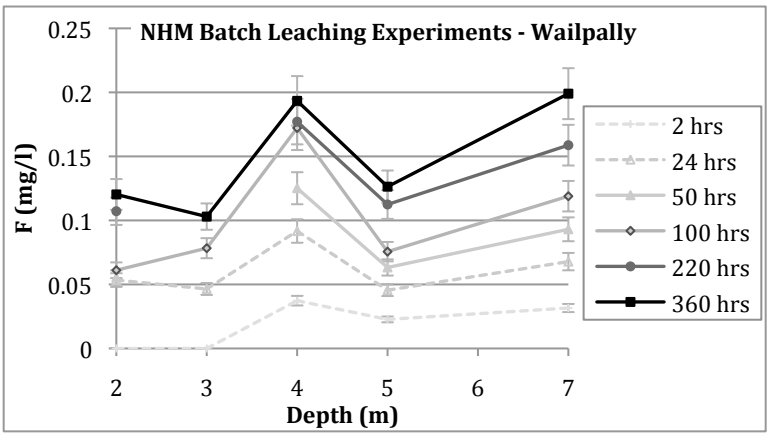

Figure 6-43 – F concentration leached from samples at different depths with time in the Wailpally Profile. NHM experiments.

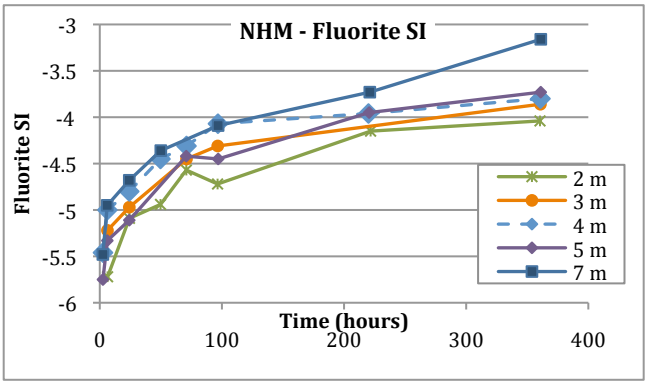

Figure 6-44 - Fluorite saturation indices (SI) determined by PHREEQC for Wailpally Profile NHM experiments

Other Elements

Concentrations of Ca, Na, K and Mg from Wailpally profile leaching experiments are given in figure 6-45 (UCL leaching) and figure 6-46 (NHM leaching). Repeat experiments give similar results for elements leached, and therefore only one set of results are given. Results from UCL and NHM experiments show similar patterns, although the leached element concentrations from UCL experiments are higher than the NHM experiments. This again is due to the method of mixing, with experiments conducted at UCL experiencing more physical breakdown than those at the NHM.

Both sets of results show increasing Ca and Mg in solution with time, with high Ca leached from samples at 3 and 5m depth and low Ca leached from the sample at 4m depth (figure 6-46). This corresponds to sample composition, with samples at depth 3 and 5m having a higher proportion of carbonate visible (see chapter 5, section 5.2 profile descriptions). The concentration of Mg leached is high from samples at 2 and 3m depth, and lower from the fresh sample W11a and samples at 7m and 4m depth (figure 6-45 and figure 6-46). In these samples Mg may be less easily removed from mineral structures. Leaching of Mg is likely to be from amphiboles, which are the principal F-bearing minerals W11a.

In both sets of experiments, the concentration of Na leached from samples at 4, 5 and 7m increases rapidly (within the first 50 to 100 hours) and then remains constant, whereas Na leached from samples at 2m, 3m and W11a remain low throughout (figure 6-45 and figure 6-46). Concentrations of K in solution show a similar response, with only K leached from the sample at 3m depth showing a large increase at the start of the experiment, and leached K from other samples remaining low. The primary location of K within the sample will be in K-feldspars, which are relatively stable minerals, and are not easily weathered.

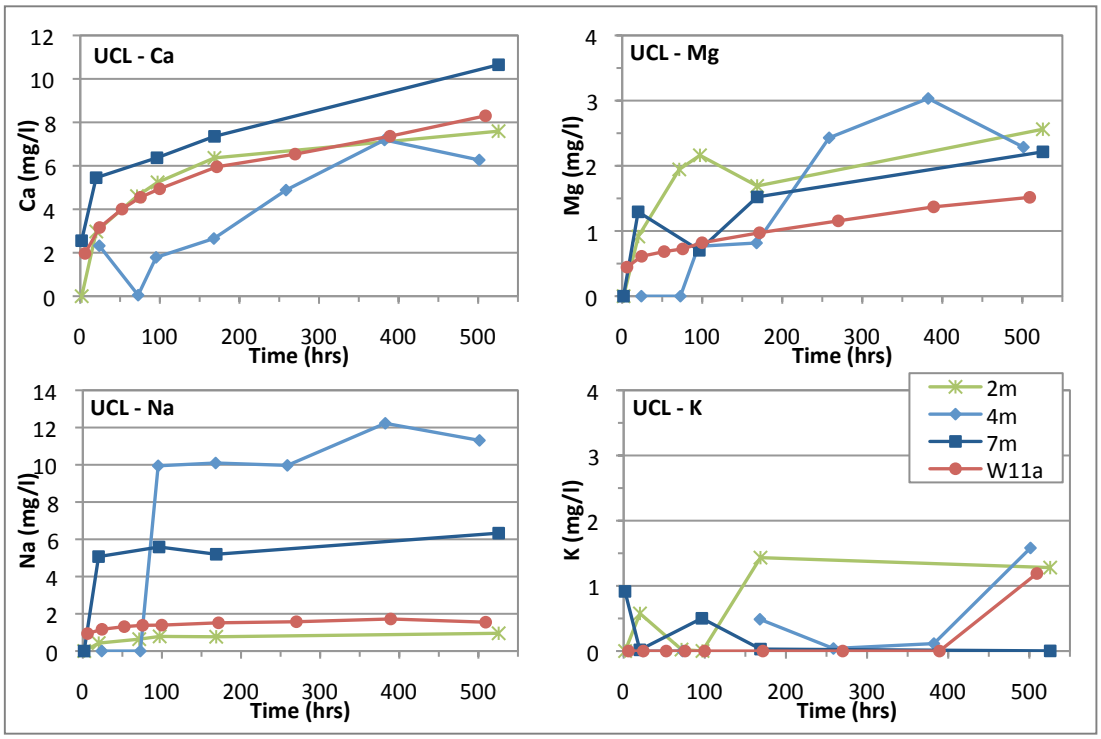

Figure 6-45 - Wailpally profile samples elements leached with time – UCL experiments

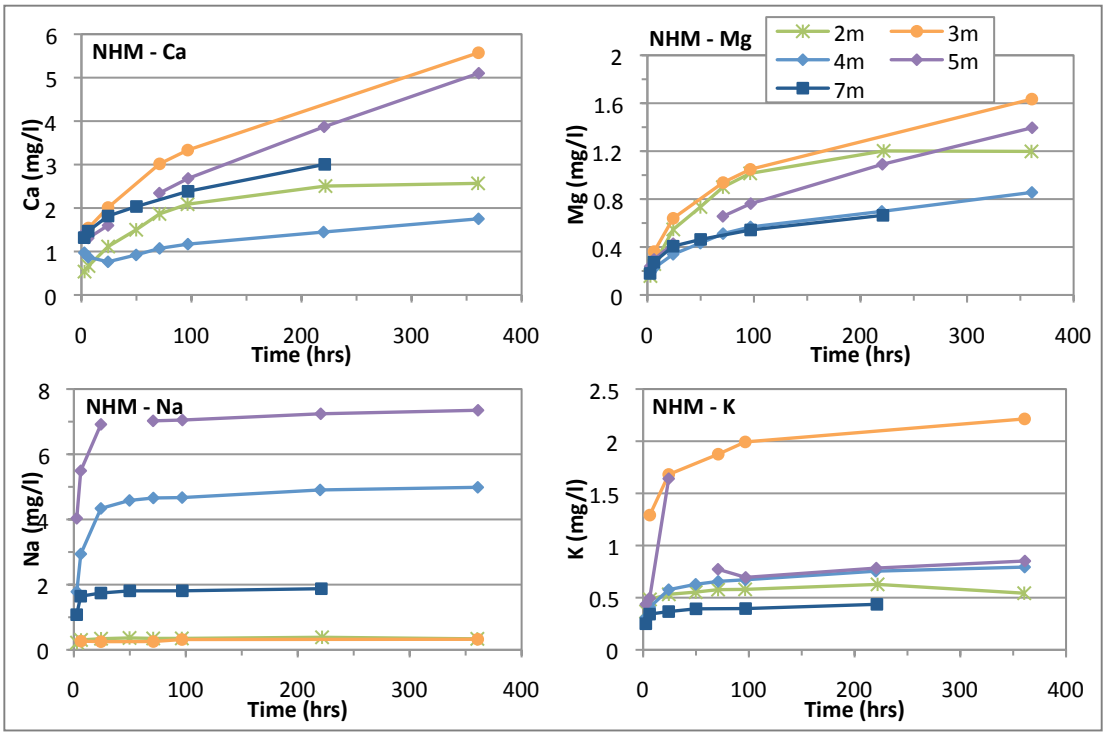

Figure 6-46 - Wailpally profile samples elements leached with time – NHM experiments

Potential Sources of Leached Fluoride – Wailpally Profile

Calculated correlation coefficients show no strong correlations (significant at the 0.05 or 0.01 level) between [F^-] and other elements in the UCL batch leaching experiments.

The NHM experiments, however, show several strong correlations (table 6-8 and figure 6-47). All samples have a strong correlation between F and Mg, indicating that F leached is likely to be from the weathering of amphiboles (which in this sample are ferro-edenite, general formula $NaCa_2(Mg,Fe)_4Al[Si_7AlO_{22}](OH)_2$). This is supported by a good correlation between [F^-] and [Na^+] and [Ca^{2+}] in many of the samples.

Amphiboles are considered to be the principal mineral F source in fresh sample W11a, contributing the largest proportion to sample total F (79% from mass balance calculations), with apatite and epidote contributing smaller amounts (12 and 6% of total, respectively). The results of profile leaching support this, with the highest F leached from the fresh sample (with high amphibole content) and from the sample at 4m depth (an amphibole rich layer), and with correlations between F and Mg (and Ca and Na) in leached solution.

The Wailpally profile samples are increasingly weathered towards the surface, with a general decrease in WRF content and F leached towards the surface (with the exception of the amphibole rich layer at 4m). Samples with higher carbonate content visible (at 3 and 5m depth) do not have a higher leached [F^-] (as observed with high carbonate fracture fill material in the Maheshwaram profile) and no fracture fill material was collected (as few fractures were present). F is most mobile from the fresh rock (W11a), and therefore interaction of groundwater with the fractured bedrock is likely to be the major source of F in groundwater. Models of F mobilisation based on this profile are developed in chapter 7.

Table 6-8- Spearman Rank Correlation Coefficient (R) for elements in Wailpally batch leaching solutions conducted at the NHM. *indicates correlation is significant at the 0.05 level, **indicates correlation is significant at the 0.01 level (shown in bold). The number of points correlated ranges from 7 to 8 apart from those for sample 3m where F-Mg, F-K and F-Na correlations are from 5 points.

Sample (NHM experiments)	F-Ca	F-Mg	F-K	F-Na	F-Cl	F-Fe
2m	**.976****	**.952****	.738*	.548	.310	-.234
3m	-	**1.000****	**1.000****	.700	-.143	-
4m	.833*	**1.000****	**1.000****	**1.000****	.595	-.265
5m	**.929****	**.964****	.643	**.964****	.595	-.236
7m	**1.000****	**1.000****	.250	**1.000****	.429	.535

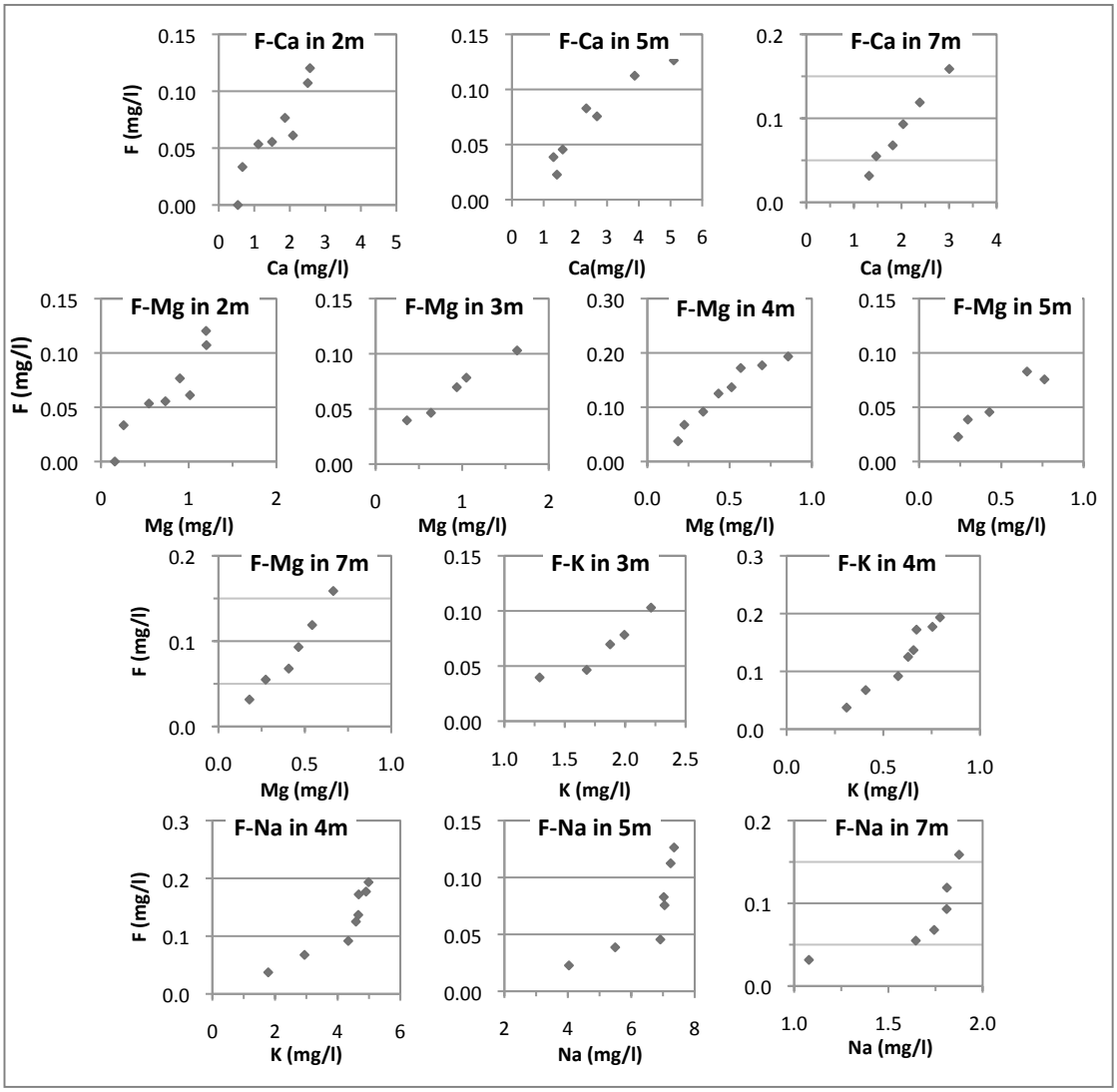

Figure 6-47 – Wailpally NHM experiments scatter plots of the concentration of F in leached solution vs. the concentration of Ca, Mg or K in leaching solutions where a strong correlation is present (see table 6-8).

6.5. Chapter Summary and Discussion

Maheshwaram and Wailpally Batch Leaching

The relative mobility of F to solution from bedrock samples from Maheshwaram and Wailpally and their weathered equivalents was investigated. The final [F^-] clearly show samples W13 (mafic vein sample), W1a (porphyritic chlorite monzogranite) and W-C (calcrete) to have much higher leachable F than other samples. The final concentrations of F^- leached have been used to derive a 'relative F source strength', which is a comparative measure of the availability of F from the samples collected across both catchments. The order of final concentration of F^- leached (from highest [F^-] leached to lowest at ~500 hours) and a semi-quantitative relative F source strength derived from this are given in table 6-9, and illustrated by catchment in figure 6-48.

Table 6-9 – Order of final [F^-] leached (from high to low, at ~500 hours) with relative source strength (10=highest) for all samples. 'MW' indicates a Maheshwaram sample, and 'WP' indicates a Wailpally sample

Sample	Name	Final [F^-] (mg/l)	Relative Source Strength
W13	Mafic vein material – WP	3.72	10
W1a	Porphyritic chlorite monzogranite - WP	2.83	7.6
W-C	Calcrete – WP	2.69	7.2
W1b	Weathered porphyritic chlorite monzogranite - WP	1.46	3.9
W11a	Amphibole granodiorite – WP	1.41	3.8
M7a	Grey monzogranite –MW	1.30	3.5
W16a	Biotite granodiorite – WP	1.17	3.1
M2b	Weathered porphyritic biotite granodiorite – MW	1.12	3.0
M3a	Pink Monzogranite – MW	0.88	2.4
M7b	Weathered grey monzogranite – MW	0.73	2.0
W16b	Weathered biotite granodiorite – WP	0.73	2.0
M2a	Porphyritic biotite granodiorite – MW	0.65	1.7
W17x	Weathered epidote quartz monzodiorite – WP	0.61	1.6
M3b	Weathered pink monzogranite - MW	0.51	1.4
W17a	Pegmatitic epidote quartz syenite - WP	0.31	0.8

The mafic vein sample (W13) consists primarily of F-bearing mica and amphiboles, the porphyritic chlorite monzogranite (W1a) contains F rich apatite, titanite, and fluorite and the calcrete (W-C) consists of calcite with adsorbed F^-. All other samples (including all Maheshwaram samples) have a final F source strength below 4 (table 6-9).

The highest F source strength sample from Maheshwaram is the grey monzogranite (M7a) which has the lowest WRF content of the Maheshwaram fresh samples, and relatively few F-bearing minerals, some with a low average F-content (e.g. biotite). The high [F^-] leached indicates a source of readily mobile F within the sample, with a high proportion of the samples F content water soluble.

For comparison, the relative source strength is also determined from the initial leached [F^-] (at 1-3 hours, table 6-10 and figure 6-48), to give the relative leachability of F upon a short water-rock interaction time. Samples with high initial F source strengths are all weathered samples, with W-C (calcrete), M2b (weathered porphyritic biotite granodiorite) and M7b (weathered grey monzogranite) having the highest source strength. All weathered samples have a higher initial relative F source strength compared to their final relative F source strength (apart from W1b and W16b) and compared to their fresh sample equivalents (apart from W1b). The majority of F is released to solution quickly from weathered samples, whereas the increase in [F^-] in fresh rock experiments is more gradual. In many cases, the initial [F^-] leached from weathered rocks is similar or higher than the equivalent fresh rock [F^-], but does not increase with time. This gives a high initial F source strength, but lower final F source strength. Initial [F^-] in leached solutions may be from F that is loosely bound. A higher proportion of sample total F is readily mobilised to solution from weathered samples (and some low WRF samples), than from fresh samples in most cases. Sample W-C has both a high initial and final F source strength as the leached solution contains high [F^-] throughout.

All Maheshwaram samples (apart from M7a) have a higher initial F source strength than final F source strength (figure 6-48).

Sample W17a (pegmatitic epidote quartz syenite) has the lowest final F source strength and contains few F-bearing minerals with a low WRF content and total F calculated by mass balance. The initial F source strength is higher, however, indicating that some F is released upon contact with water. Sample W1b has the lowest initial F source strength indicating that the weathered samples have less readily available F than other weathered samples. However, the final F source strength of W1b is the highest of the weathered samples (apart from W-C).

Table 6-10 – Order of initial [F^-] leached at 1-3 hours (from high to low) with relative source strength (10=highest) for all samples. 'MW' indicates a Maheshwaram sample, and 'WP' indicates a Wailpally sample

Sample	Name	Initial [F^-] (mg/l)	Relative Source Strength
W-C	Calcrete – WP	1.74	10
M2b	Weathered porphyritic biotite granodiorite – MW	1.03	5.9
M7b	Weathered grey monzogranite – MW	0.94	5.4
W17x	Weathered epidote quartz monzodiorite – WP	0.82	4.7
M2a	Porphyritic biotite granodiorite – MW	0.77	4.4
W16b	Weathered biotite granodiorite – WP	0.76	4.4
M3b	Weathered pink monzogranite - MW	0.72	4.1
W1a	Porphyritic chlorite monzogranite - WP	0.65	3.7
W13	Mafic vein material – WP	0.65	3.7
M3a	Pink Monzogranite – MW	0.59	3.4
W17a	Pegmatitic epidote quartz syenite - WP	0.56	3.2
W11a	Amphibole granodiorite – WP	0.44	2.5
M7a	Grey monzogranite –MW	0.43	2.5
W16a	Biotite granodiorite – WP	0.38	2.2
W1b	Weathered porphyritic chlorite monzogranite - WP	0.34	1.9

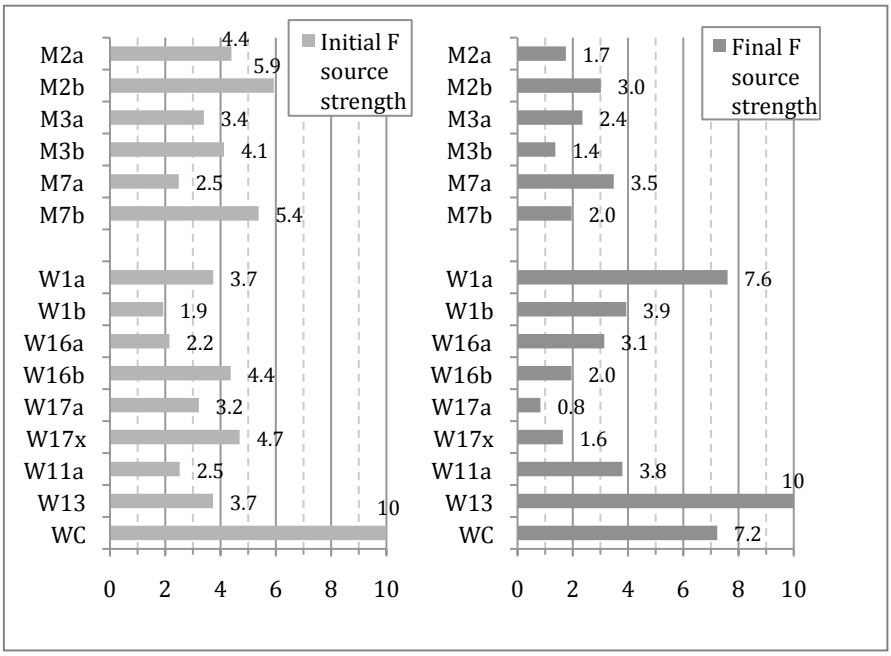

Figure 6-48 – Initial and final relative F source strength from batch leaching experiments.

The average of the initial and final relative F source strengths can be used as a comparative scale of F leachability over all samples. This average source strength takes into account the initial rapidly leached F and the longer term leachable F through prolonged contact with water (figure 6-49). Wailpally samples W-C, W13 and W1a have the highest average F source strength (these samples also have the highest final F source strength), followed by weathered Maheshwaram samples M2b

and M7b (both of which have high initial F source strength). The majority of the remaining samples have a similar average F source strength (between 2.9 and 3.2), with samples M3b, W16a and W17a having the lowest average F source strengths.

The high average F-source strength of the calcrete sample indicates that this is potentially a significant source of F to groundwater upon leaching, as well as a sink of F upon precipitation as has been previously suggested (Reddy et al., 2009).

The high source strength of mafic vein sample W13 also suggests that where present, this sample may contribute significantly to groundwater F upon leaching. High leachable F from the porphyritic chlorite monzogranite (W1a) also indicates that areas of the Wailpally catchment underlain by this geology may have high groundwater F concentrations (western hill regions).

In the Maheshwaram catchment, mobility of F is relatively lower than in Wailpally, with lower average and final F-source strengths. This is consistent with the lower groundwater F concentrations measured (Wailpally range 0.5-7.6 mg/l F (Reddy D. et al., 2010), Maheshwaram range 0.44 – 1.88 mg/l F (Sreedevi et al., 2006)). Weathered samples of Maheshwaram have higher average F source strengths than their fresh equivalent, with weathered porphyritic biotite granodiorite (M2b) and weathered grey monzogranite (M7b) having the highest average F source strength of all Maheshwaram samples. Leaching of weathered material may therefore be a significant source of F in groundwater in this catchment. High final F is leached from the fresh sample M7a which has a limited occurrence in the catchment.

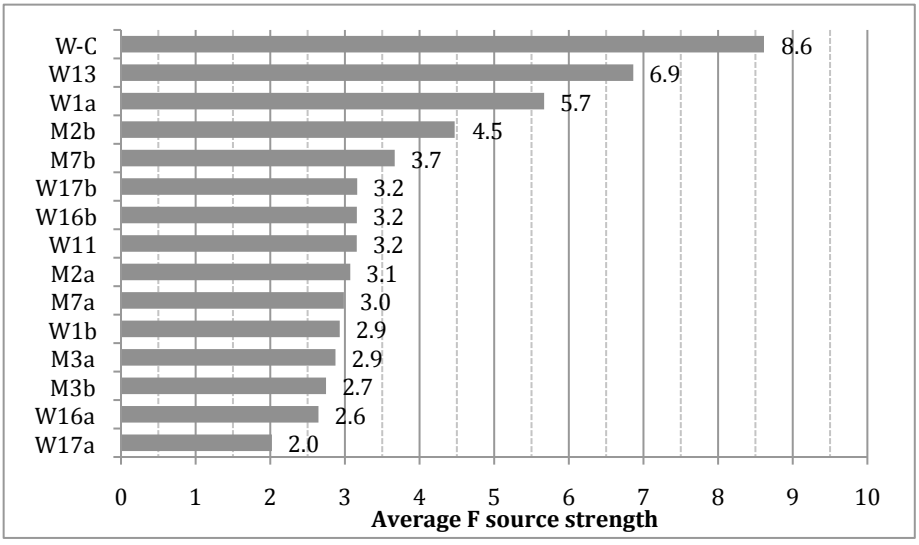

Figure 6-49 – Average F source strength for all samples in order of highest to lowest strength.

The relationship between F^- mobility (from leaching experiments) and published groundwater F concentrations are further discussed in chapter 7.

The relative F source strength can also be derived from the calculated mass balance F loss (chapter 5) which is the long term total mineralogical F loss from the fresh sample upon bedrock weathering and regolith development. The relative F source strength from mass balance is shown in table 6-11 and figure 6-50. This was not available for all samples.

The mass balance relative F source strength gives a different order of F source strength than derived from leaching results, with the porphyritic biotite granodiorite sample (M2a) as the largest F source, and the pink monzogranite (M3a) and porphyritic chlorite monzogranite (W1a) following. Relatively little F is leached from samples M2a and M3a compared to W1a, giving them a low F source strength from leaching experiments. The low relative source strength of M3a from leaching results compared to that from mass balance results may be due to unevenly distributed fluorite within the sample. The higher relative source strength of M2a calculated by mass balance than by leaching is due to the samples high WRF value compared to its low readily leachable F.

Table 6-11 – Order of Mass balance F loss and derived relative source strength (10=highest)

Sample	Name	Mass balance F loss (ppm)	Relative Source Strength
M2a	Porphyritic biotite granodiorite - MW	732	10
M3a	Pink Monzogranite - MW	642	8.8
W1a	Porphyritic chlorite monzogranite - WP	614	8.4
M4a	Amphibole monzogranite - MW	505	6.9
W16a	Biotite granodiorite - WP	265	3.6
W14a	Granodiorite - WP	75	1.0
M7a	Grey monzogranite - MW	8	0.1

In all experiments, apart from the fine size experiment (M2b – fine), fluorite saturation is not a limiting factor on solution fluoride concentrations. Where fluorite saturation is reached in the fine size fraction experiment using sample M2b, this is followed by a decrease in $[F^-]$ and $[Ca^{2+}]$ with fluorite likely to be precipitating out of solution.

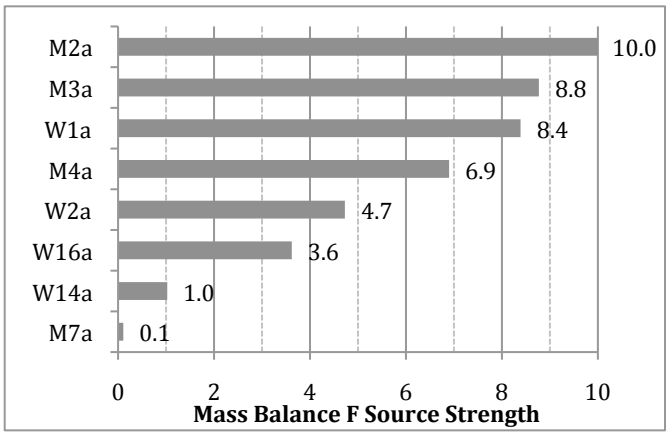

Figure 6-50 - Mass Balance F Source Strength

Sample agitation due to the method of mixing (rollers) may increase the physical weathering of the sample, increasing the concentrations of elements leached into solution. The difference between the UCL and NHM Wailpally profile experiment results indicate that sample attrition and physical breakdown do play a large role in the $[F^-]$ in leached solution in these experiments.

Where the $[F^-]$ increases with time in the fresh rock leaching experiments, this may indicate the importance of groundwater residence times on F^- concentrations, as longer water-rock interaction times are seen to result in higher leached $[F^-]$. In weathered rock experiments, F^- is released to solution quickly (within the first couple of hours), remaining relatively stable as the experiment progresses. The interaction time of groundwater with weathered rock samples is therefore less of a controlling factor on the concentration of F leached into solution.

Profile Batch Leaching

The Maheshwaram profile showed higher $[F^-]$ leached from saprolite samples than from the fresh rock sample (M2a), but with no clear correlation between leached $[F^-]$ and sample depth or WRF content. The highest F leached was from fracture fill material at 6m depth. The weathering of the fresh rock sample appears to result in the re-distribution of F to more 'available' locations within the weathered rock, which may then later be flushed by recharging waters. Models of F release to groundwater based on this profile are further developed in Chapter 7.

The Wailpally profile however shows a higher leachable [F^-] (figure 6-43) from the fresh rock sample (amphibole granodiorite, W11a) than from the weathered profile samples, although the sample at 4m depth has a final [F^-] leached that is similar to the fresh rock sample. F is most mobile from the fresh rock, consistent with the possibility that the fractured bedrock is the dominant source of F in groundwater, with possible contributions from water infiltrating through amphibole rich layers within the saprolite (such as that at 4m depth). Models of F mobilisation based on this profile are developed in chapter 7.

Chapter 7. Summary and Discussion: Conceptual Models of F Release to Groundwater

7.1 Introduction

The mineralogical mass balances determined for the principal lithologies of the two catchments (chapters 4 and 5) together with the experimental observations of F leaching to water (chapter 6) can be considered along with the measured groundwater F^- concentrations in both catchments, as a basis for the development of conceptual models of F release to groundwater, as presented below.

7.2 Groundwater F Relationships in Maheshwaram

Spatial and Temporal (Seasonal) Trends

Groundwater F data available for the Maheshwaram Catchment from 2005, pre and post monsoon (Atal, 2008), January 2006 (post-monsoon) and March 2006 (pre-monsoon) (Sreedevi et al., 2006), and from before and after the 2007-2008 monsoon (Purushotham et al., 2010) are reproduced in figure 7-1, table 7-1 and table 7-2 (with additional groundwater chemistry also given). Groundwater F concentrations over the period 2000-2004 available from Atal (2008) are illustrated in figure 7-2. Available groundwater F data are paired with sample locations in table 7-1.

Figure 7-1 – Groundwater F measurements for a) March 2006 (pre-monsoon) and b) January 2006 (post-monsoon) from Sreedevi, (2006). Blue dots indicate groundwater F values 0 - 1.5 mg/l and red dots 1.6 - 4.5 mg/l. Sample locations and geology also shown (Sreedevi et al., 2006).

Table 7-1 – Groundwater F values near Maheshwaram sample locations. A values from Atal (2008) S values from Sreedevi et al., (2006), P values from Purushotham et al., (2010),

Sample Location	Groundwater F values (mg/l F)		
	2005 (A)		
	Pre-monsoon	Post-monsoon	
M2	2.0	2.1	
M3	1.2	1.4	
M4	1.6	1.7	
M6	1.2	1.4	
M7			

Only one set of pre and post monsoon values were available for sample location M7, which is very near to sample location M3. The porphyritic epidote chlorite granodiorite sample at location M6 is not thought to be the dominant lithology in this area (a predominantly biotite granite area), and the nearest groundwater [F^-] data available, at a distance of approximately 120 m, may not correspond with sample M6.

Groundwater in the vicinity of sample location M2 (porphyritic biotite granodiorite) has the highest F^- concentrations (1.5-2.1 mg/l F, average 1.9 mg/l F), and near location M3 (pink monzogranite) the lowest F^- concentrations (0.9-1.4 mg/l F, average 1.1 mg/l F) (table 7-1).

For the period 2000 to 2004, [F^-] in groundwater fluctuates with time (figure 7-2). Groundwater [F^-] near M4 (labelled M4-1) and M2 has particularly large fluctuations (0.5 to 4.5 mg/l). Overall higher groundwater [F^-] values are observed in M4-1, M2 and M4-2, and lower values in "M7-M3".

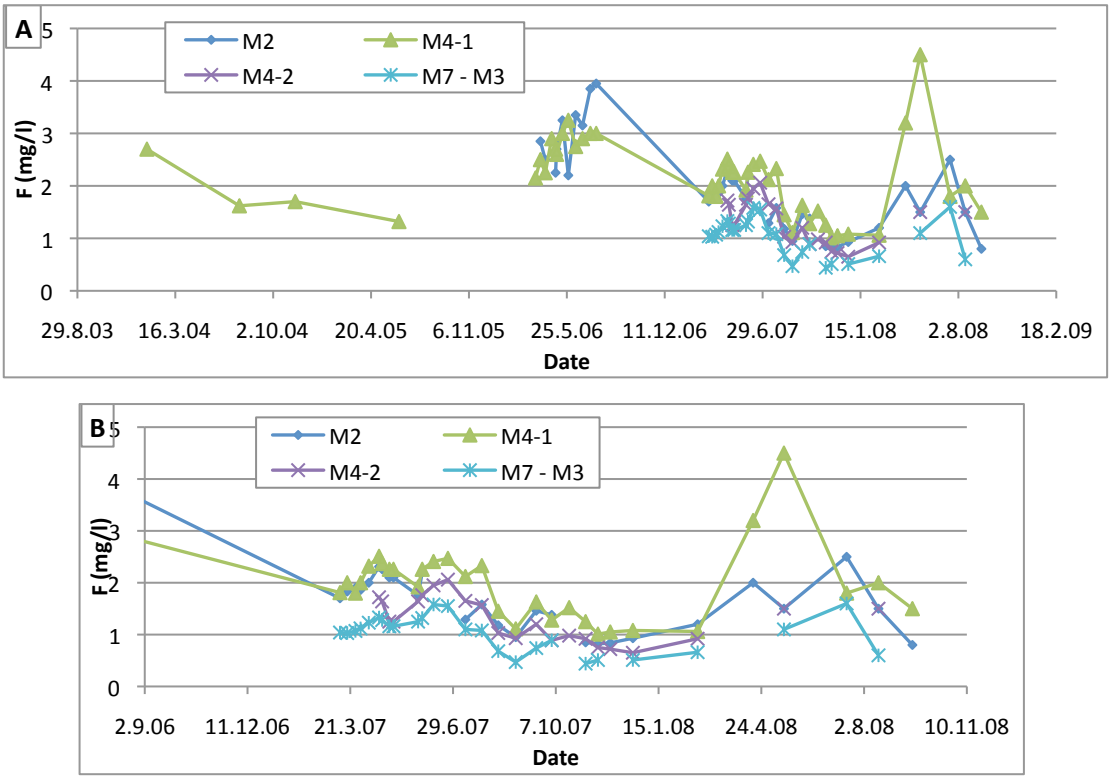

Figure 7-2 – Groundwater F measured over time from near the Maheshwaram sample locations (Atal, 2008). One groundwater sample is used to represent locations M3 and M7 due to their close proximity (shown as M7-M3). Figure B shows only the more recent section (2002-2004) of data presented in figure A.

Whole Rock Fluorine and Groundwater F^-

Groundwater F^- concentrations and whole rock fluorine (WRF) values at sample locations are shown in figure 7-3 and figure 7-4. Locations with a higher fresh rock WRF content have higher groundwater F concentrations. A similar trend is seen in weathered rock WRF values and local groundwater F^- concentrations pre-monsoon, although this trend is less apparent with post-monsoon F^- concentrations (figure 7-4).

Groundwater F^- concentrations vary with time and spatially within the areas that these samples represent. For example, in the biotite granite area (M2), groundwater [F^-] values range from 0.4 to 4.3 ppm F (figure 7-1). Spatial variations might be due to the inter-dispersed epidote chlorite granodiorite (M6a) also found in this area, local variations in mineralogy within the biotite granite or differing groundwater chemistry (see below). Temporal variations may be related to the significance of [F^-] release from the regolith following monsoon recharge.

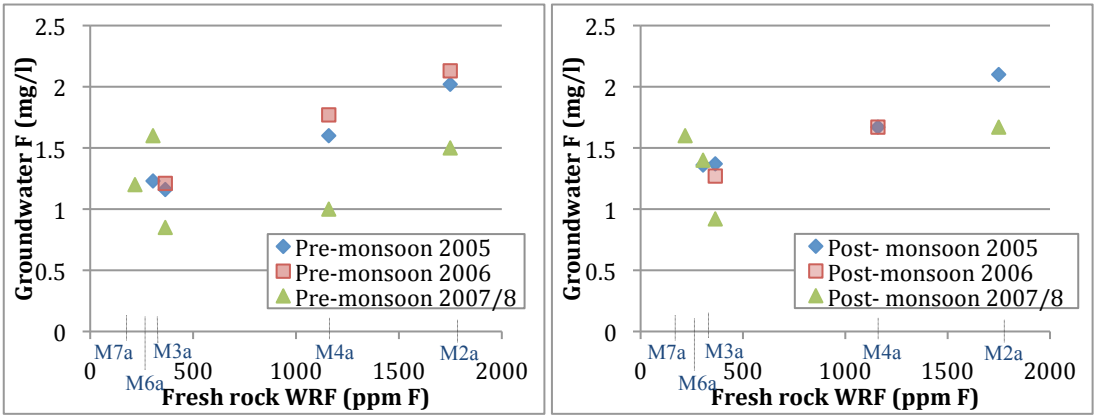

Figure 7-3 – Maheshwaram Fresh rock samples Whole Rock Fluorine (WRF) content and groundwater F concentration at locations where samples were taken. Sample names given on the x-axis. Pre and Post monsoon F values are given. F values from: 2005 values Atal (2008), 2006 values Sreedevi et al. (2006), 2007/8 values Purushotham et al. (2010).

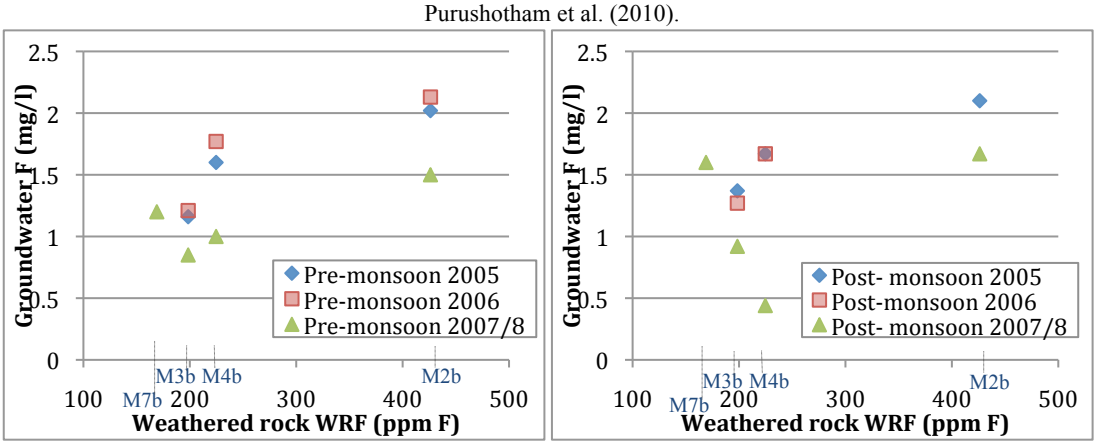

Figure 7-4 – Maheshwaram Weathered rock samples Whole Rock Fluorine (WRF) content and groundwater F concentration at locations where samples were taken. Sample names given on the x-axis. Pre and Post monsoon F values are given. F values from: 2005 values Atal (2008), 2006 values Sreedevi et al. (2006), 2007/8 values Purushotham et al. (2010).

Groundwater F^- and Weathering Release of F (from mass balance)

Mass balance calculations of F loss upon weathering and regolith development are plotted against groundwater [F^-] in figure 7-5. There is a weak trend of higher groundwater [F^-] in locations of higher calculated F loss, although this is not seen in all samples and not in all groundwater sets. F loss in sample M3 (pink monzogranite) may be anomalous because the total F calculated for this sample from mass balance is higher than chemically measured WRF concentrations (using the method by Ingram, 1970). The presence of fluorite within the M3 sample dominated the mineralogical mass balance and may not be representative at a larger volume scale.

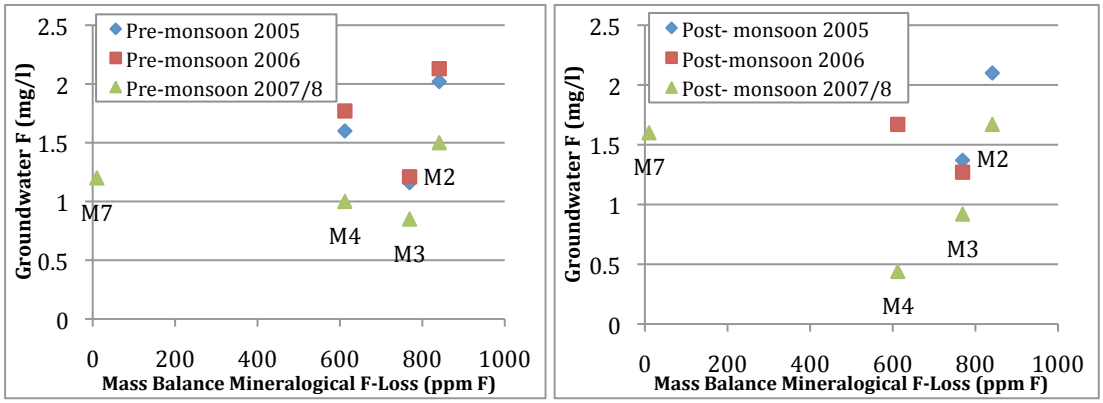

Figure 7-5 – Mass balance calculated F loss and groundwater F concentration at locations where samples were taken (Maheshwaram). Pre and Post monsoon F values are given. F values from: 2005 values Atal (2008), 2006 values Sreedevi et al. (2006), 2007/8 values Purushotham et al. (2010).

Groundwater Chemistry

Groundwater types, according to Atal's (2008) map of hydrochemistry (figure 7-6), give sample locations M3 and M7 in the zone of Ca-HCO_3 type waters, and M4, M6 and M2 in the zone of Na-HCO_3 waters (M2 and M6 are on the border), as also indicated by the pre and post monsoon groundwater chemistries in table 7-3. On a regional scale the occurrence of high F groundwaters is usually associated with Na-HCO_3 type groundwaters with high pH (Amini et al., 2008). Maheshwaram groundwaters at the sample locations are mostly neutral to alkaline pH, with approximately half of the catchment as Ca-HCO_3 and half as Na-HCO_3 water. A map of the groundwater types, groundwater F values from 2006 (Sreedevi et al., 2006) and illustrated whole rock fluorine values is given in figure 7-6. Using groundwater F values from 2006, all values above 2mg/l are located in the biotite granite area within the Na-HCO_3 zone and low groundwater F values are measured in the biotite granite

area within the Ca-HCO_3 zone (e.g. 0.5 and 0.7 ppm F - the lowest values measured in the catchment). In the intermediate and leucogranite areas slightly higher groundwater [F^-] values are measured in the Na-HCO_3 area compared to the Ca-HCO_3 area, with concentration ranging from 1 to 1.8 mg/l.

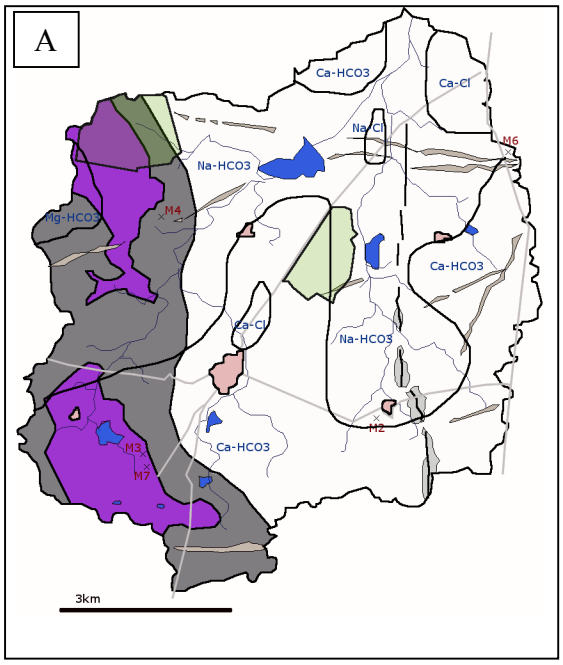

Figure 7-6 – A) Water chemistry types in the Maheshwaram catchment according to Atal (2008) B) Water chemistry types with groundwater F values from March 2006 (Sreedevi et al., 2006) and geological WRF content illustrated.

Groundwater saturation indices calculated by Atal (2008) show both pre- and post-monsoon groundwater samples to be saturated with respect to calcite and dolomite, and under-saturated with respect to fluorite. Fluorite is therefore not a limiting factor on F concentrations. Saturation with respect to calcite and dolomite will limit the Ca concentration by the precipitation of calcite, allowing for higher F concentrations in groundwater.

Groundwater flow in Maheshwaram is generally south to north, but the hydraulic gradient is shallow and in many areas flow is localised due to intense pumping, reducing outflow to the north and causing areas of stagnation (Marechal et al., 2006a). Where groundwater flow is localised it may be that the F^- concentration of groundwater more closely relates to the F content and mineralogy of the aquifer rock.

Groundwater F^- and Batch Leaching Results

The final [F^-] leached in batch leaching experiments (at 500 hours) is plotted against the groundwater F^- concentrations in figure 7-7. In the weathered rock leaching experiments, there is an approximately linear positive correlation between final [F^-] leached and groundwater [F^-], with high F leached from M2 where groundwater F^- concentrations are high, and low F leached from M3 where groundwater F^- is lower.

In the fresh rock experiments, this correlation is not apparent, with fresh rock sample M2 having low leached [F^-] compared to groundwater [F^-].

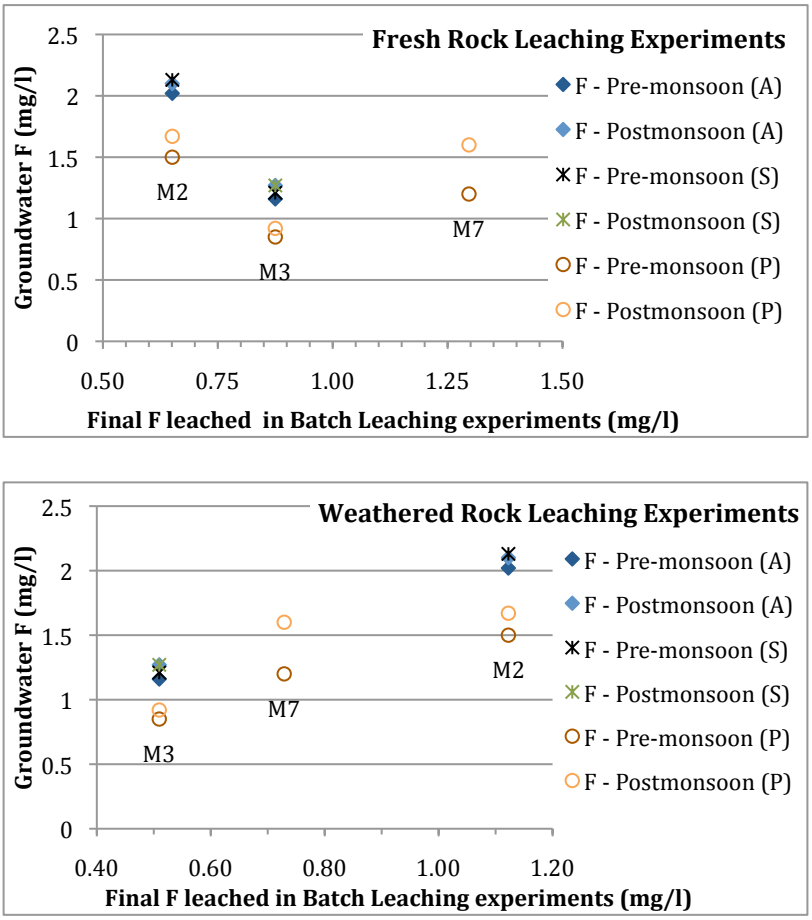

Figure 7-7 – Final [F^-] in batch leaching experiments (at ~500 hours) from Maheshwaram samples with published groundwater F data from the same location. P=values measured in 2007-2008 by Purushotham et al. (2010), S=values measured in 2005 (pre-monsoon) and 2006 (post-monsoon) by Sreedevi et al. (2006), A=values measured in 2005 by Atal (2008).

Table 7-2 - Groundwater chemistry at Maheshwaram sample sites (mg/l). Latitude and longitude in decimal degrees. F data from 2007-2008 from Purushotham et al. (2010).

Table 7-3- Groundwater chemistry at Maheshwaram sample sites (mg/l). F data from 2005 pre and post monsoon from Atal (2008).

Groundwater Chemistry Pre-Monsoon 2005															
sample site	**T(°C)**	**pH**	**EC**	**HCO_3**	**F**	**Cl**	**NO_3**	**PO_4**	**SO_4**	**Ca**	**Mg**	**Na**	**K**	**Balance**	**Water type**
M2	27.1	7.12	943	415.56	2.0	52.53	42.73	<0.5	29.98	88.43	49.53	46.94	2.2	4%	Ca-HCO_3
M3	28.2	7.17	843	407.99	1.2	48.85	21.39	<0.5	23.63	92.31	25.61	61.3	0.51	2%	Ca-HCO_3
M4	27.4	7.16	1611	586.62	1.6	197.5	21.68	<0.5	65.27	81.66	44.5	151.09	1.57	-8%	Na-HCO_3
M6	28.6	6.94	887	398.79	1.2	34.3	81.14	<0.5	21.11	91.18	38.2	34.66	2.3	0%	Na-HCO_3
Groundwater Chemistry Post-Monsoon 2005															
sample site	**T(°C)**	**pH**	**EC**	**HCO_3**	**F**	**Cl**	**NO_3**	**PO_4**	**SO_4**	**Ca**	**Mg**	**Na**	**K**	**Balance**	**Water type**
M2	26.5	6.99	1088	512.07	2.1	126.84	109.76	<0.5	58.32	118.99	75.04	69.53	2.07	0%	Na-HCO_3
M3	276	7.02	756	420.02	1.3	40.64	17.73	<0.5	21.56	82.73	22.89	55.6	0.77	-2%	Ca-HCO_3
M4	26.4	6.99	1840	642.63	1.7	232.62	46.1	<0.5	82.94	99.72	56.78	240.7	1.52	1%	Na-HCO_3
M6	27.6	6.77	905	435.16	1.4	29.75	81.2	<0.5	19.76	93.25	42.67	38.2	2.03	1%	Ca-HCO_3

7.3 Groundwater F Relationships in Wailpally

Spatial and Temporal (Seasonal) Trends

Reddy D. et al. (2010) measured groundwater [F^-] at between 1.0 and 5.8 mg/l in the Wailpally catchment, with groundwaters saturated with respect to calcite and under-saturated with respect to fluorite. A similar study by Reddy A. et al. (2010) measured groundwater F values of between 0.5 and 7.6 mg/l with an average of 2.9 mg/l in the hilly region, 3.3 mg/l in the plains and 4.6 mg/l in the discharge area, and the highest groundwater F^- concentration measured near Wailpally village.

Groundwater F^- data for the Wailpally catchment are summarised in table 7-4 (from Reddy A. et al., 2010; Nalgonda Website, 2006; Narayana et al., 2003), table 7-5 (Reddy A. et al., 2010) and figure 7-8 (Reddy D. et al., 2010). Figure 7-8 shows pre-monsoon groundwater [F^-] (2004), with groundwater near sites W14 and W16 having medium (1.6-4.0 mg/l) to high (4.1-8.0 mg/l) [F^-]. Groundwater F^- values near Antampet (near sample sites W1 and W2) have been measured at 3.7 mg/l (Narayana et al., 2003) and at 4.4 mg/l and 5.6 mg/l (Nalgonda Website, 2006) (table 7-4).

Figure 7-8 – Groundwater F values, pre-monsoon 2004-2005 from Reddy D.et al., (2010). Light blue dots indicate groundwater F values 0 - 1.5 mg/l, dark red dots 1.6 - 4.0 mg/l and bright red dots 4.1 – 8.0 mg/l. Wailpally map also shows geology, water-table contours and sample locations (modified from Dhakate et al., 2008; Reddy D. et al., 2010)

The data indicate high groundwater [F^-] near W14 (granodiorite) and W16 (biotite granodiorite) (Lachammagudem) and near W1 (porphyritic chlorite monzogranite) and W2 (porphyritic epidote granodiorite) (Anthampet). Groundwater [F^-] near site W11 (amphibole granodiorite, Kompally) and W17 (Pegmatitc epidote quartz syenite, Kurma Kothaguda) are lower, although in all cases still above the WHO guideline value of 1.5 mg/l (table 7-4).

Table 7-4 – Concentration of F^- in groundwater near Wailpally sample sites. Where there are multiple measurements near the sample site, all values are given. All groundwater F data is from Reddy A. et al. (2010), apart from *values from Nalgonda Website (updated 2006, accessed 2010), and $^+$values from Narayana et al. (2003), both of which have no season indicated.

Sample	Location	Groundwater F−		
		Pre-monsoon	Post -monsoon	Average
W14	Dharma Tanda	3.9		3.9
W14/W16	Lachammagudem	4.2 4.2	3.8 5.1	4.3
W17	Kurma Kothaguda	2.4	3.0 3.0	2.8
W11	Kompally	1.7 3.6*		2.6
W1 and W2	Anthampet	4.4* 5.6* 3.7$^+$		4.6

Whole Rock Fluorine and Groundwater F^-

Figure 7-9 shows sample WRF values and groundwater [F^-] measured near sample sites. High groundwater concentrations near W1 (porphyritic chlorite monzogranite) correspond to high whole rock fluorine (WRF) values at this location. Samples W16a and W11a have similar WRF values (824-930 ppm F) yet their corresponding groundwater [F^-] measurements are different. Fresh rock WRF content shows a slight positive correlation with groundwater F concentration (figure 7-9). However, this is reversed for weathered sample WRF values with groundwater F (figure 7-9).

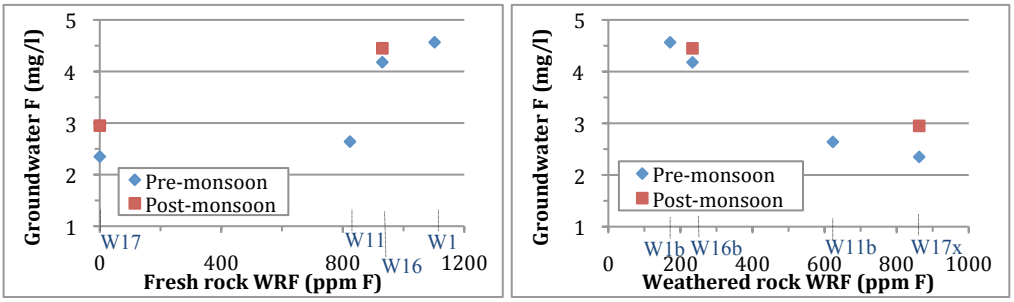

Figure 7-9 – Wailpally Whole Rock Fluorine (WRF) content and groundwater F concentration at locations where samples were taken. Sample names given on the x-axis. Pre and Post monsoon F values are given. F values from Reddy, A. et al. (2010).

Groundwater F^- and Weathering Release of F (from mass balance)

As groundwater data are limited for the locations for which mass balance F loss was calculated (locations W1, W2, W14 and W16), it is difficult to assess the correlation between F lost to groundwater upon weathering and the groundwater F^- concentration in particular areas. Overall, high F loss (752 ppm F) is calculated from the porphyritic chlorite monzogranite (W1), from Antampet, which has a high groundwater F^- concentration of 4.8 mg/l (average of data from: Narayana et al., 2003; Nalgonda Website, 2006). Low mass balance F loss (92 ppm F) is calculated for the granodiorite sample (W14), in the vicinity of which groundwater F concentrations range from 3.8 to 5.9 mg/l.

Groundwater Chemistry, Recharge and Flow

Groundwater chemistry in Wailpally is generally alkaline with an average pH of 7.7 (range 6.6-8.9), and evolves from Na-Ca-HCO_3 and Ca-Na-HCO_3 in the west to Na-HCO_3 and Na-HCO_3-Cl in the east (Reddy D. et al., 2010). High F^- groundwater is usually associated with Na-HCO_3 type groundwaters with high pH (Amini et al., 2008), although previous research by Reddy D. et al. (2010) found no correlation between groundwater type and F^- concentration in Wailpally.

The main region of groundwater recharge is in the west of the catchment, with infiltration likely to be primarily through preferred pathways of fissures and fractures. Recharge through these pathways is estimated at 16% of annual rainfall in the west and 5% in the eastern plains (average annual rainfall is 632mm/yr) (Reddy et al., 2009). Matrix recharge (piston flow) is thought to only be 1-1.5% of annual rainfall (Reddy et al., 2009). Sample W1 (porphyritic chlorite monzogranite) is representative of the lithology in the western hills of the catchment, the high WRF value of which may influence groundwater F concentrations in other areas of the catchment as the majority of rainfall recharge is in this area, with groundwater discharging in the east. The greater hydraulic gradient in Wailpally than in Maheshwaram (where several areas of stagnation are present) may lead to a less distinct correlation between aquifer bedrock fluorine content and groundwater fluorine content than seen in Maheshwaram. The principal F-bearing minerals in the catchments are also different, and so the relationship between WRF and groundwater [F^-] may be expected to differ (as also observed in leaching experiments).

Groundwater F^- and Batch Leaching Results

Figure 7-10 shows final [F^-] in batch leaching experiments with groundwater F data from the sample location. In contrast to the relationship seen at Maheshwaram, there is no clear correlation with final [F^-] leached in leaching experiments and local groundwater F^- concentrations, although high [F^-] is leached from fresh and weathered porphyritic chlorite monzogranite (W1), which corresponds to high groundwater [F^-] in this area (figure 7-10).

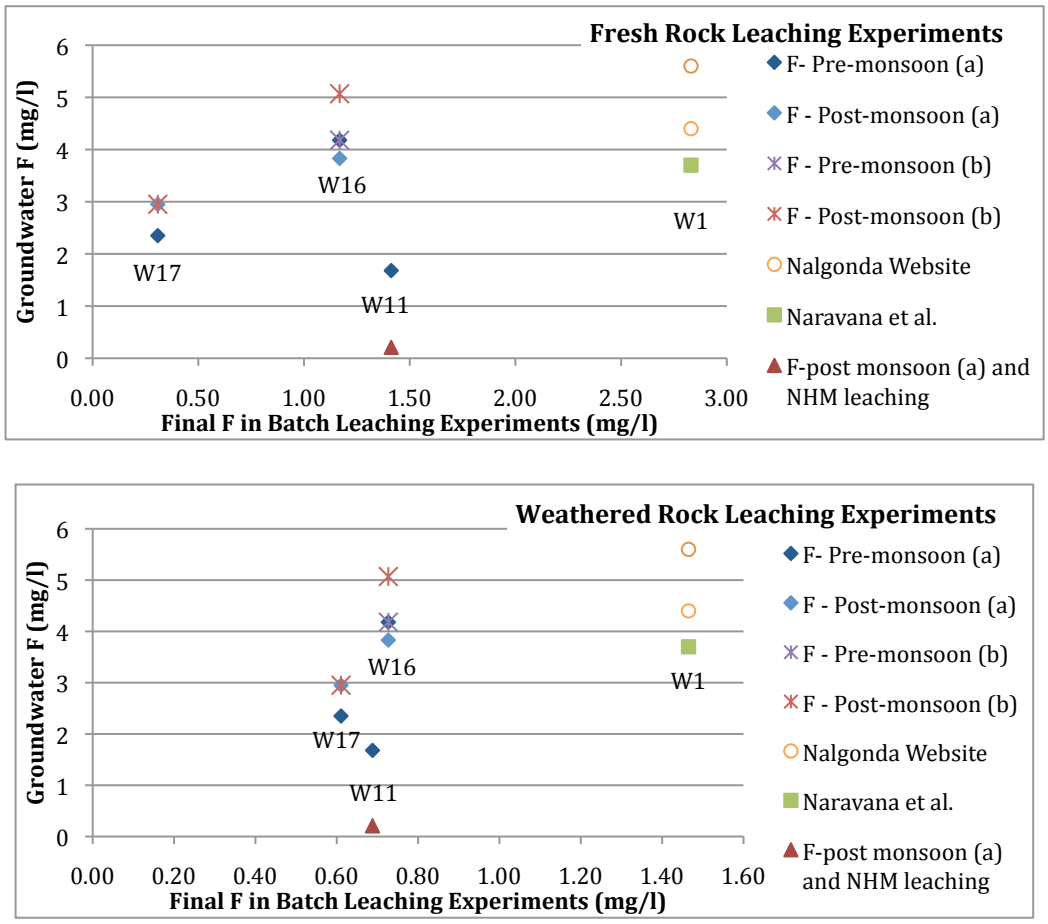

Figure 7-10 – Groundwater F near Wailpally sample sites with F leached from batch leaching experiments. Pre and Post monsoon values from Reddy A. et al. (2010). Other samples from Nalgonda Website (2006) and Narayana et al. (2003). The weathered sample at W17 (W17x) is not related to the fresh sample W17a.

Solution chemistry from batch leaching experiments differ from groundwater chemistry. In groundwater, Ca, Mg, Na and Cl are much higher than in the batch leaching solutions. F^- concentrations are also higher in groundwater than in the leached solutions (figure 7-10). In some of the leaching experiments it was apparent that the fresh rock leached F^- concentration had not reached equilibrium, and would

have likely increased if the experiment had been run for a longer period of time (e.g. in W13, W1a, W11a). Higher F^- concentrations in groundwater compared to the leaching experiments indicate that additional F is removed from the sample. This may be due to longer residence time and contact with other F-bearing minerals, and different groundwater pH conditions.

Table 7-5 – Groundwater chemistry at sites near Wailpally sample locations. Pre-monsoon samples were collected in June, and post-monsoon samples in November. All data is from Reddy A. et al., (2010). Locations shown on map in figure 7-8.

7.4 Models of F release from the bedrock

7.4.1 Catchment Fluoride Mineralogy - Summary of Research Findings

From the results of the mineralogical investigations and F mass balance calculations, and the relative F 'source strength' estimated from leaching experiments, the following observations need to be incorporated in conceptual models of F release to groundwater in the research catchments:

- *Bedrock and regolith whole rock fluorine:*

- Fresh bedrock has a higher total F content than its equivalent weathered regolith (see chapter 4, section 4.7 and chapter 5, section 5.1)
- In both catchments the highest whole rock F (WRF) content is measured in gneissic porphyritic granite (in Maheshwaram this is a biotite granodiorite, in Wailpally this is a chlorite monzogranite)
    - In Maheshwaram this covers a large proportion of the catchment area, whereas in Wailpally the high F lithology is restricted in occurrence (see chapters 4 and 5)
    - In Wailpally high WRF was also measured in mafic vein material (W13). Where present, this may be a significant source of F to groundwater.
- Low F lithologies include the grey monzogranite (M7a) in Maheshwaram and the pegmatite (W17a) in Wailpally, both of which contain few F-bearing minerals.
- In Maheshwaram there is a strong positive correlation between bedrock WRF content and groundwater F^- concentrations (figure 7-3 and figure 7-4). In Wailpally this relationship is less clear.
- In Maheshwaram there is also a positive relationship between weathered rock WRF and groundwater F^- content, however the relationship breaks down in the post-monsoon groundwater [F^-].
- In Wailpally there is a negative correlation between regolith WRF content and groundwater F^- concentrations (figure 7-9).

- F-bearing minerals present and mineral F loss on weathering:

- The principal F-bearing minerals in fresh bed-rock are apatite, biotite, amphiboles, fluorite and titanite. A summary of their occurrence and F content is given in table 7-6, and their relative contribution to total F within each sample in figure 7-11 and figure 7-12.
- The principal mineralogical contributors to groundwater [F^-] upon bedrock weathering and regolith development catchment-wide (calculated from mass balance, section 5.1.4) are:
    - Apatite and biotite in Maheshwaram
    - Amphiboles, fluorite, apatite and biotite in Wailpally
- Sources of F are present in the regolith (and also possibly in fresh bedrock samples) that are additional to those observed in optical petrology and EM analysis. These include clay minerals (measured using XRD, chapter 4, section 4.5) and may also include F sorbed to Al or Fe oxides.

- Details of profiles through the weathering rock:

- Vertical profiles through the weathered rock (section 5.2) show:
    - The fresh bedrock (deepest) to have the highest WRF content
    - The shallowest regolith samples to have the lowest WRF content, but:
        - No straightforward increase in total F content with depth through the regolith
        - Specific points at which there is a concentration of mafic minerals associated with increased WRF and [F^-] leached (batch leaching experiments).
    - The Maheshwaram profile shows:
        - Little change in whole rock chemistry with depth, apart from within fracture fill material (which has high CaO and low F content) and where mafic minerals (e.g. biotite, with high MgO and high F content) are concentrated.
        - High [F^-] leached from regolith material (especially fracture fill material) and low [F^-] leached from the fresh rock samples (section 6.5)

- The Wailpally profile shows:
  - Increased weathering in the regolith towards the surface, with depths at which mafic minerals (e.g. amphiboles) are concentrated having higher WRF content.
  - A higher [F^-] leached from the fresh rock than from the weathered regolith (section 6.5).

- The relative mobility of F from the bedrock and regolith:

- In batch leaching experiments, higher [F^-] is leached from Wailpally bedrock than from Maheshwaram bedrock, with samples W-C (calcrete), W13 (mafic vein) and W1a (porphyritic chlorite monzogranite) having the highest average F 'source strength' (figure 7-13).
- The highest Maheshwaram F average 'source strengths' are from weathered porphyritic biotite granodiorite (M2b) and weathered grey monzogranite (M7b) (both of which have low WRF content)
- Leaching experiments show that in general a higher final [F^-] is leached from fresh samples than from their weathered equivalents (see Chapter 6)
  - However, sample M2 (porphyritic biotite granodiorite) is an exception to this, with higher F leached from the weathered sample M2b
  - In addition, it is noticeable that weathered samples commonly have a higher initial (1-2 hours) [F^-] than their fresh rock equivalents
- There is no simple relationship between sample WRF content and F leached/F source strength. However:
  - Bedrock samples in Wailpally and regolith Maheshwaram samples show an approximately linear trend of increasing F leached from samples with higher WRF.
  - The percentage of total sample F leached is higher for samples with low WRF.
- In a number of leaching experiments with fresh samples, increasing water-rock interaction time results in higher leached [F^-], indicating the importance of groundwater residence time. In experiments with weathered samples however, [F^-] reaches a steady state within the duration of the experiments, indicating that long reaction times are not necessary.

- In Maheshwaram a positive correlation exists between the weathered rock samples final F source strength (from batch leaching) and groundwater F^- concentrations (figure 7-7).
- In Wailpally there is no correlation between sample's F source strength (from batch leaching) and groundwater F^- concentrations (figure 7-10).

- *Relationships between mineralogical investigations and groundwater fluorine*
  - In Maheshwaram:
    - Higher fresh rock WRF values are related to higher groundwater F^- concentrations, however this is not necessarily related to higher fresh rock leaching and more likely related to the formation of a saprolite with a high WRF content and with readily available F for leaching. The weathered rock is an important source of F for groundwater
    - Due to localised flow, effects are seen in the nearby area.
  - In Wailpally:
    - Correlations between sample WRF and groundwater F^- are not so strong. There is a slight positive correlation between fresh rock WRF and groundwater F^-, and a slight negative correlation between weathered rock WRF and groundwater F^-. The lack of clear correlations may be due to groundwater flow in Wailpally from the hills to the plains.

Table 7-6 – F-bearing minerals and the average F content (in mass %) in Maheshwaram (M) and Wailpally (W) fresh rock samples

Mineral	Occurrence	Average F content in fresh rocks (mass %)		Notes
		M	W	
Fluorite 	Rare. When present, only in small quantities (<0.2%) Pink monzogranite (M3) Porphyritic chlorite monzogranite (W1) Granodiorite (W14)	31.57	26.33	Removed upon weathering (not found in weathered samples).
Apatite 	Present in most samples. Abundance from 0.1-1.2 %.	3.16	2.75	Average F content less in weathered samples than fresh samples in M. Similar F content in all W samples.
Epidote Var 2 	Not common. Present in 5 fresh samples and 2 weathered. Abundance 0.1-0.7%	1.13	0.99	Similar composition to epidote, with higher F content.
Titanite 	Common as an alteration mineral. Present as a primary mineral only in Amphibole monzogranite (M4), Porphyritic chlorite monzogranite (W1) and Porphyritic epidote granodiorite (W2).	0.53	0.79	Average F content higher in W samples than M samples. Secondary titanite may retain F from the weathering of biotite.
Biotite 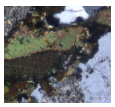	Common. Abundance ranges 0-22%	0.27	0.25	Biotite loses F upon weathering as indicated by correlation between K_2O and F content. Biotite in fresh samples have a higher F content than weathered samples. Biotite in the Amphibole monzogranite (M4a), Granodiorite (W14a) and Mafic vein material (W13) has a higher F content than other samples.
Amphiboles 	Present only in Amphibole monzogranite (M4a), amphibole granodiorite (W11a) and mafic vein material (W13). Abundance within these samples ranges 7-37%	0.24	0.20	Removed upon weathering (not found in weathered samples).
Chlorite 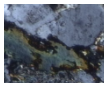	Present in most samples. Abundance 0-9%	0.03	0.02	F content low or below detection limit in all samples.
Epidote 	Present in many samples. Usually with a low abundance, however in some samples this is up to 14%	0.00	0.01	F content low or below detection limit in all samples.

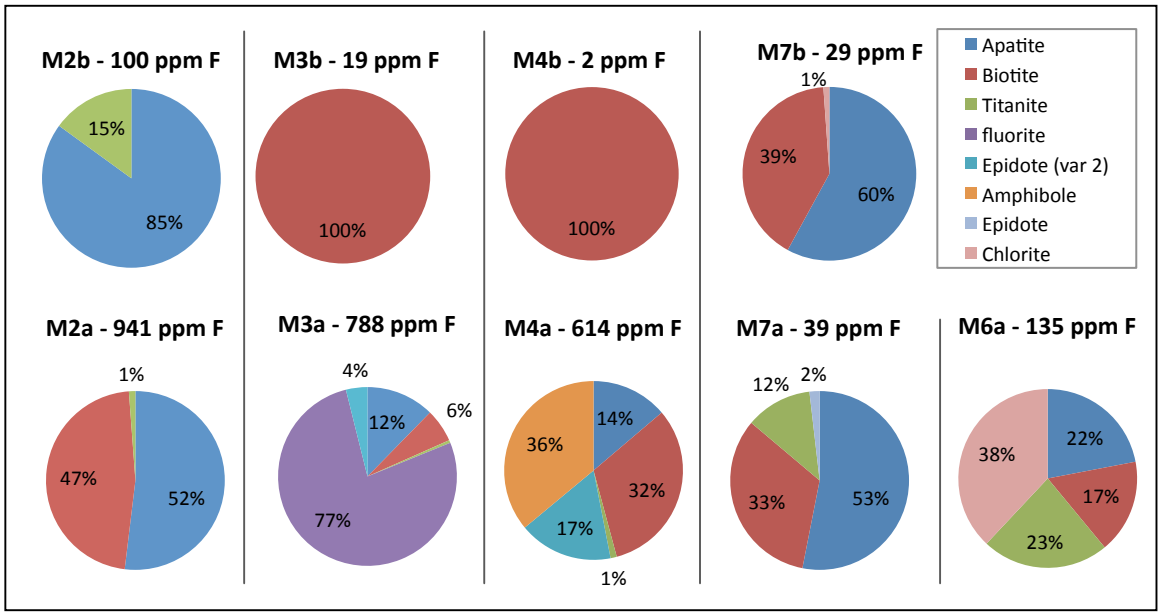

Figure 7-11 – Maheshwaram - Percentage contribution of F-bearing minerals to total rock F as calculated by mass balance.

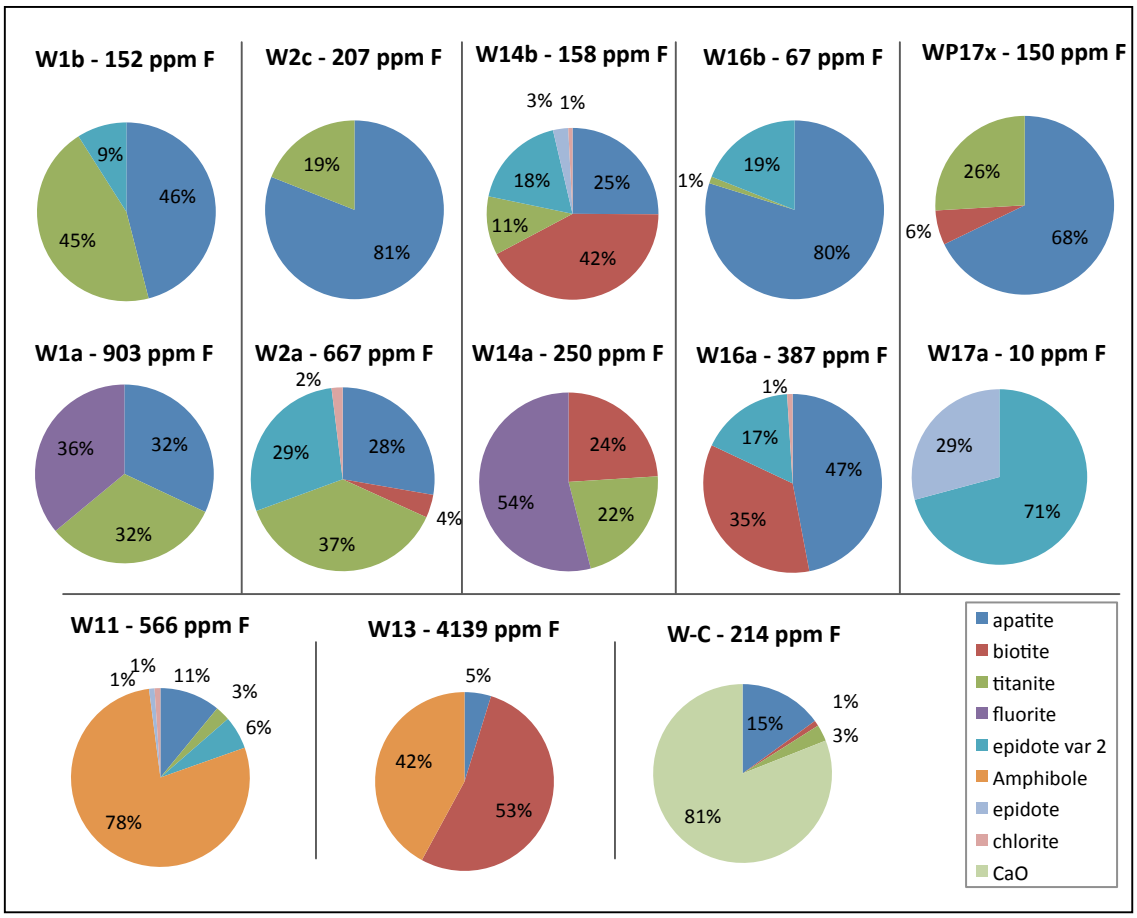

Figure 7-12 – Wailpally - Percentage contribution of F-bearing minerals to total rock F as calculated by mass balance

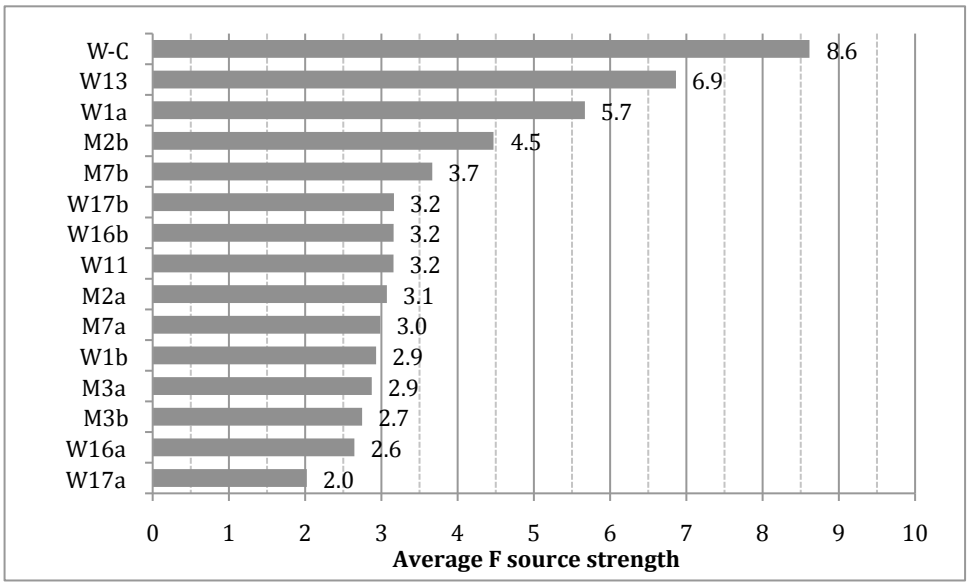

Figure 7-13 – Average relative F source strength for all samples in order of highest to lowest strength. Calculated from initial and final relative F source strengths from batch leaching experiments (chapter 6)

7.4.2 Conceptual Models of F in Groundwater at the Catchment Scale

In Maheshwaram, the gneissic porphyritic biotite granodiorite (M2a) contains the highest whole rock F content, although during leaching experiments low [F^-] is leached from this sample (mainly from biotite and apatite). Redistribution of F upon weathering (in titanite, as well as likely to clays, and sorbed to surfaces of Al and Fe minerals), with a large amount of F retained (note the high weathered sample WRF value of 426 ppm F) allows F to be more readily mobilised from the weathered regolith upon contact with water. The positive correlation between F leached from the weathered rock and groundwater F^- indicates the weathered rock to be an important influence on groundwater Fluoride. The porphyritic biotite granodiorite lithology (M2) underlies the majority of the Maheshwaram catchment (approximately 70% by area). Fluorite is not a prominent F-bearing mineral in Maheshwaram, with only sample M3a (pink monzogranite) containing small amounts of fluorite (0.2%) and with the groundwater in the catchment under-saturated with respect to fluorite. Sample M3a still has a relatively low WRF content (365 ppm F) and leaches little F on contact with water (final F concentration 0.88 mg/l). Samples M7a (leucogranite – grey monzogranite) and M6a (porphyritic epidote granodiorite) have few F-bearing minerals, with low F content, however F located in M7a is readily removed upon contact with water (mineralogical sources of F in M7a are apatite, biotite, titanite, epidote and chlorite, with clays). High F in M4a (amphibole monzogranite) is due to the presence of amphiboles and biotite.

In Maheshwaram, groundwater fluoride concentrations are higher where sample WRF is high. There is, however, variation in F content within areas of the same lithology, likely to be due to local variations in bedrock geology (either different lithologies present within the same mapped geological area, e.g. M2 and M6 are both within the 'biotite granite' area, or variation in sample mineralogy within one lithology), and variations in groundwater chemistry (with higher [F^-] associated with Na-HCO_3 waters, and low groundwater [F^-] associated with Ca-HCO_3 waters).

In Maheshwaram groundwater flow in several areas is locally compartmentalised, with a low hydraulic gradient, reduced outflow from the catchment and continuity

between groundwater from different areas minimised due to intense pumping (Marechal et al., 2006a). Where flow is more localised the high [F^-] of groundwater more closely relates to the F content and mineralogy of the aquifer rock. This is reflected in the relationship between sample WRF and groundwater [F^-] in Maheshwaram samples. When there were lower levels of groundwater abstraction, regional groundwater flow would have been more pronounced and regional hydraulic gradients would have been steeper. Under these conditions, a weaker spatial association between groundwater [F^-] and bedrock WRF might be expected.

Figure 7-14 is an illustration of the possible sources, sinks and pathways of groundwater F^- in the Maheshwaram catchment.

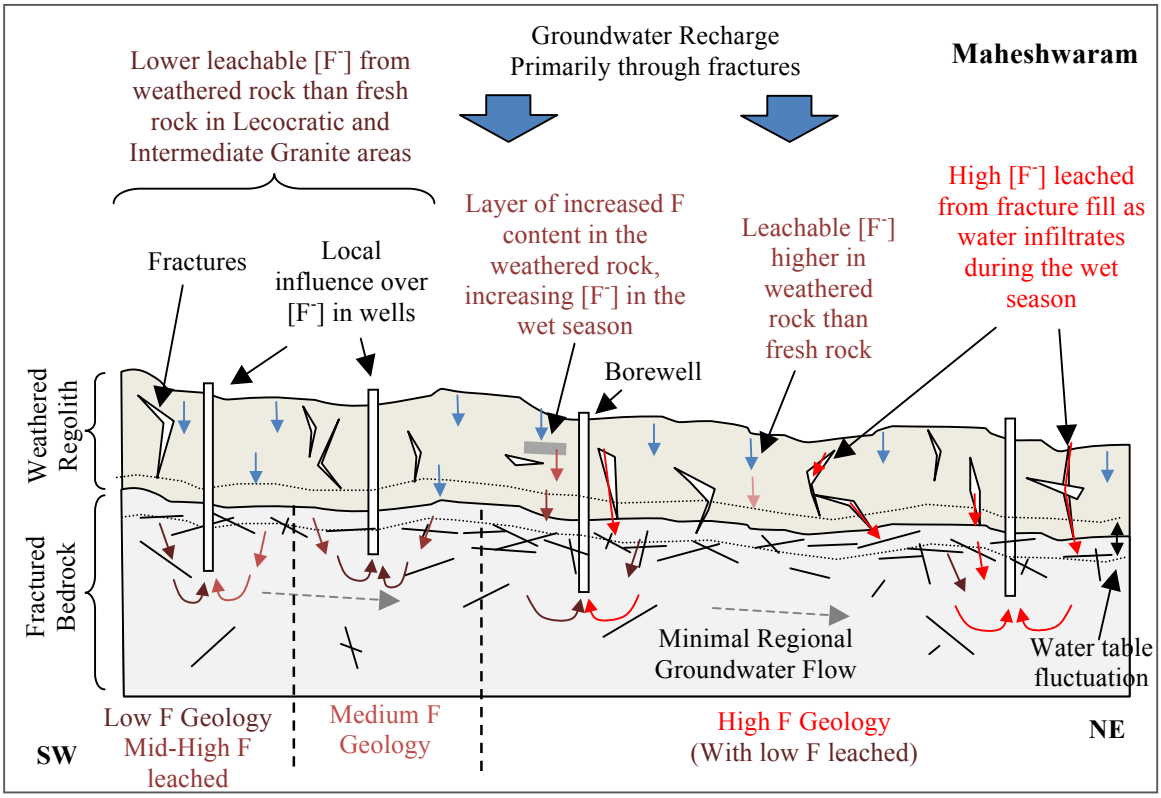

Figure 7-14 – Schematic cross section of the Maheshwaram catchment (not to scale) with potential sources, sinks and pathways of F. Low F geology in the SW of this diagram refers to the Leucogranite area (pink monzogranite M3a 365 ppm F, grey monzogranite, M7a 218 ppm F), Medium F geology refers to the Intermediate granite area (amphibole monzogranite M4a 1159 ppm F) and High F geology in the NE of this diagram refers to biotite granite (porphyritic biotite granodiorite sample M2a 1742 ppm F).

In the Wailpally catchment, very high WRF content is measured in mafic vein material (W13, 5536 ppm F) which is commonly present throughout the catchment. This mafic vein material is potentially a major source of F to groundwater, with F

readily leached in batch leaching experiments likely to be mainly from biotite and amphiboles (reaching 3.72 mg/l after 500 hours).

The highest fresh bedrock WRF content in Wailpally is in the porphyritic chlorite monzogranite (sample W1a, primary F-bearing minerals fluorite 36%, apatite 32% and titanite 32% from mass balance) which represents a small part of the catchment in the western hill regions. F leached from this sample is also high (reaching 2.89 mg/l after 500 hours and rising thereafter), with F loss mainly from fluorite (also apatite and titanite). As groundwater recharge is principally in the west of the catchment by topographic control, and the groundwater is under-saturated with respect to fluorite throughout the catchment, the porphyritic monzogranite appears to have a significant impact on [F^-] throughout the catchment. The other major fresh rock samples in Wailpally also have high WRF values (930 ppm F in W16a, 824 ppm F in W11a) apart from the pegmatites which contain few F-bearing minerals. Overall the primary F-bearing minerals in the catchment are apatite, titanite, fluorite and amphiboles, with biotite and epidote var 2 also important in some samples. Fresh bedrock contains more F than its weathered equivalents. Batch leaching experiments also show higher [F^-] leached from fresh rocks than from their weathered equivalents. Layers of concentration of F-bearing minerals in the regolith may be important sources of F to recharging water during the wet season.

Calcrete, widely present throughout the catchment, incorporates F into its structure and may therefore be a sink for F on initial formation. The formation of calcrete will moderate [Ca^{2+}] in groundwater and allow an increase in [F^-] where the groundwater is under-saturated with respect to fluorite. However, on contact with water F is readily lost from calcretes (batch leaching final [F^-] 2.69 mg/l after 500 hours). Calcrete may therefore be a sink of F during its precipitation in the dry season, and a source of F upon leaching in the wet season.

In Wailpally the correlation between fresh bedrock samples and groundwater F^- concentrations is less clear, with a negative correlation seen between weathered regolith samples and groundwater F^-. This may be due to the more pronounced hydraulic gradient and more extensive regional groundwater flow than in the Maheshwaram catchment. Local variations may result from calcrete precipitation or leaching, or from the presence of mafic veins with high F content. This is the

conceptual basis for much variation in groundwater F through the catchment. Figure 7-15 is an illustration of the possible sources, sinks and pathways of groundwater F in the Wailpally catchment.

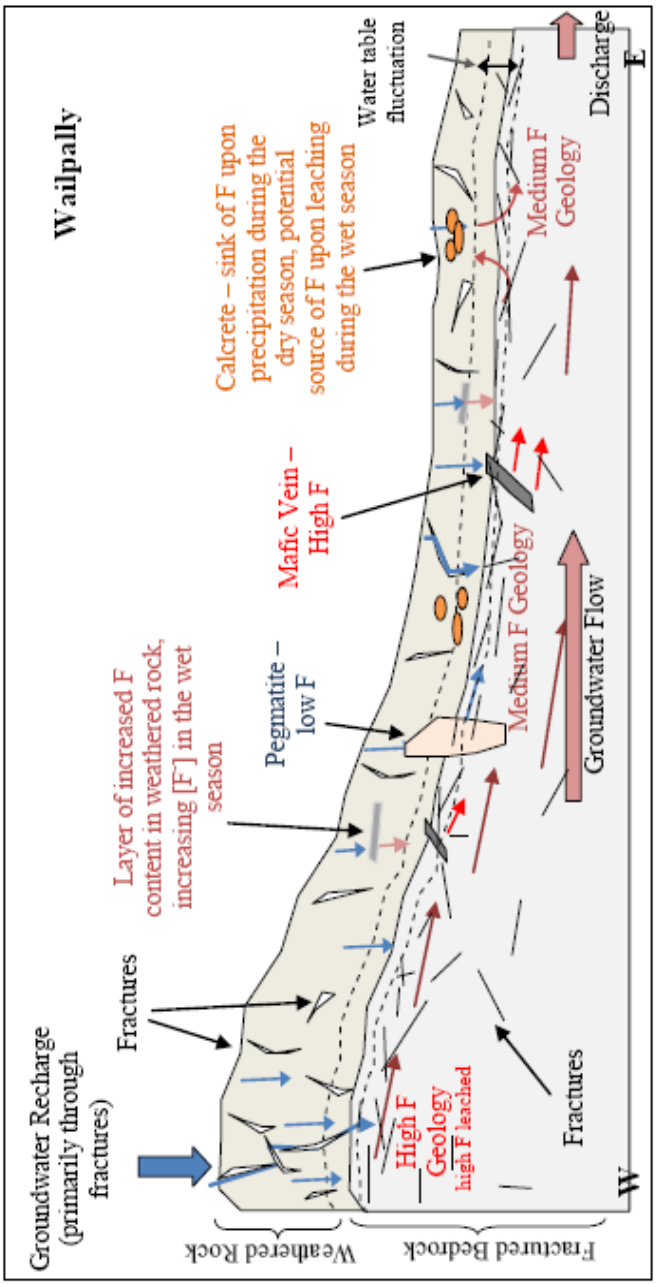

Figure 7-15 – Schematic cross section of the Wailpally catchment with potential sources, sinks and pathways of F. High F geology in the west refers to the porphyritic granites with high F content and high F leached in batch leaching experiments (e.g. W1a, porphyritic chlorite monzogranite, 1102 ppm F). Medium F geology refers to biotite granodiorites (W16a, 930 ppm F), amphibole granodiorites (W11a, 824 ppm F) and granodiorites (W14a). Diagram not to scale.

7.4.3 Conceptual Models of F in Groundwater at a Local Scale

Results from the profile samples and leaching experiments suggest two modes of weathering and F release to groundwater (figure 7-16 and figure 7-17).

In the Maheshwaram porphyritic biotite granodiorite (M2) profile, the weathered saprolite has a lower WRF content than the fresh rock, but a higher leachable F concentration (as observed in leaching experiments). The weathering profile contains many preserved fractures, with fill material containing readily water soluble F (high F source strength), although with a moderate WRF content (423 ppm F). Layers within the profile with a higher proportion of mafic F-bearing minerals are also present. Leaching experiments from the fresh rock sample result in the lowest leached [F^-], whereas the fracture fill material and saprolite with a high mafic proportion result in the highest leached [F^-]. The higher availability of F for release from the saprolite would result in increased F^- concentration in infiltrating rain waters, with increasing F also leached from layers with a higher content of F-bearing minerals (figure 7-16). As fractures are thought to be the main route of recharge to the underlying aquifer from monsoon rainfall, recharging water passing through fractures with high leachable F would become enriched in F^- and provide a source of F^- to groundwater. An increase in infiltrating water due to extensive irrigation may also result in a similar increase in groundwater fluoride concentrations. Figure 7-16 shows a model of weathering and F distribution in this profile (model A), illustrating the potential sources and pathways of F to groundwater, and the resultant seasonal groundwater F^- patterns. The water table was much shallower ~30 years ago, before extensive groundwater abstraction began in the catchment, and was within the weathered regolith. This would have resulted in a much less pronounced seasonal variation of [F^-] and a different overall groundwater [F^-]. However, no groundwater [F^-] data are available for this period for comparison.

In the Wailpally profile WRF content and final [F^-] leached is highest in the fresh rock (amphibole granodiorite) and lowest in the shallow samples (at 2 and 3m depth). The profile contains a layer with high mafic content, high WRF and high leached F. The profile contains few preserved fissures and no calcrete was observed. Figure 7-17 shows a model of weathering and F distribution in this profile (model B), with F that

is readily lost from the bedrock removed upon weathering, and the F remaining in the saprolite located in minerals where it is less mobile. The mode of release of F to groundwater is therefore primarily from F-bearing minerals in the fractured fresh bedrock, with a smaller amount of additional F mobilised from the regolith. Figure 7-17 illustrates potential sources and pathways of F to groundwater, and the resultant patterns of transience in groundwater [F^-]. A shallower water table in the past (~30 years ago) may have resulted in a lower overall groundwater [F^-] due to the relatively lower F^- leached from the weathered saprolite. However, no groundwater F data for this past period are available for comparison.

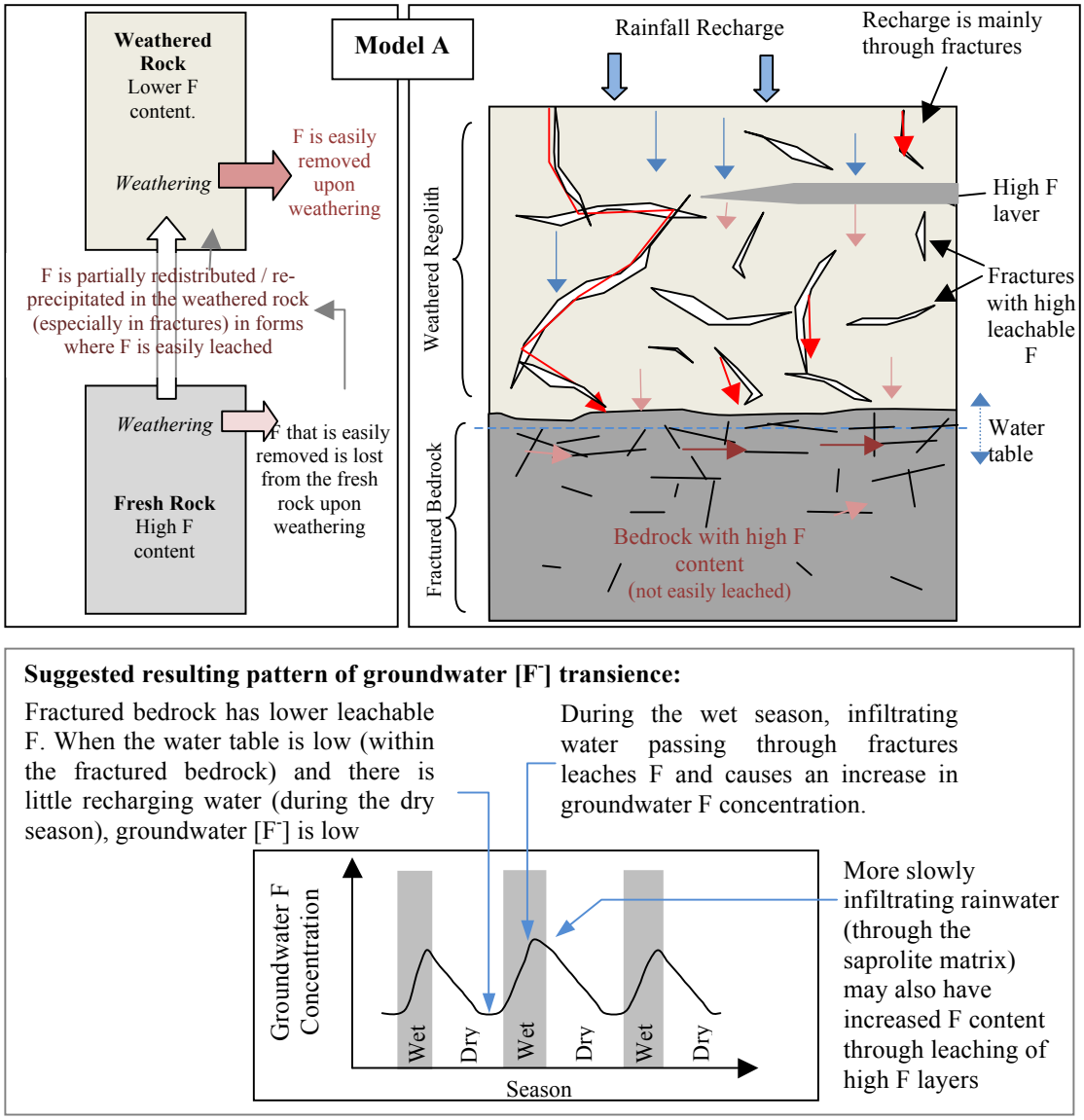

Figure 7-16 – Model A of weathering and F distribution, and diagram of potential sources and pathways of F based on Model A. Based on profile at M2 - porphyritic biotite granodiorite in Maheshwaram. A suggested resultant pattern of transience is illustrated below model A.

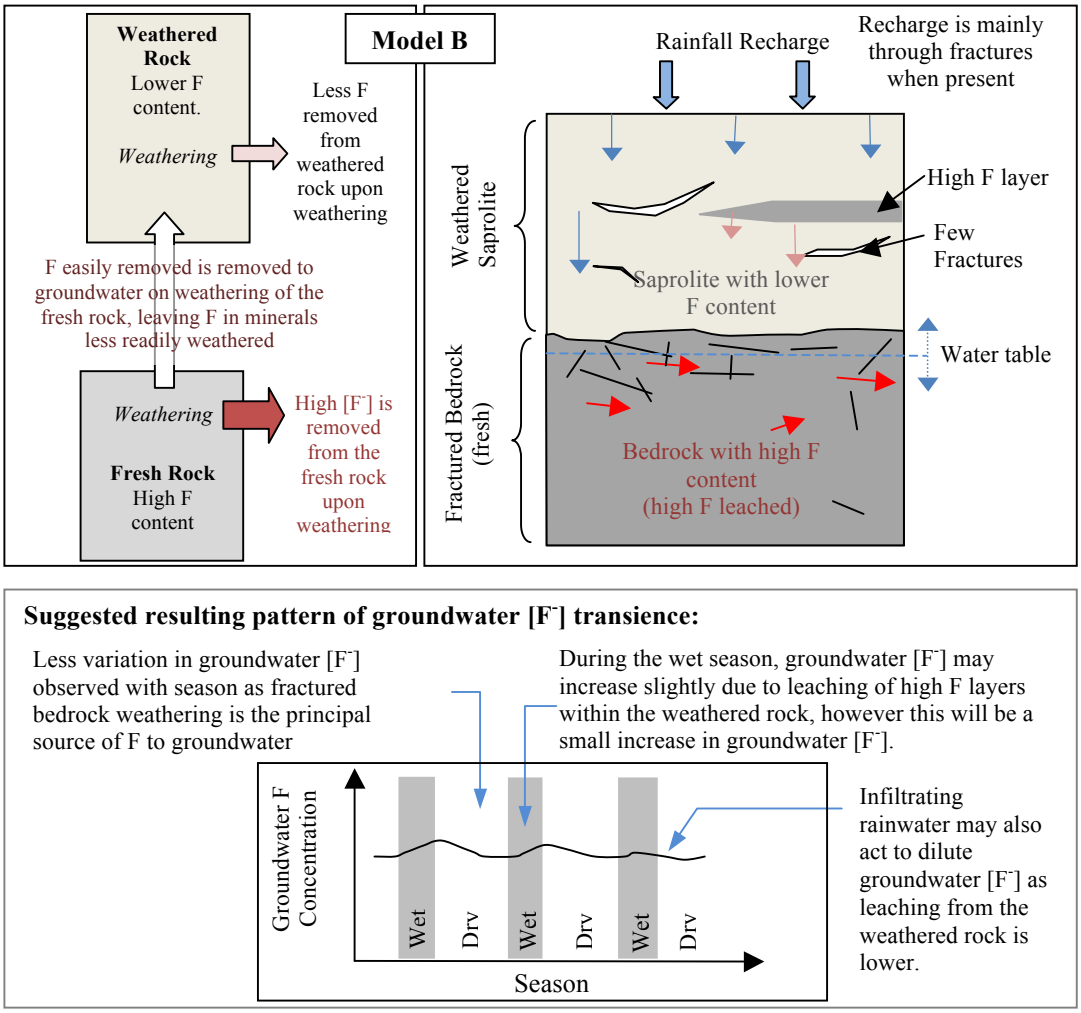

Figure 7-17 – Model B of weathering and F distribution, and diagram of potential sources and pathways of F in weathering. Based on profile at W11 – Amphibole granodiorite in Wailpally. A suggested resultant pattern of transience is illustrated below model B.

Although Model A is based on a profile from Maheshwaram, and Model B on a profile for Wailpally, both models of weathering and F release may be relevant for different areas in each catchment. Leaching experiments gave overall higher F concentrations leached from the Maheshwaram profile (model A) than from the Wailpally profile (model B). The difference in the profiles and the sources and concentration of F leached to groundwater locally appear to be related to the hydrological and geological context.

7.4.4 The Significance of the Hydrological and Geological Context on Profile Models

The Hydrological Context:

The regolith profiles examined in the Maheshwaram and Wailpally catchments are located in different situations within their respective catchment. The porphyritic biotite granodiorite profile (M2) from Maheshwaram is located in the upper reaches (south) of the catchment. The weathering profile here is thick, with many preserved fissures. Groundwater generally flows from this area to regions of discharge towards the north, but much of the catchment is subject to low groundwater flow and stagnation on account of excessive groundwater pumping (Marechal et al., 2006a).

The amphibole granodiorite profile (W11) from Wailpally is located on the plains, in the lower reaches of the catchment near the region of groundwater discharge. Water flows to this area from the higher ground in the hilly upper reaches in the west of the catchment and from the nearby tank. The weathering profile is thinner and more thoroughly weathered than the profile in Maheshwaram. Few preserved fissures were seen in this profile, possibly due to its location within the catchment.

The Geological Context:

The sources and distribution of F within the profile depends on the presence and abundance of F-bearing minerals. The fractured bedrock in the Maheshwaram profile is a gneissic porphyritic biotite granodiorite, and in the Wailpally profile is an amphibole granodiorite. The main sources of F to groundwater in the Maheshwaram profile (M2) are biotite and apatite (from mass balance and leaching experiments) and in the Wailpally profile (W11) from amphiboles (magnesio-hornblende). The sources and mineralogy of F in other samples has previously been discussed.

In both profiles, layers with a high mafic content and high whole rock fluorine were observed. These are likely to be due to natural variations in the distribution of F-bearing mafic minerals in the fresh rock, leading to layers of higher WRF in the saprolite. F leached from these samples is higher than other weathered sample

leaching, and infiltrating water passing through these layers may have increased F^- concentration. Infiltration of water, however, is mainly through preserved fractures, with more limited matrix flow. Therefore layers of high whole rock F may have only a limited impact on groundwater F concentrations.

Fracture fill material in Maheshwaram contains disseminated carbonate minerals and clays with readily leachable F. Apart from fracture fill material, the Wailpally profile overall has a higher CaO content than the Maheshwaram profile. Calcrete is observed in many locations in the Wailpally catchment, but appears absent from the Maheshwaram catchment. Calcrete has been suggested both as a sink of F upon deposition (Jacks and Sharma, 1995 in the Southern India context; Reddy D. et al., 2010 in the Wailpally catchment) and a factor increasing the potential of groundwater to attain high [F^-] as Ca is removed from solution where groundwater is under-saturated with respect to fluorite. In Wailpally calcrete was seen to be commonly present in the surface soils and also as layers within the saprolite. While the precipitation of calcrete may be a sink of F from groundwater upon precipitation, leaching experiments show that a very high F^- concentration is rapidly leached from calcrete, making it also a potential source of F. Where calcrete is present, infiltrating water may leach F and increase the F content of groundwater. This may occur in a similar way to F leaching from fracture fill in model A above, although possibly on a larger scale as calcrete deposits are more extensive, with higher leached [F^-] than from the fracture fill material (figure 7-15).

7.5 Implications for Long-Term Bedrock Weathering and Regolith Development

The weathering of F-bearing minerals from bedrock leads to loss of F to groundwater and to the redistribution of F within the regolith profile. Mass balance calculations demonstrate mineralogical F distribution within the profile and allow for the estimation of mineralogical F losses. Whole rock chemistry and whole rock fluorine chemical analysis indicate chemical changes that have occurred upon weathering and regolith development. Groundwater F^- concentrations available from the two research catchments can be combined with the whole rock chemical analyses to estimate F-flux and long-term bedrock weathering rates with regard to fluorine. These estimates are described in the following sections.

7.5.1 Groundwater F-Flux, Regolith Age and Weathering Rate

The difference in WRF content between fresh bedrock and the weathered equivalent regolith gives an indication of F lost through long-term weathering. This can be used with the groundwater F^- concentration to estimate a minimum groundwater flux (expressed as an equivalent depth of water) required to remove the observed amount of F from the fresh rock. The minimum F loss from the profile is calculated using:

$$F_{lost} = F_{fresh} - F_{weathered}$$

Where F_{lost} is the difference in total F content between a fresh sample and its weathered equivalent (mg/kg), F_{fresh} is the F content of fresh rock (mg/kg) and $F_{weathered}$ is the F content of weathered rock (mg/kg).

The amount of water required to remove the mass of F lost (A_w, in L per Kg of rock being weathered) is calculated using:

$$A_w = F_{lost} / F_{groundwater}$$

Where $F_{groundwater}$ is the concentration of F in groundwater (mg/l). The minimum equivalent depth of water required in the weathering process (D_{min} in mm) is then calculated from:

$$D_{min} = A_w \times \partial \times h$$

Where ∂ is the density of rock (kg/m^3) and h is the depth of weathering (m).

This can be considered against the average annual recharge (R, in mm/year) in the catchment (estimated as a proportion of rainfall), to estimate the duration of weathering (T, in years), which is a maximum value by this approach:

$$T=D_{min}/R$$

The weathering flux (Q) is then:

$$Q = \frac{F_{lost}}{T}$$

For comparison with published weathering fluxes, it is useful to compute the flux (Q) in units of moles/m^2/s, using F_{lost} in moles/m^2, and time (T) in seconds in the above equation.

This estimate takes no account of the following:

- Rainfall and recharge variation over the time period
- Physical erosion of the regolith (i.e. the time calculated refers to the observed regolith thickness only)
- Variation in groundwater fluoride concentration (i.e. F is assumed to be removed at a constant rate) over the time period
- Fluorine sequestration in the regolith profile (i.e. the method establishes a minimum groundwater flux and a maximum duration of weathering)
- Non-mineralogical inputs of F.

Within these limitations, the catchment-wide values of D_{min}, T and Q have been calculated for Maheshwaram and Wailpally (table 7-7), as well as at sample locations (table 7-8).

Table 7-7 – Catchment wide weighted averages for D_{min}, T and Q for Maheshwaram and Wailpally.

	Maheshwaram	**Wailpally**
Minimum depth of water (D_{min}) (mm)	23,009,000	6,391,000
Weathering Duration (T) (years)	5.7×10^5	1.7×10^5
Weathering flux (Q) (moles/m^2/s)	1.16×10^{-7}	2.46×10^{-7}

Table 7-8– Calculated D_{min}, T and Q at sample sites in Maheshwaram and Wailpally

	Maheshwaram				**Wailpally**		
	M2	**M3**	**M4**	**M7**	**W1**	**W16**	**W11**
Minimum depth of water (D_{min}) (mm)	22,803,000	5,960,000	33,393,000	1,404,000	16,394,000	8,013,000	2,547,000
Weathering Duration (T) (years)	5.6×10^5	1.5×10^5	8.2×10^5	3.5×10^4	1.6×10^5	2.5×10^5	8.1×10^4
Weathering flux (Q) (moles/m^2/s)	1.27×10^{-7}	7.66×10^{-8}	9.22×10^{-8}	9.49×10^{-8}	7.87×10^{-7}	2.31×10^{-7}	1.41×10^{-7}

The values used in these calculations are:

- Density 2700 kg/m^3 (an average granite density)
- Recharge:
  - In Maheshwaram, as 5% of average annual rainfall (812mm/year) (Chand et al., 2005)
  - In Wailpally, as 16% of average annual rainfall (632mm/year) in the east of the catchment, and as 5% of average annual rainfall in the central and west of the catchment (Reddy et al., 2009).
- Depth of weathering in Maheshwaram locations from Dewandel et al. (2006) and in Wailpally locations from a weathering thickness map (Dhakate et al., 2008).

Within the Wailpally catchment, calculated values of D_{min}, weathering duration and weathering flux are smaller from sample W11, located in the discharge region of the catchment, than for samples W16 and W1, located towards the centre of the catchment. Individual sample locations within the Maheshwaram catchment show no apparent spatial trends in weathering duration or rate.

The catchment-wide values calculated for the weathering duration and weathering flux in each catchment are the same order of magnitude (table 7-7). The values for the minimum depth of water (and the weathering duration) are higher in Maheshwaram than in Wailpally, however the weathering flux calculated is higher in Wailpally. As the groundwater F concentration is higher in Wailpally than Maheshwaram, this removes F from the profile at a faster rate than in Maheshwaram, giving a lower depth of water required and a higher weathering rate.

7.5.2 Long-Term Weathering Rates from Element Profiles

The estimates of weathering flux above do not take into account changes in volume and density that may occur during regolith formation, and calculate the F-flux based on recently measured F^- concentrations in groundwater, average rainfall and estimated recharge.

Long-term weathering rates (weathering flux) incorporating density and volume change, that do not rely on current climate and groundwater conditions, can also be calculated from element profiles, determined from the ratio of a chemical species in the regolith to that in the bedrock, and dependent on changes in the bedrock/regolith density and volume (Brimhall and Dietrich, 1987). The ratio is calculated as follows:

$$\frac{C_{j,w}}{C_{j,P}} = \frac{\rho_P}{\rho_w} \frac{1}{(\varepsilon + 1)} (1 + \tau_j)$$

Where $C_{j,W}$ is the concentration of species j in the weathered rock, $C_{j,P}$ is the concentration of species j in the bedrock, ρ_w is the density of the weathered rock, ρ_P is the density of the bedrock, ε is the strain factor and τ is the mass transfer coefficient.

The strain factor can be calculated from the ratios of the concentrations of an inert reference element, i. Elements commonly used are Zr, Ti, Nb, Y and sometimes Al (White et al., 1998). The strain factor is equal to V_w/V_p-1 (where V is volume) and therefore in iso-volumetric saprolite formation should be close to zero. The strain factor can be calculated using the following equation:

$$\varepsilon_j = \frac{\rho_P C_{i,P}}{\rho_w C_{i,w}} - 1$$

The mass transfer coefficient, τ , is calculated using the following equation:

$$\tau_j = \frac{\rho_w C_{j,w}}{\rho_P C_{j,P}} \left(\varepsilon_{j,w} + 1\right) - 1$$

The total mass loss of element j ($\Delta M_{j,r}$) in moles/m^2 is given by:

$$\Delta M_{j,r} = \left(\rho_P \frac{C_{j,P}}{m_j} 10^4\right) \int_{z=0}^{z=d} \tau_{j,w} dZ$$

Where m_j is the atomic weight of species j, and d is the total profile depth. The total mass loss is then used to calculate the weathering flux ($Q_{j,r}$, in moles/m^2/s) based on the age of the profile (t, seconds) (equation below).

$$Q_{j,r} = \frac{\Delta M_j}{t}$$

These equations were used to estimate the mass loss of fluorine from the weathering profiles and the weathering flux (based on fluorine loss) of the profiles. Bedrock density was taken as equivalent to 2700 kg/m^3. The porosity of the weathered regolith is given as 10% by Dewandel et al. (2006), therefore a regolith density of 2450 kg/m^3 was estimated. This gives a calculated strain factor (ε_j) of near to zero for the majority of profiles, hence confirming to an iso-volumetric weathering regime. The age of the weathering profiles are also required. This was taken from the weathering duration calculated in section 7.6.1 above.

Table 7-9 shows the estimated ΔM_j (total mass loss) for F, Mg and Na, using Ti as the reference (immobile) element. Whole rock chemistry results show an apparent retention of TiO_2 between fresh and weathered pairs (section 4.8). However, due to apparent titanite enrichment upon weathering from whole rock chemistry results in sample M3, Al is used as the reference element as an alternative. Similar F mass losses are calculated for the Wailpally and Maheshwaram samples, with F mass loss less than Mg and Na mass loss in the majority of samples. A smaller F mass loss may

result from to the lower mobility of F compared to Mg and Na, as some F may be sequestered in the weathered regolith. Calculated mass losses for Mg and Na are an order of magnitude or two larger than those calculated for Puerto Rico granite by White et al. (1998) (ΔM_{Na} 1.2 x10^4, ΔM_{Mg} 6.4 x10^3).

The long-term weathering flux (Q) for F, Mg and Na calculated for each sample location using ΔM values and weathering times calculated in section 7.6.1 are shown in table 7-10.

Table 7-9- Total mass loss ΔM_j (moles/m^2) determined for F, Mg and Na. Ti used as reference element (except for sample M3, where Al is used). Mass loss for sample W11 calculated using the profile sample at 7m depth as the weathered equivalent sample.

ΔM_j	M2	M3	M4	M7	W1	W16	W11
F	2.1 x10^5	1.8 x10^5	3.0 x10^6	2.8 x10^5	6.1 x10^6	9.0 x10^5	9.6 x10^5
Mg	3.5 x10^6	1.8 x10^6	6.5 x10^7	3.2 x10^6	3.2 x10^7	3.5 x10^7	6.6 x10^5
Na	9.8 x10^6	2.0 x10^7	1.3 x10^8	-4.4 x10^6	7.3 x10^8	8.5 x10^7	4.5 x10^7

Table 7-10 – Long-term weathering F (Q) flux in moles/m^2/s determined from ΔM_F (using reference element Ti, except sample M3 where Al is used)

Q	M2	M3	M4	M7	W1a	W16a	W11a-7m
F	1.2 x10^{-8}	5.0 x10^{-8}	1.7 x10^{-7}	3.3 x10^{-7}	1.2 x10^{-6}	1.1 x10^{-7}	3.8 x10^{-7}
Mg	2.0 x10^{-7}	5.0 x10^{-8}	1.7 x10^{-7}	3.7 x10^{-6}	6.3 x10^{-6}	4.3 x10^{-6}	2.6 x10^{-7}
Na	5.5 x10^{-7}	5.0 x10^{-7}	3.7 x10^{-6}	4.6 x10^{-5}	1.4 x10^{-4}	1.1 x10^{-5}	1.8 x10^{-5}

7.5.3 Comparison with Published Weathering Rates

A summary of catchment-wide calculated weathering F-flux is given in table 7-11. The weathering F-flux by both methods is of the same order of magnitude, although the weathering F-flux calculated from ΔM_F for Maheshwaram is approximately half that calculated from F loss calculations.

The catchment-wide calculated weathering duration (from F) for each catchment is given in table 7-12. The weathering duration is also calculated from average denudation rates for southern India from Gunnell (1998), calculated assuming the average long-term chemical weathering rate is of the same order of magnitude as the average long-term physical erosion rate, as suggested by White et al. (1998), Braun et al. (2009) and Green et al. (2006). The weathering duration calculated from F loss (section 7.6.1) is of the same order of magnitude as those calculated from average

denudation rates from Gunnell (1998) giving a degree of confidence in an estimate of the duration of weathering responsible for the preserved regolith in Andhra Pradesh to be in the order of 300,000 years (table 7-12).

Comparison of weathering flux estimated here with published data (table 7-13) shows the weathering F flux calculated in Maheshwaram and Wailpally to be higher than the majority of published weathering rates for other elements (Mg, K, Si, Na, Ca).

Table 7-11 – Summery of weighted average catchment weathering F Flux (Q) calculated from methods described in section 7.6.1 and 7.6.2

Weathering F- Flux (Q, weathering rate) in moles/m^2/s		
Calculation:	**Maheshwaram**	**Wailpally**
Calculated from F loss calculations (section 7.6.1)	1.16×10^{-7}	2.46×10^{-7}
Calculated from ΔM_F	6.12×10^{-8}	3.41×10^{-7}

Table 7-12 – Summary of weighted average catchment weathering time (years) calculated using methods described in section 7.6.1 and from average denudation rates of Gunnell (1998)

Weathering Duration (age of profile) in Years		
Calculation:	**Maheshwaram**	**Wailpally**
F loss calculations from WRF (section 7.6.1)	5.7×10^5	1.7×10^5
Average denudation rates (from Gunnell, 1998)	2.23×10^5	3.13×10^5

Table 7-13– Long-term weathering flux calculated from changes in regolith chemistry. ^Based on chemical changed between inner (fresh) and outer (weathered) portions of basaltic clasts. +Calculated at a basin scale from precipitation and stream water chemistry

Weathering Flux (Q) moles/m^2/s					
	Maheshwaram **This Study**	Wailpally **This Study**	Puerto-Rico – Quartz Diorite White et al. (1998)	Costa Rica, weathering rinds on basaltic clasts^. Sak et al. (2004)	Puerto Rico – Quartz Diorite+ Turner et al. (2003)
F	1.16×10^{-7} 6.12×10^{-8}	2.46×10^{-7} 3.41×10^{-7}			
Mg	4.7×10^{-7}	1.7×10^{-6}	1.0×10^{-9}	6.1×10^{-10}	2.7×10^{-9}
K			8.2×10^{-10}	2.5×10^{-11}	1.0×10^{-9}
Si			1.7×10^{-8}	6.0×10^{-9}	2.6×10^{-10}
Na	2.7×10^{-6}	1.1×10^{-5}	1.9×10^{-9}	6.4×10^{-10}	5.8×10^{-9}
Ca			2.7×10^{-9}	1.5×10^{-9}	6.6×10^{-9}

A higher weathering flux calculated for Maheshwaram and Wailpally compared with published results may result from the methods of calculation. The weathering flux

calculated by Sak et al. (2004) is from basaltic clasts collected from alluvial fill terraces, and the weathering flux calculated by Turner et al. (2003) uses differences between the flux of the solute in stream water and in meteoric water. The higher weathering flux may also result from a stronger monsoon climate or from the different geological history of weathering.

The calculation of silicate weathering fluxes is important in the estimation of CO_2 sequestration rates (as silicate weathering involves CO_2 consumption). This is the first estimate for Southern India using the above method, and is yet to be supported or verified by additional calculations to be expected from Braun et al. (2009).

7.6 Summary and Discussion

Summary

This research has been based on parallel studies of two catchments in Andhra Pradesh. Through mineralogical and chemical analyses, batch leaching experiments and the development of an F mass balance, the principal mineralogical sources of F and their relative importance and spatial variation in the two catchments have been identified. The effect of weathering and regolith development on F distribution and F loss in the principal lithologies present, and the relative source strength of F to groundwater from the catchment sample lithologies have also been determined.

The principal F-bearing minerals in the fresh bedrock are apatite, biotite, fluorite, amphiboles and titanite. The occurrence and distribution of these minerals varies with lithology. The presence of high F fluorite does not necessarily indicate high bedrock total F or high leachable F. Fresh bedrock has a higher whole rock fluorine content than its weathered equivalent, with gneissic porphyritic granites having the highest whole rock fluorine content. In Maheshwaram this lithology underlies a large area of the catchment (~70% by area), while in the Wailpally catchment this lithology is confined to the upland areas (~10% of the catchment). Similar ranges of bedrock whole rock fluorine are found in both catchments. Bedrock whole rock fluorine content is not directly related to leachable F (source strength) or groundwater F^- concentration, although in Maheshwaram there is a distinct positive correlation between bedrock whole rock fluorine and groundwater F^-.

Mass balance calculations show that in the majority of cases over 60% of the bedrock F content has been removed as a result of long-term weathering and regolith development. The principal mineralogical loss of F is from biotite and apatite in Maheshwaram, and from fluorite, apatite and biotite (and amphiboles) in Wailpally. Sources of F are present in the regolith that are additional to those observed in optical petrology and EM analysis. These include clay minerals (as observed in XRD) and may also include F adsorbed to Al and Fe oxides. Features of the weathered regolith with high leachable F include fracture fill and layers of high mafic content. Where

present these may be a significant source of F to groundwater upon water infiltration and leaching. In laboratory experiments higher [F^-] is leached from the fresh bedrock than from weathered regolith in the majority of cases, apart from the porphyritic biotite granodiorite (M2), which covers a large area of Maheshwaram. Here, infiltration following the monsoon season or due to intensive irrigation may increase groundwater [F^-] through leaching of the regolith. The significance of F mobilisation from the regolith in Maheshwaram has important implications for the widespread policy of artificial recharge as a groundwater management technique.

Based on batch leaching experiments, a scale of relative F 'source strength' has been developed, which shows calcrete, mafic vein material and the porphyritic granites of Wailpally to have the most readily leachable F, and pegmatites of Wailpally to have the least. During these experiments the concentration of F^- leached from bedrock increases with time, therefore longer bedrock water-rock interaction time (groundwater residence time) may increase [F^-] in groundwater. In contrast, F is leached rapidly from the regolith, indicating that long reaction times are not necessary. Fluorite saturation is not a limiting factor on F concentrations in either catchment.

The differences in catchment topography, weathering styles and groundwater flow affect the sources and pathways of F to groundwater as described in conceptual models. The observed regolith thickness has been shown to have developed over ca. 300,000 years.

Discussion and Suggestions for Further Research

This research has highlighted similarities and differences between the two catchments studied, including those of geology, F-mineralogy, topography, groundwater flow and F leachability. These observations have been incorporated into catchment-scale conceptual models of F in groundwater. Detailed profile sampling of one location in each catchment has led to the development of conceptual models of F in groundwater at a local scale. The widespread presence of calcrete in Wailpally and its apparent absence from Maheshwaram is significant and is linked in the conceptual models to the contrasting groundwater [F^-] distribution. These models attempt to explain the

spatial and seasonal variations observed in both catchments, and highlight the variety of factors which control groundwater F^- concentrations. The variation in controls of groundwater F concentrations between the two catchments highlights the need for case by case site evaluation prior to the selection of an appropriate fluoride management technique.

Development of quantitative descriptions of mineralogical F sources in the two catchments and conceptual models of F release from bedrock and regolith to groundwater should form the basis for further research on the issue of groundwater F^- occurrence, including:

- Further investigation of the processes of weathering and controls on F distribution within the weathering profile. For example:
    - Investigation of calcrete occurrence in Wailpally, a more detailed description of its formation, F-content and leachability, and by implication, explanation for its absence in Maheshwaram
    - The analysis of additional weathering profiles to give a wider understanding of weathering processes and the effect of mineralogical F distribution
    - Investigation of the clay minerals present and their F content using XRD with aligned powdered samples and whole rock fluorine analysis with sample separation prior to analysis. Analysis of the composition of fracture fill material by these methods may aid the understanding of the source of the readily leachable F from this material.
    - Specification of chemical equations describing the weathering of F-bearing minerals as indicated by the EM-EDX analysis
- Modelling of these proposed reactions:
    - Modelling of mineral weathering and the relative dissolution and contribution of different minerals to groundwater chemistry using precipitation and groundwater chemistry with bedrock mineralogy.
    - Further development of batch leaching experiments, with measurements of pH and bicarbonate content as well as longer term batch leaching or column experiments, to enable modelling of the kinetics of the simulated water-rock reactions

- Further development of the Ingram (1970) whole rock fluorine analytical method to achieve more accurate whole rock fluorine results. This may include some of the suggestions of Stecher (1983).
- Transient, depth-specific sampling of pore-water through the regolith to scrutinise the response to monsoon recharge.
- Transient sampling of pore-water down-gradient of sites of surface water tanks and dams constructed for recharge enhancement, to investigate the possible unintentional release of F under this style of catchment management.

References

Abdelgawad, A. M., Watanabe, K., Takeuchi, S., and Mizuno, T., 2009, The origin of fluorine-rich groundwater in Mizunami area, Japan - Mineralogy and geochemistry implications: Engineering Geology, v. 108, p. 76-85.

Agarwal, M., Rai, K., Shrivastav, R., and Dass, S., 2002, A study on fluoride sorption by Montmorillonite and Kaolinite: Water, Air and Soil Pollution, v. 141, p. 247-261.

AIST website, 2009, National Institute of Advanced Industrial Science and Technology Website: http://staff.aist.go.jp/nomura-k/english/itscgallary-e.htm.

Aizawa, S. and Akaiwa, H., 1995, Geochemical behaviour of fluorine during the formation of Pleistocene limestones in Yoron-Jima Island, South-western Japan: Bulletin of the Chemical Society of Japan, v. 68, p. 825-830.

Amini, M., Mueller, K., Abbaspour, K. C., Rosenberg, T., Afyuni, M., Moller, K. N., Sarr, M., and Johnson, C. A., 2008, Statistical modelling of global geogenic fluoride contamination in groundwaters: Environmental Science and Technology, v. 42, p. 3662-3668.

Andezhath, S. K. and Ghosh, G., 1999, Fluorosis management in India: the impact due to networking between health and rural drinking water supply agencies: IAHS Publication, v. 260, p. 159-166.

Andhra Pradesh Online, 2008, Water Resources Information System http://irrigation.cgg.gov.in/jsp/wris.jsp.

Anthoni, J. F., 2000, Seafriends: Soil use, sustainability and conservation. Website http://www.seafriends.org.nz/enviro/soil/claylay.gif.

Anthony, J. W., Bideaux, R. A., Bladh, K. W., and Nichols, M. C., 1997, Handbook of mineralogy: Tuscon, Arizona, Mineral Data Publishing.

Antipin, V. S., Savina, E. A., and Mitichkin, M. A., 2006, Geochemistry and formation conditions of rare-metal granites with various fluorine-bearing minerals (Fluorite, Topaz, and Cryolite): Geochemistry International, v. 44, p. 965-975.

Apambire, W. B., Boyle, D. R., and Michel, F. A., 1997, Geochemistry, genesis, and health implications of fluoriferous groundwaters in the upper regions of Ghana: Environmental Geology, v. 33, p. 13-24.

Appelo, C. A. J. and Postma, D., 1996, Geochemistry, groundwater and pollution: A.A. Balkema.

Atal, S., 2008, Investigation of hydro-geochemical factors controlling excessive fluoride in granitic hard rock terrain: with special reference to Maheshwaram watershed, Andhra Pradesh [PhD thesis]: Osmania University.

Avishek, K., Pathak, G., Nathawat, M. S., Jha, U., and Kumari, N., 2010, Water quality assessment of Majhiaon block of Garwa district in Jharkhand with special focus on fluoride analysis: Environmental Monitoring and Assessment, v. 167, p. 617-623.

Bailey, J.C., 1977, Fluorine in Granitic rocks and melts: A review: Chemical Geology, v. 19, p. 1-42.

Bancroft, G. M., Metson, J. B., and Kresovic, R. A., 1987, Leaching studies of natural and synthetic titanites using secondary ion mass spectrometry: Geochimica et Cosmochimica Acta, v. 51, p. 911-918.

Banks, D., Reimann, C., RØyset, O., Skarphagen, H., and Sæther, O. M., 1995, Natural concentrations of major and trace elements in some Norwegian bedrock groundwaters: Applied Geochemistry, v. 10, p. 1-16.

Bateman, R. M. and Catt, J. A., 1985, Modification of heavy mineral assembages in English coversands by acid pedochemical weathering: Catena, v. 12, p. 1-21.

Bell, F. G., 2000, Engineering properties of soils and rocks: Oxford, Blackwell Science.

Bhagavan, S. V. B. K. and Raghu, V., 2005, Utility of check dams in dilution of fluoride concentration in ground water and the resultant analysis of blood serum and urine of villagers, Anantapur District, Andhra Pradesh, India: Environmental Geochemistry and Health, v. 27, p. 97-108.

Bisdom, E. B. A., Stoops, G., Delvigne, J., Curmi, P., and Altemuller, H. J., 1982, Micromorphology of weathering biotite and its secondary products: Pedologie, v. 32, p. 225-252.

Boyle, D. R. and Chagnon, M., 1995, An incident of skeletal fluorosis associated with groundwaters of the maritime carboniferous basin, Gaspé region, Quebec, Canada: Environmental Geochemistry and Health, v. 17, p. 5-12.

Brandt, F., Bosbach, D., Krawczyk-Barsch, E., Thuro, A., and Bernhard, G., 2003, Chlorite dissolution in the acid pH-range: A combined microscopic and macroscopic approach: Geochimica et Cosmochimica Acta, v. 67, p. 1451-1461.

Braun, J. J., Descloitres, M., Riotte, J., Fleury, S., Barbiero, L., Boegen, J. L., Violette, A., Lacarce, E., Ruiz, L., Sekhar, M., Mohan Kumar, M. S., Subramanian, S., and Dupre, B., 2009, Regolith mass balance inferred from combined mineralogical, geochemical and geophysical studies: Mule Hole gneissic watershed, South India: Geochimica et Cosmochimica Acta, v. 73, p. 935-961.

Brimhall, G. H. and Dietrich, W. E., 1987, Constitutive mass balance relations between chemical composition, volume, density, porosity, and strain in metasomatic hydrochemical systems: Results on weathering and pedogenesis: Geochimica et Cosmochimica Acta, v. 51, p. 567-587.

Brinda, K., Rajesh, R., Murugan, R., and Elango, L., 2010, Fluoride contamination in groundwater in parts of Nalgonda District, Andhra Pradesh, India: Environmental Monitoring and Assessment.

Carrillo-Rivera, J. J., Cardona, A., and Edmunds, W. M., 2002, Use of abstraction regime and knowledge of hydrogeological conditions to control high-fluoride concentration in abstracted groundwater: San Luis Potosí basin, Mexico: Journal of Hydrology, v. 261, p. 24-47.

Chae, G. T., Yun, S. T., Kwon, M. J., Kim, Y. S., and Mayer, B., 2006, Batch dissolution of granite and biotite in water: Implication for fluorine geochemistry in groundwater: Geochemical Journal, v. 40, p. 95-102.

Chand, R., Hodlur, G. K., Ravi Prakash, M., Mondal, N. C., and Singh, V. S., 2005, Reliable natural recharge estimated in granitic terrain: Current Science, v. 88, p. 821-824.

Chandrawanshi, C. K. and Patel, K. S., 1999, Fluoride deposition in Central India: Environmental Monitoring and Assessment, v. 55, p. 251-265.

Chaudhary, V., Kumar, M., Sharma, M., and Yadav, 2010, Fluoride, boron and nitrate toxicity in ground water of northwest Rajasthan, India: Environmental Monitoring and Assessment, v. 161, p. 343-348.

Chorley, R. J., 1969, The role of water in rock disintegration, in Chorley, R. J., ed., Water, Earth and Man: A Synthesis of Hydrology, Geomorphology and Socio-economic Geography: London, Meuthuen young books, p. 135-155.

Correns, C. W., 1956, The geochemistry of the halogens: Physics and Chemistry of the Earth, v. 1, p. 181-233.

Costa, J. E. and Cleaves, E. T., 1984, The piedmont landscape of Maryland: A new look at an old problem: Earth Surface Processes and Landforms, v. 9, p. 59-74.

Cremer, M. and Schlocker, J., 1976, Lithium borate decomposition of rocks, minerals and ores: American Mineralogist, v. 61, p. 318-321.

Currell, M., Cartwright, I., Raveggi, M., and Han, D., 2011, Controls on elevated fluoride and arsenic concentrations in groundwater from the Yuncheng Basin, China: Applied Geochemistry, (in press).

Dai, S., Ren, D., and Ma, S., 2004, The cause of endemic fluorosis in Western Guizhou Province, Southwest China: Fuel, v. 83, p. 2095-2098.

Datta, D. K., Gupta, L. P., and Subramanian, V., 1999, Dissolved fluoride in the Lower Ganges-Brahmaputra-Meghna River system in the Bengal Basin, Bangladesh: Environmental Geology, v. 39, p. 1163-1168.

Davraz, A., Sener, E., and Sener, S., 2008, Temporal variations of fluoride concentrations in Isparta public water system and health impact assessment (SW-Turkey): Environmental Geology, v. 56, p. 159-170.

Deer, W. A., Howie, R. A., and Zussman, J., 1992, An introduction to the rock forming minerals: Hong Kong, Longman Scientific and Technical.

Dewandel, B., Lachassagne, P., Wyns, R., Marechal, J.C., and Krishnamurthy, N.S., 2006, A generalized 3-D geological and hydrogeological conceptual model of granite aquifers controlled by single or multiphase weathering: Journal of Hydrology, v. 330, p. 260-284.

Dhakate, R., Negi, B. C., and Singh, V. S., 2006, Electrical resistivity survey to delineate groundwater potential zones in Granitic terrain, Nalgonda district, India: Asian Journal of Water, Environment and Pollution, v. 5, p. 17-25.

Dhakate, R., Singh, V. S., Negi, B. C., Chandra, S., and Rao, V. A., 2008, Geomorphological and geophysical approach for locating favourable groundwater zones in granitic terrain, Andhra Pradesh, India: Journal of Environmental Management, v. 88, p. 1373-1383.

Dhiman, S. D. and Keshari, A. K., 2006, Hydrochemical evaluation of high-fluoride groundwaters: a case study from Mehsana District, Gujarat, India: Hydrological Sciences Journal, v. 51, p. 1149-1162.

Dorozhkin, S. V., 1997, Surface reactions of apatite dissolution: Journal of Colloid and interface Science, v. 191, p. 489-497.

Drever, J. I. and Clow, D. W., 1995, Weathering rates in catchments: Reviews in Mineralogy and Geochemistry, v. 31, p. 463-483.

Edmunds, M. and Smedley, P., 2005, Fluoride in natural waters, in Selinus, Alloway, Centeno, Finkelman, Fuge, Lindh, and Smedley, eds., Essentials of medical geology: impacts of the natural environment on public health: London, Elsevier, p. 301-329.

Farooqi, A., Masuda, H., and Firdous, N., 2007, Toxic fluoride and arsenic contaminated groundwater in the Lahore and Kasur districts, Punjab, Pakistan and possible contaminant sources: Environmental Pollution, v. 145, p. 839-849.

Fawell, J., Bailey, K., Chilton, J., Dahi, E., Fewtrell, L., and Magara, Y., 2006, Fluoride in drinking-water, IWA publishing.

Frost, B. R., Chamberlain, K. R., and Schumacher, J.C., 2000, Sphene (titanite): Phase relations and role as a geochronometer: Chemical Geology, v. 172, p. 131-148.

Fuge, R., 1988, Sources of halogens in the environment, influences on human and animal health: Environmental Geochemistry and Health, v. 10, p. 51-61.

Fuge, R. and Andrews, M.J., 1988, Fluorine in the UK environment: Environmental Geochemistry and Health, v. 10, p. 96-104.

Fuhong, R. and Shuqin, J., 1988, Distribution and formation of high-fluorine groundwater in China: Environmental Geology and Water Science, v. 12, p. 3-10.

Gaciri, S. J. and Davies, T. C., 1993, The occurrence and geochemistry of fluoride in some natural waters of Kenya: Journal of Hydrology, v.143, p. 395-412.

Gaus, I., Shand, P., Gale, I.N., Williams, A.T., and Eastwood, J.C., 2002, Geochemical modelling of fluoride concentration changes during Aquifer Storage and Recovery (ASR) in the Chalk Aquifer in Wessex, England: Quarterly Journal of Engineering Geology and Hydrogeology, v. 35, p. 203-208.

Gautam, R. and Bhardwaj, N., 2010, Groundwater quality assessment of Nawa Tehsil in Nagaur district (Rajasthan) with special reference to Fluoride: Environmentalist, v. 30, p. 219-227.

Genxu, W. and Guodong, C., 2001, Fluoride distribution in water and the governing factors of environment in arid north-west China: Journal of Arid Environments, v. 49, p. 601-614.

Giudry, M. W. and MacKenzie, F. T., 2003, Experimental study of igneous and sedimentary apatite dissolution: Control of pH, distance from equilibrium, and temperature on dissolution rates: Geochimica et Cosmochimica Acta, v. 67, p. 2949-2963.

Gizaw, B., 1996, The origin of high bicarbonate and fluoride concentrations in waters of the Main Ethiopian Rift Valley, East African Rift System: Journal of African Earth Sciences, v. 22, p. 391-402.

Goldich, S. S., 1938, A study in rock-weathering: The Journal of Geology, v. 46, p. 17-58.

Gosselin, D. C., Headrick, J., Harvey, F. E., Tremblay, R., and McFarland, K., 1999, Fluoride in Nebraska's groundwater: Groundwater Monitoring and Remediation, p. 87-95.

Green, E.G., Dietrich, W.E., and Banfield, J. F., 2006, Quantification of chemical weathering rates across an actively eroding hill-slope: Earth and Planetary Science Letters, v. 242, p. 155-169.

Gunnell, Y., 1998, Present, past and potential denudation rates: is there a link? Tentative evidence from fission-track data, river sediment loads and terrain analysis in the South Indian shield: Geomorphology, v. 25, p. 135-153.

Guo, Q., Wang, Y., and Guo, Q., 2010, Hydrogeochemical genesis of groundwaters with abnormal fluoride concentrations from Zhongxiang City, Hubei Province, central China: Environmental Earth Sciences, v. 60, p. 633-642.

Guo, Q., Wang, Y., Ma, T., and Ma, R., 2007, Geochemical processes controlling the elevated fluoride concentrations in groundwaters of the Taiyuan Basin, Northern China: Journal of Geochemical Exploration, v. 93, p. 1-12.

Gupta, S., Banerjee, S., Saha, R., Datta, J.K., and Mondal, N., 2006, Fluoride geochemistry of groundwater in Nalhati-1 block of the Birbhum District, West Bengal, India: Fluoride, v. 39, p. 318-320.

Gupta, S. K., Deshpande, R. D., Agarwal, M., and Raval, B. R., 2005, Origin of high fluoride in groundwater in the North Gujarat-Cambay Region, India: Hydrogeology Journal, v. 13, p. 596-605.

Haamer, K., 2006, Hydrochemistry and sources of fluoride in Silurian-Ordovician aquifer system, [MSc Thesis]: University of Tartu, Institute of Geology.

Hagen, A. R., 1975, Studies of Fluorapatite: II. The Solubility Behaviour: Journal of Dental Research, v. 54, p. 384-393.

Handa, B. K., 1975, Geochemistry and genesis of fluoride-containing ground waters in India: Groundwater, v. 13, p. 275-281.

Harrington, L. F., Cooper, E. M., and Vasudevan, D., 2003, Fluoride sorption and associated aluminium release in variable charge soils: Journal of Colloid and interface Science, v. 267, p. 302-313.

Hitchon, B., 1995, Fluorine in formation waters, Alberta Basin, Canada: Applied Geochemistry, v. 10, p. 357-367.

Hodson, M. E., 2002, Variation in element release rate from different mineral size fractions from the B horizon of a granitic podzol: Chemical Geology, v. 190, p. 91-112.

Hughes, J. M., Cameron, M., and Crowley, K.D., 1989, Structural Variations in natural F, OH and CL apatites: American Mineralogist, v. 74, p. 870-876.

Ingram, B .L., 1970, Determination of Fluoride in Silicate Rocks without Separation of Aluminium Using a Specific Ion Electrode: Analytical Chemistry, v. 42, p. 1825-1827.

Ishikawa, K., Eanes, E. D., and Tung, M. S., 1994, The effect of supersaturation on apatite crystal formation in aqueous solutions at physiological pH and temperature: Journal of Dental Research, v. 73, p. 1462-1469.

Jacks, G., Bhattachary, P., Chaudhary, V., and Singh, K. P., 2005, Controls on the genesis of some high-fluoride groundwaters in India: Applied Geochemistry, v. 20, p. 221-228.

Jacks, G., Rajagopalan, K., Alveteg, T., and Jonsson, M., 1993, Genesis of high-F groundwaters, southern India: Applied Geochemistry, p. 241-244.

Jacks, G. and Sharma, V. P., 1995, Geochemistry of calcic horizons in relation to hillslope processes, southern India: Geoderma, v. 67, p. 203-214.

Jeffery, P. J. and Hutchinson, D., 1986, Chemical methods of rock analysis: Oxford, Pergamon Press.

Jerzykowska, I., Michalik, M. and Drewnik, M., 2007, Accessory minerals in podzolic soils and the Tatra MTS: Weathering microtextures and stability order: Minerlogia Polonica – Special Papers, v. 30.

Jha, S. K., Nayak, A. K., and Sharma, Y. K., 2010, Potential fluoride contamination in the drinking water of Marks Nagar, Unnao district, Uttar Pradesh, India: Environmental Geochemistry and Health, v. 32, p. 217-226.

Jiang, E. T. and Peacor, D.R., 1994, Formation of corrensite, chlorite and chlorite-mica stacks by replacement of detrital biotite in low-grade pelitic rocks: Journal of Metamorphic Geology, v. 12, p. 867-884.

Karro, E. and Rosentau, A., 2005, Fluoride levels in the Silurian-Ordovician aquifer system of Western Estonia: Fluoride, v. 38, p. 307-311.

Kau, P. M. D., Smith, D. W., and Binning, P., 1997, Fluoride retention by kaolin clay: Journal or Contaminant Hydrology, v. 28, p. 267-288.

Kau, P. M. H., Smith, D. W., and Binning, P., 1998, Experimental sorption of fluoride by kaolinite and bentonite: Geoderma, v. 84, p. 89-108.

Keshavarzi, B., Moore, F., Esmaeili, A., and Rastmanesh, F., 2010, The source of fluoride toxicity in Muteh area, Isfahan, Iran: Environmental Earth Sciences, v. 61, p. 777-786.

Khandare, A. L., Rao, G. S., and Balakrishna, N., 2007, Dual energy x-ray absorptiometry (DXA) study of endemic skeletal fluorosis in a village of Nalgonda District, Andhra Pradesh, India: Fluoride, v. 40, p. 190-197.

Kilham, P. and Hecky, R.E., 1973, Fluoride: Geochemical and ecological significance in East African waters and sediments: Liminology and Oceanography, v. 18, p. 932-945.

Kim, K. and Jeong, G. J., 2005, Factors influencing natural occurrence of fluoride-rich groundwaters: A case study in the South-eastern part of the Korean peninsula: Chemosphere, v. 58, p. 1399-1408.

Kreidler, E. R. and Hummel, F. A., 1970, The Crystal Chemistry of Apatite: Structure Fields of Fluor- and Chlorapatite: The American Mineralogist, v. 55, p. 170-184.

Kruse, E. and Ainchil, J., 2003, Fluoride variations in groundwater of an area in Buenos Aires Province, Argentina: Environmental Geology, v. 44, p. 86-89.

Kumar, D. and Ahmed, S., 2003, Seasonal behaviour of spatial variability of groundwater level in a granitic aquifer in monsoon climate: Current Science, v. 84, p. 188-196.

Kumar, V. V., Sai, C. S. T., Rao, P. L. K. M., and Rao, C. S., 1991, Studies on the distribution of fluoride in drinking water sources in Medchal Block, Ranga Reddy District, Andhra Pradesh, India: Journal of Fluoride Chemistry, v. 55, p. 229-236.

Kundu, N., Panigrahi, M. K., Tripathy, S., Munshi, S., Powell, M. A., and Hart, B. R., 2001, Geochemical appraisal of fluoride contamination of groundwater in the Nayagarh District of Orissa, India: Environmental Geology, v. 41, p. 451-460.

Lang, L.-O., 2000, Heavy mineral weathering under acidic soil conditions: Applied Geochemistry, v. 15, p. 415-423.

Leeuw, N.H. and Cooper, T.G., 2003, A Computational Study of the Surface Structure and Reactivity of Calcium Fluoride: Journal of Materials Chemistry, v. 13, p. 93-101.

Levinson, A.A., 1974, Introduction to exploration geochemistry: Wilmette, Illinois, Applied Publishing Ltd.

Lian-Fang, W. and Jian-Zhong, H., 1995, Outline of control practice of endemic fluorosis in China: Social Science and Medicine, v. 41, p. 1191-1195.

Lindahl, C. B. and Mahmood, T., 1995, Fluorine compounds, inorganic, in Howe-Grant, M., ed., Fluorine Chemistry: A Comprehensive Treatment: John Wiley and Sons, p. 27-33.

Loughnan, F. C., 1969, Chemical weathering of the silicate minerals: New York, American Elsevier Publishing Company, Inc..

Madhavan, M. and Subramanian, V., 2002, Fluoride in fractionated soil samples of Ajmer district, Rajasthan: Journal of Environmental Monitoring, v. 4, p. 821-822.

Malcherek, T., Domeneghetti, C. M., Tazzoli, V., Salje, E. K. H., and Bismayer, U., 1999, A high temperature diffraction study of synthetic titanite CaTiSiO4: Phase Transitions, v. 69, p. 119-131.

Mamatha, P. and Rao, S. M., 2010, Geochemistry of fluoride rich groundwater in Kolar and Tumkur Districts of Karnataka: Environmental Earth Sciences, v. 61, p. 131-142.

Mandinic, Z., Curcic, M., Antonijevic, B., Carevic, M., Mandic, J., Djukic-Cosic, D., and Lekic, C., 2010, Fluoride in drinking water and dental fluorosis: Science of the Total Environment, v. 408, p. 3507-3512.

Marechal, J. C., Ahmed, S., Engerrand, C., Galeazzi, L., and Touchard, F., 2006a, Threatened groundwater resources in rural India: An example of monitoring: Asian Journal of Water, Environment and Pollution, v. 3, p. 15-21.

Marechal, J. C., Dewandel, B., Ahmed, S. K., Galeazzi, L., and Zaidi, F.K., 2006b, Combined estimation of specific yield and natural recharge in a semi-arid groundwater basin with irrigated agriculture: Journal of Hydrology, v. 329, p. 281-293.

Mesdaghinia, A., Vaghefi, K. A., Montazeri, A., Mohebbi, M. R., and Saeedi, R., 2010, Monitoring of fluoride in groundwater resources of Iran: Bulletin of Environmental Contamination and Toxicology, v. 84, p. 432-437.

Meshri, D. T., 1995, Fluorine Compounds, Inorganic (Aluminum), in Howe-Grant, ed., Fluorine Chemistry: A Comprehensive Treatment: John Wiley and Sons, p. 33-47.

Middelburg, J. J., Van Der Weijden, C. H., and Woittiez, J. R. W., 1988, Chemical processes affecting the mobility of major, minor and trace elements during weathering of Granitic rocks: Chemical Geology, v. 68, p. 253-273.

Misra, A. K., Mishra, A., and Premraj, 2006, Escalation of groundwater fluoride in the Ganga Alluvial Plain of India: Fluoride, v. 39, p. 35-38.

Mondal, N. C., Prasada, R. K., Saxena, V. K., Singh, Y., and Singh, V. S., 2009, Appraisal of high fluoride zones in groundwater of Kurmapalli watershed, Nalgonda district, Andhra Pradesh (India): Environmental Earth Sciences, v. 59, p. 63-73.

Morton, A. C. and Hallsworth, C. R., 1999, Processes controlling the composition of heavy mineral assemblages in sandstones: Sedimentary Geology, v. 124, p. 3-29.

Motalane, M. P. and Strydom, C. A., 2004, Potential groundwater contamination by fluoride from two South African phosphogypsums: Water SA, v. 30, p. 465-468.

Msonda, K. W. M., Masamba, W. R. L., and Fabiano, E., 2007, A study of fluoride groundwater occurrence in Nathenje, Lilongwe, Malawi: Physics and Chemistry of the Earth, v. 32, p. 1178-1184.

Mueller, W. H., 1995, Fluorine compounds, inorganic (Sodium), in Howe-Grant, ed., Fluorine Chemistry: A Comprehensive Treatment: John Wiley and Sons, p. 186-188.

Munoz, J. L. and Ludington, S.D., 1974, Fluoride-hydroxyl exchange in biotite: American Journal of Science, v. 274, p. 396-413.

Muralidharan, D., Nair, A. P., and Sathyanarayana, U., 2002, Fluoride in shallow aquifers in Rajgarh Tehsil of Churu District, Rajasthan - an arid environment: Current Science, v. 83, p. 699-702.

Nalgonda Website, 2006, Nalgonda F levels www.nalgonda.org/fluorosis/fluoridelevels.htm, p. Accessed 2010.

Narayana, A. S., Khandare, A. L., and Krishnamurthi, M. V. R. S., 2003, Mitigation of Fluorosis in Nalgonda District Villages, p. 98-106.

Naseem, S., Rafique, T., Bashir, E., Bhanger, M. I., Laghari, A., and Usamani, T. H., 2010, Lithological influences on occurrence of high-fluoride groundwater in Nagar Parkar area, Thar Desert, Pakistan: Chemosphere, v. 78, p. 1313-1321.

Natarajan, V. and Mohan Rao, V. R., 1974, Hydrochemical investigation for fluorine bearing minerals in the Kangla and Hallia river basins, Nalgonda district, Andhra Pradesh, p. 37-46.

Natarajan, V. and Murthy, S. R. N., 1974, Fluorite bearing granites of Sivanagudem area, Nalgonda district, Andhra Pradesh, p. 49-53.

Nesbitt, H. W. and Young, G. M., 1984, Prediction of some weathering trends of plutonic and volcanic rocks based on thermodynamic and kinetic considerations: Geochimica et Cosmochimica Acta, v. 48, p. 1523-1534.

Nicolli, H. B., Suriano, J.M., Gomez Peral, M.A., Ferpozzi, L.H., and Baleani, O.A., 1989, Groundwater contamination with arsenic and other trace elements in an area of the Pampa, Province of Córdoba, Argentina: Environmental Geology and Water Science, v. 14, p. 3-16.

Nkotagu, H. H., 2009, Hydrogeochemistry of fluoride and salinization mechanism of groundwater in the Singida region, central Tanzania, in Titus, R., Beekman, H., Adams, S., and Strachan, L., eds., Water Research Commission, p. 80-90.

Nordstrom, D. K. and Jenne, E. A., 1977, Fluorite solubility equilibria in selected geothermal waters: Geochimica et Cosmochimica Acta, v. 41, p. 175-188.

Nouri, J., Mahvi, A. H., Babaei, A., and Ahmadpour, E., 2006, Regional pattern distribution of groundwater fluoride in the Shush aquifer of Khuzestan County, Iran: Fluoride, v. 39, p. 321-325.

Ozvath, D. L., 2006, Fluoride concentrations in a crystalline bedrock aquifer Marathon County, Wisconsin: Environmental Geology, v. 50, p. 132-138.

Padfield, T. and Grey, A., 1971, Major element rock analysis by X-ray Fluorescence - A simple fusion method: Philips Analytical Equipment Bulletin, v. FS35.

Pan, Y. and Fleet, M. E., 1990, Halogen-bearing Allanite from the White River Gold occurrence, Hemlo area, Ontario: Canadian Mineralogist, v. 28, p. 67-75.

Paoloni, J. D., Fiorentino, C. E., and Sequeira, M. E., 2003, Fluoride contamination of aquifers in the southeast sub-humid Pampa, Argentina: Environmental Toxicology, v. 18, p. 317-320.

Parkinson, D., 1999, Sources and controls of fluoride in groundwater of the Arusha Region, Northern Tanzania, [PhD Thesis]: UCL.

Pauwels, H. and Ahmed, S., 2007, Fluoride in groundwater: origin and health impacts: Geosciences - La revue du BRGM pour une terre durable, v. 5, p. 68-73.

Perez, E. S. and Sanz, J., 1999, Fluoride concentration in drinking water in the province of Soria (Central Spain) and caries in children: Environmental Geochemistry and Health, v. 21, p. 133-140.

Pettijohn, F. J., 1941, Persistence of heavy minerals and geologic age: The Journal of Geology, v. 49, p. 610-625.

Preston, J. and Smith, C.B., 2002, Amphibole Calculation Sheet.

Purushotham, D., Prakash, M. R., and Rao, A. N., 2010, Groundwater depletion and quality deterioration due to environmental impacts in Maheshwaram watershed of R.R. district, AP (India): Environmental Earth Sciences, v. Online.

Putnis, A., 1992, Introduction to mineral sciences: Cambridge University Press.

Rango, T., Bianchini, G., Beccaluva, L., and Tassinari, R., 2010, Geochemistry and water quality assessment of central Main Ethiopian Rift natural waters with emphasis on source and occurrence of fluoride and arsenic: Journal of African Earth Sciences, v. 57, p. 479-491.

Rao, A. T., Rao, G. A., and Rao, P. P., 1979, Fluorian allanite from calc-granulite and pegmatite contacts at Garividi, Andhra Pradesh, India: Mineralogical magazine, v. 43, p. 312.

Rao, N. S., 2003, Groundwater quality: focus on fluoride concentration in rural parts of Guntur district, Andhra Pradesh, India: Hydrological Sciences Journal, v. 48, p. 835-847.

Rao, N. S., 2006, Seasonal variation of groundwater quality in a part of Guntar District, Andhra Pradesh, India: Environmental Geology, v. 49, p. 413-429.

Rao, N. S., 2008, Fluoride in groundwater, Varaha River Basin, Visakhapatnam District, Andhra Pradesh, India: Environmental Monitoring and Assessment.

Rao, N. S. and Devadas, D. J., 2003, Fluoride incidence in groundwater in an area of Peninsular India: Environmental Geology, v. 45, p. 243-251.

Rao, N. V., Rao, N., Rao, K. S. P., and Schuiling, R. D., 1993, Fluorine distribution in waters of Nalgonda District, Andhra Pradesh, India: Environmental Geology.

Rao, P.B., Subrahmanyam, K., and Dhar, R.L., 2001, Geoenvironmental effects of groundwater regime in Andhra Pradesh, India: Environmental Geology, v. 40, p. 632-642.

Rashid, S. A., 2008, Major and trace elements distribution in a weathering profile of a granite gneiss at higher altitudes: Current Science, v. 95, p. 1474-1478.

Reddy, A. G. S., Reddy, D. V., Rao, P. N., and Prasad, K. M., 2010, Hydrogeochemical characterization of fluoride rich groundwater of Wailpally watershed, Nalgonda District, Andhra Pradesh, India: Environmental Monitoring and Assessment, v. 171, p. 561-577.

Reddy, D. V., Nagabhushanam, P., Sukhija, B. S., and Reddy, A. G. S., 2009, Understanding hydrological processes in a highly stressed granitic aquifer in southern India: Hydrological Processes, v. 23, p. 1282-1294.

Reddy, D. V., Nagabhushanam, P., Sukhija, B. S., Reddy, A. G. S., and Smedley, P. L., 2010, Fluoride dynamics in the granitic aquifer of the Wailpally watershed, Nalgonda District, India: Chemical Geology, v. 269, p. 278-289.

Reed, 1996, Electron Microprobe Analysis and Scanning Electron Microscopy in Geology.

Robinson, W.O. and Edgington, G., 1946, Fluorine in soils: Soil Science, v. 61, p. 353.

Rushton, K. R., 1986, Vertical flow in heavily exploited hard rock and alluvial aquifers: Ground Water, v. 24, p. 608.

Rutley, F., 1988, Rutley's elements of mineralogy: London, Unwin Hyman.

Sak, P. B., Fisher, D. M., Gardner, T. W., Murphey, K., and Brantley, S. L., 2004, Rates of weathering rind formation on Costa Rican basalt: Geochimica et Cosmochimica Acta, v. 68, p. 1453-1472.

Sarma, D. R. R. and Rao, A. L. N., 1997, Fluoride concentrations in ground waters of Visakhapatnam, India: Bulletin of Environmental Contamination and Toxicology, v. 58, p. 241-247.

Satsangi, G. S., Khare, A. L. P., Singh, S. P., Kumari, K. M., and Srivastavam S. S., 1998, Composition of rain water at a semi-arid rural site in India: Atmospheric Environment, v. 32, p. 3783-3793.

Savenko, A. V., 2001, Interaction between Clay Minerals and Fluorine-Containing Solutions: Water Resources, v. 28, p. 274-277.

Saxena, V. K. and Ahmed, S., 2003, Inferring the chemical parameters for the dissolution of fluoride in groundwater: Environmental Geology, v. 43, p. 736.

Saxena, V. K. and Ahmed, S., 2001, Dissolution of Fluoride in groundwater: A water-rock interaction study: Environmental Geology, v. 40, p. 1084-1087.

Shah, M. T. and Danishwar, S., 2003, Potential fluoride contamination in the drinking water of Naranji area, Northwest Frontier Province, Pakistan: Environmental Geochemistry and Health, v. 25, p. 475-481.

Siddiqui, A. H., 1955, Fluorosis in Nalgonda district, Hyderabad - Deccan: British Medical Journal, v. 2, p. 1408-1413.

Skjelkvåle, B. L., 2007, Factors influencing fluoride concentrations in Norwegian lakes: Water, Air and Soil Pollution, v. 77, p. 151-167.

Smedley, P. L., Nicolli, H. B., Macdonald, D. M. J., Barros, A. J., and Tullio, J. O., 2002, Hydrogeochemistry of arsenic and other inorganic constituents in groundwaters from La Pampa, Argentina: Applied Geochemistry, v. 17, p. 259-284.

Sreedevi, P. D., Ahmed, S., Made, B., Ledoux, E., and Gandolfi, J. M., 2006, Association of hydrogeological factors in temporal variations of fluoride concentration in a crystalline aquifer in India: Environmental Geology, v. 50, p. 1-11.

Srikantha, R., Viswanatham, K. S., Kahsai, F., Fisahatsion, A., and Asnekkash, M., 2002, Fluoride in groundwater in selected villages in Eritrea (North East Africa): Environmental Monitoring and Assessment, v. 75, p. 169-177.

Stecher, O., 1983, Fluorine in twenty-two international reference rock samples and a compilation of fluorine values for the USGS reference samples: Geostandards Newsletter, v. 7, p. 283-287.

Stolt, M. H., Baker, J. C., and Simpson, T. W., 1992, Characterization and genesis of saprolite derived from gneissic rocks of Virginia: Soil Science Society of America Journal, v. 56, p. 531-539.

Stormer, J. C. and Carmichael, I. S. E., 1970, Villiaumite and the occurrence of fluoride minerals in igneous rocks: The American Mineralogist, v. 55, p. 126-134.

Sujatha, D., 2003, Fluoride levels in the groundwater of the South-East part of Ranga Reddy District, Andhra Pradesh, India: Environmental Geology, v. 44, p. 587-591.

Tebbutt, T. H. Y., 1983, Relationship between natural water quality and health, Paris, UNESCO.

Tilley, D. B. and Eggleton, R. A., 2005, Titanite low-temperature alteration and Ti mobility: Clays and Clay Minerals, v. 53, p. 100-107.

Tindle, A., 2009, Chlorite formula unit calculator and variety namer, The Open University.

Tirumalesh, K., Shivanna, K., and Jalihal, A. A., 2007, Isotope hydrochemical approach to understand fluoride release into groundwaters of Ilkal area, Baglakot District, Karnataka, India: Hydrogeology Journal, v. 15, p. 598.

Toledo, M. C. M., Lenharo, S. L. R., Ferrari, V. C., Fontan, F., Parseval, P., and Leroy, G., 2004, The compositional evolution of apatite in the weathering profile of the Catalao I Alkaline-Carbonatitic Complex, Goias, Brazil: The Canadian Mineralogist, v. 42, p. 1139-1158.

Troll, G., Farzaneh, A., and Cammann, K., 1977, Rapid determination of fluoride in mineral and rock samples using an ion selective electrode: Chemical Geology, v. 20, p. 295-305.

Tseng, W. J., Lin, C. C., Shen, P. W., and Shen, P., 2005, Directional/acidic dissolution kinetics of (OH,F,CL)-bearing apatite: Journal of Biomedical Materials and Research Part A, v. 76, p. 753-764.

Tugrul, A. and Zarif, I. H., 1999, Correlation of mineralogical and textural characteristics with engineering properties of selected granitic rocks from Turkey: Engineering Geology, V. 51, p. 303-317.

Turner, B. D., Binning, P., and Stipp, S. L. S., 2005, Fluoride removal by Calcite: Evidence for fluorite precipitation and surface adsorption: Environmental Science and Technology, v. 39, p. 9561-9568.

Turner, B. F., Stallard, R. F., and Brantley, S. L., 2003, Investigation of in situ weathering of quartz diorite bedrock in the Rio Icacos basin, Luquillo Experimental Forest, Puerto Rico: Chemical Geology, v. 202, p. 313-341.

UNICEF, 2008, Fluoride in water: An overview.

Valenzuela-Vasquez, J., Ramirez-Hernandez, J., Reyes-Lopez, J., Sol-Uribe, A., and Lazaro-Mancilla, O., 2006, The origin of fluoride in groundwater supply to Hermosillo City, Sonora, Mexico: Environmental Geology, v. 51, p. 17-27.

Varughese, K. and Moreno, E. C., 1981, Crystal growth of calcium apatites in dilute solutions containing fluoride: Calcified Tissue International, v. 33, p. 431-439.

Vivona, R., Preziosi, E., Madé, B., and Giuliano, G., 2007, Occurrence of minor toxic elements in volcanic-sedimentary aquifers: a case study in central Italy: Hydrogeology Journal, v. Online only.

Warren, C., Burgess, W. G., and Garcia, M. G., 2005, Hydrochemical associations and depth profiles of arsenic and fluoride in quaternary loess aquifers of northern Argentina: Mineralogical magazine, v. 69, p. 877-886.

White, A. F., Blum, A. E., Schulz, M. S., Davidson, V. V., Stonestrom, D.A., Larsen, M., Murphy, S.F., and Eberl, D., 1998, Chemical weathering in a tropical watershed, Luquillo Mountains, Puerto Rico: I. Long-term versus short-term weathering fluxes: Geochimica et Cosmochimica Acta, v. 62, p. 209-226.

White, A. F., Blum, A. E., Schulz, M. S., Huntington, T. G., Peters, N .E., and Stonestrom, D.A., 2002, Chemical weathering of the Panola Granite: Solute and regolith elemental fluxes and the weathering rate of biotite: Water Rock Interactions, Ore Deposits, and Environmental Geochemistry: A Tribute to David A Crerar, v. The Geochemical Society, Special Publication No. 7, p. 37-59.

WHO, 1993, Guidelines for drinking-water quality. Second edition, Geneva, World Health Organisation.

Wilson, M., 1975, Chemical weathering of some primary rock-forming minerals: Soil Science, v. 119, p. 349-355.

Wondwossen, F., AstrØm, A. N., Bjorvatn, K., and Bårdsen, A., 2004, The relationship between dental caries and dental fluorosis in areas with moderate- and high-fluoride drinking water in Ethiopia: Community Dentistry and Oral Epidemiology, v. 32, p. 337-344.

Yong, L. and Hua, Z. W., 1991, Environmental characteristics of regional groundwater in relation to fluoride poisoning in North China: Environmental Geology and Water Science, v. 18, p. 3-10.

Young, S. M., Pitawala, A., and Ishiga, H., 2010, Factors controlling fluoride contents of groundwater in north-central and northwest Sri Lanka: Environmental Earth Sciences, v. Online.

Zhu, M. X., Ding, K. Y., Jiang, X., and Wang, H. H., 2007, Investigation of co-sorption and desorption of fluoride and phosphate in a red soil of China: Water, Air and Soil Pollution, v. 183, p. 455-465.

Zhu, M. X., Xie, M., and Jiang, X., 2006, Interaction of fluoride with hydroxyaluminium-montmorillonite complexes and implications for fluoride-contaminated acidic soils: Applied Geochemistry, v. 21, p. 675-683.

Appendix 1. An Experimental Study of Fluorapatite Scale Formation in Drinking Water

1.1 Abstract

Scale formation is a common problem in water supplies in the UK. In areas where phosphate (P) is added (to reduce lead concentrations at customer taps through plumbosolvency) along with fluoride (F) (for dental health reasons), fluorapatite ($Ca_{10}(PO_4)_6F_2$) scale can form. This is usually associated with heating systems and appliances.

This study aims to investigate the reaction kinetics and the factors governing apatite scale formation in water systems due to the addition of phosphate (as H_3PO_4) and fluoride (as NaF). This was done using generic synthetic waters (one hard water and one soft water) and phosphate and fluoride dosing in varying quantities (similar to those used by water companies) and at different temperatures. Concentrations of Calcium (Ca) and P were monitored and the results modelled using a sigmoidal curve which could be fitted to the data collected.

1.2 Introduction

The addition of both P and F to drinking water can lead to the precipitation of fluorapatite scale upon heating (particularly in areas where water is naturally high in Ca). In many areas of the UK, both of these elements are added to water supplies.

In 95% of the UK's water supplies, phosphate is added to reduce lead concentrations at customer taps through plumbosolvency reduction (phosphate acts as a corrosion inhibitor, reducing the ability of the water to dissolve lead, therefore reducing the concentration of lead in the water) (CIWEM policy, 2005). Lead, a poisonous substance, can build up in the body and cause health problems, especially in young children where it may affect mental development and growth (DWI Lead information 2008). The UKs maximum lead concentration in drinking water is currently 25ppm, which will be reduced to 10ppm in 2013 (3 Valleys Lead information guide, 2008). High lead concentrations are a problem particularly in areas with lead water pipes. Lead was generally used to make water pipes up to the 1970's (they are now mostly copper, iron or plastic). In the UK, approximately 40% of properties are supplied by lead pipes. Simply replacing all of the lead pipes is problematic for a number of reasons; ownership of the pipes may be split between the water supplier and the property owner, the cost of replacement is high (replacing all lead pipes in the UK would cost £8-10 billion), and in some areas the density of lead pipes may be high and cause considerable disturbance. Some water companies are undergoing a replacement scheme for lead pipes in public buildings and opportunistic replacements of lead connection pipes (CIWEM policy, 2005).

Plumbosolvency treatments require correct pH conditions (a pH higher than 8.0 is desirable), correct dosing (usually 0.5-1.5ppm P), sufficient organics removal and a lack of significant iron discolouration problems (CIWEM policy 2005).

Fluoride, an essential element which helps the formation of strong bones and teeth, is added to water supplies in some areas to reduce dental carries. The minimum recommended concentration of F in drinking water is 0.5ppm and the maximum is 1.5ppm. Concentrations greater than this may lead to fluorosis (brittle bones/teeth). Fluoridation of water supplies aims at a target concentration of 1ppm. Currently in England the water supply of around 6 million people has natural, or fluoridated water with 1ppm F. Water fluoridation in the UK is currently in practice in areas of the North West (e.g. Crewe), the West midlands (e.g. Birmingham) and the North East (e.g. Lincoln). The government department of health views water fluoridation as a way to improve oral health, especially of children in less affluent areas where tooth brushing may not be as regular as it should (Department of Health Guidance 2008). The 2003 Water Act legally requires water suppliers to carry out fluoridation of drinking water if requested to do so by a Strategic Health Organisation (DWI fluoridation 2008).

As in some areas both P and F are being added, upon heating this can lead to the formation of fluorapatite scale ($Ca_{10}(PO_4)_6F_2$). This can cause problems such as blockages and poor aesthetics in customers appliances (boilers, kettles), and hot water pipes. This study aims to investigate the factors governing the reaction kinetics. The experiments conducted followed a series of similar experiments run at the Natural History Museum (NHM).

1.3 Apatite – Structure and Chemistry

The most stable and common calcium phosphate minerals are apatites (general formula: $Ca_{10}(PO_4)_6(OH,F,Cl)_2$, with differences in OH, F and Cl causing differences in chemical behaviours). This includes the end members Fluorapatite ($Ca_{10}(PO_4)_6F_2$), Chlorapatite ($Ca_{10}(PO_4)_6Cl_2$), and Hydroxyapatite ($Ca_{10}(PO_4)_6OH_2$), and their solid solution. Fluorapatite is the most common of these. Substitutions can occur in the apatite structure, carbonate substitution for example (which can happen in two locations in the apatite structure) gives carbonate fluorapatite or carbonate hydroxyapatite. Natural Fluorapatite minerals have the space group $P6_3/m$, and usually differ from synthetic structures, possibly due to differences in anion ordering caused by impurities and vacancies (Hughes et al., 1989).

The precipitation of apatite from aqueous species can be written as:

$$10Ca^{2+} + 6HPO_4^{2-} + 2F^- = Ca_{10}(PO_4)_6F_2 + 6H^+$$

The precipitation of apatite is dependent on the super-saturation of the solution, with crystallisation in homogeneous solution taking place in two stages (nucleation and growth of the nuclei). Growth is suggested to be controlled by surface diffusion of the growth units to the active growth units.

Initial precursor phases may also be initially formed as more than one calcium phosphate may be supersaturated. The addition of fluoride to solutions already supersaturated with respect to hydroxyapatite is seen to significantly change precipitation kinetics (Varughese and Moreno, 1981).

The formation of apatite scale is associated with heating, where there are high concentrations of Ca, P and F in the water. This is because the solubility of fluorapatite decreases with increasing temperature (log Keq values become more negative. This is known as retrograde solubility, where solubility decreases with increasing temperature) (Walker and Valsami-Jones E., 2007). Therefore at higher temperatures, fluorapatite can precipitate at lower concentrations of P, Ca and F and at lower pH values.

Fluorapatite dissolution has also been found to be dependent on pH (Giudry and MacKenzie, 2003).

Several difficulties may be found when conducting spontaneous precipitation experiments. Low reproducibility and low accuracy can result from changes in the supersaturated phase as the experiment progresses (due to the precipitation phase lowering the ionic activities of the precipitation components), or phases forming and subsequently dissolving yielding a different calcium phosphate. Seeded experiments can be done at lower super-saturations, however these tend to precipitate rapidly (Valsami-Jones E. and Wilson, 2003).

1.4 Methodology

In order to investigate the precipitation of fluorapatite scale in drinking water, two synthetic waters were produced (one hard and one soft water) using the method outlined by Smith et al 2002. The chemical composition of these waters according to Smith et al (2002) is shown in table a.1-1. The composition of the soft water did not vary significantly through the experimentation period. The composition of the hard water remained fairly constant for 9 months, but then was remade using the same method due to declining Ca concentrations.

In order to investigate the reaction kinetics and factors governing apatite scale formation, experiments were run to investigate the affects of varying P and F dosing, temperature (min 25°C, max 85 °C) and pH in both of the synthetic waters.

Previous studies at the NHM have shown that variations of temperature and P concentration to have the greatest impact on the onset time of precipitation of fluorapatite, therefore these parameters were varied widely to see the resulting changes.

Dosing concentrations similar to those used in the water industry were chosen for investigation (F dosing of 0.5-1.5ppm, P dosing of 0.5-2.0ppm). P was added as H_3PO_4, and F was added as NaF. PH was adjusted using NaOH or HNO_3 (as these would not affect the initial saturation of hydroxyapatite or fluorapatite end members). The parameters used for the experiments are shown in table a.1-2.

One hundred ml of the synthetic waters (dosed with P and F, and pH adjusted) was placed in a bottle and heated and shaken in a hot water bath, with 2ml samples of the water taken every 2 hours. The samples were filtered through a 2um filter, and stabilised

using 2% HNO_3. Analysis was by ICP-AES. It is important to make sure that no particles enter the samples as they may act as seeds to aid precipitation. Blank runs with no P or F dosing or pH adjustments were also run.

Table A.1-1- chemical composition of hard (Rostherne Mere) and soft (Esthwaite) waters made according to (Smith et al., 2002)

The precipitation of apatite was monitored by the concentration of P in solution as this was the most sensitive an indicator of precipitation; Ca concentrations are fairly high in the synthetic waters (at least in the hard water) and would therefore only show a small change, and F losses would be much smaller due to the stoichiometry of fluorapatite.

Table A.1-2 - Hard and soft water propensity tests showing the dosing, temperature and pH variations used for experiments. Each experiment was repeated (between two and four repeat runs). H denotes experiments using synthetic hard water, and S denotes experiments using synthetic soft water. Comments of 'rapid ppt' denote rapid precipitation. Times given in comments column indicate rough onset times of precipitation.

P and F dosing H water - 85					
Test No.	**P (ppm)**	**F (ppm)**	**pH**	**Temperature**	**Comments**
H1	0.9	0.5	8.0	85	Rapid ppt
H2	1.5	0.5	8.0	85	Rapid ppt
H3	2.0	0.5	8.0	85	Rapid ppt
H4	0.9	1	8.0	85	Rapid ppt
H5	1.5	1	8.0	85	Rapid ppt
H6	2.0	1	8.0	85	Rapid ppt
H7	0.9	1.5	8.0	85	Rapid ppt
H8	1.5	1.5	8.0	85	Rapid ppt
H9	2.0	1.5	8.0	85	Rapid ppt

Ph differences - 85					
Test No	**P(ppm)**	**F(ppm)**	**pH**	**Temperature**	**comments**
H10	1.5	1	8.5	85	Rapid ppt
H11	1.5	1	7.4	85	Rapid ppt

P and F dosing S water - 85					
Test No.	**P (ppm)**	**F (ppm)**	**pH**	**Temperature**	**comments**
S1	0.9	0.5	7.8	85	60-140hrs
S2	1.5	0.5	7.8	85	30-50h
S2b	1.5	0.5	7.8	85	5-22hr
S3	2.0	0.5	7.8	85	30-50h
S3b	2.0	0.5	7.8	85	5-22hr
S4	*0.9*	*1*	*7.8*	*85*	2-18h
S5	1.5	1	7.8	85	No Change
S6	2.0	1	7.8	85	Rapid ppt
S7	0.9	1.5	7.8	85	Rapid ppt
S8	1.5	1.5	7.8	85	Rapid ppt
S9	2.0	1.5	7.8	85	Rapid ppt
S10	0.5	1.0	7.8	85	Rapid ppt

S water with lower P dosing					
Test No	**P(ppm)**	**F(ppm)**	**pH**	**Temperature**	**comments**
S24	0.5	0.5	7.8	85	Rapid ppt
S25	0.5	1	7.8	85	Rapid ppt
S27	0.75	0.5	7.8	85	Quick
S28	0.75	1	7.8	85	Quick
S40	0.5	0.75	7.8	85	100-200 hrs
S41	0.9	0.75	7.8	85	~40 hrs
S42	1.5	0.75	7.8	85	~5 hrs

1 litre H and S - 55					
Test No	**P(ppm)**	**F(ppm)**	**pH**	**Temperature**	**comments**
H12 – 1litre	3.9	3	8.0	55	No Change
S12- 1 litre	3	3	7.8	55	No Change

Temperature change H water					
Test No	**P(ppm)**	**F(ppm)**	**pH**	**Temperature**	**Observations**
H14	0.9	1.5	8.0	55	No Change
H15	1.5	1.5	8.0	55	~25hrs
H16	2.0	1.5	8.0	55	No Change
H17	0.9	1.5	8.0	25	No Change
H18	1.5	1.5	8.0	25	No Change
H19	2.0	1.5	8.0	25	No Change
H20	0.9	1.5	8.0	70	by 100hrs
H21	1.5	1.5	8.0	70	by 100hrs
H22	2.0	1.5	8.0	70	by 100hrs
H23	0.9	1.5	8.0	55	Between 200 and 500 hours
H24	1.5	1.5	8.0	55	No Change
H25	2.0	1.5	8.0	55	No Change
NH26	0.9	0.3	8.0	85	Rapid ppt
NH27	1.5	0.3	8.0	85	Rapid ppt
NH28	2.0	0.3	8.0	85	Rapid ppt

Temperature change S water					
Test No	**P(ppm)**	**F(ppm)**	**pH**	**Temperature**	**Observations**
S34	0.9	1	7.8	70	No Change

S35	1.5	1	7.8	70	No Change
S36	2.0	1	7.8	70	No Change
S37	0.9	1	7.8	55	No Change
S38	1.5	1	7.8	55	No Change
S39	2.0	1	7.8	55	No Change

1.5 Sigmoidal Curve fitting

The changes in the concentration of P in solution with time can be fitted to a four parameter sigmoidal curve of the form:

$$y = y0 + \frac{a}{1 + exp^{-\left(\frac{x-x0}{b}\right)}}$$

where y is concentration of P (ppm), x is time (hours/days), y0 is the initial concentrations of P, a is the negative difference between the initial and final concentrations of P (therefore usually close to y0), x0 is the midpoint at the steepest gradient of the sigmoid curve (in hours), and b is a constant (Wilson and Valsami-Jones E., 2004).

The sigmoid curve has three key stages relevant to this study. The first stage marks the onset stage when P concentration in the solution is constant and associated with the formation of crystal nuclei in the solution. The second stage is marked by a rapid decrease in P concentration and associated with the major phase of fluorapatite precipitation from the solution. The third and final stage marks the loss of P from the solution (Wilson and Valsami-Jones E., 2004). Figure A.2-1 shows an example of the curve fitted to P concentration, and the stages of the curve.

Figure A.1-1 - Example of curve fitting to reducing P concentrations in solution, showing the induction period and precipitation periods 1 and 2 (Wilson and Valsami-Jones E., 2004).

From the curve (by taking derivatives) it is possible to calculate:

- The onset time of precipitation
- The end of precipitation
- The maximum rate of precipitation
- The average rate of precipitation
- These values can be used to quantify the reaction kinetics for each experiment.

1.6 Results and Discussion

Temperature variations

Temperature has a large effect on precipitation rates. This is as would be expected, as the solubility of fluorapatite decreases with increasing temperature (as discussed above).

Figure A.1-3 and figure a.1-4 show results from the temperature experiments. At 25°C no significant change in P concentrations occurred in both the soft and hard waters (figure a.1-3 and figure a.1-4). Soft water (S-water) experiments showed no changes at 55 °C after one week in the 100ml experiments (figure a.1-3), or after 6.5 weeks in the 1 liter experiments (figure a. 1-2). No change is seen at 70°C after 200 hours. A decrease in P is only seen at 85 °C, and this is fairly rapid (within 2-4 hours).

This is different to the hard water (H-water) experiments (figure a.1-4), which show no change at 25 °C, but do show a decrease in P at 55°C. However this does not happen until 40-90 hours. In the 1 liter experiments (figure a. 1-2) this was sometime between 20 and 45 weeks (unfortunately no data is available in between these dates). In the 100ml experiments (figure a.1-4), the lowest concentration of P (0.9ppm) showed no change at 55°C even after 3 weeks (500 hours), whereas the higher P concentration experiments showed a decrease in P at 55°C by 500 hours (not shown in figure). The hard water experiments also showed a decrease in P concentrations at 70°C by 100 hours. At 85°C P was rapidly depleted (within the first 2-4 hours) as seen in figure a.1-4.

All of the further hard water experiments conducted at 85°C showed a similar rapid decrease in P concentrations, in these cases no comparisons were possible between different P and F dosing and pH.

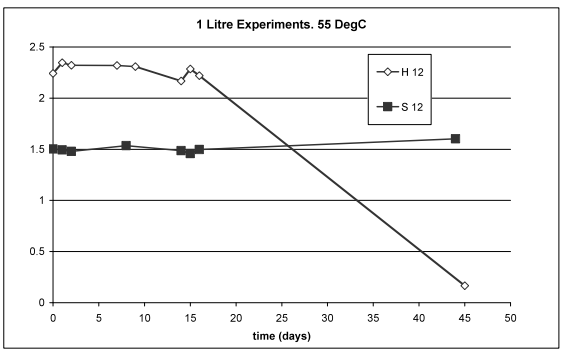

Figure A. 1-2- 1 liter dosing experiments. H12 dosed with 3.9ppm P and 3ppm F, S12 dosed with 3ppm F and 3ppm P.

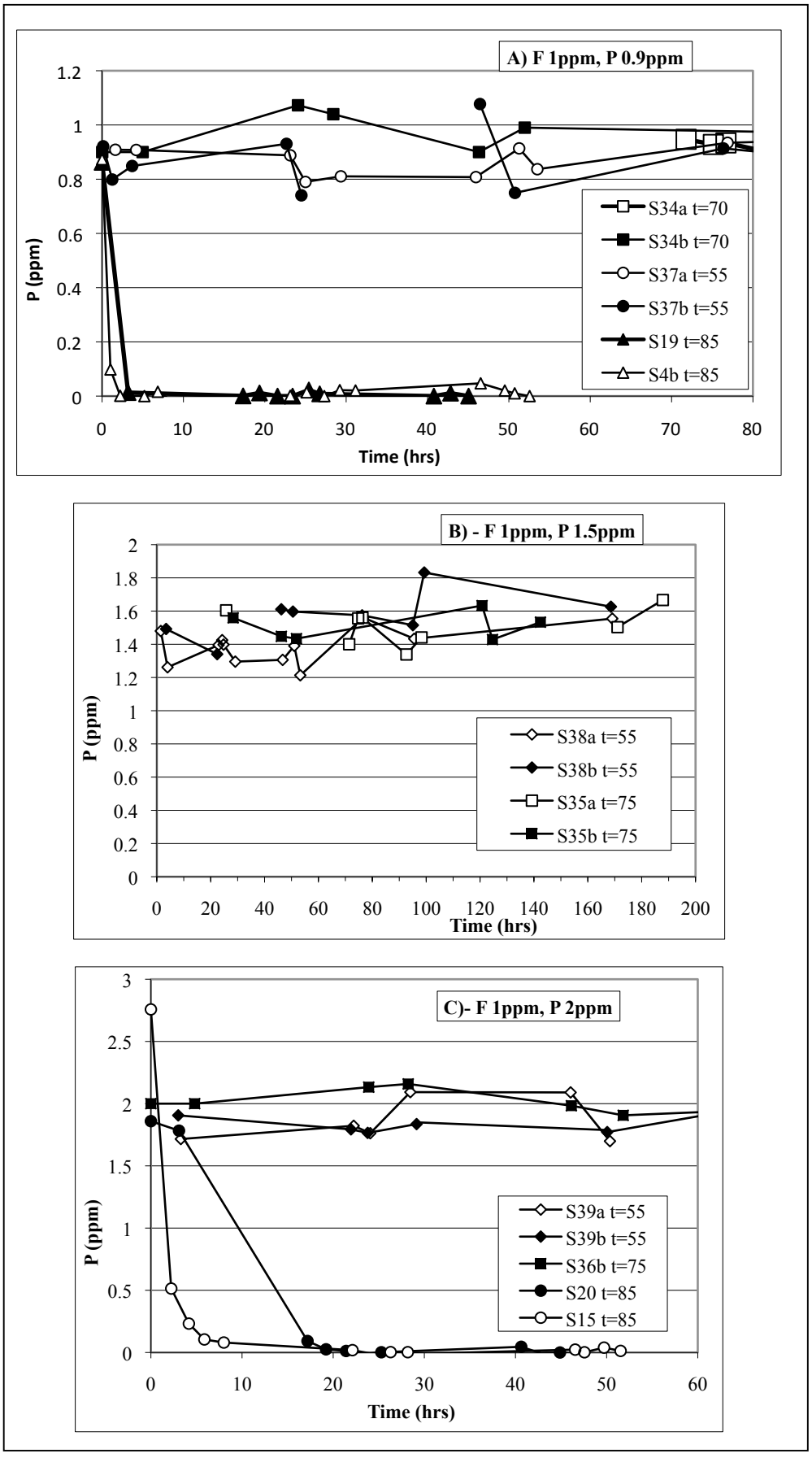

Figure A.1-3- Temperature (t) variations Soft Waters. F dosing constant at 1ppm for all figures. P dosing in A) - 0.9ppm, in B) – 1.5ppm, C) - 2ppm.

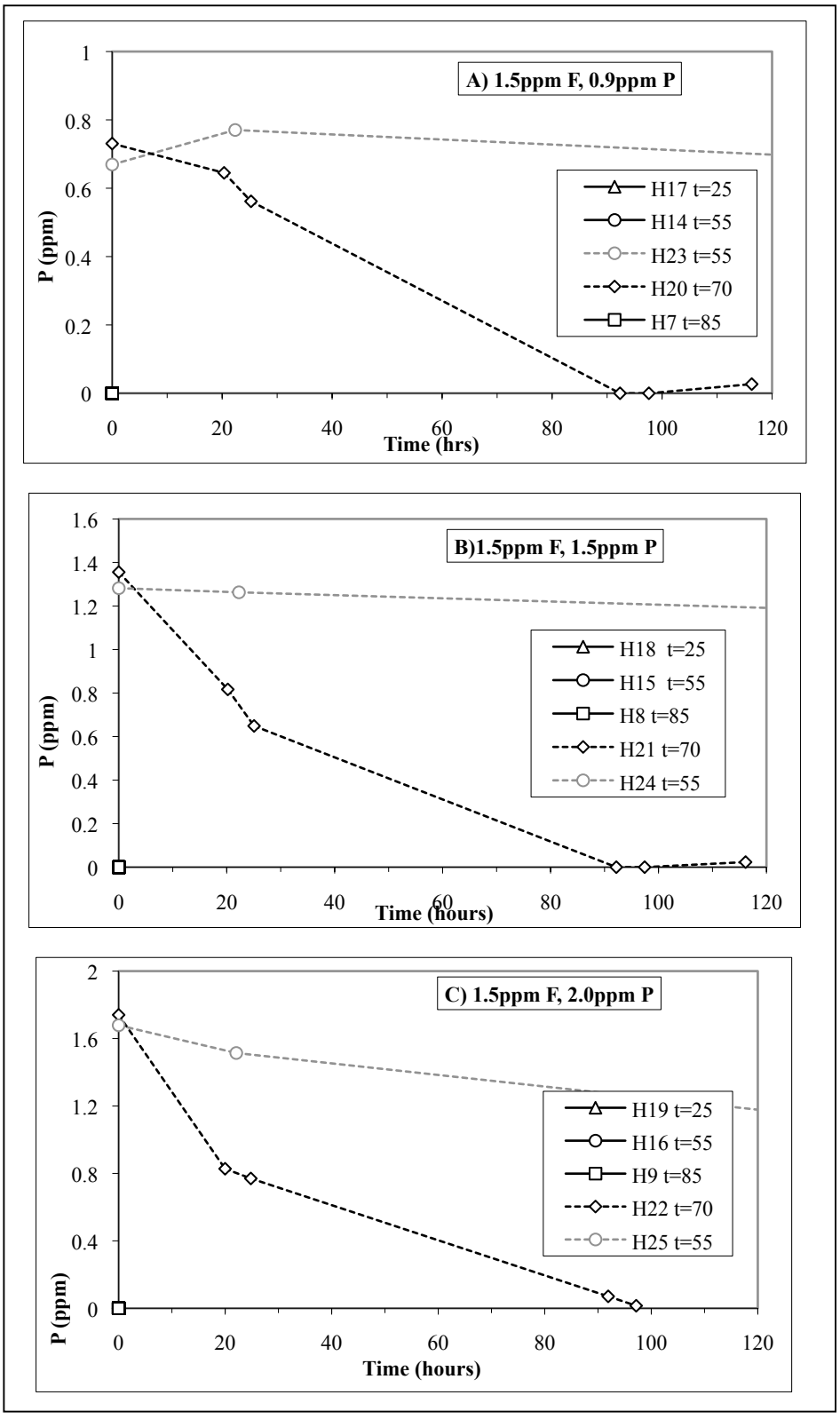

Figure A.1-4. Variations in Temperature (t) in Hard water P and F dosing experiments. F dosing fixed at 1.5ppm. P dosing varies, in A) - 0.9ppm P, in B) – 1.5ppm P, in C) -2.0ppm P

P and F dosing

The soft water experiments conducted at 85 °C showed a slower onset to that of the hard water experiments, allowing comparisons between P and F dosing and sigmoidal curve plotting. Blank runs showed little changes in P over time. Figure A. 1-5 to figure a. 1-7 show P dosing of soft water. Sigmoidal curve plotting was used to model this data and find onset times (table a. 1-3), however this was only possible for S2 and S3 (and repeats) and S41 and S42, due to poor lack of data around the onset time in S1 (and S1b), and S40. The repeats of S1-3 are shown in figure a. 1-6. It can be seen in this figure, and in table a. 1-3, that although both sets of repeats show a similar relationship (higher P dosing giving shorter onset times), the actual onset times are very different. Repeat experiments in this project often showed different results for onset times (although similar relationships) highlighting the difficulties in repetition of precipitation kinetics experiments (mentioned previously).

These experiments show that the onset time of precipitation is affected by the P dosing, with higher P dosing leading to reduced onset times. This is quantified in the sigmoidal curve plotting, where the onset time and final time are greater for S2 than S3 and also greater for S41 than S42.

Higher F values are also seen to lead to reduced onset times (figure a.1-8) however this was only seen here for one set of parameters.

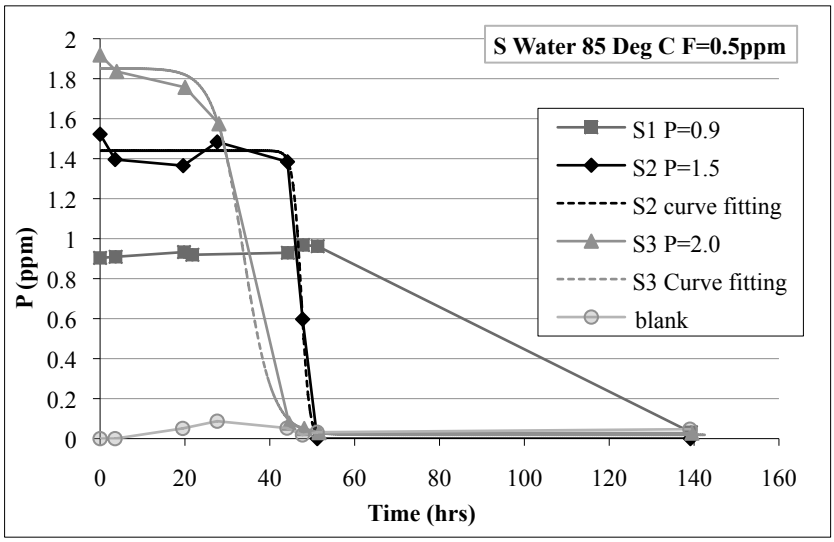

Figure A. 1-5 - P dosing of Soft water. F concentration set at 0.5ppm. Dotted line shows curve fitting. T = temperature.

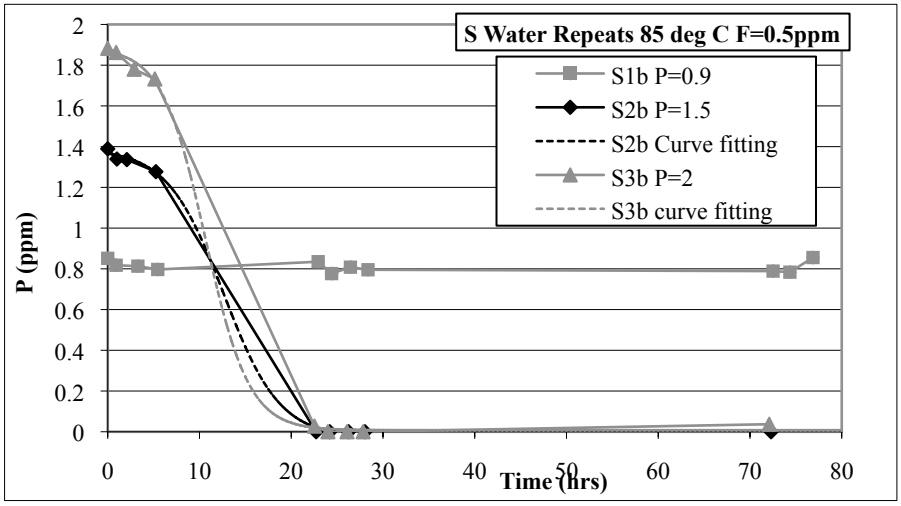

Figure A. 1-6 - S water repeats of S1b-S3b. P dosing of Soft water, F concentration set at 0.5ppm. Dotted line shows curve fitting. T = temperature.

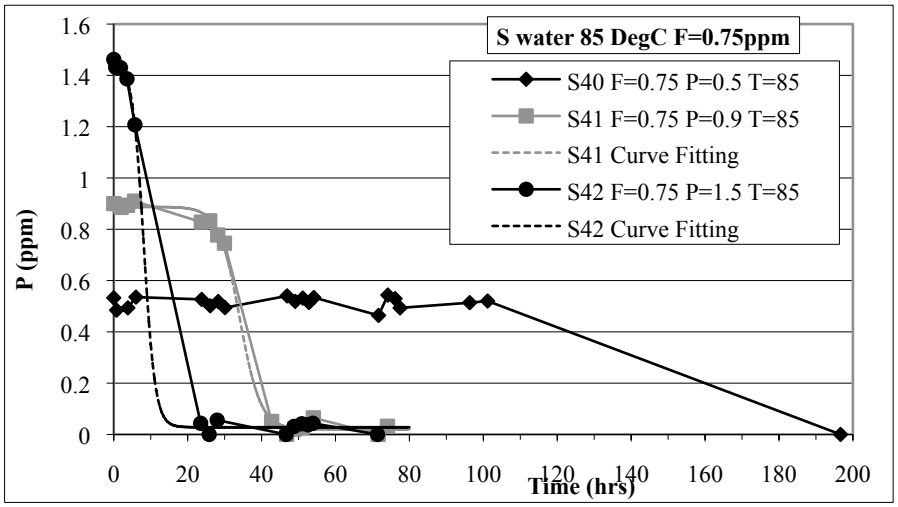

Figure A. 1-7 - P dosing of Soft water. F concentration set at 0.75ppm. Dotted lines show curve fitting. T = temperature.

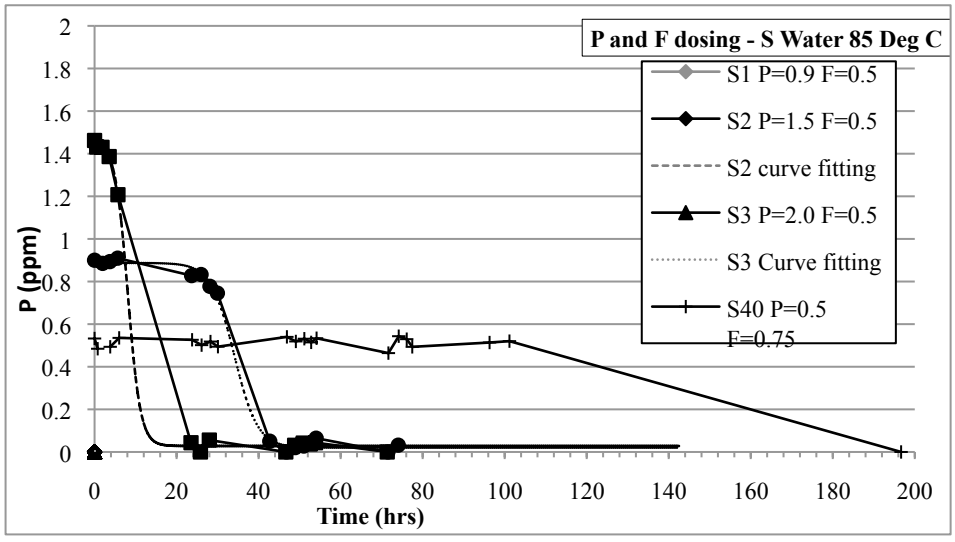

Figure A.1-8- Comparing F dosing and P dosing. Dotted lines show curve fitting

Table A. 1-3- Sigmoidal curve fitting for S2 and S3 (and repeats of these), and for S41 and S42. Curve plotting only possible for S2, S3, S2b, S3b, S41 and S42 due to poor data around the onset time in S1, S1b and S40.

Sample	pH	P	F	Onset time	Final time	Ave rate (ppm/hr)	Max rate (ppm/hr)
S2	7.8	1.5	0.5	46.160	48.678	0.333	0.380
S3	7.8	2	0.5	29.234	38.232	0.118	0.134
S2b	7.8	1.5	0.5	8.598	16.642	0.102	0.116
S3b	7.8	2.0	0.5	7.522	13.794	0.173	0.197
S41	7.8	0.9	0.75	30.340	37.810	0.067	0.076
S42	7.8	1.5	0.75	6.076	10.141	0.203	0.231

Hard water P dosing experiments at the same temperatures (85 ˚C) and dosing showed immediate decreases in P concentrations (figure a. 1-9). No comparisons were possible from this data. Hard water F dosing experiments (85˚C) also showed a rapid decrease in P concentrations (figure a. 1-10).

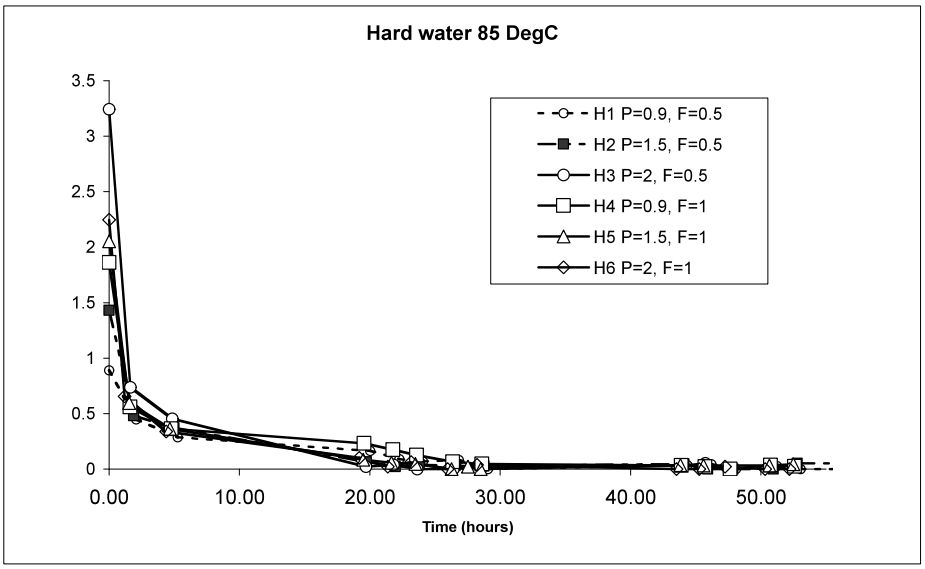

Figure A. 1-9- Hard water P and F dosing experiments at 85 °C.

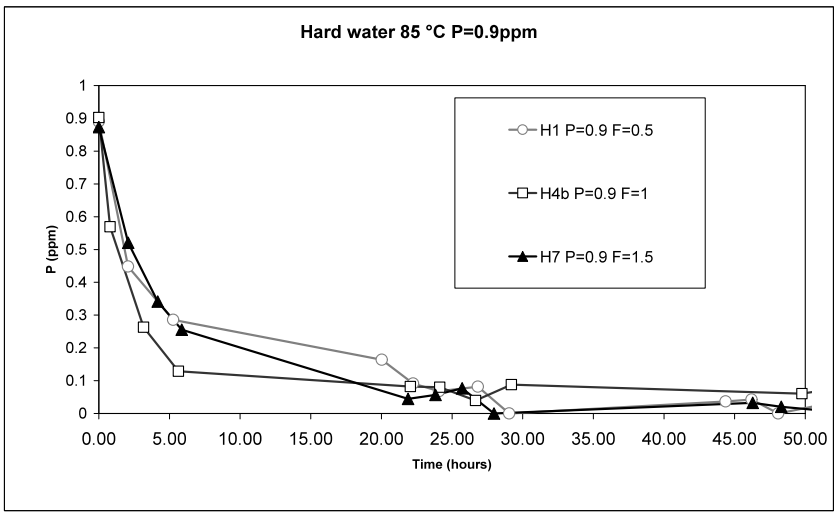

Figure A. 1-10- F dosing. P=0.9. 85 ˚C.

Hard water pH experiments were also carried out at 85 ˚C (figure a. 1-11). These also show a rapid decrease in P concentration, and no curve plotting was possible. However it is possible to see from the graph a rough trend of faster precipitation at higher pH values, although this cannot be quantified.

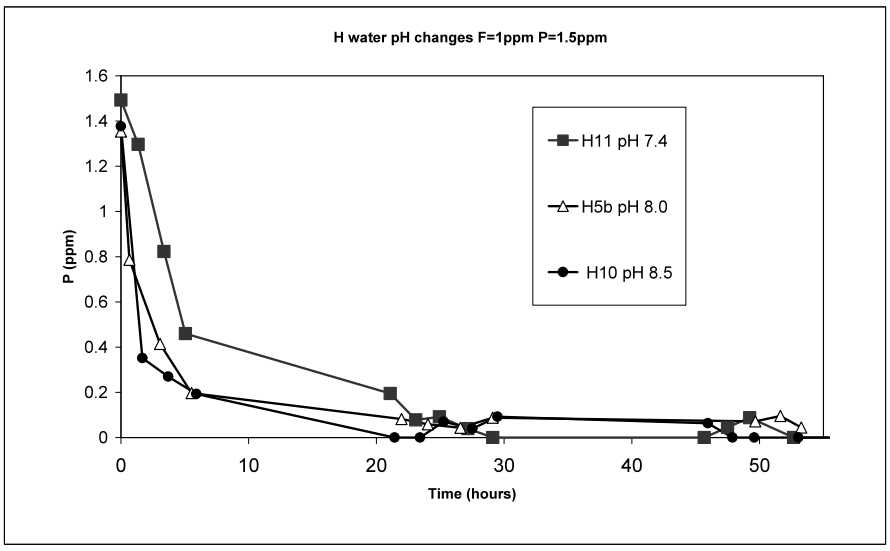

Figure A. 1-11- H water pH experiments. F=1ppm, P=1.5ppm, 85 ˚C.

1.7 Conclusions

Analysis of the results of these experiments were difficult due to short precipitation onset times (so that they could not be measured) and low reproducibility of results. This can be shown in the differences between repeats of S-water experiments S1-S3 (figure a. 1-5 and figure a. 1-6). Although in both sets of experiments, the trend of shorter onset times of precipitation with increasing P were seen, the timings were very different when comparing sets.

Soft water temperature experiments showed no precipitation occurred at or below 75˚C, but did occur at 85˚C (figure a.1-3). H water experiments showed precipitation did occur at 70˚C and above, but not at 55˚C or lower (figure a.1-4).

Both S-water and H-water experiments showed the importance of temperature on apatite precipitation. Increasing temperatures reduce the solubility of fluorapatite and allows precipitation at lower P and F concentrations than would be necessary for precipitation at lower temperatures. The H-water experiments show this relationship more fully with precipitation onset time being shorter at 85˚C than at 70˚C. The lack of precipitation at 70 ˚C in the S-water experiments compared to the H-water experiments is probably due to the different hardness and concentrations of Ca in the waters (i.e. initial saturation index of apatite in solution).

From the Soft water P dosing experiments (S1-3 and repeats, figure a. 1-5 and figure a. 1-6), it can be seen that onset times of precipitation are affected by initial P concentrations, with higher concentrations corresponding to shorter onset times. This can be shown by the onset times calculated from the sigmoidal curve plotting (table a. 1-3). Initial F concentrations are also seen to affect onset time of precipitation in figure a.1-8 (and associated sigmoidal curve plotting in table a. 1-3), again showing shorter onset times with higher F concentrations.

H-water dosing experiments at 85 ˚C showed rapid loss of P within the first hour or two (figure a. 1-9), which did not allow for comparisons. F dosing experiments in both H-water and S-water showed similar rapid loss of P in the initial stages (figure a. 1-10).

These precipitation rates are very high for such waters and concentrations of F and P (which are close to the levels added, or the required concentrations, of water companies). Previous experiments on apatite precipitation at the NHM showed much slower onset times for hard and soft waters of very similar concentrations. The differences may be due to small differences in water chemistry, or due to the presence of seeds in these experiments (such as small amounts of dust etc). Full caution was taken to avoid this. The low reproducibility of these results show that these experiments can be slightly unpredictable.

1.8 Further Work

There are several areas of this study that can be developed further, some of which may be investigated in the coming year. This future work includes:

- Scale characterisation (of that produced in the lab from dosing of both the hard and soft synthetic waters)
- Analysis of fluorine concentrations with time.
- Carbonate analysis of the synthetic waters to investigate the effect of carbonate on fluorapatite precipitation

- Further experiments using different water compositions and/or different temperatures to achieve more results that can be compared and analysed using sigmoidal curve fitting, to quantify the precipitation kinetics.
- Analysis of the synthetic waters and modelling of the reactions using PHREEQC.
- Comparison with precipitation in natural waters (rather than synthetic waters)

References Cited

Giudry, M.W. and MacKenzie, F.T., 2003, Experimental study of igneous and sedimentary apatite dissolution: Control of pH, distance from equilibrium, and temperature on dissolution rates: Geochimica et Cosmochimica Acta, v. 67, p. 2949-2963.

Hughes, J.M., Cameron, M., and Crowley, K.D., 1989, Structural Variations in natural F, OH and CL apatites: American Mineralogist, v. 74, p. 870-876.

Smith, E.J., Davidson W., and Hamilton-Taylor, J., 2002, Methods for preparing synthetic freshwaters: Water Research, v. 36, p. 1286-1296.

Valsami-Jones E. and Wilson, J., 2003, Calcium Phosphate Scale Formation. Natural Hisotry Museum desk study report, Research and Consultancy Project.

Varughese, K. and Moreno, E.C., 1981, Crystal growth of calcium apatites in dilute solutions containing fluoride: Calcified Tissue International, v. 33, p. 431-439.

Walker, C. and Valsami-Jones E., 2007, Fluorapatite scale study. Natural History Museum Progress report, Research and Consultancy Project.

Wilson, J. and Valsami-Jones E., 2004, Calcium phosphate scale formation. Natural History Musuem progress report, Consultancy and Research Project.

Appendix 2. Details of Analytical Methods

2.1 Thin Section Preparation:

A rectangular slab of rock (approximate dimensions 2.5×5×1.5 cm) was cut using a rock saw. This was ground to ensure the slab is completely flat and of the appropriate dimensions. The slab is then ground further using a Logitech machine with 300 then 600 dpi grit for ~10 minutes. The flatness of the slab is checked, and if completely flat, the slab is mounted onto a piece of cut glass of specified thickness and size (using a hot plate, mounting adhesive and press), reduced in thickness using a Petri-Thin machine (which grinds down the surface of the rock), ground further on the Logitech, then ground by hand using 320, 600 and finally 1000 dpi grit until the sample is of the appropriate thickness (quartz should move from pink to yellow to white as the thickness decreases). The sample is then polished further and either covered for optical microscope work or left uncovered for EM work.

2.2 Whole Rock Chemistry Method

Sample whole rock chemistry (WRC) was measured at the Natural History Museum (NHM) using the following method:

- Weigh 100 ±2 mg of sample in a clean platinum/5% gold crucible
- Weigh 300 ± 10 mg of lithium metaborate (LiBO2) flux into the crucible.
- Mix the sample and the flux together by stirring with a platinum rod or spatula
- Heat the crucible over a meker burner, covering the ½ to ¾ of the crucible with the lid. The flux will melt and the fusion should begin. Swirl the melt occasionally to ensure there is no sample powder residue and that the molten material is together.
- Continue heating until fusion is complete (~10 minutes)
- Carefully roll the molten bead around the inside of the crucible to collect any residue, the tip the crucible so that the molten bead rolls to the side of the crucible. Remove from the heat and allow the bead to cool on the side of the crucible.
- Direct a jet of water on the outside of the crucible on the side that the bead is cooling on to help the bead break cleanly from the crucible side.
- Tip the bead into approximately 100 ml of 10% HNO3 in a plastic beaker. Stir with a magnetic flea.
- Pour some of the solution in the beaker back into the crucible to dissolve any residue (leave this for 1 hour, and then return the solution to the plastic beaker).

- Place a lid over the beaker and continue stirring the solution until the bead dissolves (leave overnight).
- To check that the crucible is clean, heat it uncovered to bright red heat for about 10 minutes. Any Iron for example, that has alloyed with the Pt/Au will appear on the surface as a dark stain that can be removed with a small amount (1ml) of concentrated HCl, which should be placed on a hot plate for 10-15minutes and then the solution added to the beaker containing the dissolving fusion bead.
- Once the bead is dissolved, transfer the solution into a 250ml volumetric flask, ensuring that all of the liquid is washed into the flask and none is lost (washing the lid, beaker, magnetic flea and funnel used with deionised water and adding this liquid to the volumetric flask). Make the volume up to 250ml with deionised water and mix well by inverting and shaking the flask at least 3 times.
- Transfer 50ml of the solution to a plastic bottle for storage, washing the bottle out with the solution from the volumetric flask twice beforehand.
- Discard the remaining liquid and wash the volumetric flask and funnel 3 times with deionised water.
- Samples are analysed using ICP-AES

Two repeat samples were prepared (M2a –porphyritic biotite granodiorite and W17a, pegmatite epidote quartz syenite). Repeat measurements give similar results indicating a good method and well mixed samples (Table A. 2-1).

Table A. 2-1– Repeat whole rock chemical analysis of sample W17a

W17a	Al2O3	CaO	Fe2O3	K2O	MgO	MnO	Na2O	P2O5	SiO2	TiO2
WRC -1	17.6	1.12	0.80	11.4	0.08	0.008	2.17	<	64.0	0.03
WRC -2	17.7	1.10	0.80	11.4	0.08	0.008	2.14	<	64.3	0.02
Difference	0.04	-0.02	0.00	-0.03	0.00	0.00	-0.02	-	0.32	0.00

2.3 Whole Rock Fluorine method, after Ingram 1970.

The method used was that of Ingram (1970), with minor alterations (see below). The method involves preparing and measuring a set of standard F solutions, and the preparation and measurement of dissolved sample solutions.

Preparing Standard Solutions:

A range of solutions were prepared of known F concentrations for use as standards to calibrate the fluoride ISE. These were prepared from a known standard solution (1000ppm F) diluted with deionised water into plastic volumetric flasks. The range of standards used was as follows:

- 0.25-10ppm F (first 2 calibrations). Lowest calibrated F value 250 ppm F
- 0.1 to 10 ppm F (next 3 calibrations). Lowest calibrated F value 100 ppm F
-

Measurement and calibrating was done using the following method:

- 10ml of standard solution and 10ml of TISAB (total ionic strength adjustment buffer) were added to a plastic beaker
- The solution is measured using the ISE, the mV reading taken after a total of 3 minutes (with the solution stirred using a magnetic stirrer for the first minute)
- After each measurement the ISE is rinsed with deionised water and dried
- The same method of measurement is used for the samples as the standards. ISE readings for the lowest standard (0.1 ppm F) may take longer to stabilise, therefore this standard is measured for a longer period of time with mV readings noted with time. It was found that the initial reading of the day took up to 10 minutes to stabilise, but subsequent (later?) readings of low standards stabilised within the 3 minutes.
- Values of mV should decrease with increasing F concentration, and should give a range of approx. 54-59 mV difference between standards with F concentrations an order of magnitude different (the electrode slope)
- Standard values are plotted with log F concentrations on the x-axis and mV on the y-axis. A trend line is drawn through the plotted values, giving an equation for the calculation of F concentrations in samples from mV readings
- Three chosen standards (0.1, 1 and 10ppmF) are measured frequently (after ever 4-5 samples measured) to check for drift, and the full set of standards are measured at least after every 12 samples measured (in some cases more frequently than this)

Sample Preparation:

The samples were analysed in two sets using the following method:

- Crush and powder rocks to form a fine powder
- Weigh approximately 0.2 g of sample in a platinum crucible, recording the exact weight (to 3 or 4 decimal places)
- Weigh 1g of sodium carbonate into the crucible

- Weigh 0.2g of zinc oxide into the crucible
- Mix thoroughly with a plastic tipped rod
- Place the crucible with lid in a furnace at 950 °C for 1 hour and 30 minutes. The lid should not be fully covering the crucible, but left with a small gap at the side. Remove and allow to cool
- Place crucible in a plastic beaker and fill with deionised water so that the level of water is just above the edge of the crucible.
- Cover the beaker with a plastic lid to reduce loss by evaporation
- Place the beaker in a steam bath and leave for 12 hours
- Remove the beaker from the steam bath. Remove the crucible from the beaker and wash the inside and outside with deionised water, emptying the washing water back into the plastic beaker. Break up any loose bits in the crucible and wash into the beaker.
- Filter the contents of the beaker through a 40 watman filter paper in a filter funnel, into a plastic 200ml volumetric flask.
- Wash down the filter paper with 0.1 sodium carbonate solution
- Add 2ml of 50% HCL and shake well
- Pipette out 10ml of sample into a plastic beaker. Add to this 10ml of TISAB buffer
- Measure samples using the ISE in the same way as the standards are measured (total of 3 minutes, stirred with a magnetic stirrer for the first minute)
- Rinse the fluoride ion selective electrode with deionised water between each use
- To find the F values of the samples from mV readings use the equation of the trend line plotted from the standard samples, multiply by 1000 and then multiply by 0.2/actual weight of the sample measured during sample preparation

Repeats of several samples were prepared, as well as repeat ISE measurements of all the sample solutions. Repeat samples and repeat measurements are averaged to give final F concentration. One geological sample (G2) was also prepared for measurement.

Method development:

The method was developed from the Ingram (1970) method to maximise the removal of F from the sample and according to the performance of the Fluoride ISE. Developments included using a larger weight of sample, sodium carbonate and zinc oxide, increasing the dilution volume and increasing the time in the furnace and in the steam bath. Results from early trial measurements (using a different ISE electrode – ELIT model 8221) and later measurements using the developed method (using a more stable ISE, EDT model QSE333) as well as mass balance total F values are given in Table A. 2-2.

ISE Measurements

ISE mV readings should be higher for higher F solutions. The ISE is immersed in the solution (both the standards and the samples) for a set length of time, set at 3 minutes for both runs. The initial measurement of the run (of the lowest standard solution) was found to take a longer time to stabilise than later readings. Therefore the ISE is immersed in low F solution (0.1 ppm F) for up to 30 minutes at the beginning of the run, before the first set of standards are measured.

Table A. 2-2– Total Fluorine calculated by Mass balance and by Ingram Whole Rock Fluorine (WRF) chemical methods. Includes trial method as well as developed method (see appendix for details).

Sample	Rock Type	EM Mineral Mass Balance	Ingram WRF - Trial	Ingram WRF - Developed		
				Aug/2010	Dec/2010	Average
M2a	Porphyritic Gneissic Chlorite Biotite Granodiorite	788	746	1770	1729	**1749**
M2b	Weathered sample	84	513		426	**426**
M3a	Pink Monzogranite	658	457		365	**365**
M3b	Weathered sample	16	302		198	**198**
M4a	Amphibole Monzogranite	514		1261	1057	**1159**
M4b	Weathered sample	9	395	208	228	**225**
M6a	Porphyritic Epidote Chlorite Granodiorite	108		320	320	**305**
M7a	Grey Monzogranite	33	320		218	**218**
M7b	Weathered sample	25	270		132	**169**
W1a	Porphyritic Chlorite Monzogranite	732		1102		**1102**
W1b	Weathered sample	118		171		**171**
W16a	Biotite Granodiorite	324		930		**930**
W16b	Weathered sample	56		233		**233**
W17a	Pegmatitc Epidote Quartz Syenite	8		<100		**<100**
W17x	Weathered Monzodiorite	128		863		**863**
W11a	Amphibole Granodiorite	474		824		**824**
W13	Mafic Vein material	3903		5536		**5536**
WC	Calcrete	207		266		**266**
G2	Geological Standard (should be 1280 ±80 ppm F)	n/a	1065	976	958	

For the EDT QSE333 fluoride electrode the manufacturers' guidelines state that a slope of 54-59 mV should be observed between measurements of standard solutions that are an order of magnitude apart. Differences of less than this will result in a steeper gradient and therefore reduce the accuracy of the calibration (as a small change in mV reading would lead to a larger

change in F concentration), whereas differences greater than this are preferable. Differences in mV readings and R^2 values from the logarithmic trend line from calibrations during measurement of runs 1 and 2 are given in Table A. 2-3

The decade differences measured are mostly within the stated range for measurements of F standards between 1 and 10 ppm F, but are lower (down to 35.5 mV) when measuring the difference between lower standards of 0.1 and 1 ppm F. The decade difference between standards of 0.1 and 1ppm F are lower in the second run than the first run. In all cases the regression line through the calibration standards shows a good fit (R^2>0.98) Table A. 2-3.

Run 1 standard solution measurements for calibration sets A to E as well as drift check (D/C) marks are given in Table A. 2-4. Standard solutions drift during the day, with mV values gradually decreasing through the day. Standard solution 0.25ppm changes very rapidly between set A and set B which may indicate contamination. Standard 0.25ppm F is therefore not used in calibration of sets B to E. The drift in the standard samples is plotted in Figure A. 2-1.

Potential sources of error in the Ingram (1970) ISE method include (Stecher, 1983):

- Inhomogenety of samples – samples may not be thoroughly homogenised and since only a small amount of the sample is used for analysis it is important that this fairly represents the whole rock
- The effectiveness of fluorine extraction during solution preparation, although this is not possible to determine
- Sorption onto container walls may cause drift; this can be reduced by using plastic vessels which do not adsorb as much fluoride as glass.
- Fluoride contamination of buffer
- Illumination effects – it has been found that changes in ambient illumination may cause drift in the electrode potential in the first hour or so
- Interference of elements such as Al can be reduced by the use of a buffer (TISAB buffer used in this experiment).
- Dissolution of and adsorption of fluoride onto, the membrane can caused poor measurements of F at low concentrations. This can be ‘cleaned’ or freshened by rubbing the bottom of the electrode with a very fine sand paper.
- Memory effect – when a low F solution is measured after a high F solution, the electrode may give falsely high mV readings due to the ‘memory’ of the previous solution. To reduce this, the electrode was thoroughly rinsed between samples and the electrode was allowed to stabilise before readings taken (this usually happened within 3 minutes).

- The electrode is likely to vary with temperature; therefore it should be kept at a constant temperature throughout the experiment.

Table A. 2-3- Decadal differences and R^2 values of calibration graphs for WRF. Decade differences should show an mV difference of 54-59. Values of F of standards and lowest calibrated F value are for F in solution. A F value of 0.1ppm F in solution corresponds to a WRF value of 100ppm F, a F value of 0.25ppm F in solution corresponds to a WRF value of 250ppm F. R^2 values are calculated from logarithmic regression of standards.

Run	Calibration	Decade Difference in F standards		lowest calibrated F value (ppm F)	R^2
		F standards measured (ppm F)	mV difference		
1	A	1 to 10	58.9	250	0.9986
	B	1 to 10	58.3	250	0.9835
	C	0.1 to 1	53.2	100	0.9993
		1 to 10	58.8		
	D	0.1 to 1	52.7	100	0.9992
		1 to 10	58.5		
	E	0.1 to 1	52.1	100	0.9989
		1 to 10	58.9		
2	A	0.1-1	40.8	100	0.9916
		1-10	56.9		
	B	0.1-1	45	100	0.9953
		1-10	57.4		
	C	0.1-1	35.5	100	0.9841
		1-10	57.1		
	D	0.1-1	36.8	100	0.9856
		1-10	57.2		

Table A. 2-4 - mV readings for standard solutions in sets A to E and drift check marks (D/C). Two measurements were taken of solution 0.25ppm F in calibration set B.

Standard F value (ppm F)	mV reading for each Calibration Set							
	A	B		D/C	C	D/C	D	E
0.1					103.8	103.0	100.8	99.1
0.25	81.4	70.4	69.5	69.4	69.1		66.7	65.5
1	51.0	50.5		50.4	50.6	49.4	48.1	47.0
2	32.4	32.0			32.0		29.9	
5	9.8	9.6			9.6		7.3	6.0
10	-7.9	-7.8		-8.6	-8.2	-9.4	-10.4	-11.9

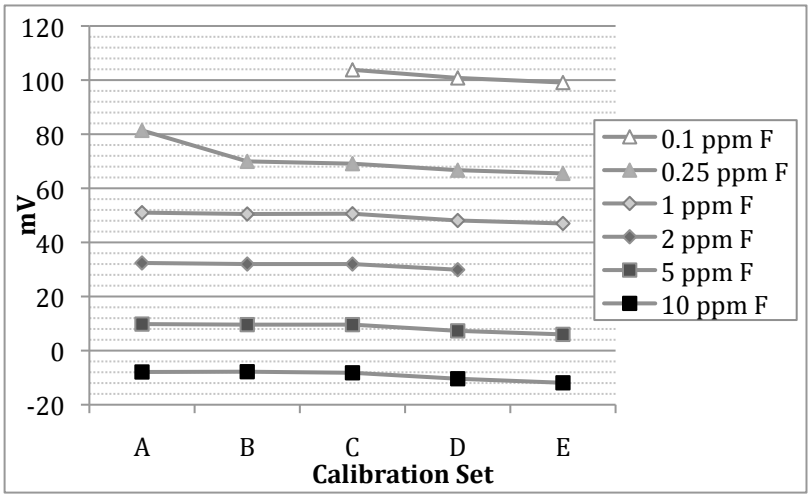

Figure A. 2-1 – Drift of standard mV measurements between calibration sets (run 1)

Full caution was taken to avoid error where possible. Powdered samples were thoroughly mixed, plastic contains were used for all solutions, the lab was kept at a constant temperature and illumination throughout the measurements, the electrode was thoroughly rinsed between readings, and freshened using very fine sandpaper prior to use and a TISAB buffer was used.

References Cited

Ingram, B.L., 1970, Determination of Fluoride in Silicate Rocks without Separation of Aluminium Using a Specific Ion Electrode: Analytical Chemistry, v. 42, p. 1825-1827.

Stecher, O., 1983, Fluorine in twenty-two international reference rock samples and a compilation of fluorine values for the USGS reference samples: Geostandards Newsletter, v. 7, p. 283-287.

Appendix 3. Further Details of Batch Leaching

Method

The method for batch leaching experiments was as follows:

- Dry the rock sample and crush to size 0.5-2mm. Sieve to remove any small or large material.
- Weigh 40g of the rock sample into a 250ml high-density polythene bottle
- Add 200ml of de-ionised water, and place the lid tightly on the bottle.
- Place the bottle on a roller for constant movement of the material and water, at room temperature.
- Duplicate each rock sample, and run a blank for each set of samples.
- Each bottle is sampled every 2 hours on the first day of the experiment, then at approximately 24, 32, 48, 72 and 96 hours, and then twice a week for the next 3 weeks.
- To sample, remove the bottle from the roller and leave to stand for 3 minutes. Remove exactly 4 ml of liquid using a syringe, and place in a tube. Place the tube in a centrifuge for 4 minutes to separate any solid material that may have been removed from the sample bottle. Remove the liquid with a syringe and filter through a 0.45um filter tip. Divide this into two sample tubes:
- 1ml in one tube, for analysis with IC (analysis of F and Cl). Store in a refrigerator
- 3ml in a second tube, acidified (with a single drop of 50% nitric acid) for analysis by ICP-AES (analysis of Ca, Mg, Na, K, and Fe and P if possible)
- Replace the cap on the sample bottle and shake briefly to disturb any settled material. Replace on the roller.
- For ICP-AES analysis, 2ml of the acidified sample is added to 2ml of deionised water to increase the volume available for analysis.

Anomalous Results

The results of the blank runs and the comparison of results from repeats allowed for the identification of anomalous results, some of which resulted from contamination of the samples. Sample contamination was only observed in one set of batch leaching experiments using Wailpally samples.

In the Wailpally batch leaching experiments, some fluoride IC measurements were very high (up to ~13mg/l). In some cases the blank measurement at the same time interval also had a very high F concentration, and in a few samples, high Cl, S and N were also measured.

The high F results were found to be due to a double-peak being present at the fluoride interval (F peak should be at 1.19 minutes) (figure a. 3-1 to figure a. 3-4). This can result in a high F reading as:

- The second peak may increase the F peak intensity or width due to their close proximity (figure a. 3-1)
- The double peak may be measured as one peak by the IC software (figure a. 3-2 and figure a. 3-3)
- The second peak may be mis-identified as the F peak, when it is not (figure a. 3-4)

Where possible the two peaks were resolved and new measurements of F calculated from the F peak alone. In many cases it is not possible however to resolve the peaks. The second peak is most likely from organic matter present in the samples or from contamination. Fluoride values where a double peak is clearly seen have been removed from the results.

The vials used are acid cleaned and rinsed with de-ionised water and should not be a cause of contamination.

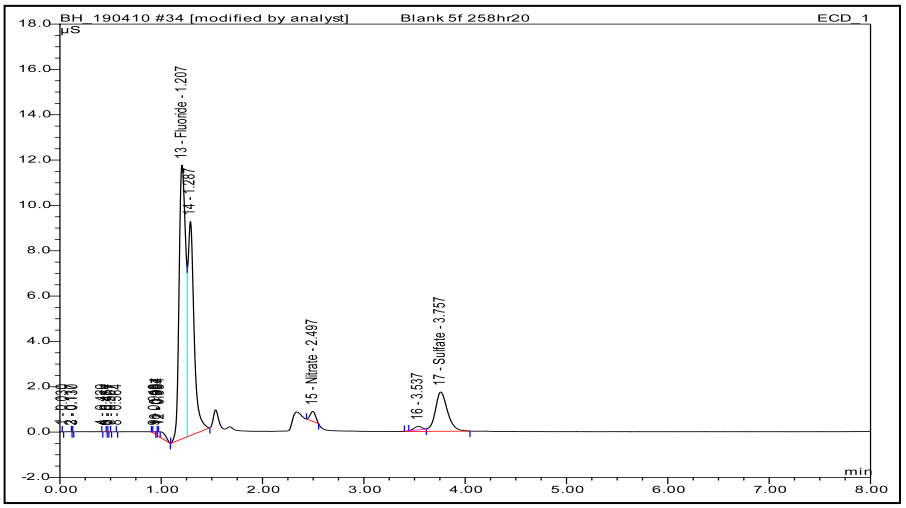

Figure A. 3-1 – Double peak observed with the fluoride peak (peaks 13 and 14)

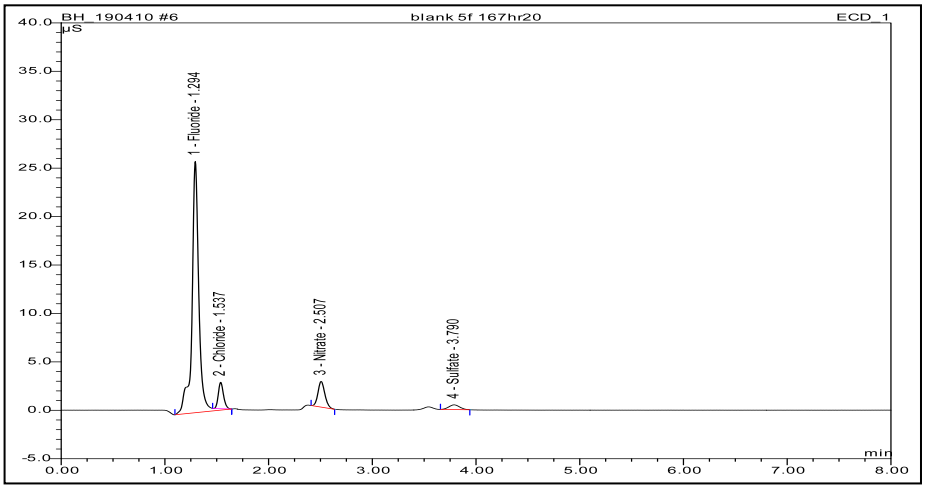

Figure A. 3-2 – A 'hump' is seen at the beginning of the F peak. The F peak is large and slightly delayed (at 1.294 minutes). The small 'hump' may be the true F peak, which has merged with the larger near-by peak.

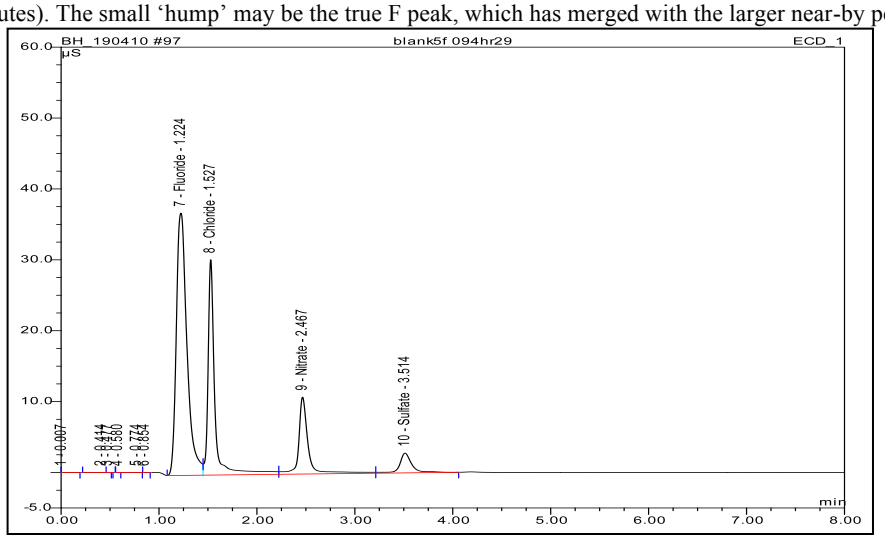

Figure A. 3-3 – The F peak here is very broad, suggesting another substance may be present here.

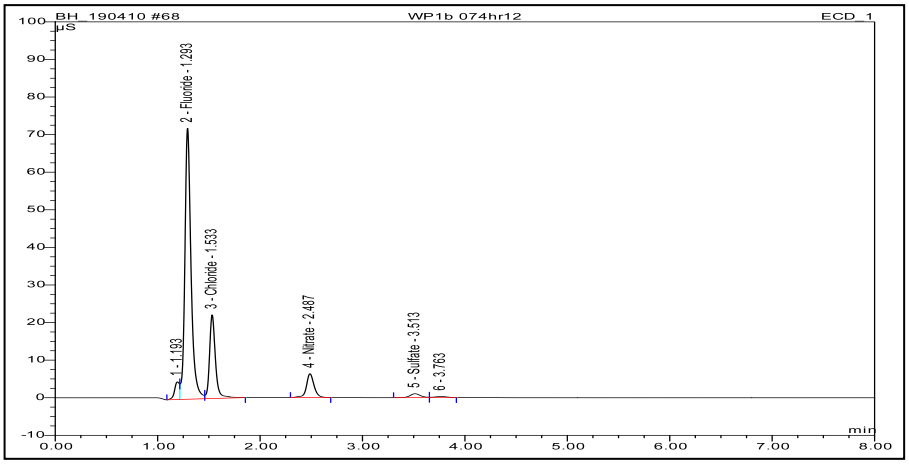

Figure A. 3-4 – A 'hump' seen at the beginning of the first peak. This is likely to be the fluoride peak (at 1.193 minutes), however the software has identified the second peak (at 1.29 minutes) as the fluoride peak.

An investigation of potential contamination from the filters used was carried out by the sampling of a blank run, filtering some samples, and leaving some samples un-filtered. Unfiltered blanks have low/no F, whereas filtered blanks have anywhere from 0.5 to 5 mg/l F

(figure A. 3-5). The filters may therefore be a source of F contamination to the samples. The filters used were VWR sterile cellulose acetate filters, pore size 0.45µm, and should contain no fluoride or organic matter. As this contamination was only observed in one set of leaching experiments it may be assumed that several of the filters from the pack used for these experiments were the cause of such contamination, but that not all filters were contaminating the samples. Previous blank runs for Maheshwaram batch leaching experiments measured low/no fluoride.

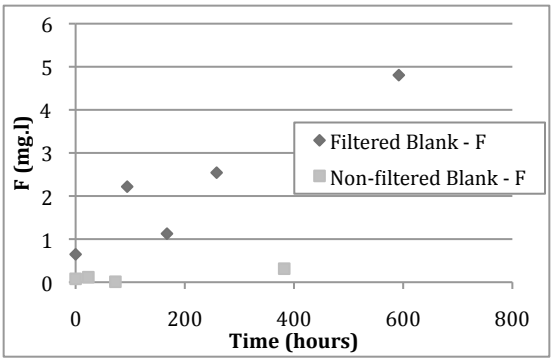

Figure A. 3-5 – F measurements for filtered and non-filtered blank samples